



**ROBERT GORDON  
UNIVERSITY • ABERDEEN**

## **OpenAIR@RGU**

### **The Open Access Institutional Repository at Robert Gordon University**

<http://openair.rgu.ac.uk>

#### **Citation Details**

**Citation for the version of the work held in 'OpenAIR@RGU':**

**BUCHAN, B. E., 2011. Formulation studies on cysteamine for the treatment of nephropathic cystinosis. Available from *OpenAIR@RGU*. [online]. Available from: <http://openair.rgu.ac.uk>**

#### **Copyright**

Items in 'OpenAIR@RGU', Robert Gordon University Open Access Institutional Repository, are protected by copyright and intellectual property law. If you believe that any material held in 'OpenAIR@RGU' infringes copyright, please contact [openair-help@rgu.ac.uk](mailto:openair-help@rgu.ac.uk) with details. The item will be removed from the repository while the claim is investigated.

FORMULATION STUDIES ON CYSTEAMINE FOR  
THE TREATMENT OF NEPHROPATHIC CYSTINOSIS

BARBARA ELIZABETH BUCHAN

FORMULATION STUDIES ON CYSTEAMINE FOR  
THE TREATMENT OF NEPHROPATHIC CYSTINOSIS

BARBARA ELIZABETH BUCHAN

A thesis submitted in partial fulfilment of the  
requirements of the  
Robert Gordon University  
for the degree of Doctor of Philosophy

August 2011

## **Declaration**

This thesis in candidature for the degree of Doctor of Philosophy has been composed entirely by myself. The work which is documented was carried out by myself unless otherwise stated. All sources of information contained within the text which have not arisen from the results generated have been specifically acknowledged.

Barbara Elizabeth Buchan

**Barbara Elizabeth Buchan**

**PhD**

**Formulation Studies on Cysteamine for the Treatment of Nephropathic Cystinosis**

**Abstract**

Nephropathic cystinosis is a rare autosomal recessive disease characterised by raised lysosomal levels of cystine in the cells of almost all organs. It is treated by regular oral and topical administration of the aminothioliol, cysteamine (Cystagon™), which possesses an offensive taste and smell. The oral form frequently causes emesis, and should be administered every six hours to be maximally effective. The topical eye drop treatment requires hourly application to be most effective. In an attempt to reduce this frequency and improve the treatment, the preparation and evaluation of three alternative cysteamine containing formulations (suppositories, long-acting ophthalmic gels and an inhaler) was undertaken.

The physicochemical properties, stability and release profiles of the active (cysteamine or phe conjugate) from the formulations were evaluated. The suppositories released cysteamine over a 20-40 minute period with a  $T_{75}$  = 10-13 minutes. They were most stable at 4°C. The analysis of the ophthalmic gels demonstrated that a weak gel network was formed at low shear stress, the bioadhesion of the gel was increased with inclusion of a cysteamine derivative (e.g. mean force of 0.067N compared to 0.107N with compound included) and eight-hour, first order release from the gel was observed. There was significant adhesion observed between the ophthalmic gels and bovine corneal tissue. The pulmonary microspheres were spherical and within the optimum size range for deep lung delivery (1-5  $\mu$ m). However, Andersen Cascade Impactor analysis revealed poor deep lung penetration.

In conclusion, these results demonstrated that more development work was required to produce a useful pulmonary formulation of cysteamine, however, formulation of an ocular applicable gel or suppository was readily

achievable. The suppository preparations may be particularly beneficial for the treatment of infants, whilst the ophthalmic gel preparations could be developed for daily or overnight use. With respect to pulmonary delivery, microspheres in the optimum size range were produced. However, deep lung targeting was prevented by static agglomeration, which requires further investigation.

**Keywords:** Cystinosis, formulation, rectal, ophthalmic, pulmonary, bioadhesive, gel, polymer, modified release.

## Contents

<b>Declaration</b>	3
<b>Abstract</b>	4
<b>Contents</b>	6
<b>Acknowledgements</b>	11
<b>List of tables</b>	13
<b>List of figures</b>	15
<b>List of abbreviations</b>	19
<b>Preface</b>	22
<b>Chapter 1 – General introduction</b>	25
1.1 Nephropathic cystinosis	26
1.2 History of nephropathic cystinosis	27
1.3 Genetics	32
1.4 Cystinosis pathophysiology	33
1.5 Cystinosis sub-categories	35
1.6 Cysteamine	36
1.7 Cystamine	37
1.8 Problems arising from cysteamine treatment	38
1.9 Other barriers to effective treatment	39
1.10 Economical considerations	40
1.11 Recent advances	41
1.12 Alternative routes	42
1.13 Aims of the project	44
<b>Chapter 2 – Analytical methods</b>	48
2.1 Introduction	49
2.2 Phe conjugate synthesis	49
2.3 Partition coefficient studies	52
2.4 Ellman's reagent	53
<b>Chapter 3 – Rectal formulations</b>	57
3.1 Introduction	58
3.1.1 Suppository history	58
3.1.2 Rectal anatomy and first-pass effect	58
3.1.3 Second-generation suppositories	60
3.1.4 In-situ gelling suppositories	60
3.1.5 Cysteamine suppositories	61
3.1.6 Suppository bases	62
3.1.6.1 Polyethylene glycols	62
3.1.6.2 Witepsol	63
3.1.6.3 Gelucire	63
3.1.6.4 Poloxamers	64
3.2 Materials and methods	64
3.2.1 Materials	64
3.2.2 Suppository manufacture	65
3.2.3 Dissolution studies	66
3.2.4 Hot-stage microscopy studies of suppositories and excipients	67

3.2.5 Cooling profile studies	67
3.2.6 Active dispersion studies	68
3.2.7 Suppository mould temperature studies	68
3.2.8 Stability tests	69
3.3 Results and discussion	70
3.3.1 Dissolution studies	70
3.3.2 Hot-stage microscopy studies	73
3.3.3 Cooling profile studies	77
3.3.4 Active dispersion studies	78
3.3.5 Suppository mould temperature studies	79
3.3.6 Stability tests	80
3.3.6.1 DSC results: T0, T6 months, T12 months comparison	80
3.3.6.2 Infrared spectroscopy after 1 week, 3 months, 6 months and 12 months	83
3.3.6.3 Correlation between DSC plots and IR percentage match results	85
3.4 Conclusions	86
<b>Chapter 4 - Ophthalmic formulations</b>	<b>88</b>
4.1 Introduction	89
4.1.1 History of cysteamine eye drops	90
4.1.2 Eye anatomy	92
4.1.3 Mucus	93
4.1.4 Delivery systems for ophthalmic symptoms of cystinosis	94
4.1.4.1 In-situ gelling polymers	94
4.1.4.2 Bioadhesive and mucoadhesive polymers	95
4.1.5 Gellan gum	97
4.1.6 Carbomer 934	97
4.1.7 Xanthan gum	98
4.1.8 Hydroxypropyl methylcellulose (HPMC)	99
4.1.9 Thiolated polymers	99
4.1.10 In-vitro testing	101
4.2 Materials and methods	101
4.2.1 Materials	101
4.2.2 Gel manufacture	102
4.2.3 pH studies	103
4.2.4 Optical transmission	103
4.2.5 Rheology studies	104
4.2.6 Dissolution studies	104
4.2.6.1 Phe conjugate (6) studies	104
4.2.6.2 Cysteamine hydrochloride studies	105
4.2.7 Bioadhesion studies	106
4.2.8 Stability tests	107
4.3 Results and discussion	107
4.3.1 pH studies	107
4.3.2 Optical transmission	108
4.3.3 Rheology studies	110
4.3.3.1 Carbomer 934 gels	110
4.3.3.2 Xanthan gum gels	114
4.3.3.3 HPMC gels	116
4.3.4 Dissolution studies	118
4.3.4.1 Phe conjugate as active	118

4.3.4.2 Cysteamine hydrochloride as active	120
4.3.5 Bioadhesion studies	122
4.3.5.1 Oscillation rheology	124
4.3.6 Stability tests	125
4.3.6.1 Carbomer 934	125
4.3.6.2 Xanthan gum	128
4.3.6.3 HPMC	131
4.4 Conclusion	132
<b>Chapter 5 – Respiratory formulations</b>	<b>135</b>
5.1 Introduction	136
5.1.1 History of respiratory delivery	136
5.1.2 Pulmonary delivery in cystinosis	137
5.1.3 Lung anatomy	137
5.1.4 Inhaled bioavailability	140
5.1.5 Inhaler types	140
5.1.6 Fate of inhaled microparticles	143
5.1.7 Microsphere production	144
5.1.7.1 Milling	145
5.1.7.2 Emulsion solvent evaporation	145
5.1.7.3 Spray drying	145
5.1.8 Static electricity and agglomeration	147
5.1.9 Poly(D,L-lactide)	150
5.1.10 In-vitro testing	152
5.2 Materials and methods	155
5.2.1 Materials	155
5.2.2 Cysteamine bitartrate synthesis	155
5.2.3 Microsphere preparation	156
5.2.4 Microscope analysis	158
5.2.5 Scanning Electron Microscopy (SEM)	159
5.2.6 Particle size analysis	159
5.2.7 Moisture content of microspheres	160
5.2.8 Drug content of microspheres	160
5.2.9 Blend with lactose	160
5.2.10 In vitro powder aerolisation: Pre-clean	161
5.2.11 Andersen Cascade Impactor: Testing	161
5.2.11.1 ACI set up	161
5.2.11.2 Respiratory powder testing	162
5.2.11.3 ACI wash down	163
5.2.11.4 Respiratory powder analysis	163
5.2.12 ACI pressure and flow testing	164
5.2.13 Dissolution testing	165
5.2.14 Stability testing	165
5.3 Results and discussion	166
5.3.1 Cysteamine bitartrate synthesis and analysis	166
5.3.2 Microscope analysis	166
5.3.3 Scanning Electron Microscope (SEM) analysis	168
5.3.4 Particle size analysis	170
5.3.5 Moisture content of microspheres	172
5.3.6 Drug content of microspheres	173
5.3.7 Blend with lactose	173
5.3.8 Andersen Cascade Impactor: Analysis	177

5.3.9 ACI pressure and flow testing	179
5.3.10 Dissolution testing	180
5.3.11 Stability tests	180
5.4 Conclusions	183
<b>Chapter 6 – General discussion and future work</b>	<b>186</b>
6.1 Rectal delivery	187
6.2 Ophthalmic delivery	189
6.3 Pulmonary delivery	191
6.4 Cysteamine bitartrate's indications in other disease states	192
6.5 General conclusion	193
<b>References</b>	<b>194</b>
<b>Appendices I-III</b>	<b>217</b>
<b>Supporting studies</b>	<b>221</b>
<b>Communications associated with this thesis</b>	<b>222</b>

Till a' the seas gang dry, my dear,  
And the rocks melt wi' the sun;  
And I will luv thee still, my dear,  
While the sands o' life shall run.

**A red, red rose**

**Robert Burns**

**1794**

## Acknowledgements

This PhD would not have been possible or as enjoyable without the help and support from many wonderful people. I owe you all much more than a free cappuccino.

I must first of all thank my three brilliant supervisors, Graeme Kay, Kerr Matthews and Don Cairns, for all their hard work, patience, support and advice over the years. I have loved working on this project, due largely to their dedication and enthusiasm. Thanks must also go to the devoted staff of The Robert Gordon University, in particular Liz Hendrie, Laurie Mearns, Moira Middleton, Dorothy Moir, Vivienne Hamilton, Moira Innes, Maureen Byres, Raymond Reid, Kirstin and John, who have provided invaluable technical support and a richt guid blether. The Cystinosis Foundation UK, who funded my second and third years and provided travel funding to Portland and Tenovus Scotland, who provided funding for consumables have made it all possible. Thanks also to the UK Resource Centre for Women in Science, Engineering & Technology who provided valuable financial support for travel to the CRS conference in Portland.

Many thanks to my parents Colin and Betty, who helped me through my first year and have supported me throughout my education even though they have no idea what it is I do, and my lovely Auntie Nannie, who gave great words of support and encouragement from across the pond. Thanks must also go to my awesome second Mum Liz, for all her help and support as my soon-to-be-Mother-in-law. You have more energy than a big bag of energetic things! To my fellow PC27 Post-Graduate students; whether playing American football, going for coffee or gossiping, you have made me laugh and helped me through a fair few crises. Karen, Clare, Owen, Scott, Clare and Lisa, Olga, Amina, Martha, Noelle and Pramod, I wish you all lots of love and the best of luck. Many thanks also to Sukanta, Bridgeen, Alberto and Ziad for all your patient and hands-on chemistry help.

Thanks to McIntosh Donald of Portlethen, who gave me hundreds of cow's eyes for free, and in particular Brian Christie, who did all the dirty work. To Emma Hector, who picked up the eyes when my car was in the shop, and who patiently waited while they were removed from their respective heads, and Olga and Karen, who helped me to dissect my first cow eyes, and laughed at me until I could stomach it myself without full body protection, I can only say thank you!

Many thanks must also go to the engineering boys from downstairs, who dealt with my endless requests for yet more stainless steel plates, foot pumps and pressure gauges. Thanks to Robert Lothian, school of computing at RGU, who gave me invaluable help with the statistics I had forgotten, and Rachel Knott, who gave me outstanding help with statistics and SPSS.

Many thanks also to Dan Alexander, Gary Cannon and Mike Ramsey at GSK, Ware, for all their generosity and help with the Andersen Cascade Impactor and with the pulmonary delivery work.

To Moira, thank you for all your amazing help and support during my third year.

Special mention must go to the brilliant crew at Starbucks, Upperkirkgate, who have become firm friends. Liz, Craig, Marta, Blair, Katy, Jo, Iain, Justyna, Mike and Nadia, I know you are all destined for great things. You have kept me sane through my write up and made me laugh until I cried. I love you all.

And finally Stuart, my best friend and better half by far, I can't begin to describe how much you've helped me. You made sure I was never alone during this process, and were always ready with some good advice, a cup of tea and a cuddle. I am truly lucky to have found you.

## List of tables

Table 1. Summary of the most common symptoms of cystinosis	35
Table 2. Summary of the experimentally obtained partition coefficient values	53
Table 3. A summary of the suppository batches made and their characteristics	66
Table 4. Summary of phe conjugate release studies	71
Table 5. Summary of cysteamine hydrochloride release studies	73
Table 6. DSC analysis data of the suppositories from six different starting mould temperatures	79
Table 7. Average temperatures and relative humidities in each storage chamber	80
Table 8. DSC analysis data of selected suppository samples over time	81
Table 9. The group frequencies used for identification of the suppository samples	84
Table 10. Suppository stability over time, presented as percentage match to sample at $T_0$	85
Table 11. Summary of all gels tested	103
Table 12. pH effect on all gels after active addition	108
Table 13. Optical transmission of the three gels and two commercial gels	109
Table 14. Viscosity coefficient values for carbomer 934 gels containing different cysteamine compounds	111
Table 15. Oscillatory data for carbomer 934 gels	113
Table 16. Viscosity coefficient values for xanthan gels containing different cysteamine compounds	115
Table 17. Oscillatory data for xanthan gels	115
Table 18. Viscosity coefficient values for HPMC gels containing different cysteamine compounds	117
Table 19. Oscillatory data for HPMC gels	118
Table 20. Average membrane rod areas for each gel	118
Table 21. Results of the Higuchi model analysis on each of the three gels	120

Table 22. Results of bioadhesion assay for carbomer 934	122
Table 23. Results of bioadhesion assay for xanthan gum gels	123
Table 24. Results of bioadhesion assay for HPMC gels	123
Table 25. Synergy tests using oscillatory rheology	125
Table 26. Cut-off diameters in the ACI	154
Table 27. The ten batches of microspheres were manufactured according to the conditions shown	157
Table 28. Final spray drying conditions used for optimum microsphere separation	158
Table 29. Summary of the powders tested	163
Table 30. Sequential ACI stages, with corresponding flask size	164
Table 31. Summary of the particle size results for Batch 9 microspheres	171
Table 32. Moisture content of Batch 9 microspheres over time	172
Table 33. The average room temperature and relative humidity at ACI testing, and standard deviation between readings	177
Table 34. Summary of the powder batch characteristics	177
Table 35. ACI cut-off diameters and the corresponding powder deposition	178
Table 36. IR analysis of Batch 9 microspheres stored in varying conditions, compared with $T_0$	181
Table 37. A summary of the suppository batches made and their characteristics.	219

## List of figures

Figure 1. The relationship between cysteine and cystine, and how cysteamine removes cystine from the lysosome.	29
Figure 2. Location of chromosome 17p13 (CTNS), the gene deletion responsible for cystinosis.	32
Figure 3. Image of dissected nephrons from a cystinosis patient, which display a marked narrowing at the start of the proximal section (the characteristic 'swan-neck' deformity).	34
Figure 4. Cysteamine.	36
Figure 5. Cystamine.	38
Figure 6. Phe conjugate	49
Figure 7. Synthesis of the phe conjugate.	50
Figure 8. A scan of UV absorbance highlighting the lambda max for phe conjugate.	51
Figure 9. Linear regression produced for the phe conjugate, with the corresponding correlation coefficient.	52
Figure 10. The mechanism of thiol detection by Ellman's Reagent	54
Figure 11. A plot of concentration versus absorbance for a series of DTNB solutions	54
Figure 12. A diagram of the three rectal veins: 1 superior rectal vein; 2 middle rectal vein; 3 inferior rectal vein	59
Figure 13. Molecular structure of polyethylene glycol, where n = number of repeating subunits, e.g. n = 34 would produce PEG 1500.	63
Figure 14. Suppository sample points for uniform content studies.	68
Figure 15. Percentage release of the phe conjugate from PEG Blends A, B and C over time (n = 7, 9 and 6 respectively).	70
Figure 16. Percentage release of cysteamine hydrochloride from PEG Blends A, B and C over time (n = 6, 5 and 5 respectively).	72
Figure 17. Optical micrographs of: a. Cysteamine hydrochloride at 25°C, b. cysteamine hydrochloride at 25°C (heated to melting point then re-crystallised), c. PEG 8000, d. PEG 8000 at 25°C (heated to melting point (62°C) then recrystallised), and e. PEG 600 at 5°C (heated to 50°C and recrystallised).	74

Figure 18. Optical micrographs of, a. PEG 14000 at 25°C (heated to its melting point (62°C) and recrystallised), b. PEG blend A at 25°C (suppository), c. PEG blend B at 25°C (suppository), and d. PEG blend C suppository at 25°C.	75
Figure 19. Three PEG blend suppositories average cooling profiles	77
Figure 20. Section comparison of the melt phase between the tip, middle and edge areas of the PEG Blend A suppository containing cysteamine hydrochloride.	78
Figure 21. DSC plot of PEG blend C suppositories over time, stored at 21°C.	82
Figure 22. DSC plots of PEG blend C suppositories over time, stored at 4°C.	82
Figure 23. Regions of the IR spectra used for comparison in this study.	84
Figure 24. Diagram of the cornea.	89
Figure 25. Structural repeating unit of carbomer 934, where $n \approx 2000$	98
Figure 26. Structural repeating unit of xanthan gum, $n \approx 500$	99
Figure 27. Structural repeating unit of HPMC, $n \approx 500$	99
Figure 28. Synthesis scheme for the generation of polymer–cysteamine conjugates.	100
Figure 29. Rheology of 1% w/w carbomer 934 with 0.5% cysteamine hydrochloride	111
Figure 30. Continuous flow curves for carbomer 934 gels containing different cysteamine compounds at 34°C.	112
Figure 31. 1% w/w carbomer 934 with 0.5% cysteamine hydrochloride oscillation results.	113
Figure 32. 1% w/w xanthan gum with 0.5% cysteamine hydrochloride.	114
Figure 33. Effect of active addition on xanthan gels.	114
Figure 34. Oscillatory shear data for xanthan gels.	115
Figure 35. 1% w/v HPMC displayed a Newtonian rheology.	116
Figure 36. Effect of active addition on the viscosity of HPMC gels.	116
Figure 37. 1% w/v HPMC with 0.5% cysteamine hydrochloride oscillation results.	117

Figure 38. Percentage release of carbomer 934.	118
Figure 39. Percentage release of xanthan gum.	119
Figure 40. Percentage release of HPMC.	119
Figure 41. Percentage release of cysteamine hydrochloride from carbomer 934 gels.	121
Figure 42. Carbomer 934 gel stability containing no active.	126
Figure 43. Carbomer gel stability over time containing phe conjugate.	126
Figure 44. Carbomer gel stability over time containing cysteamine hydrochloride.	127
Figure 45. Carbomer 934 oscillation data over time.	128
Figure 46. Effect of time on the viscosity of xanthan gels containing no active.	129
Figure 47. The rheology of xanthan gum containing cysteamine hydrochloride over time.	129
Figure 48. Oscillatory results for xanthan gum over time.	130
Figure 49. Rheology of HPMC containing no active over time.	131
Figure 50. The rheology of HPMC over time, containing cysteamine hydrochloride.	131
Figure 51. Oscillatory data of HPMC gels over time.	132
Figure 52. Diagram of particle sizes for lung delivery, with the corresponding Andersen Cascade Impactor (ACI) stages	138
Figure 53. The Handihaler <sup>®</sup> device used in this project.	141
Figure 54. Diagram of a typical bench top spray dryer.	146
Figure 55. Monomeric repeating unit of Poly(D,L-lactic acid), where $n \approx 7700$	150
Figure 56. Detail of the internal structure of the ACI (Copley Scientific Ltd, Nottingham, UK).	153
Figure 57. Optical micrographs of the progressing blends, illustrating the particles becoming more discreet; a. Batch 2, b. Batch 3, c. Batch 8, and d. Batch 8 showing particles of 3-5 $\mu\text{m}$ .	167
Figure 58. Optical micrographs illustrating the spherical final particles, a. Batch 9 particles of 2-3 $\mu\text{m}$ , and b. Batch 9 particles of 2-4 $\mu\text{m}$ .	167
Figure 59. SEM images showing, a. Batch 2 showing signs of spheres (x 10K), and b. Batch 3 becoming more spherical and displaying hard bridges between particles (x 10K).	169

Figure 60. SEM images showing, a. Batch 8 showing fully formed microspheres, with many still connected (x 10K), and b. Batch 9 with complete microspheres within the desired size range (1-6µm) (x 2K).	169
Figure 61. SEM images of Batch 9, the batch chosen for further analysis (magnification: a – x 5.37K, b – x 11.71K, c – x 6.28K, d – x 8.06K).	170
Figure 62. SEM of 100µm lactose, showing large planar particles with minor asperities (x 4.68K).	174
Figure 63. The BP lactose grade possesses many areas for drug particle attachment (x 10K).	174
Figure 64. The spray dried/USP lactose has extensive regions for particle attachment (x 10K).	175
Figure 65. SEM of a 50:50 mix of 100 µm lactose with Batch 9 microspheres, with the microspheres clearly attached to the carrier lactose particles (x 2.1K).	176
Figure 66. Comparison of storage effects on the most successful powder blend, T = throat, P = pre-separator.	178
Figure 67. Cysteamine bitartrate release from the microspheres over time (n = 4).	180
Figure 68. Images of, a. Batch 9 microspheres stored at 4°C for 1 week, and b. Batch 9 microspheres stored at 30°C, 75% RH for 1 week.	181
Figure 69. TGA plot comparing Batch 9 microspheres from T1 day and T6 weeks, stored at 30°C and at 75%RH.	182

## Abbreviations

ACI	Andersen Cascade Impactor
AUC	area under the curve
Boc-Phe-OSu	Boc protected phenylalanine
BP	British Pharmacopoeia
CD <sub>3</sub> OD	deuterated methanol
d	doublet
DBU	1,8-Diazabicyclo[5.4.0]undec-7-ene
DCM	Dichloromethane
DPI	dry powder inhaler
DSC	Differential Scanning Calorimetry
DTNB	5,5'-dithiobis(2-nitrobenzoate), Ellman's Reagent
ETC	Environmental Test Chamber
FPD	fine particle dose
G'	storage modulus
G''	loss modulus
HCl	hydrochloride
HPMC	Hydroxypropyl methylcellulose
IR	Infra Red
IV	Intra venous
kb	kilo bases
kDa	kilodaltons
kPa	kilopascal
kV	kilovolts
J/g	Joules per gram (heat capacity)
L	Litre
λ <sub>max</sub>	lambda max
LSD	Lysosomal Storage Disease
m	multiplet
MeOD	deuterated methanol
mg	milligrams
MHz	megahertz
ml	millilitres
MMAD	mass median aerodynamic diameter

mmHg	millimetres of mercury
ms	milliseconds
mTorr	millitorr
m/z	mass-to-charge ratio
N	Newtons
NaHSO <sub>4</sub> .H <sub>2</sub> O	sodium hydrogen sulphate monohydrate
NaOH	sodium hydroxide
nm	nanometers
nmol	nanomole
pA	picoamps
PAA	Poly(acrylic acid)
Pa.s	Pascal second
PEG	Polyethylene glycol
Phe	Phenylalanine
PLA	Poly (D,L-lactide), Resomer <sup>®</sup> R 202s
ppm	parts per million
% RH	percentage relative humidity
rpm	revolutions per minute
Sat	saturated
SEM	Scanning Electron Microscope
SLF	Simulated Lachrymal Fluid
SMPB	Sorensens Modified Phosphate Buffer
t	Triplet
T <sub>0</sub>	Time zero
Tan δ	tan delta
TFA	Trifluoroacetic acid
Tg	Glass transition temperature
TGA	Thermogravimetric Analysis
TNB	2-nitro-5- thiobenzoate
µg	microgram
µL	micro litres
µm	micrometers
UV	Ultra Violet
W <sub>ad</sub>	work of adhesion
W/g	change in heat capacity



## **Preface**

This thesis presents and discusses data produced during a pharmaceuticals research project. The project aimed to improve upon the current oral capsule and eye drop treatments for Nephropathic Cystinosis. This disease, which affects around 2000 people globally, is characterised by poor growth, rickets and renal failure in children. If untreated, the disease will cause death by age twelve. Currently, cystinosis is treated with cysteamine bitartrate as an oral capsule and topical eye drop. This treatment, in combination with renal transplantation can improve symptoms and delay renal failure, allowing patients to conduct normal activities and live into their 30s or 40s. However, the current treatment cysteamine bitartrate produces side effects which can be prohibitive to compliance. These include frequent nausea and vomiting, odiferous breath and sweat and a challenging dosage regime. This project addressed these issues through the formulation of three alternative dosage forms, which aimed to reduce or eliminate these side effects.

Chapter one is an introduction to cystinosis, its symptoms, history and treatments. Chapter two outlines the analytical methods used in this project and the preformulation work conducted, including cystamine derivitisation. Chapter three describes the rectal formulation work and the subsequent analysis of the forms, including hardness testing, dissolution and microscope analysis. Chapter four outlines the ophthalmic formulations developed during the project. Analysis of these forms including dissolution, rheology and long-term stability tests are described. Chapter five details the pulmonary delivery work, and analysis of the powders including electron microscope and impactor work is described. Chapter six is a discussion of the conclusions of the project, with an exploration of areas for further work.

For my beloved Stuart.



# **Chapter 1 – General Introduction**

## **Chapter 1 – General Introduction**

### **1.1 Nephropathic Cystinosis**

Nephropathic Cystinosis is a rare genetic disease characterised primarily by extremely high intracellular levels of the amino acid cystine, electrolyte imbalance, proximal renal tubular dysfunction (Fanconi syndrome) and general failure to thrive (1,2). The accumulation of cystine as crystals in most tissues leads to the progressive impairment and dysfunction of multiple organs, such as the pancreas, brain and thyroid (3). The incidence of cystinosis is one in 100,000 – 200,000 live births, and affects approximately 2000 patients in the world, although there are believed to be many more undiagnosed cases (4). It is reported that some infants will die due to dehydration and electrolyte imbalance from Fanconi syndrome without diagnosis (5). In the USA alone there are 500-600 reported cases, with between 20 and 40 born each year (5). In the US, 1.4% of children on dialysis have cystinosis, while 2% of paediatric renal transplants are due to the disease (3).

Cystinosis is categorised as a Lysosomal Storage Disorder (LSD), which is a group of progressive disorders that share multi-organ failure as an endpoint, and is notable as the first disease in this group to be treatable (3,5). As with all LSDs, no signs of abnormality are displayed at birth; the first symptoms of glomerular dysfunction begin to appear at around 6-12 months of age (2). Without treatment most children will reach end-stage renal failure by age 9 (5), and grow at 50-60% of the expected rate. By the age of eight an untreated child with cystinosis will be the height of a healthy 4-year old (5), and, if non-compliant with treatment, may not reach four feet in height. Patients with cystinosis have normal intelligence, but possess extremely poor spatial awareness, and this can cause learning difficulties in early school life as many tasks such as reading and mathematics are based on this skill. However, many patients have finished school and gone into higher education (6).

## 1.2 History of nephropathic cystinosis

One hundred years ago, the disease cystinosis was almost unknown. The Swiss biochemist Abderhalden first reported the symptoms of cystinosis in a patient, following an autopsy of a 21-month-old child in 1903. The child was suspected of suffering from malnutrition, however the autopsy revealed abnormally high levels of the amino acid cystine accumulated as crystals in the liver and spleen (7). He recognised that the disease was genetic as five members of the same family had been afflicted, and called it "Familial Cystine Diathesis". There were several similar cases reported around Europe in the following decades (8,9,10). These cases all bore striking similarities and showed several common components; rickets, glucosuria and hypophosphatemia. However, it wasn't until 1936 that Fanconi realised there was a link between these cases and renamed the condition "nephrotic-glucosuric dwarfism with hypophosphatemic rickets".

Burki, working in 1941, first documented the ocular symptoms of cystinosis (11). Both the posterior ophthalmic segments such as optic nerve and retina, as well as anterior portions such as conjunctiva, iris, ciliary body and cornea were found to accumulate cystine crystals. The crystals deposit slowly in the cornea through infancy until they become apparent at around 16 months of age (12). Photophobia and, ultimately, blepharospasm affect the quality of life such that the slightest glimmer of sunlight can be debilitating (2).

In 1943 three researchers linked hyperaminoaciduria to the disease and, in combination with an improved qualitative method for detection, this then became a crucial starting point for future detection and research (8). At first it was hypothesised that perhaps a low kidney threshold for amino acids was the cause of high levels being found in the urine, despite normal levels in the blood. However, in 1952 Bickel realised that the kidneys were being progressively damaged, and therefore the problem had to lie elsewhere. Bickel renamed the disease "Lignac-Fanconi's Disease", or even "cystine storage disease with amino-aciduria", after discovering that cystine was being accumulated in lympho-glandular tissue and bone marrow (10).

Three major breakthroughs occurred in cystinosis in the late 1960s. Kidney transplants became more commonplace, immunosuppressant drugs were developed and a more sensitive method for the detection of cystine was developed (13). Schulman, Schneider and Patrick et al discovered that cystine accumulated within the lysosomes of cells. They began to investigate several compounds as potential cystinosis treatments. This led to the biggest breakthrough in cystinosis to date (14); It was discovered that the aminothiols cysteamine depleted cystine from cells safely and effectively (15).

Subsequent clinical trials of cysteamine in a healthy human volunteer revealed that liver function tests, haematology and electrolyte balance tests all remained within normal ranges, however an episode of grand mal seizures in the volunteer led to the premature cessation of the trial (15). It was concluded that this was due to the cysteamine directly, as the patient had been treated with 90 mg/kg cysteamine for 4 weeks. Once treatment stopped, the seizures did not return. Although these results indicated a rapid elimination of cystine from the cells, it was concluded that a larger cohort was needed to fully test the new treatment (15). Cysteamine therapy was later found to rapidly deplete leukocytes of cystine, with minor side effects. Almost all of the ocular tissues are treated by the oral administration of cysteamine apart from the cornea, which remains unaffected by systemic treatment due to its avascular nature (12,16). This meant a topical treatment was required for the corneal crystals alone. More details of the ophthalmic symptoms are found in Chapter 4.

Lysosomes were recognised as playing a central role in this disease and, in 1982, Gahl et al and Jonas et al both characterised this further: cystine is transported out of normal lysosomes by a specific carrier system which is defective in cystinotic patients (17,18). However, other amino-acid specific transporters remain intact. Gahl also provided a proof by showing that heterozygotes for the disease take exactly twice as long to clear cystine from lysosomes compared to healthy cells (17). Recently, Gahl has continued this genetic work, and demonstrated that heterozygotes for the disease carry exactly half the number of cystine carriers (5).

The exact mechanism whereby cysteamine depletes lysosomes of cystine was hypothesised by Thoene et al, and finally confirmed in 1985 by Gahl et al; a cysteine and cysteamine mixed disulphide is formed (19). When administered cysteamine accumulates within the acidic environment of the lysosome and forms an intracellular mixed disulphide (cysteine – cysteamine) by a disulphide exchange reaction (figure 1). This molecule can then exit the lysosome and enter the cytoplasm. As a footnote the paper cites Pisoni et al’s work of 1985, describing how the mixed disulphide molecule is structurally similar to Lysine and its corresponding transporter is intact and recognises the molecule, allowing the passage into the cytoplasm (20).

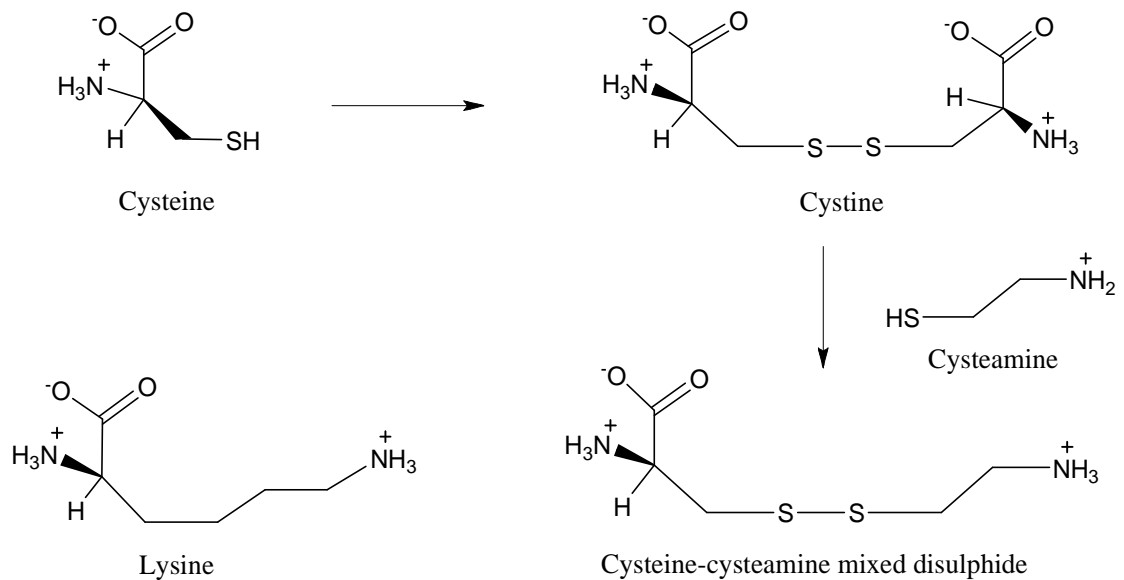


Figure 1. The relationship between cysteine and cystine, and how cysteamine removes cystine from the lysosome.

Cysteamine eye drops were first documented in 1987, when Gahl et al and Dufier et al both reported initial findings on its novel use (16,21). To date the corneal crystals are treated using this topical form of cysteamine eye drops, which must be administered hourly in addition to the oral capsule to achieve the maximum benefit.

In 1987 a study was conducted which investigated the treatment of 93 children with cysteamine. This aimed to elucidate the long term effects of

the drug on the disease and the symptoms, with particular focus on renal function (22). The findings were supportive of previous work in that cysteamine was found to be very effective at depleting intracellular cystine. However this study also revealed the possibility that diligent therapy, if started early enough, could maintain glomerular function at the same level or even prevent the need for renal transplantation completely (22). The study also found an improvement in the growth profiles for the children. This provided a real impetus to provide early diagnosis and treatment as well as reiterating the importance of regular and compliant use. This study concluded that research should continue to develop a more palatable form of cysteamine, and makes reference to phosphocysteamine, a prodrug phosphorothioester, where the thiol group was masked in order to reduce or eliminate the smell and taste.

Phosphocysteamine was investigated for an alternative to cysteamine in 1988, when Gahl et al performed a study comparing the standard treatment cysteamine with the phosphorothioester (23). The smell and taste was also improved and the bioavailability maximised due to reduced protein binding. Phosphocysteamine is a prodrug and therefore it must be de-phosphorylated to be activated. It was hypothesised that this occurred intracellularly, thereby directly targeting the stored cystine. It was concluded that cysteamine and the prodrug, when taken orally, can be regarded as equivalent and should be equally effective for treating cystinosis.

Cystinosis patients are now living much longer because of improvements in treatment, but also have to face the increased likelihood of more varied complications. In 1987 Broyer et al studied 19 patients aged 15-26 years with good graft survival following a kidney transplant and noted their extra-renal complications that have only become apparent recently after an improvement in treatment. They described blindness, hypothyroidism, insulin-dependent diabetes, liver enlargement, hypersplenism, repeat gross epistaxis and encephalopathy, and how these effected the patients (24). This is an added burden to those with the disease and their carers and families, increasing the number of medicines to be taken and time spent

receiving treatment. In 1990 a study revealed the extent of swallowing dysfunction experienced by cystinotic patients, a late complication stemming from a build up of cystine crystals within the lysosomes of muscle cells (25). In a study of 43 patients, 17-79% presented with abnormalities in swallowing. There is a large variation in the percentage as the patients were grouped by age and the complications tend to be age dependant. Difficulties included weakness of the lips and tongue, dysphagia, dry mouth and dysphonia and at least one patient has been recorded to choke and die of aspiration. Apart from continuing cysteamine therapy to try to limit the damage to muscles, the importance of "therapeutic manoeuvres" such as thickening and pureeing food are emphasised in order to limit these deaths.

The importance of early initiation of cysteamine therapy was again reported following two studies conducted in the early 1990s (1,26). The findings showed that in order to prolong life and reduce or avoid complications, therapy should continue after renal transplantation. These conclusions were taken a step further when Gahl, Markello and Bernardini reported that children treated adequately with cysteamine resembled healthy children with respect to height and, remarkably, renal function (27). Predominantly this occurs only when therapy is started early in life, as the kidneys go through a rapid development stage during the first 3-4 years of development. If the kidneys can be preserved of their function during this time, then subsequent renal deterioration will be minimised or even avoided. This of course will only be the case if therapy is administered every 6 hours, every day, for life. These findings demonstrate that if that regimen is adhered to, some children might avoid the need for renal transplantation altogether. The paper concludes with the statement: "Since irreversible kidney damage before diagnosis limits the ultimate benefit of cysteamine therapy, early diagnosis and treatment are critical in this disease". These researchers all come to the same conclusion: diagnose cystinosis quickly and treat effectively to ensure the best possible outcome.

### 1.3 Genetics

Cystinosis is caused by a defect in the CTNS gene. This is a 12 exon gene within 23 kb of DNA which codes for a 367-amino acid lysosomal transport protein called Cystinosin. In approximately 56-76% of white western patients, 12% of Italian patients and 18% of French Canadians, this defect is caused by a 57 kb deletion removing the first 10 exons (28), and is thought to have arisen in Germany in 500 A.D. (29) There are more than 100 known CTNS mutations (5,30). Other originating mutations, W138X and G339R have been identified amongst French Canadians and Amish Mennonites in Ontario (5). One in 150 – 200 people in the USA have a CTNS mutation (5). There are also known genetic clusters in French Canadians, and Brittany in France reports incidence of the disease at one in 26,000 live births (5). The gene responsible for the disease was discovered in 1995 and mapped in 1998 to chromosome 17p13 by Antignac et al, and named CTNS (figure 2) (5,6,31).

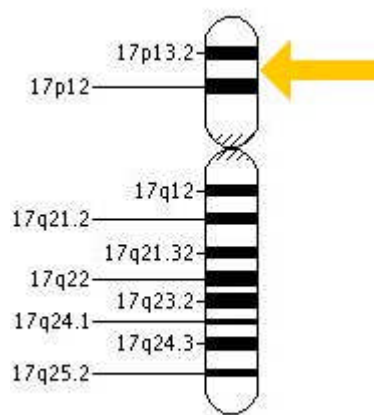


Figure 2. Location of chromosome 17p13 (CTNS), the gene deletion responsible for cystinosis (32).

It was discovered that the locus was deleted in 23 out of 70 patients. This knowledge gives patients the hope of better diagnosis and a genetic cure in the future, although for now cysteamine is the best treatment available. This knowledge also allowed scientists to explore the disease through artificially created cystinotic mice in labs, probing deeper into the mechanisms of cell apoptosis and ultimately widening the platform from which a new treatment or cure will be sought. Prenatal diagnosis is now

possible, as well as diagnosis of the 57 kb deletion (33). If a child is diagnosed with cystinosis, subsequent pregnancies can be tested at 8-10 weeks of gestation with tissue, or at 14-16 weeks with amniotic fluid. The placenta can also be tested at birth for cystine (5).

#### **1.4 Cystinosis pathophysiology**

The amino acid cystine should be transported into the cytoplasm of healthy cells for processing. In cystinosis however, it accumulates inside the lysosomes to 10-1000 times the level seen in healthy cells where it crystallises, causing cell death leading to organ failure (34). This crystallisation is widespread throughout the majority of the tissues and organs in the body. Initially however, it is most apparent in the kidneys and eyes as these organs are more sensitive to cystine accumulation (33). Renal tubules show a characteristic 'swan-neck' deformity (figure 3), which then progresses to interstitial nephritis and necrosis (5).



Figure 3. Image of dissected nephrons from a cystinosis patient, which display a marked narrowing at the start of the proximal section (the characteristic 'swan-neck' deformity) (35).

If left untreated symptomatic deterioration leads to death by the second decade of life (30). At diagnosis, 85% of children with cystinosis are malnourished and classified as failure to thrive due to frequent emesis and false satiety. This lack of appetite is caused by poor eating habits and large liquid intake (5). Table 1 summarises the most frequently seen symptoms, irrespective of age.

Table 1. Summary of the most common symptoms of cystinosis (3).

Organ/system	Common symptoms
Renal	Polyurea Polydipsia Renal failure
Hepatic	Hepatomegaly
Ocular	Photophobia Visual impairment Poor visual spatial processing Blindness
Musculo-skeletal	Muscle wasting Rickets Swallowing difficulties Inter-costal muscle weakness
Reproductive	Hypogonadism Azoospermia
Other	Short stature Diabetes Hypothyroidism Alzheimer's disease Epilepsy

### 1.5 Cystinosis sub-categories

Cystinosis presents as three different forms with varying levels of severity. Infantile cystinosis is the most severe, progressive form comprising 95% of cases. Patients with this form have two severe CTNS mutations (5). Juvenile cystinosis (also known as intermediate or adolescent) is a milder form, with diagnosis in the second or third decade of life. Here patients carry one mild and one severe CTNS mutation (5). Although a milder form, renal failure still occurs. Ocular cystinosis (also called adult or benign) only presents as crystals in corneas and bone marrow, and does not progress to renal failure (5). Patients with ocular cystinosis have one mild and one

severe CTNS mutation, or two mild mutations. In total there are around 40 patients worldwide who suffer from the milder forms of cystinosis, and therefore the focus of this project was on the more severe infantile form (5).

## 1.6 Cysteamine

Cystinosis is treated by the systemic and topical administration of the amino-thiol cysteamine (figure 4). Cysteamine, which is used therapeutically in the bitartrate form as Cystagon™, has been used to great effect since the 1970s and its introduction has completely altered the prognosis of the disease. With early and diligent therapy, cystinosis patients can prevent or delay most of the non-renal complications and extend their lives into a fourth or fifth decade, live independently and even have children (5,36). The renal damage is continuous however, and decline is inevitable (5). The treatment is available as an oral capsule, and also as a liquid eye drop.

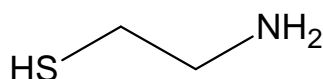


Figure 4. Cysteamine.

Once absorbed after administration, cysteamine enters the lysosomes of cells. Due to the compound's primary amine group and the acidic environment of the lysosome, cysteamine attracts a positive charge and concentrates there (5,37). Within the lysosome it reacts with the trapped cystine, forming a lysine isostere: a mixed cysteine – cysteamine disulphide, which, due to its structural and spatial similarity to the amino acid lysine, can exit through the unaltered transport mechanism for lysine (38) (Figure 1). This mimic can be transported out of lysosomes and into the cytosol of the cell (39). The monomer cysteine can also exit via its specific transporter into the cytoplasm. The clinical endpoint and target for treatment is a blood cystine level of less than 1 nmol per milligram of protein (40).

Through strict and regular use this treatment has been reported to remove up to 95% of the crystallised cystine from cells, and has been known to slow or, in some cases, prevent the development of renal failure (5,7,27,41). Many other extra renal symptoms show benefit from regular, compliant use, such as growth retardation and hypothyroidism (36,42). The likelihood of complications such as myopathy, neuropathy and diabetes mellitus occurring are reduced the longer the patient takes cysteamine (36). The life expectancy of patients who adhere to treatment has now extended to 20, 30 and even 40 years of age, due to the advent of safer kidney transplants and powerful immunosuppressant drugs (43). It is not a cure however; the disease progresses continuously until death, caused in most cases by sepsis or respiratory problems (5).

Continuation of cysteamine treatment post kidney transplant is vital, as crystals continue to accumulate in other tissues and organs (3,36). Although the transplanted kidney would be largely free of cystine crystals, some do accumulate due to invasion by host macrophages (5). As a result of life-lengthening improvements in treatment, the crystals now have more time to accumulate and cause damage in multiple organ systems. Thus a plethora of previously unproblematic complications are now major factors on quality of life, such as generalised muscular wasting leading to swallowing difficulties, corneal and retinal crystals, diabetes, cerebral degeneration and cardiovascular disease (28,44,45). Once patients enter their twenties, the central nervous system begins to show signs of deterioration, and most patients display mental deterioration, pyramidal signs and extreme loss of short-term visual memory (3).

## **1.7 Cystamine**

Research on cystamine (figure 5), the disulphide form of cysteamine, has found that it is almost as effective as cysteamine at depleting cystine from lysosomes, in every tissue apart from the cornea (5,29,37). This is contradictory to previous reports. Although it is known that cystamine is reduced to cysteamine in vivo, this cannot happen in the corneal tissues.

The reason for this is most likely to be extracellular crystals, which may have become extracellular by extrusion or through cell death. These crystals do not exist in an acidic environment like those inside lysosomes, which attract cysteamine, and trap the molecule by addition of a positive charge (37). Therefore cysteamine remains oxidised in the cornea, and also does not concentrate within a certain organelle.

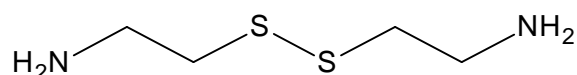


Figure 5. Cysteamine.

Cysteamine also has proven benefits in the treatment of neurodegenerative diseases such as Parkinson's, Alzheimer's and Huntington's Disease (HD) (46-49). By converting to cysteamine in vivo, the anti-oxidative properties have been shown to prolong the life of HD-transgenic mice (50).

### **1.8 Problems arising from cysteamine treatment**

Cysteamine causes a range of side effects, largely due to the high dose which is required. High blood levels of cysteamine must be achieved as much of the drug is lost to first-pass metabolism (36). A large proportion of the administered drug will also bind to circulating proteins and cannot be absorbed (40,47). Neutral and acidic drugs bind to albumin which is basic, while basic drugs bind to glycoproteins in the blood.

The cysteamine treatment regime for cystinosis is a lifelong commitment. Patients should aim to take their oral dose at regular 6-hour intervals for the treatment to work effectively. The plasma half-life of cysteamine is 1.88 hours (33), with blood levels peaking at 1h, and rapidly declining thereafter (5). This requires a nightly oral dose, which affects the quality of life of patients and families (36). The cysteamine eye drops have a very short residence time and require application every hour whilst awake (51-53). The drug also has a foul taste and smell akin to rotten eggs, which regularly induces vomiting after ingestion (36). In approximately 10-15%

of patients this can be severe enough to halt therapy (5). Cysteamine and its malodorous metabolites are subsequently excreted in breath and sweat. This can be a major barrier to compliance, especially when the child enters education. Cysteamine also has the potential to cause potentially serious stomach irritations, with 97% of patients reporting gastrointestinal symptoms (54,55). In many patients this can be severe enough to significantly limit therapy (56). It is caused by a combination of gastric acid hypersecretion, reverse peristalsis and bile reflux. These factors, coupled with delayed gastric emptying and reduced mucus and bicarbonate production, causes gastric ulcers and nodules (42,57). All of these gastric symptoms must be treated rigorously with proton pump inhibitors. Compliance can therefore be a major barrier to effective treatment, leading to significant morbidity.

### **1.9 Other barriers to effective treatment**

Cystinosis patients receive other medication and electrolyte treatments in addition to cysteamine therapy. Patients must also receive potassium, bicarbonate, calcium, vitamin D and phosphate for treatment of rickets and Fanconi syndrome. Carnitine is frequently deficient in patients with kidney disease, and is required for muscle function. Sodium excretion is normally only 2-3 mg/kg/day, but in cystinosis patients this can be as high as 13 mg/kg/day. As a consequence, patients crave salty foods, and should be allowed free access to these (43). Saline supplements may also be administered if necessary. Patients with cystinosis frequently receive Indomethacin, which acts in two ways. By sensitising the kidney to antidiuretic hormone and thereby lowering the glomerular filtration rate, water losses can be reduced. Consequently, the urinary losses of salts is reduced, relieving the polyurea and polydipsia, increasing the appetite, energy and overall well-being (5). Although this therapy can reduce salt excretion by 20-30%, these supplements have a strong potential for causing gastric ulcers (56). Indomethacin and salt administration can be enough to boost growth after diagnosis; however growth hormone is frequently administered before patients enter puberty, in an attempt to

achieve a normal adult height. Sex hormones can also improve height if administered, in addition to producing secondary sexual characteristics. Patients must also be encouraged to drink water continually.

Growth in infancy is dependent upon nutrition, and the maximum growth velocity is seen between birth and 12 months. Parents should therefore be counselled on diet, and advised to aim for 60% carbohydrates, 10% protein and 30% lipids with a view to gaining weight (5,6). Anti-rejection treatments are always given after transplantation, and these can introduce new problems such as recurrent infections and Cushingoid effects (28). Studies have shown that 50% of all 10-year old cystinosis patients are hypothyroid (5).

Compliance with these additional treatments in combination with adequate cysteamine therapy can lead to a normal growth rate (5). The maintenance dose of cysteamine for children under the age of twelve or weighing less than 50 kg is 60-90 mg/kg/day in divided doses, every 6 hours. The typical adult dose is 500 mg every six hours but can be as much as 750 mg (4).

### **1.10 Economical considerations**

A study was conducted in 1997 to examine the cost-effectiveness of cysteamine as a treatment for cystinosis (58). As patients requiring Cystagon™ are few in number, pharmaceutical companies can be reluctant to pursue a drug which provides little return on their efforts. The American study reported that cysteamine treated patients have a median renal survival time of 15 years as opposed to 10 years without the treatment. However, the levels of compliance with therapy were not taken into account and so this should be seen as a conservative figure. Patients receiving therapy before renal failure occurs were found to incur \$234,000 of lifetime costs, while those not receiving treatment were estimated at costing \$238,000 each. The report also produces figures that support the use of cysteamine post transplant. Additional lifetime costs would be \$27,000 at low levels, and \$17,256 at high levels of efficacy in delaying renal failure.

The authors of this study admit that these figures are conservative, and yet still produce a convincing argument for the use of the drug.

### **1.11 Recent advances**

Until recently, the mechanism by which cystine crystal accumulation resulted in widespread apoptosis and organ failure was unclear. The cause of such renal sensitivity was also unknown. It is now believed to be caused by a synergistic failure of intracellular organelles, particularly involving abnormal mitochondria and elevated Reactive Oxygen Species (ROS) production, which gives rise to widespread apoptosis (39). Autophagy also appears inhibited and this, coupled with a lack of ATP production, is thought to cause particular damage to the kidneys (39). The damaged tissue is then replaced with fibrous tissue (5).

More recently, it has been demonstrated that early diagnosis and initiation of confluent therapy can salvage kidney function; for each month of treatment the patient receives before the age of 2 years approximately 14 months of subsequent kidney function is retained (5), while some later complications may also be avoided or delayed.

Cysteamine was found to be teratogenic and fetotoxic in 1998, and hence is not recommended during pregnancy or nursing (33). This is thought to be due to the generation of hydroxyl radicals (56). Patients hoping to conceive are advised to suspend cysteamine therapy during gestation and nursing, which carries risks to the patient.

A new side effect of oral cysteamine has recently been reported, and appears to be linked with higher than recommended doses when administered over time. Lesions on the elbows and knees similar to Ehlers-Danlos syndrome have been reported, as well as bone lesions. This is seen primarily in patients who are receiving three larger than recommended doses per day, instead of the typical four times a day regime (59). This is

frequently done in an attempt to achieve normality and stability in the patient's routine. Symptoms always resolve after dosage reduction.

Researchers working at King's College in London recently made a breakthrough in renal transplantation. If an organ to be transplanted is washed out with an engineered drug solution before transplantation, graft survival time can be doubled (60). Currently, less than half of all transplanted kidneys are still functioning after ten years. The new drug solution also maintains the kidney more effectively during transit from donor to recipient, allowing these kidneys, which would have previously been disregarded for transplant, to become useable thus increasing the amount of potential donor organs available. This drug solution is hoped to reach the market by 2015 (60). Cystinosis patients generally experience better graft survival compared to primary kidney diseases; after ten years, 90% of transplants are still functioning (27,28).

### **1.12 Alternative routes**

Cysteamine has been used intra-venously for long-term treatment of cystinosis on only two occasions. Therapeutic levels were established at 6mg/kg every 8 hours, with a maximum of 40 mg/kg in 24 hours (56), where the typical oral requirements are 60-90 mg/kg a day. It has been reported that a single IV dose kept cystine levels at a therapeutically acceptable level for 24 hours (15). This is probably due to the avoidance of the first-pass effect. This has led researchers in San Diego to develop an enteric-coated form. This is achieved by spray drying the drug with vegetable fat. Early in 2007 Schneider and Dohil logged a patent for "Enterically coated cysteamine, cystamine and derivatives thereof" (61). This was achieved by coating commercially available cysteamine bitartrate with the polymer Eudragit<sup>®</sup>, to allow dispersion only at pH 5.5-6 (36). In 2006 the University of San Diego published findings from research which formed the foundation for the patent idea in which cysteamine was administered to three different areas of the gastrointestinal tract via a naso-enteric catheter (47,62). The small intestine was found to absorb the drug

in the most effective manner, as well as producing the greatest cystine depletion when compared to the stomach and colon. After the patent was logged a one-year trial of the form was commenced.

Trials of this new formulation have demonstrated that the enteric-coated form has equivalent efficacy to 6-hourly Cystagon™ when given twice a day (36). In addition, a reduction in dose of 40% was achievable, allowing relief from side effects. However, some patients experienced erratic cystine levels, and the cause of this was unclear. A twice-daily administered capsule at 60% of the current dose has demonstrated efficacy in maintaining cystine levels at the target level during a small clinical study involving five cystinosis patients, although two of the children still required acid suppression therapy (36,63). One patient maintained target cystine blood levels for 15 hours, while another maintained these levels for 24 hours. The capsules contain coated microbeads, allowing sprinkling onto food and the avoidance of swallowing large capsules. Phase 3 clinical trials began in July 2010 and are still ongoing, comparing the new formulation against Cystagon™, but it is hoped that this new capsule will replace and improve upon the current oral treatment (36).

Developing a form of cysteamine with a gastro resistant coating may be one step towards a better side effect profile for the drug, and may relieve some of the troublesome symptoms associated with it. The researchers believe that a controlled release preparation targeted directly to the small intestine will lessen the dosing frequency and thereby improve quality of life. This is the latest finding in a line of gastric research at the University of California, San Diego, and will hopefully produce results which are of relevance to this research project (63).

Bone marrow cell transplantation is used in other LSDs such as Hurler disease and adrenoleukodystrophy (ADL), to slow or prevent disease progression, and has recently been investigated for cystinosis (3,64). Post-transplant, the cystine content in the kidneys was reduced by 70%, with improved renal function and normal serum urea and creatinine levels. The transplanted cells were also found in other tissues, including eye, brain and

liver, and in all organs the cystine content was reduced (3,64). Delivery of the CTNS gene directly into organs has also been trialled but with limited success (3). Cystinosis cannot be excreted by cells, and therefore, while the local delivery of an enzyme can greatly improve other LSDs, cystinosis requires the integration of cells with the functional protein (3).

Prodrugs have been used effectively for other diseases and are also being investigated for cystinosis. Prodrugs are inactive upon administration and become activated once metabolised by the body. Examples include 5-Fluorouracil and Sulfasalazine. They are particularly effective with foul-tasting drugs. Researchers at Robert Gordon University and Sunderland University are developing and testing forms which mask the taste and increase the potency of the current drug, with a potential reduction in unpleasant side effects (52,65). In addition, these prodrugs have been designed to release multiple cysteamine compounds once activated, allowing lower doses to be administered. These experimental compounds have proven non-toxic and efficient at depleting cystine (66-68).

### **1.13 Aims of the project**

The current oral and ophthalmic treatment for cystinosis often meets with resistance from patients. A combination of the drug's putrid taste and gastric side effects, as well as a demanding dosage regime results in frequent non-compliance. A sulphurous body odour post-administration is also very unpleasant. This is highlighted during infancy and puberty, when compliance is particularly low (4). A study by the World Health Organisation has shown that compliance with chronic medication as prescribed is generally around 50%, regardless of the disease, the age of the patient or the location in the world (69). Refusal of medication is a serious barrier to effective treatment and avoidance of morbidity and mortality. Studies have shown that strict compliance with cysteamine can drastically improve long-term outcomes, and may delay or prevent the need for renal transplantation (2,58). This has led to several alternative therapies being investigated, including IV administration, stem cell and

bone marrow replacements, pro-drugs and lipophilic derivatives of cysteamine (42).

Formulation science may provide a way to improve the current medication, significantly improving the lives of sufferers and those who care for them. By reducing the taste and frequency of administration through alternative dosage forms, ease of administration of cysteamine could be improved. The main aim of this project was to develop alternative formulations of cysteamine which could reduce or eliminate some of the side effects which are evident using the current oral capsule and ophthalmic eye drop, thereby improving the quality of life for those affected.

There were three areas of focus for the delivery of cysteamine; rectal, ophthalmic and pulmonary. Administration of cysteamine via the rectum should reduce or eliminate the first-pass metabolism by the liver, allowing a smaller dose to be given daily. This will eliminate the gastric irritation currently seen with the oral capsule, avoiding the taste, smell and subsequently reducing the body odour. It will also be a useful dosage form in paediatric treatment of cystinosis and when the oral route is compromised.

By formulating cysteamine as a bioadhesive ophthalmic gel with controlled drug release, it is hypothesised that administration frequency will be greatly reduced, allowing once or twice-daily dosing instead of the current hourly requirement. In addition, the gel will be pH neutral to eliminate the stinging associated with the current eye drop, and the rheology will alter to reflect the situation in the eye. This should allow pain-free blinking, without the gel flowing out of the eye. These formulation changes should reduce the burden of treatment and improve compliance, producing long-term prevention of ophthalmic morbidity such as blindness.

Delivery of biodegradable polymer-coated cysteamine microspheres to the respiratory tract will eliminate the foul taste and smell along with the gastric symptoms experienced at present. A smaller dose may be permissible due to the avoidance of the first-pass effect. It may also open the possibility of

sustained release, allowing a reduction in the six-hourly recommended dosage with the oral capsule.

The central objective was to improve upon the dosage forms in which cysteamine is currently administered to infants and young children, and eliminate or reduce the side effects commonly experienced with the oral capsule and eye drop. It was hypothesised that these new formulations might, in turn, lead to increased compliance through puberty and into adulthood, and subsequently reduce morbidity and mortality in the latter stages of the disease.

In addition, there may be the possibility of incorporating other drugs into the ophthalmic gel base, allowing versatility for a range of eye diseases which require chronic medication such as glaucoma and dry-eye syndrome. As cysteamine also has a potential benefit in the treatment of Alzheimer's and Huntington's diseases, there may also be a wider-reaching benefit to those patients in the future.



## **Chapter 2 – Analytical methods**

## Chapter 2 – Analytical methods

### 2.1 Introduction

Cysteamine does not possess a UV-active chromophore. Therefore, to enable UV detection, the molecule requires either derivitisation or to be tagged by a UV-active agent. Two separate methods were used to detect cysteamine in this project; conjugation with phenylalanine (derivitisation), and the use of thiol detector DTNB (tagged). The use of DTNB was preferable, as the chemical and physical properties of cysteamine were unaltered.

### 2.2 Phenylalanine conjugate synthesis

Cysteamine and cystamine do not possess a chromophore and therefore are UV transparent, thus monitoring their release from formulations is very difficult. A phenylalanine conjugate (phe conjugate) was developed to 'light-up' the molecule, allowing quantitative determination of release of the active from the dosage form via UV spectroscopy (Figure 6). Cystamine, the disulphide of cysteamine was used in the synthesis. This was used to avoid the use of protecting agents for the thiol group and concerns about its oxidation.

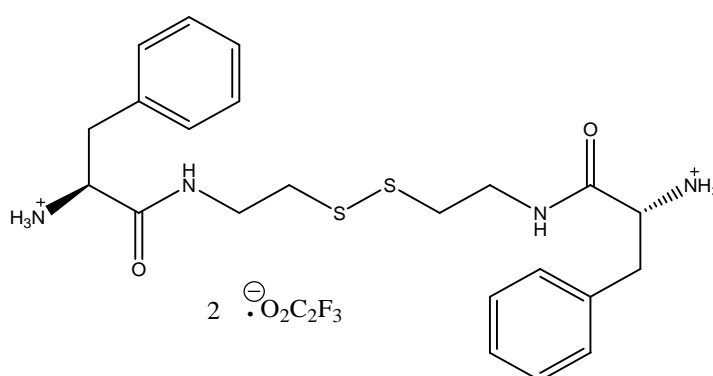


Figure 6. Phe conjugate

Cystamine dihydrochloride was reacted with two equivalents of 1,8-diazabicycloundec-7-ene (DBU) in dichloromethane (DCM), converting the cationic tertiary amino groups to primary amino groups. Two equivalents of

Boc-L-phe N-hydroxysuccinimide ester (Boc-Phe-OSu) was added to the stirred solution. The amino terminal is tBoc protected and the carboxy terminal is activated as the OSu ester. Deprotection was achieved by stirring in trifluoroacetic acid (TFA). The resultant gum-like solid was triturated with ethanol, followed by drop wise addition of diethyl ether to yield the final experimental compound (figure 7). More details can be found in the experimental section, appendix I.

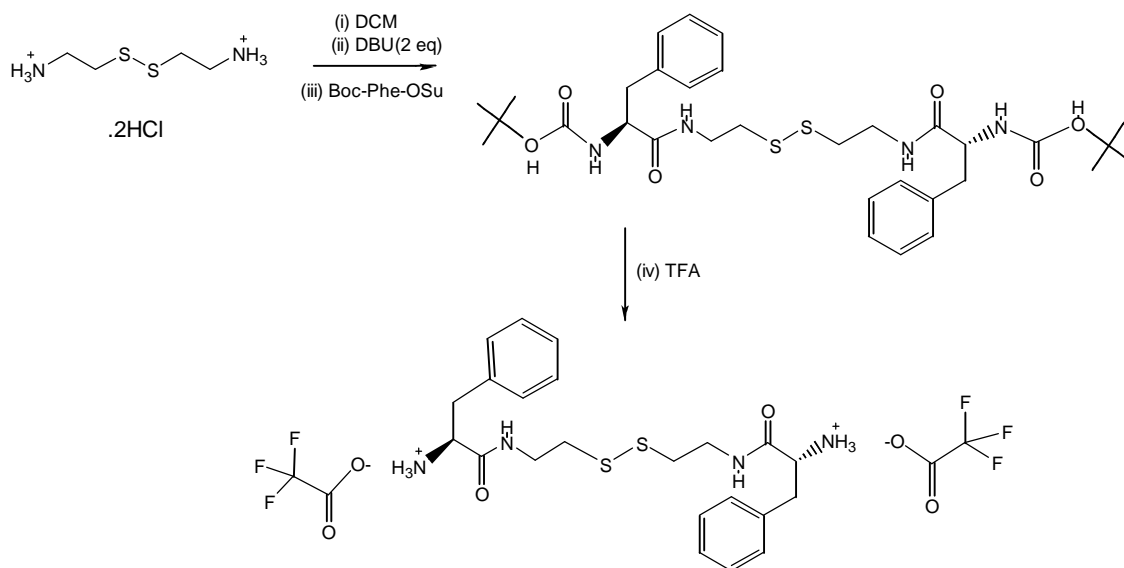


Figure 7. Synthesis of the phe conjugate.

The compound was fully characterised by <sup>1</sup>HNMR and Mass Spectroscopy. The presence of a doublet centred at 3.1 ppm represented methylene protons of the phenylalanine residue. There were also characteristic aromatic signals centred around 7.35 ppm which corresponded to the phenyl ring of the phenylalanine residue. The multiplets centred at 2.64 and 3.39 ppm represented the methylenes of the cystamine residue. All remaining protons were fully assigned (appendix I). The electrospray mass spectrum had a base peak at m/z 453.2 (100%), which corresponded to the molecular mass of the phe conjugate.

The UV absorbance lambda max, the wavelength at which most light is absorbed, was analysed in triplicate, and found to be at 256 nm for the phe conjugate (figure 8). Using three sets of standards at known

concentrations, linear regressions were produced in triplicate and used to quantify the release from formulations (figure 9).

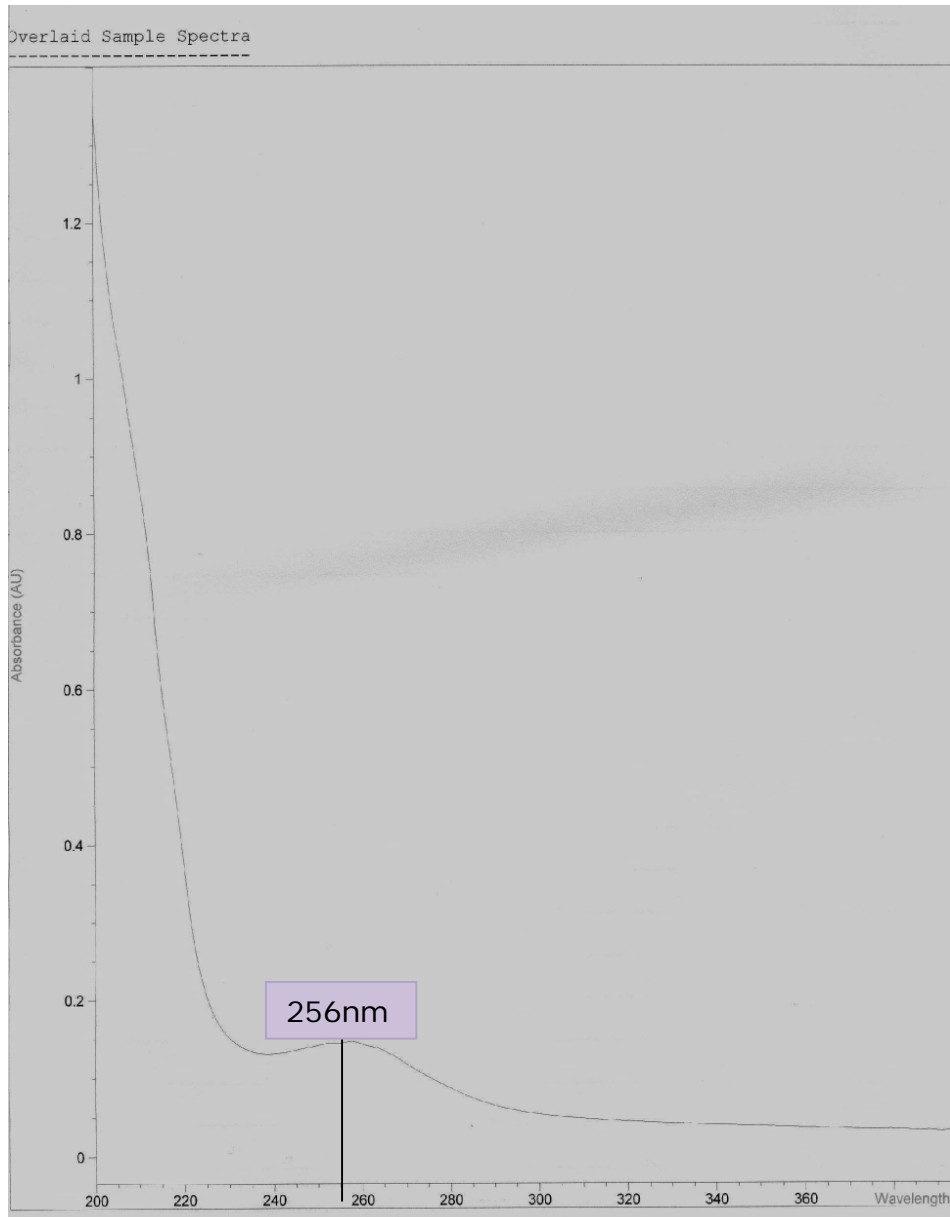


Figure 8. A scan of UV absorbance highlighting the lambda max for phe conjugate.

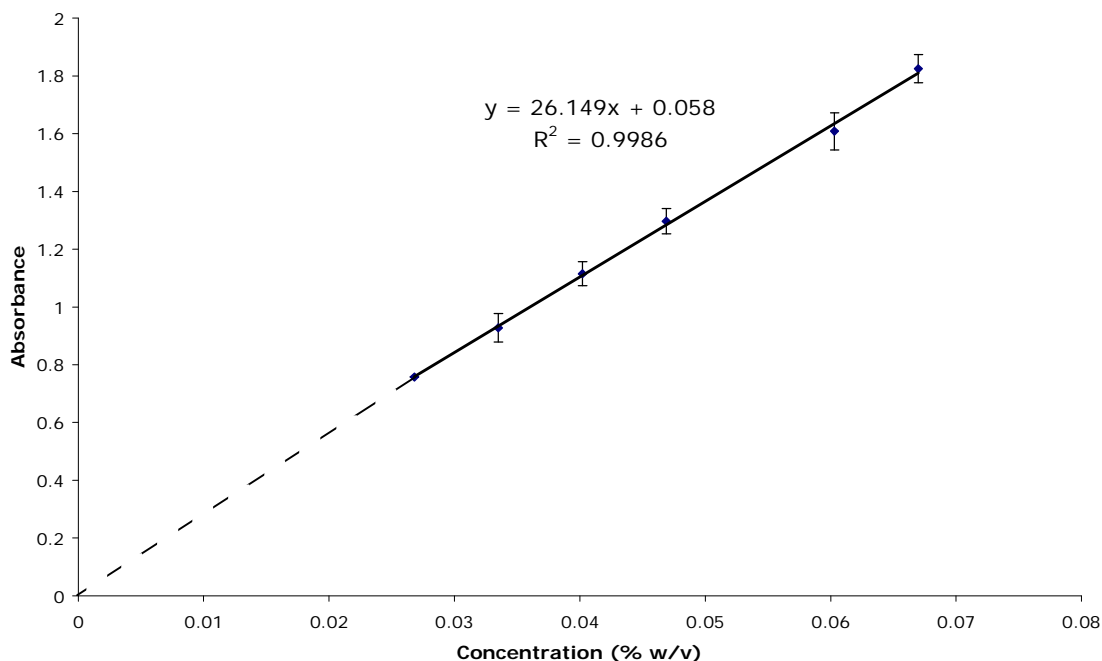


Figure 9. Linear regression produced for the phe conjugate, with the corresponding correlation coefficient.

### 2.3 Partition coefficient studies

The cornea is composed of three alternating hydrophilic and lipophilic layers, thus any drug targeting the tissue has to be partially soluble in both. Three different software applications were used, in triplicate, to calculate the partition coefficient values for cysteamine and cystamine from the chemical structure, including Chemdraw software (Chemsoft, Cambridge, England). The calculated value was found to be -0.47 and -1.59, respectively (70,71). A partition coefficient value of less than zero is relatively hydrophilic, while a value of 10 is very hydrophobic (71). These values indicate suitability for ophthalmic delivery, due to both compound's solubility in both oil and water phases.

Using a standard method, the partition coefficients of cysteamine and phe conjugate were determined experimentally (72). Chloroform was used as the oil layer instead of Octanol, as it has a much lower boiling point and is easier to evaporate than Octanol (73). Both water and Simulated

Lachrymal Fluid (SLF) buffer at pH 7.4 were used as the aqueous layer. The buffer represented aqueous compartments within the body (74). Each test was performed in triplicate (table 2). The partition coefficient of cysteamine was found to be -0.32 for water and -0.47 when buffer was used, which were both similar to the calculated value. This is an ideal value for ophthalmic delivery due to the balance between lipophilicity and hydrophilicity. The partition coefficient for phe conjugate was -1.89 with water and -0.16 with buffer as the aqueous layer.

Table 2. Summary of the experimentally obtained partition coefficient values (n = 3).

Drug (aqueous/organic phase)	Average partition coefficient ( $\pm$ SD)
Cysteamine (water/chloroform)	-0.32 ( $\pm$ 0.14)
Cysteamine (buffer/chloroform)	-0.47 ( $\pm$ 0.12)
Phe conjugate (water/chloroform)	-1.89 ( $\pm$ 0.25)
Phe conjugate (buffer/chloroform)	-0.16 ( $\pm$ 0.11)

## 2.4 Ellman's reagent

The lack of a chromophore in both cysteamine hydrochloride and cysteamine bitartrate makes the use of Ellman's reagent necessary. By addition of this compound, the release of these drugs from formulations can be measured. Ellman's reagent, also known as 5,5'-dithiobis(2-nitrobenzoate) (DTNB), is a disulphide which readily reacts with free thiols to form a mixed disulphide (75). The colourless DTNB forms a mixed disulphide compound with the thiol of interest, cysteamine in this case, which in turn releases a molecule of thionitrobenzoic acid (TNB) (Figure 10). Measurement of TNB can be used to assess the quantity of thiol present in a sample as the stoichiometry is 1:1 (75). The yellow-coloured TNB molecule has an absorption maximum at 440 nm (76,77).

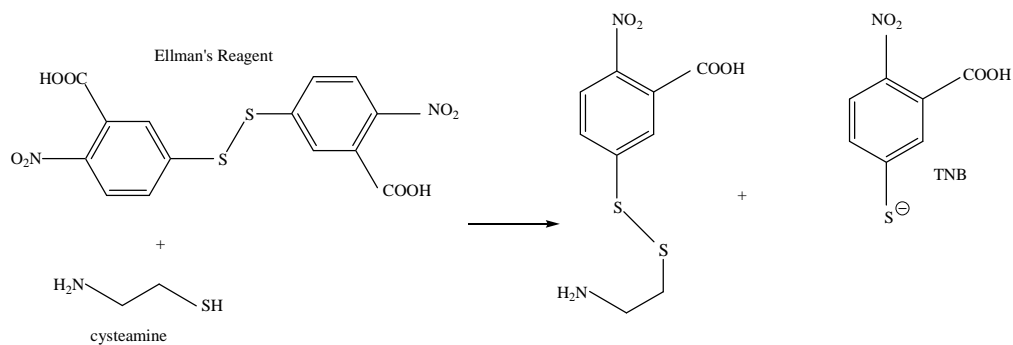


Figure 10. The mechanism of TNB release.

By equimolar addition of Ellman's reagent to the dissolution media, samples can be analysed in a UV spectrophotometer, and the results inserted into a linear regression equation (figure 11).

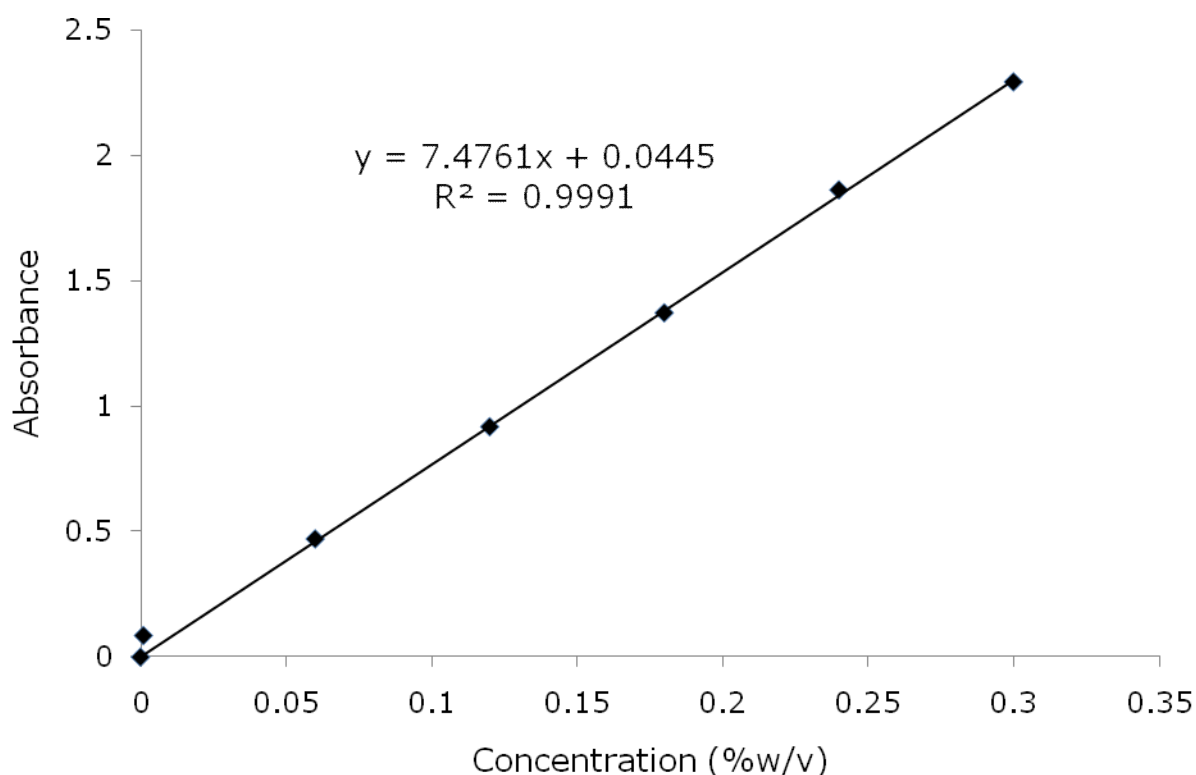


Figure 11. A plot of concentration versus absorbance for a series of DTNB solutions.

DTNB is sensitive to light, and therefore the reaction was undertaken in a darkroom. The disulphide is susceptible to photolysis (being broken down by light) when in solution, particularly when exposed to natural light (78). The reactive TNB species is unaffected by light however (figure 10).

Daylight is intense at around 325 nm, a wavelength at which Ellman's reagent is particularly sensitive, whereas fluorescent light is less intense at this wavelength (78). All reactions using DTNB were performed either in a darkroom devoid of any natural light and with minimal artificial light, or in low light levels using aluminium foil to fully enclose reaction vessels.



## **Chapter 3 – Rectal formulations**

## **Chapter 3 – Rectal formulations**

### **3.1 Introduction**

Suppositories were initially investigated to improve upon the current oral capsule treatment for cystinosis. Suppositories are frequently overlooked as a drug delivery system, consisting of around 1% of all formulation types in both the US and the UK (74,79). However, they can avoid many of the problems encountered with the oral route of delivery. They may also be beneficial for treating conditions in infancy, when capsules are difficult to administer, or when the oral route is compromised.

#### **3.1.1 Suppository history**

The earliest recorded use of suppositories was in 1550 BC, which has been documented in ancient Egyptian papyrus records (79). Local and systemic conditions were treated, using base ingredients such as wax or lard, very similar to those used currently. During the early 1700s, the liquid bases cocoa butter and glycerin were used, introducing a need for suppository moulds which were first manufactured in 1874. The moulds in general use today for small batch manufacturing are almost identical to those first pioneered (79). More recently, suppositories have been manufactured in plastic moulds, which also functions as packaging (80). Examples of commonly used suppositories include bisacodyl for constipation, ondansetron for nausea and vomiting, and diclofenac for pain relief.

#### **3.1.2 Rectal anatomy and first-pass effect**

First pass metabolism can greatly reduce the bioavailability of an orally administered drug, before it reaches the systemic circulation (81). Enzymes present in the gut and liver metabolise the drug, significantly reducing the concentration before the systemic system can be reached. There are several ways to avoid the first pass effect, including the buccal

and sublingual routes, however the malodorous and irritating nature of cysteamine makes these routes unsuitable. The rectal route of administration can largely avoid the phenomenon of first-pass effect. This results from one of the three rectal veins draining into the hepatic system, while the middle and lower veins bypass this and drain directly into the systemic circulation (Figure 12). If the suppository is positioned correctly, the drug should not be subjected to the first pass effect. This potentially allows a smaller dose to be administered, thereby reducing or eliminating some of the unpleasant side effects.

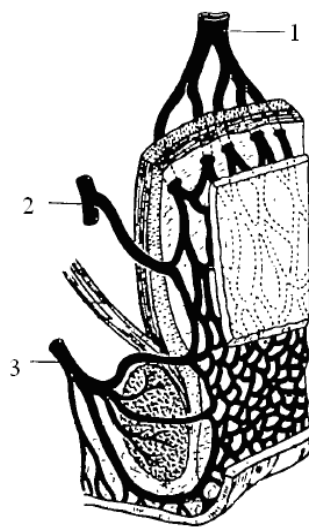


Figure 12. A diagram of the three rectal veins: 1. superior rectal vein, 2. middle rectal vein, 3. inferior rectal vein (82).

In order to ensure accurate placing within the rectum, patients should be counselled upon receiving the suppositories. The following instructions are general for all suppositories:

1. Lie down on the left side, with the upper leg bent.
2. Once the packaging has been removed, moisten the suppository with water, if required.
3. Gently push the suppository into the rectum a finger's depth, at an angle towards the belly button, so that it is directly in contact with the rectal wall.

4. Remove the finger, and hold together the buttocks until the urge to defecate ceases.
5. Try to retain the suppository for at least 20 minutes after insertion by limiting mobility (79).

### **3.1.3 Second-generation suppositories**

Suppositories have long been recognised for their advantages over the more traditional oral route, and this is illustrated to some extent in the paper by Hermann published in 1995 (83), which reported on the potential for the sustained release of drugs from suppositories. This research also demonstrated that suppositories can be extremely useful as a dosage form and perhaps more beneficial than tablets in certain circumstances. Unfortunately, due to a cultural reluctance to accept and regularly use these dosage forms, particularly in Japan and certain Western cultures, potential benefits are being shunned in favour of an easy-to-swallow tablet or capsule (74,79). In the USA, less than 1% of drugs are manufactured as suppositories, whereas in Germany suppositories may make up as much as 5% of the market (79). Rectal formulations are useful tools, particularly in a case such as this where the taste and side effects renders the task of swallowing a tablet very unpleasant and foreboding (84,85). This is especially true if the suppository is modified from a solid to a semi-solid, to make it even more comfortable and bring even greater advantages to the patient. Such an improvement exists with in situ gelling forms.

### **3.1.4 In situ gelling suppositories**

Research on the applications and benefits of in situ gelling suppositories began in the last few years of the 20<sup>th</sup> Century. Various active compounds have been used and tested, but the fundamental formulation technology is consistent. During 1998 and 1999, work undertaken by Kim et al vastly expanded knowledge of these forms, through tests on propranolol and acetaminophen in situ gelling mucoadhesive suppositories (84,86-89). The

research reports on the benefits of these forms when compared to conventional suppositories; the avoidance of the first pass effect and a reduction in discomfort (86). However, the work also highlights the limitations of in situ gelling suppositories such as the possible spread to the colon leading to drainage into the hepatic portal vein (86). These suppositories can be modified from a liquid form to an in situ gelling form, to improve their function further, through the inclusion of a bioadhesive component (88). The suppository can then be administered as a liquid which gels with the heat in the rectum, reducing spreading and maximising bioavailability. This work produced a form which gelled at 37°C, was retained in the rectum and stayed present for up to 6 hours (88). The in situ gelling suppository also displayed an appropriate gel strength and bioadhesive force, demonstrating the potential benefits for human use (87). Kim et al then incorporated propranolol into the formulation, using the same liquid suppository technology as before (89), although comparing different mucoadhesive polymers such as HPC, PVP and sodium alginate. The preparations which included sodium alginate and polycarbophil demonstrated a 71% and 68% increase in bioavailability respectively when compared to conventional suppositories. In addition, some important findings with regard to rectal irritation by mucoadhesive polymers are discussed; it was found that sodium alginate, when used alone, did not irritate the rectal lining, although all others studied were found to increase the proportion of severely damaged epithelium. This issue is a potential concern as the form is in constant direct contact with the mucosal membrane, and is also for a lifelong treatment regime. Kim et al made strong arguments for the use of the novel systems, and the results further enhanced their hypothesis (88).

### **3.1.5 Cysteamine suppositories**

Van't Hoff was the first to deliberate on the possibility of delivering cysteamine as a rectal formulation for the treatment of cystinosis (90). Eight patients with cystinosis were each given cysteamine rectally as a gel in a study conducted at Guy's Hospital in London in 1991. In three younger

children the form was well tolerated, although it caused defecation 30 minutes after the dose was administered to three older children. None of the children suffered diarrhoea, vomiting or rectal bleeding during the study. There was also a dramatic decrease in the odiferous smell of thiol on the patient's breath. After the trial, however, it was reported that two out of three patients stopped the rectal dose and recommenced the oral form, one because of diarrhoea and the other experienced minor rectal bleeding. Other problems were a reduced absorption compared to the oral route and importantly, no significant effect on the mean cystine leukocyte concentration. The authors concluded that this was caused by the expulsion of the doses after 30 minutes (90). However, the parents felt that compliance, including that for other medications and treatments had improved, due to less vomiting along with greatly reduced smell and taste. Van't Hoff and his team concluded that rectal cysteamine was feasible and safe (90).

### **3.1.6 Suppository bases**

The ideal suppository base should be: solid at room temperature, rapidly melting once inserted in the body, compatible with active components, non-irritating and stable (80). There are several commonly used bases, four of which were investigated in this project.

#### **3.1.6.1 Polyethylene Glycols**

Polyethylene Glycols (PEGs) were introduced in 1937, and are still widely used today (79). They are water-soluble polymers of ethylene oxide and water, and are available in a range of molecular weights, each having corresponding melting points (figure 13). The numerical component of their name refers to the average molecular weight of the polymer. Lower weight PEGs such as PEG 100 are clear liquids at room temperature and higher weights such as 8000 are white, waxy solids. PEGs of different molecular weights can be blended together to produce a water-soluble suppository

base with the required physical characteristics, and this makes PEGs a popular choice for suppositories. When formulated as a suppository, the PEG base is dissolved into the rectal fluid, allowing the active ingredient to be released. Diffusion through the rectal epithelium and into the plasma occurs across the concentration gradient (79).

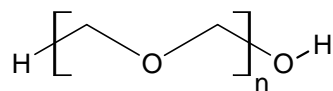


Figure 13. Molecular structure of polyethylene glycol, where n = number of repeating subunits, e.g. n = 34 would produce PEG 1500.

Local irritation is a potential side effect of chronic suppository use but this can be reduced by moistening the form with water prior to insertion (79). Hyperemia has also been reported with the chronic use of PEG-based suppositories (91).

### 3.1.6.2 Witepsol

Witepsol is a fatty suppository base, composed of triglycerides of saturated vegetable fatty acids (C12-C18), with varying proportions of monoglycerides (79). There are many different grades available. The grade used in this project is Witepsol W35, which has a melting range of 33.5 - 35.5°C. It is white and odourless. It is used in the manufacture of Gyno-pevaryl 1<sup>®</sup> pessaries for the treatment of fungal infections, and Anodesyn<sup>®</sup> suppositories for the treatment of haemorrhoids (74).

### 3.1.6.3 Gelucire

Gelucire is composed of glycerol esters of saturated C12 - C18 fatty acids. Gelucire is available in a wide range identified by melting point and hydrophilic-lipophilic balance (HLB). It has many uses depending on these values, including bioavailability enhancer and controlled-release agent.

Therefore the grade used in this project Gelucire 39/01 has a melting point of 39°C and an HLB of 1, which is hydrophobic in nature (92). Gelucire is sold under the trade name Suppocire<sup>®</sup> for the formulation of suppositories (93).

#### **3.1.6.4 Poloxamers**

Poloxamers are versatile non-ionic block copolymers, composed of a central poly(propylene oxide) backbone chain, with a poly(ethylene oxide) chain down each side. They have been used as surfactants and as cell culture media (94,95). The Poloxamer grades F68 and F127 were used in this project; the 'F' denotes the form at room temperature (flakes), while the first two digits, when multiplied by 100, gives the approximate molecular weight of the poly(propylene oxide) component. The final number, when multiplied by ten, gives the percentage of poly(ethylene oxide) content. Poloxamers have been investigated as liquid suppository vehicles for paracetamol and diclofenac sodium (96,97).

### **3.2 Materials and methods**

#### **3.2.1 Materials**

Cysteamine hydrochloride and Polyethylene Glycol grades 400, 600, 1000, 1500, 3000, 4000, 6000, 8000 and 14000 were obtained from Sigma. Witpsol W35 was obtained from Gattefosse (St-Priest, France). Gelucire 39/01 was purchased from Sasol GmbH (Witten, Germany). Poloxamers F68 and F127 were purchased from BASF SE (Ludwigshafen, Germany). DTNB was purchased from Molekula (Gillingham, UK). Tris buffer and Tween 80 were purchased from Fisher. Phe conjugate was manufactured as outlined in Chapter 2.

### 3.2.2 Suppository manufacture

To allow for wastage, the weight of eight suppositories was calculated for a six-form, nominal 1g mould. The calibration value was calculated for each mould, and the displacement value was calculated for each drug. The bases were weighed out accurately on a Mettler AE50 analytical balance, along with the active (Ohio, USA). The bases were heated and blended together, before addition of either cysteamine hydrochloride or phe conjugate. This mix was then thoroughly stirred. The resultant liquid was poured into the mould and allowed to cool. The tops were then trimmed with a spatula, and the final forms removed from the mould, bottled and labelled (74). The surfactant Tween 80 was used in some formulations to ensure the fatty bases were sampled accurately from the dissolution media.

The suppository bases gelucire, witepsol, PEG and Poloxamer were investigated; both lipophilic and hydrophilic bases and also blends were examined for optimum characteristics. As 10 mg/kg was used for previous rectal delivery of cysteamine hydrochloride, the concentrations 30 mg and 60 mg were used as nominal values (90). Until further tests are carried out in vivo, the correct dose cannot be determined. These initial studies demonstrated that the bases can tolerate varying drug loading. The characteristics of all suppositories made are summarised in appendix II.

Suppository hardness was tested on an Erweka TBH28 hardness tester (Heusenstamm, Germany). A result of at least 1.8 – 2 kg is considered acceptable for suppositories (79). If the inert suppository blend produced unsatisfactory results, no further testing was performed. The suppositories with the best characteristics based on appearance, hardness and dissolution tests were selected for further testing (Table 3). The final three suppositories selected for further characterisation were blend 17 hereafter designated "A" (40% PEG 8000, 60% PEG 600), blend 10 ["B"] (40% PEG 14000, 60% PEG 600) and blend 1 ["C"] (PEG 1500). The lipophilic bases Gelucire and Witepsol demonstrated complete melting within two minutes, increasing the risk of drug loss through expulsion and were therefore eliminated from the study.

Table 3. A summary of the batches made and their characteristics.

Suppository batch	Composition (%w/w)	Hardness without active	Hardness including active (cysteamine HCl)	Appearance
17 'A'	PEG 8000 40% PEG 600 60%	19 N, 1.94 kg	9 N, 0.92 kg	Uniform white
10 'B'	PEG 14000 40% PEG 600 60%	17 N, 1.73 kg	12 N, 1.22 kg	Uniform white
1 'C'	PEG 1500 100%	30 N, 3.06 kg	27 N, 2.75 kg	Opaque

### 3.2.3 Dissolution studies

Dissolution tests were performed in a six-chambered Sotax CH-4123 dissolution tank (Basel, Switzerland). The dissolution test method followed the standard BP test for suppositories: one suppository in a stainless-steel basket, rotating at 100 rpm in a 1 L water bath at 37°C, sampling at 5 minute intervals for 1 hour (BP 2005 Edition). The dissolution medium was altered depending on the active used. At present, there is no simulated rectal fluid available for in vivo testing (98). However, rectal fluid is known to possess a pH which is very close to neutral, around 7.2 - 7.4, as well as a negligible buffer capacity. The release was measured by UV spectrometry, and the samples were returned to the tank after analysis.

Suppositories containing the phe conjugate as the active were initially tested. The absorbance for each sample was measured at 256 nm, the corresponding  $\lambda_{max}$  of the phe conjugate. Deionised water was used as the dissolution medium.

Cysteamine hydrochloride was then used as the active, as this is the drug used in the treatment of cystinosis. It was established that the release of cysteamine could be measured quantitatively via free sulphhydryl concentration through the use of DTNB (figure 11). Studies were performed which demonstrated that linearity was achievable, allowing accurate concentrations to be calculated from an unknown sample. Absorbance was

measured at 440nm. The dissolution medium was 90% v/v deionised water and 10% v/v 1 M Tris buffer solution at pH8, as DTNB is water insoluble. An equimolar weight of DTNB to cysteamine was dissolved in each dissolution tank. For the reasons described in Chapter 2, the tank was surrounded with aluminium foil, and the experiment undertaken in a room void of natural light.

### **3.2.4 Hot-stage microscopy studies of suppositories and excipients**

The active and inactive excipients were studied using a hot-stage microscope, to examine the exact interaction of the suppository ingredients and their crystalline characteristics. Samples were viewed through a Leica DM 2500M microscope connected to a Leica DFC 420 camera (Leica Microsystems GmbH, Germany) for analysis. The microscope was fitted with 5x, 10x, 20x, 50x and 100x lenses.

Samples were placed within a hot stage, which could be heated to 100°C and cooled to -50°C using liquid nitrogen (Linkam, Tadworth, UK). The images were taken with cross-polarising filters in order to distinguish between crystalline and non-crystalline structures. Thus, all dark areas are unorganised, non-crystalline structures, and light areas are ordered crystalline structures.

### **3.2.5 Cooling profile studies**

The cooling profile of a suppository gives a unique thermal history, altering crystal size and geometry. This affects how the suppository melts and dissolves once administered. To determine the precise cooling profile of the forms, an experiment was performed in which a thermal probe was positioned in the suppository mould, and the molten suppository mixture poured. This was performed in triplicate.

### 3.2.6 Active dispersion studies

Due to gravitational settling, there is a possibility that the tip might contain more drug than the rest of the form (79). To ensure uniform drug loading, three separate areas of the suppository were sampled and compared using a DSC Q100 Differential Scanning Calorimeter from TA instruments (Delaware, USA): the side, the middle and the tip (Figure 14). Samples of uniformly less than 10 mg were placed in a standard aluminium pan for DSC analysis, and the lid crimped on. The reference pan was empty. The DSC was set to a heat-cool-heat cycle, where the sample was equilibrated at 0°C, then heated to 100°C at 10°C per minute, equilibrated at 100°C, then cooled at 10°C per minute to 0°C, before being heated again to 100°C at 10°C per minute. This was undertaken in triplicate. This method of DSC analysis was identical throughout the project.

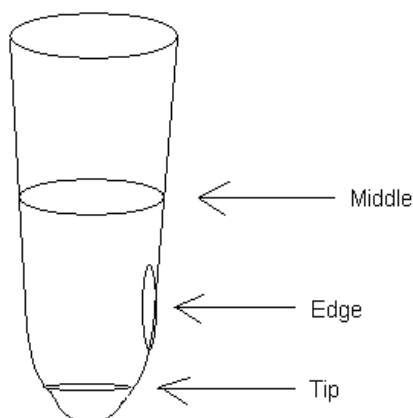


Figure 14. Suppository sample points for uniform content studies.

### 3.2.7 Suppository mould temperature studies

The temperature of the suppository mould may affect the final form's characteristics, as differing rates of cooling affect the crystal size, producing forms with different thermal histories. Suppositories were analysed using DSC to ensure that the starting temperature of the mould did not affect the final form. Six batches of suppository blend A, each containing 30 mg of cysteamine hydrochloride were manufactured, with the mould set at a

different temperature for each; 28.5, 30.5, 38, 46, 52 and 58°C. Room temperature was taken as 21°C.

### 3.2.8 Stability tests

Stability studies were conducted over a 12-month period. Upon manufacture ( $T_0$ ), the suppositories were stored under three different environmental conditions in order to analyse their stability; a refrigerator (4°C), a store containing a desiccator with saturated sodium hydrogen sulphate solution at 20°C and 52% RH (99), and an Environmental Test Chamber (ETC) (Copely, Nottingham, England) set at 30°C and 75% Relative Humidity (74). These conditions were selected to analyse cold storage, typical home storage and accelerated testing. As the suppositories had low melting points, it was decided to reduce the commonly used accelerated temperature from 37°C to 30°C. The temperature in each of the storage areas was monitored daily. DSC and IR Spectroscopy analysis was then performed every week for one month, every month for 3 months, and subsequently every 3 months for 12 months, and compared with the results from the suppositories at  $T_0$  (74). In combination with other techniques, infrared (IR) spectroscopy was used to monitor changes over time in the suppositories. IR Spectroscopy of the samples was performed using a Nicolet IS10 IR from Thermo Scientific (Fisher, UK) with a Smart iTR attachment and a diamond HATR (horizontal attenuated total reflectance). It has been used previously with cysteamine (100). Infrared spectroscopy of a compound produces a spectrum, the patterns and peaks of which relate to the vibration of the compound's different molecular bonds caused by the electromagnetic energy (101). These bonds vibrate upon the absorption of energy, producing a unique peak or set of peaks on the spectrum which can therefore be used for identifying the compound. Thiol groups have an IR sample frequency of between 2600 to 2550  $\text{cm}^{-1}$ , while disulphides are found between 620 and 600  $\text{cm}^{-1}$  (101). A sample of a cysteamine hydrochloride suppository will only exhibit evidence of a disulphide bond if oxidation has occurred, highlighting the instability of the formulation. A

disulphide bond is present in the phe conjugate samples, allowing a comparison to be made between the two actives.

### 3.3 Results and discussion

#### 3.3.1 Dissolution studies

The following plot (figure 15) illustrates the release of the active from the three PEG suppository bases over time. They were undertaken using the phe conjugate (6) as the active, in PEG blends A, B and C.

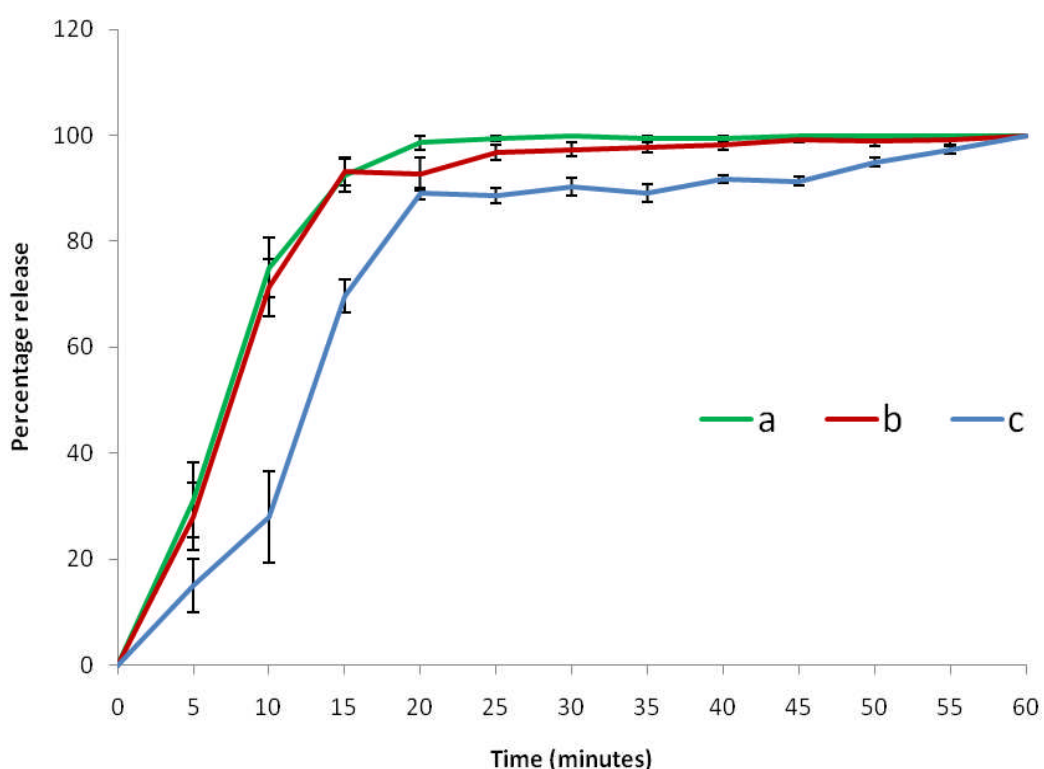


Figure 15. Percentage release of the phe conjugate from PEG Blends A, B and C over time (n = 7, 9 and 6 respectively).

It is evident that there is a large variation in release onset in forms A, B and C.  $T_{100}$  for PEG blends A, B and C were observed at 20, 45 and 60 minutes respectively (n = 5-9). PEG blend C released the phe conjugate more slowly than PEG blends A and B, and this may be due to the greater hardness of blend C (table 3).

The fatty bases Witepsol and Gelucire produced a more homogenous blend and melted instantly (data not shown), whereas the PEG bases produced a more desirable dissolution profile and dissolved more slowly over time (Table 4). It was decided to continue studies using PEG bases only, as they produced a more prolonged release of 40-60 minutes compared to 2 minutes for witepsol and gelucire. This slower dissolution of the PEGs allows the drug to be in contact with the rectum for longer where it is more likely to be absorbed into the body, whereas a sudden melt over 2 minutes increases the chances of drug loss through expulsion.

Table 4. Summary of phe conjugate release studies

Percentage release	Time to release phe conjugate (minutes)				
	PEG blend A	PEG blend B	PEG blend C	Gelucire	Witepsol
10%	2	2	3	0.5	0.5
25%	5	5	9.5	1	1
50%	7	7.5	12.5	2	2
75%	10	10	17	2.5	2.5
100%	20	45	59	4.5	4.5

The following plot (figure 16) illustrates the release of the active from the three suppository bases over time. Cysteamine hydrochloride was used as the active (4), formulated into suppository bases PEG blends A, B and C.

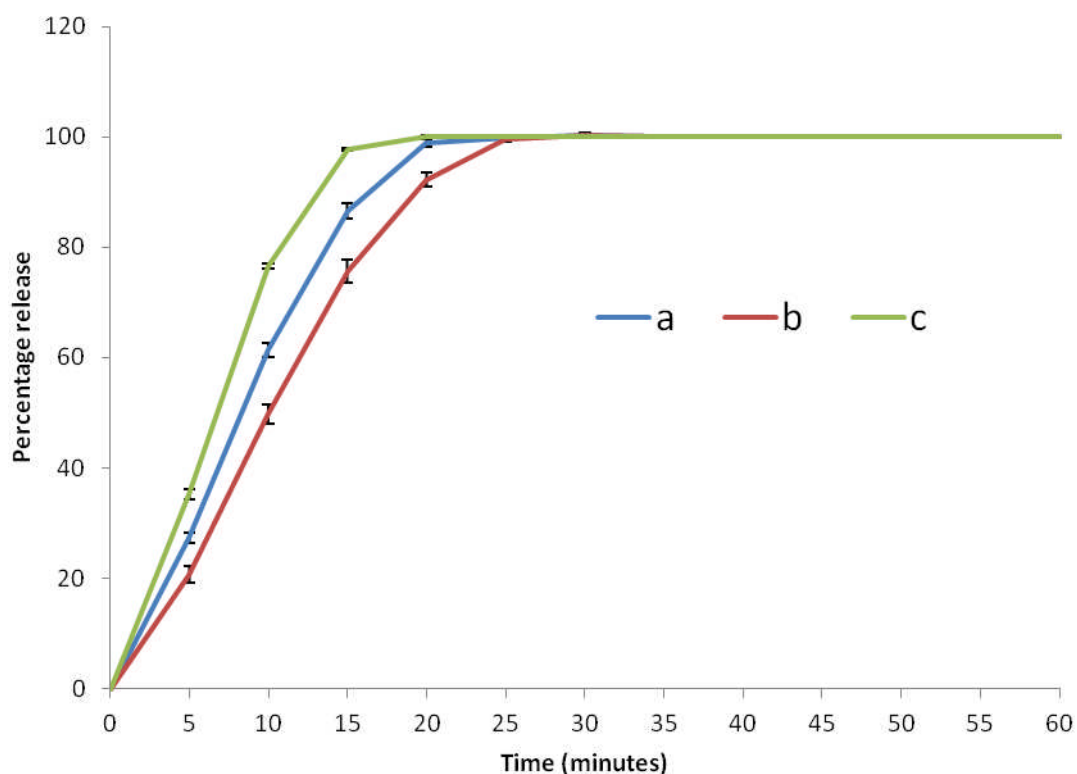


Figure 16. Percentage release of cysteamine hydrochloride from PEG Blends A, B and C over time (n = 6, 5 and 5 respectively).

All three PEG blends containing cysteamine hydrochloride as the active displayed more reproducible profiles than dissolution using the phe conjugate. The PEG bases should dissolve at the same rate in every reproduction of the test, therefore this may have been due to non-uniform drug loading of the phe conjugate. The UV-tagged phe conjugate was developed initially to monitor release from the forms, as there is a lack of chromophore in cysteamine. Cysteamine hydrochloride is also a very difficult drug to formulate. At room temperature it rapidly oxidises to the disulphide form cystamine, which has been shown to deplete cells of cystine but which is not licensed to do so (5,15,29). It is also extremely hygroscopic and deliquescent, absorbing moisture from the air to become a liquid. As UV-tagging the cystamine chemically alters the drug, a more suitable method of monitoring release was found with DTNB. Thus, release could be measured while the structural properties of the active remained unaltered. Analysis continued using cysteamine hydrochloride as the active. A summary of the release times are shown in table 5.

Table 5. Summary of cysteamine hydrochloride release studies

Percentage release	Time to release cysteamine hydrochloride (minutes)		
	PEG blend A	PEG blend B	PEG blend C
10%	1.75	2.5	1.75
25%	5	6.5	4.5
50%	9	10	7
75%	13	15	9.5
100%	26	26	17

The data produced using Ellman's reagent to detect the release of cysteamine hydrochloride demonstrated excellent reproducibility (average standard error of the mean for PEG Blend: A – 0.39, B – 0.58, C – 0.14). However, initial studies using Ellman's Reagent produced results that showed a distinct decline in absorbance after full release of cysteamine hydrochloride (average 3-5% reduction after full release). In an attempt to eliminate this, aluminium foil was used to limit the exposure to natural light as much as possible. DTNB is known to be photosensitive (75,78). The results produced in the dark environment showed an elimination of the decline that was previously seen.

### 3.3.2 Hot-Stage Microscopy studies

Figures 17 and 18 examine the suppository excipients, along with the suppository PEG blends A, B and C. Within each image, the dark areas represent unorganised, non-crystalline structures, whereas the light areas correspond to crystalline structures.

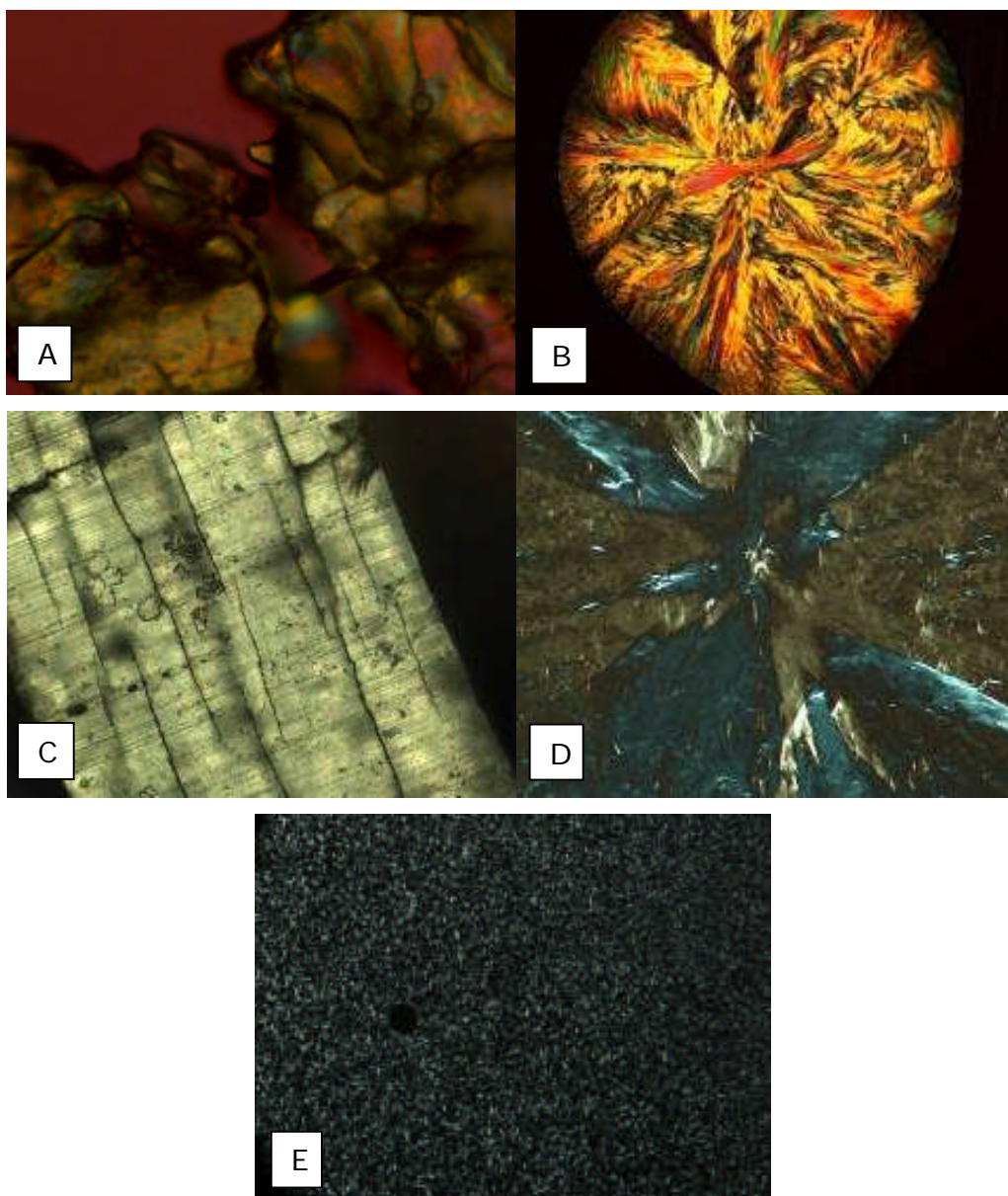


Figure 17. Optical micrographs of: A. cysteamine hydrochloride at 25°C, B. cysteamine hydrochloride at 25°C (heated to melting point then cooled), C. PEG 8000, D. PEG 8000 at 25°C (heated to melting point (62°C) then cooled), and E. PEG 600 at 5°C (heated to 50°C and recrystallised).

Cysteamine hydrochloride possesses a triclinic crystal structure (102). This is an unsymmetrical structure, with the three crystal vectors of unequal length and non-perpendicular intersection (103). PEG 1500 at 25°C (results not shown) displayed a tetragonal structure similar to that of PEG 8000, where one axis is much longer than the other two, forming a cuboid shaped crystal. Peg 600 is liquid at room temperature, and indeed displayed a disordered structure with cross-polarised light (results not shown). These

results demonstrated that lower molecular weights of PEG possess a lower degree of crystallinity below their melting point.

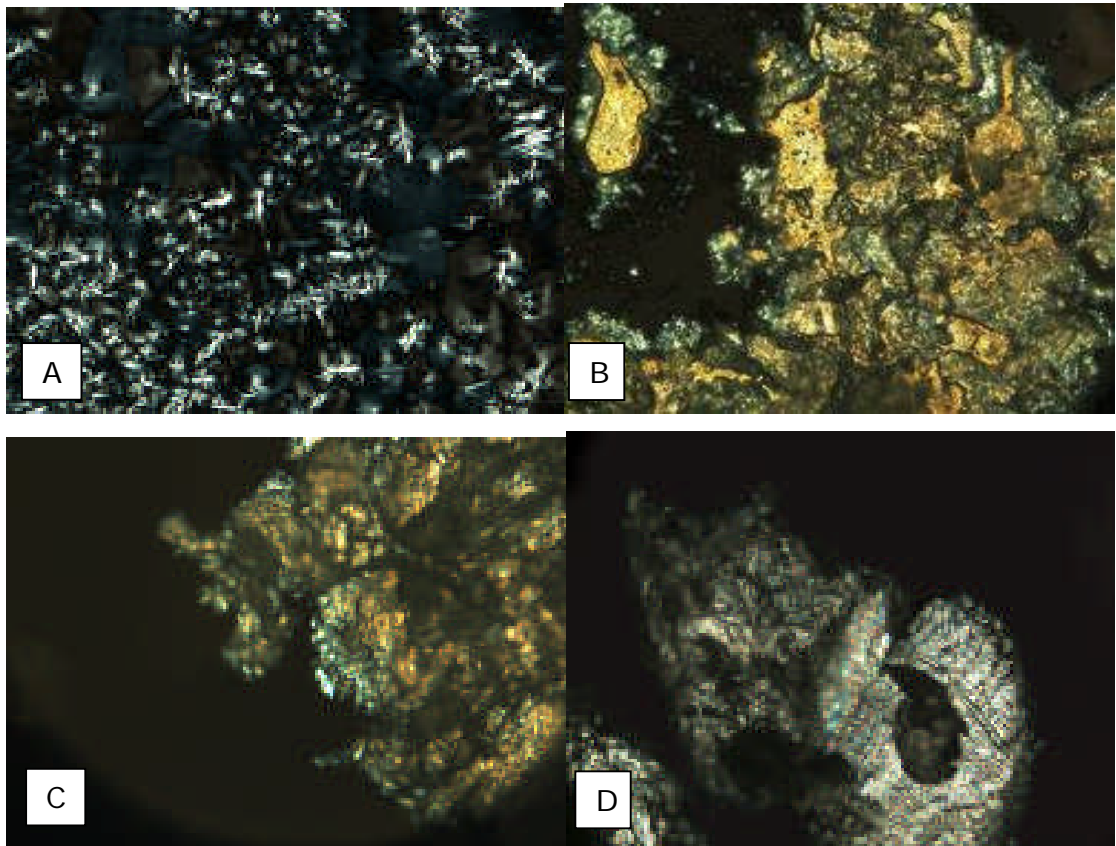


Figure 18. Optical micrographs of, A. PEG 14000 at 25°C (heated to its melting point (62°C) and cooled), B. PEG blend A at 25°C (suppository), C. PEG blend B at 25°C (suppository), and D. PEG blend C suppository at 25°C.

Figure 18 shows evidence of homogenous suppository mixes, where the suppository possesses a uniform appearance. This homogeneity suggested that cysteamine hydrochloride was well dispersed within the suppository. The PEG blend C suppositories were the most stable formulation when observed over time. Both PEG blend A and B displayed a 'sweaty' appearance, in that beads of liquid were clearly visible on the surface. This was more pronounced in PEG blend A. The liquid was viscous and foul smelling, possibly indicating the presence of cysteamine hydrochloride. If left in the open for a few hours, the volume of this liquid increased to the point where the form was completely covered. When this liquid was studied

on the hot stage microscope, there were no crystals observed. When cooled to  $-20^{\circ}\text{C}$  with liquid nitrogen, a crystal structure did form similar to the needle crystal structure displayed by cooled PEG 600 (figure 17E). There was one crystal evident of unknown composition. To determine if cold storage affected this 'sweating' phenomenon, PEG Blend A suppositories were kept in a freezer for 1 month. When removed, the form appeared normal, without any 'sweating' evident. However, within seconds a large amount of this liquid was again produced by the suppository. Cysteamine hydrochloride crystals were also left out in the open, and after 20 minutes had become a viscous liquid. Cysteamine hydrochloride is known to be extremely hygroscopic. However, if a PEG Blend C suppository containing 30 mg of cysteamine hydrochloride is exposed to room temperature for 24 hours, there is no evidence of any 'sweating'.

From the evidence obtained phase separation is the most likely cause for this phenomenon. There may be a 'demixing' of the PEG and cysteamine hydrochloride components. Crystal ripening, where the PEG recrystallises over time to a lower free energy state may also be expelling the cysteamine hydrochloride from the suppository. This 'microcrystalline phase separation' forces the hygroscopic cysteamine hydrochloride to the outside of the suppository, where it attracts environmental moisture. The deliquescence is almost instantaneous, where it appears that a liquid is being produced from the suppository. Thus, the 'sweat' observed may be a concentrated aqueous solution of cysteamine hydrochloride. Table 3 also illustrates that there has been a large decrease in suppository hardness after cysteamine hydrochloride addition, particularly in PEG blend A. This is observed to a lesser degree in PEG blend B, and only slightly in PEG blend C. There may therefore be an incompatibility between cysteamine hydrochloride and PEG blends A and B, which manifests as 'sweating'.

### 3.3.3 Cooling profile studies

Each of the three suppository PEG blends A, B and C were monitored for temperature changes during the cooling period after being poured into moulds (Figure 19). This cooling profile gives an indication of the individual thermal history of each form. If cooled quickly, the suppository base would be composed of small crystals, whereas a faster cool would produce larger crystals. This difference in crystal size would affect how the suppository dissolves in the rectum.

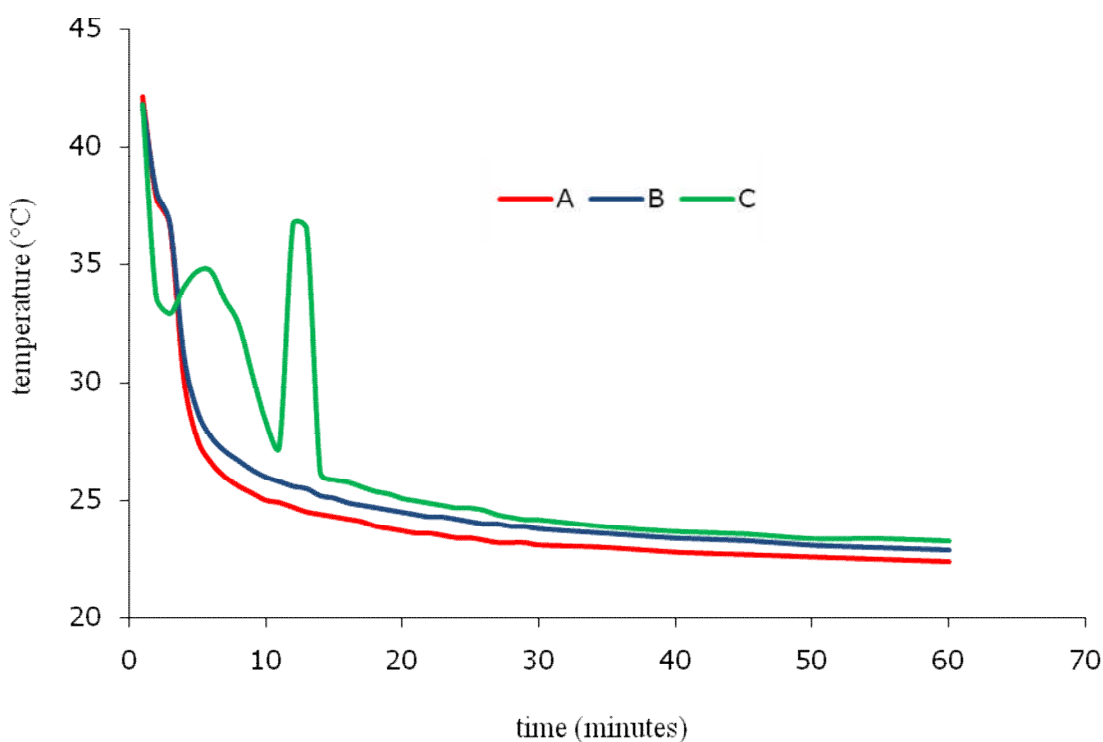


Figure 19. Three PEG blend suppositories average cooling profiles, n = 3.

Whilst PEG Blend A and B displayed very similar cooling profiles, the PEG Blend C suppositories cooled in a very different way. PEG Blends A and B displayed a sudden drop in temperature as the hot molten mixture hits the cooler mould, with a plateau after three minutes when the temperature neither rises nor falls. There is then a gradual temperature decrease, eventually reaching a point where the mould and form are almost the same temperature. Blend C also displays the characteristic initial drop, however this is followed by a large increase in temperature. This exothermic peak is the heat of crystallisation of the suppository base. There is also a heat of

crystallisation for PEG blends A and B, however this is much smaller and is observed as the plateau in temperature. This smaller heat of crystallisation observed in PEG blends A and B is due to a lower degree of crystallinity observed in lower molecular weight PEGs.

### 3.3.4 Active dispersion studies

To ensure cysteamine hydrochloride was evenly dispersed throughout the suppository, samples were taken from three separate sections of the suppository (figure 14) and analysed using DSC (Figure 20).

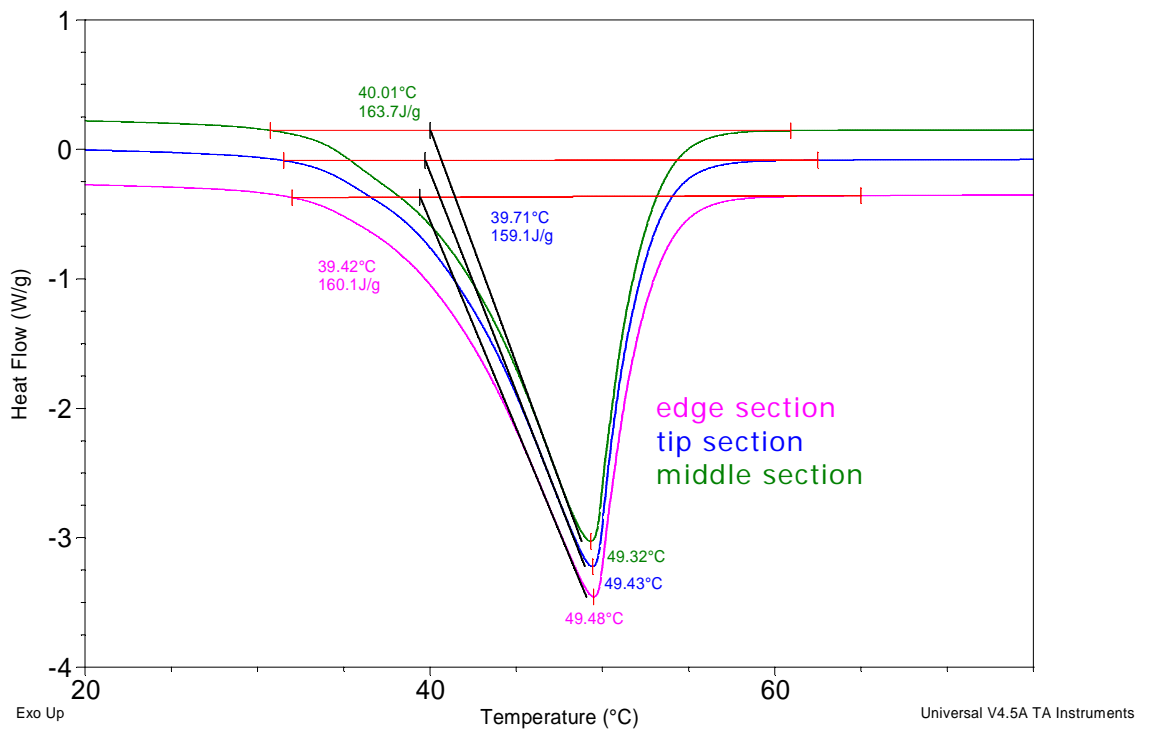


Figure 20. Section comparison of the melt phase between the tip, middle and edge areas of the PEG Blend A suppository containing cysteamine hydrochloride.

It is evident from figure 20 that there is minimal difference between the tip, edge and middle sections, which is indicative of a uniform crystallinity within the PEG suppository.

### 3.3.5 Suppository mould temperature studies

Suppository mould temperatures were recorded, and the characteristics of each complete suppository were analysed. Suppository hardness and appearance remained unaffected by the change in mould temperature, and the suppositories were analysed further by DSC (table 6).

Table 6. DSC analysis data of the suppositories from six different starting mould temperatures.

Suppository mould starting temperature (°C)	Melting onset temperature (°C)	Energy of transition (J/g)
28.5	50.08	76.63
30.5	50.46	76.37
38	50.58	73.54
46	50.81	75.37
52	51.76	75.88

There is a general trend for the melting point of the suppositories to increase as the mould temperature increases. This is caused by a slower cooling rate, producing larger crystals of PEG. When PEG is cooled quickly, the chains are random and unordered. The suppository exists at too high an energy state for the molecules. Over time, these chains will move to a state of lower energy, becoming more aligned and increasing the level of crystallinity. This process is accelerated if heat is supplied to the form. If PEG is cooled at a slower rate, the chains align in a more linear manner, and crystal size is increased (104). This produces a more stable suppository over time, which is less likely to degrade in storage before use. All of the tested suppositories were manufactured with the same starting mould temperature, 22°C, and therefore the crystal size are uniform across the batches manufactured. The energy of transition values decrease as a function of temperature. This is evidence of a decrease in the degree of crystallinity in the samples over time, caused by water absorption ('physical ageing'). This contradicts the melting point data. The evidence suggests that two opposing phenomena are competing to both increase and decrease

the degree of crystallinity, one as a result of 'crystal ripening' (increase), and the other caused by water absorption (decrease). In 'crystal ripening', the larger the crystals are, the lower the free energy that the sample possesses. This is thermodynamically more desirable than smaller crystals. It appears that these analyses have measured the 'net effect' of these two phenomena.

### 3.3.6 Stability tests

The temperature and relative humidity in each of the three storage chambers were monitored continuously throughout the 12 months. The average values are shown in Table 7.

Table 7. Average temperatures and relative humidities in each storage chamber, with standard deviations.

	Refrigerator	Store	ETC
Average temperature	3.7°C (± 0.8)	20.3°C (± 1.9)	29.9°C (± 1.0)
Average relative humidity	9.2% (± 0.3)	52%	76.4% (± 2.0)

#### 3.3.6.1 DSC results: T0, T6 months, T12 months comparison.

The suppositories were tested by DSC at 6 months and 12 months for melting point, energy of transition and peak temperature. This data was compared with the starting point, time zero (T<sub>0</sub>). Selected analysis data is presented in table 8 as a percentage increase or decrease in these parameters over time, as well as two example plots (figures 21 and 22).

Table 8. DSC analysis data of selected suppository samples over time (n = 3).

Suppository sample	Time zero	T 6 months	T 12 months
	Melting point (°C)	Melting point (%°C)	Melting point (%°C)
	Energy of transition (J/g)	Energy of transition (%J/g)	Energy of transition (%J/g)
	Peak temperature (°C)	Peak temperature (%°C)	Peak temperature (%°C)
PEG blend A 4°C storage	50.55	0.75↑	1.84↓
	71.84	5.78↑	13.1↑
	56.44	0.5↑	2.3↓
PEG blend A 21°C storage	50.70	2.25↑	0.32↓
	83.77	10.7↑	15.91↑
	57.71	0.66↑	0.88↓
PEG blend A 30°C storage	50.52	3.82↓	11.6↓
	75.32	11.74↑	19.33↑
	56.60	1.54↓	8.98↓
PEG blend B 4°C storage	51.39	1.46↑	0.6↓
	73.44	9.89↑	12.43↑
	57.77	0.17↓	2.2↓
PEG blend B 21°C storage	50.35	4.61↑	1.25↑
	67.18	28.57↑	33.94↑
	56.65	2.97↑	0.26↑
PEG blend B 30°C storage	50.73	1.71↑	1.59↓
	80.09	7.6↑	13.65↑
	57.62	0.9↓	2.92↓
PEG blend C 4°C storage	41.16	3.77↑	2.33↑
	159.4	12.83↑	16.56↑
	50.30	0.6↓	0.42↓
PEG blend C 21°C storage	41.07	3.63↓	8.45↓
	165.9	3.86↑	5.42↑
	50.27	2.11↓	5.78↓
PEG blend C 30°C storage	49.97	1.28↓	30.64↓
	164.50	3.71↑	4.86↓
	40.92	5.96↓	12.95↑

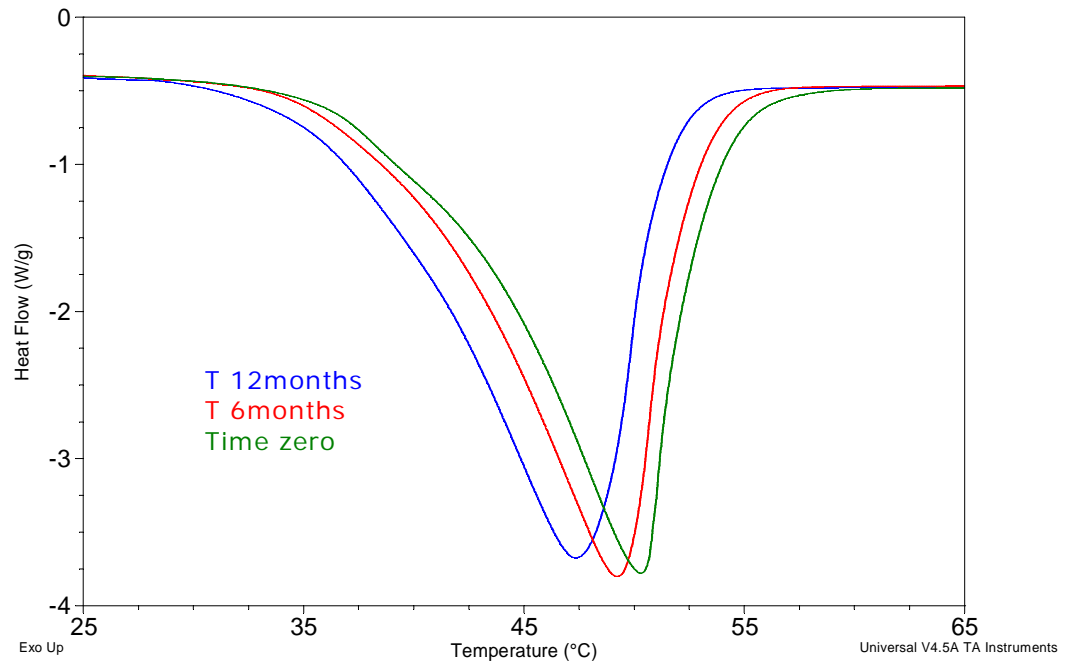


Figure 21. DSC plot of PEG blend C suppositories over time, stored at 21 °C.

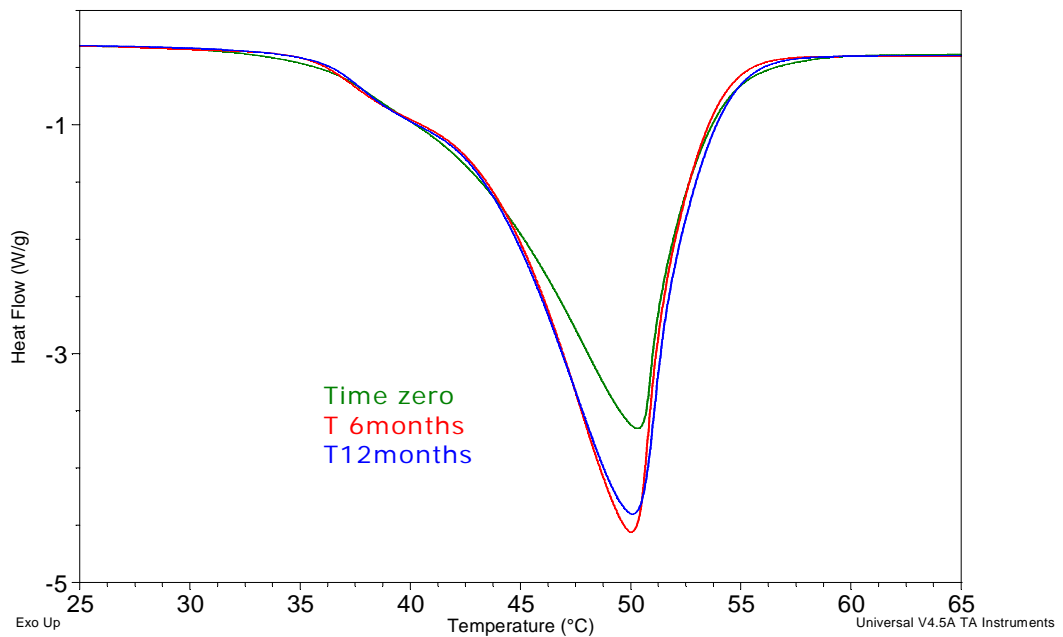


Figure 22. DSC plots of PEG blend C suppositories over time, stored at 4 °C.

The melting points of the PEG blend suppositories demonstrated stability over time, with the exception of PEG blend A stored at 30°C (11.6% decrease) and PEG blend C stored at 21°C (8.45% decrease). Both the melting points and peak temperature values have decreased, demonstrating deterioration of these samples over time. Both of these storage conditions possess a high relative humidity, and therefore water penetration is

probably the main reason for deterioration. Cysteamine hydrochloride is extremely deliquescent, and exposure to water is likely to be the main factor for the stability of the suppositories. The storage at 30°C and 75% RH is representative of accelerated stability testing, and therefore PEG blend A should be stored at 21°C or below, with a low relative humidity.

Over 12 months, the energy of transition of each sample has increased without exception. This is due to an increase in the crystallinity of the samples over time, caused by 'crystal ripening'. When heat is supplied to the sample, this process of crystal enlargement is accelerated. This is illustrated in samples PEG blend A stored at 30°C, and PEG blend B stored at 21°C. Over twelve months, the energy of transition has increased by 19.33% and 33.94% respectively. As discussed previously, the energy supplied to the forms as heat during twelve months of accelerated storage testing has altered the thermal energy, aligning the PEG chains in a less chaotic manner (104). Overall, the DSC analysis over 12 months demonstrated that the PEG blend C suppositories were most stable when stored at 4°C. PEG blend A suppositories displayed deterioration when stored in excessive temperature and humidity conditions.

#### **3.3.6.2 Infrared Spectroscopy after 1 week, 3 months, 6 months and 12 months.**

Infrared spectroscopy of a chemical produces a spectrum, the patterns and peaks of which relate to the absorption of the electromagnetic energy by the chemical's different molecular bonds (101). These bonds vibrate upon the absorption of energy, producing a unique peak or set of peaks on the spectrum which can therefore be used for identifying the compound (table 9). The bonds can vibrate in many specific ways, such as twisting, wagging or stretching. Each of the suppository samples were, over time, scanned by IR spectroscopy and added to a compound library. A percentage match was then performed on each sample (Figure 23 and table 9).

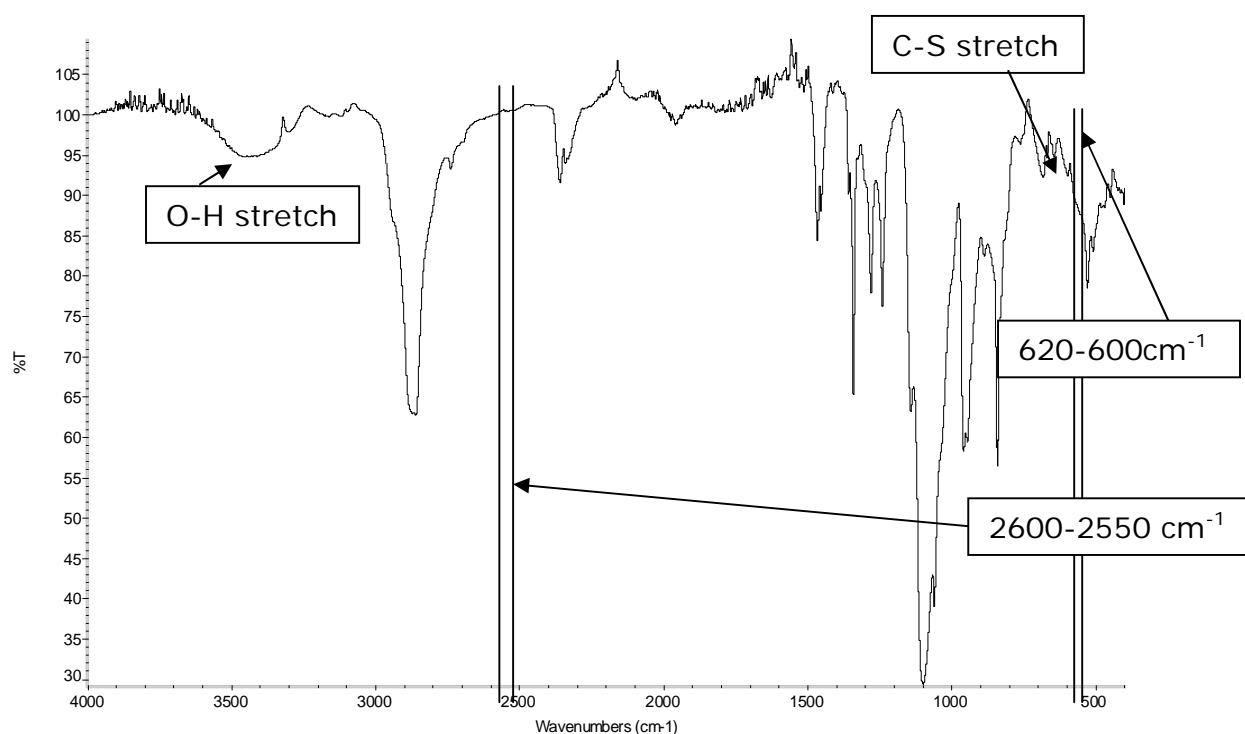


Figure 23. Regions of the IR spectra used for comparison in this study (PEG blend C).

Table 9. The group frequencies used for identification of the samples (101).

Group frequency (cm <sup>-1</sup> )	Functional group/assignment
3400-3380	O-H stretch
2600-2550	S-H stretch
710-685	C-S stretch
620-600	S-S stretch

The oxidation of cysteamine to cystamine was the basis of comparisons made between samples. This would produce a peak in the region of disulphide bond stretches, i.e. 620-600 cm<sup>-1</sup>, and allow the identification of sample degradation.

Each suppository was analysed over time using the IR spectrometer, and compared to the suppositories at time zero. The results are shown in table 10 (selected examples only).

Table 10. Suppository stability over time, presented as percentage match to sample at T<sub>0</sub> (selected data only).

Suppository blend/storage conditions	Percentage match to sample at T <sub>0</sub>
PEG blend C, 4°C	99.2% at 3 months
	98.84% at 12 months
PEG blend A, 4°C	97.4% at 3 weeks
PEG blend C, 21°C	98.94% at 6 months
PEG blend B, 21°C	97.95% at 12 months
PEG blend C, 30C, 75% RH	98.94% at 6 months

The stability tests using IR analysis demonstrated that PEG blend C is the most stable in all conditions, with minimal changes over six months at room temperature and accelerated tests, and up to twelve months stability when stored at 4° C. PEG blend B shows evidence of stability over twelve months at room temperature. PEG blend A shows evidence of degradation when subjected to a range of storage conditions, and therefore is unsuitable for the rectal delivery of cysteamine.

### 3.3.6.3 Correlation between DSC plots and IR percentage match results

The IR percentage match data supports the DSC plots. This is evidence of correlation between the two methods which allows a more conclusive result to be produced. For example, PEG blend C stored at 21°C displayed a 98.94% match at 6 months (table 10), and the IR plot illustrated stability over time (results not shown).

These stability test results support previous results, and indicate that PEG Blend C was the most stable formulation over a 12-month period. The suppositories stored at 4°C were generally more stable than those stored at higher temperatures, although PEG blend C displays long term stability even at room temperature. PEG blend B suppositories were stable over time at room temperature. PEG blend A suppositories displayed long term instability in all storage conditions. There is correlation between the DSC

and IR results. By utilizing two techniques a comprehensive comparison can be made. PEG blend C displays ideal stability over time in a range of storage conditions (refrigerator, room temperature, accelerated stability tests).

### **3.4 Conclusions**

Various suppository bases were investigated for suitability for the incorporation of cysteamine hydrochloride and the phe-cysteamine conjugate. Melting point, hardness, stability and appearance were analysed, and the three suppository bases with the most suitable characteristics were chosen for further study. PEG Blends A, B and C were made and characterised. Blend C displayed good qualities (i.e. complete, reproducible release after 30 minutes, stability over 12 months at 4°C) required for the delivery of cysteamine hydrochloride to the rectum. DSC analysis indicated that cysteamine hydrochloride was dispersed uniformly in the suppositories. Dissolution studies using the phe-cysteamine conjugate revealed 20-60 minute release, while cysteamine hydrochloride as the active component demonstrated 17-26 minute release on average. The stability tests indicate that 4°C provided the ideal storage conditions over a 12-month period. Formulation C is the most stable over time, followed by B. Blend A is the least stable form, and even when stored in the refrigerator it is subject to degradation. There is also evidence of an incompatibility between cysteamine hydrochloride and PEG Blends A and B, and this may be due in part to a 'demixing' of the PEG and cysteamine. There is evidence that crystal ripening over time is forcing the expulsion of the cysteamine hydrochloride to the outside surfaces of the suppository. The highly deliquescent cysteamine then quickly dissolves in environmental moisture, forming droplets of liquid on the surface of the suppositories. For these reasons, PEG blends A and B would not be suitable for the rectal delivery of cysteamine. Analysis indicates that PEG blend C would be an ideal suppository base for the delivery of cysteamine hydrochloride.

These tests demonstrate that cysteamine hydrochloride can be formulated as a suppository. This may be of particular benefit when treating cystinosis during infancy, when swallowing capsules is difficult or when the oral route is compromised. Future work with the suppositories may involve the development of in situ gelling forms.

# **Chapter 4 – Ophthalmic formulations**

## Chapter 4 - Ophthalmic formulations

### 4.1 Introduction

The deposition of cystine crystals in the cornea is one of the most troublesome complications affecting cystinosis patients. The crystals become noticeable when the entire peripheral stroma and endothelium have become packed, usually around the age of 6-8 years. However, the crystals are always present by 16 months (5). Photophobia and, ultimately, blepharospasm affect the quality of life such that the slightest glimmer of sunlight can be debilitating (2). Sunglasses are often worn, and lights dimmed (5). The tissue can become so packed that it causes the Bowman's membrane to rupture, causing pain (Figure 24) (6).

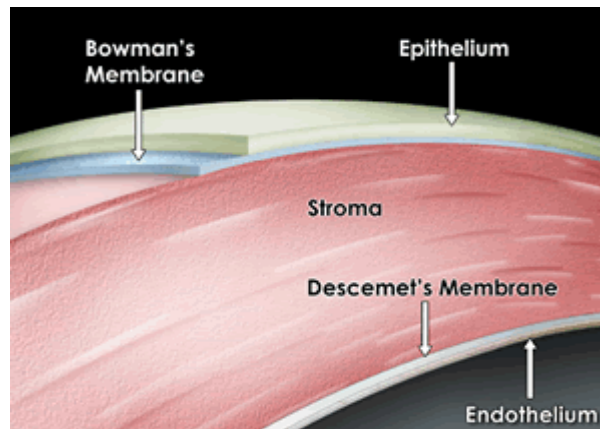


Figure 24. Diagram of the cornea.

In addition, the crystals' accumulation over a period of years can cause corneal scars and sores, keratitis and cataracts, as well as calcification in the form of band keratopathies to form, and ultimately corneal breakdown (45). A study showed that 15% of Cystinosis patients over ten years of age had corneal ulcerations (23).

Ophthalmic problems are not limited to the accumulation of cystine crystals in the cornea. Cataracts can be caused by the steroid treatment post-renal transplant (45). Angle closure glaucoma can also develop (5). Retinal blindness occurs in 3-5% of untreated adults, with optic nerve swelling

another potential cause for this (105). Phthisis bulbi, where the body of the eye shrinks and vision is lost, is a potential endpoint (21).

The oral form of cysteamine treatment can treat most of the ophthalmic symptoms, but has no effect on depleting corneal crystals due to a lack of vasculature in the cornea, and therefore cysteamine must be administered topically in the form of eye drops (21). Corneal transplantation is now an option, however the transplanted tissue re-accumulates crystals over time, and so topical treatment is still required (12,37).

Cysteamine is available in an eye drop form and has been shown to work well. Due to concerns over the formulation's instability at room temperature, the FDA required additional efficacy data and has only recently approved this current treatment (4). It readily oxidises to the disulphide form cystamine, the efficacy of which is controversial (22,33). The only way to overcome this problem is to store the drops in a freezer or remove all oxygen by storing under Argon, which is not commercially or domestically practical. Researchers are aware of the limitations and inconvenience of this current eye drop treatment, and attempts have been made to resolve it (106).

Compliance with the eye drops is a major factor however, as in order to achieve the maximum benefit these drops have to be routinely inserted every hour while awake. They also cause some discomfort by stinging (5). Thus there is a need for a once or twice-daily dosage preparation, to give relief from these ocular symptoms whilst allowing minimal interference to everyday life.

#### **4.1.1 History of cysteamine eye drops**

Topical cysteamine was first documented in 1987, when Gahl et al and Dufier et al both reported initial findings on its novel use (16,21). Both sources were experimental and conducted in a small population. The Dufier study was conducted over a 26-year follow-up period however, and showed

promise for the future use of the eye drops. Gahl's team performed in vitro studies in rabbits, and subsequently set up a controlled double-blind clinical trial in two patients under two years of age. Gahl was also the first to try and explain the reason for the ineffectiveness of systemic cysteamine on the ophthalmic complications, and hypothesised it was due to the cornea's lack of vasculature. Initial findings were encouraging, and the drug's use in this way was deemed safe and effective at depleting corneal crystals, at least in patients under two years of age.

This led to more in-depth investigations, which tested the eye-drop's toxicity and efficacy in different age ranges. Topical cysteamine in the form of eye drops was repeatedly shown to be safe at a concentration of 0.5% w/v while side effects were minor and infrequent, and corneal crystals were effectively depleted to a level which meant normal activities could be performed (37,105,107,108). The possibility of crystal deposition reversal was suggested by the results of a 4-year study (108). Noble's research from 1991 highlighted the importance of compliance with regard to efficacy of the drops and even severe prolonged symptoms were shown to benefit (109). Therefore this new eye drop treatment had the potential to transform the lives of sufferers.

Since being introduced, many more trials have reiterated the previous findings that topical cysteamine eye drops are extremely beneficial to those with this complication. In 1998, Gahl et al compared topical cysteamine with the disulphide form cystamine, as cysteamine rapidly oxidises to the disulphide form at room temperature and therefore has special storage requirements (37). Despite a conclusion of no efficacy of the disulphide form, the team did discover that the crystals exist extracellularly in addition to the currently known intracellular crystals. Gahl et al working in 2000 discovered that the extent of crystal accumulation in the cornea, measured using the standardised Corneal Cystine Crystal Score (CCCS) method is a direct indication of the course and severity of the disease (12). They noticed a link between severity of the individual's CTNS mutations and the rate of crystal build up. The reversibility of the complication through compliant use of eye drops was cemented; however this will not be the case

if a band keratopathy has occurred. Non-compliance is seen as a major barrier to improvement of symptoms, as the drops require administration 8-12 times per day in order to be effective. This paper also contemplates on future studies: could early preventative therapy with the topical formulation actually prevent ophthalmic complications from occurring?

A more recent study attempted to alter the current eye drops to allow storage at room temperature (106). This new formulation included monosodium phosphate and disodium EDTA, however was not as effective at depleting cystine as the current therapy.

#### **4.1.2 Eye anatomy**

The structure and defence mechanisms of the eye make it incredibly difficult to target therapeutically. The avascular cornea receives nutrients from lachrymal fluid and aqueous humor (110). Lachrymal fluid constantly washes the surface, binding proteins and degrading through metabolism, while eye lids blink out any particles and increase tear production (111). The cornea has five, hard to penetrate, layers of alternating hydrophilic and hydrophobic cell types which exhibit tight junctions. The outermost layer is the epithelium, which is negatively charged and lipophilic, behind which are the Bowman's membrane, and the stroma. This layer provides the cornea with 90% of its thickness, and is composed mainly of water. Below the stroma is Descemet's membrane, and finally the endothelium (110) (figure 24).

Of the three distinct corneal layers, the epithelium, the stroma and the endothelium, the epithelium provides the greatest hurdle as it is lipophilic and acts as a barrier to ion transport and to the absorption of hydrophilic drugs such as cysteamine bitartrate. The tight junctions of the corneal epithelium serve as a selective barrier for small molecules and prevent the diffusion of macromolecules via the paracellular route (112). Non-corneal absorption, on the other hand, involves drug penetration across the

conjunctiva and underlying sclera into the uveal tract and vitreous humor (112) and is important for the absorption of large, hydrophilic molecules.

Current understanding of ocular pharmacokinetics involves mixing of the eye drops with lachrymal fluid, produced at a rate of 0.5-2.2  $\mu\text{L}/\text{min}$ , resulting in a short contact time with ocular tissue (113). Subsequent drainage towards the nasolachrymal duct during blinking results in extensive elimination of the applied solution and contact times varying from 1-2 minutes (114) to 5 minutes (115) have been reported. This mix of lachrymal fluid and instilled medication is subsequently absorbed through the conjunctival bloodstream, and can cause potentially serious side effects (116). The rapid drainage rate is due to the tendency of the eye to maintain its residence volume at  $\sim 10 \mu\text{L}$ , while a typical eye dropper delivers around 30  $\mu\text{l}$  and consequently, the overall absorption and bioavailability of a topically applied drug is typically less than 5% (117,118). These barriers make it extremely difficult for the instilled eye drop to be retained at the eye surface long enough to exert its full therapeutic effect.

#### **4.1.3 Mucus**

The mucus which covers the eye is constantly being produced by goblet cells within the conjunctiva and then digested, which makes it difficult for both pathogens and drugs to reach the corneal surface. Pathogens and drugs must move through the layers of mucus quickly, to reach the epithelium before they are lost to the nasolacrimal ducts. The mucus also traps any foreign particle, and wraps it in a thin mucus coat before the particle is swept away with blinking (119). Mucin is composed of mucin glycoproteins, lipids, inorganic salts and as much as 95% water (120). The thickness of the mucus layer ranges from 0.05 to 1.5  $\mu\text{m}$  (121). Mucus is a negatively-charged, viscoelastic, shear-thinning gel which is replaced every 10 minutes with lachrymal fluid (122). This high turnover rate of tear fluid, in combination with the other protective mechanisms such as frequent

blinking and tight cell junctions ensures that the eye remains clear of pathogens and foreign bodies, and may impair mucoadhesion (123).

#### **4.1.4 Delivery systems for ophthalmic symptoms of cystinosis**

The largest improvement upon the poor bioavailability of eye drops can be achieved by either improving corneal permeability or prolonging the corneal residence time of the ophthalmic dosage form (124). This project focussed on extending corneal contact time using ophthalmic gels.

##### **4.1.4.1 In situ gelling polymers**

In situ gelling polymers have the potential to improve ophthalmic drug bioavailability through prolonged contact of the drug with the ocular tissues. In situ forming hydrogels exhibit the desirable properties of eye drops, whilst combining the efficacious nature of ophthalmic inserts. Introduced within the last 20 years and technically more complex than traditional eye drops, they embody everything necessary in an ophthalmic delivery form; easy to make and use, liquid until they come into contact with the eye, a gel once instilled, minimal interference with vision, comfortable, non toxic and no need for removal (116).

Hydrogels are composed of three-dimensional aqueous gel networks which swell rapidly to retain large volumes of water within their structure (125). The gelling process can be triggered in different ways. A rise in temperature can cause gelation to occur, through the formation of hydrophobic interactions between polymer chains (125). The chemical class Pluronics, which are used in multiple applications such as emulsification and drug delivery are an example of a polymer which gels upon a rise in temperature. The gelling process can also be triggered by a change in pH, through the ionisation of particular groups within the polymer chain. Carbomer, used as a thickening agent and an emulsifier, is an example of an acrylic acid polymer which gels under rising pH conditions. Ionic

changes can also initiate gelling, by cross-linking negatively-charged polymer chains with positive ions (cations) (126). Gellan gum gels in this manner, making it suitable for ophthalmic applications. When added to water, these compounds swell and maintain water (125). The gels take 24 hours to fully hydrate and swell, and are left for this period in a refrigerator. The formed gels have to possess high viscosity when there is little or no shear stress placed upon them, and low viscosity under high stress conditions, thus ensuring maximum comfort to the user during blinking and causing minimal interference with vision. Human lachrymal fluid has been measured with a viscosity of 0.0006 Pa.s (120), giving an indication of the level of viscosity acceptable in the eye. There has been much research on hydrogels undertaken, and the conclusions are similar; well tolerated, non-toxic delivering effective 8-hour sustained delivery (126-130).

#### **4.1.4.2 Bioadhesive and mucoadhesive polymers**

Bioadhesion describes a situation where a material is held onto the surface of a biological tissue for extended periods (120). Some polymers can bind to the mucin layer, and are termed mucoadhesive. This is not in fact true bioadhesion, as the adherence occurs between the polymer and the mucus layer which covers the eye, allowing minimal disruption to vision (121). Certain polymers such as carbomer 934 have been shown to bind to corneal epithelium (bioadhesive), and be retained in the eye for over 2 hours in vivo (120). In 2001, Pan et al demonstrated that an ion-activated device was developed from carbomer 934 and Methocel E50LV as a viscosity enhancing agent, and found to be extremely well tolerated, non-irritant and delivered the active pharmaceutical ingredient over an 8-hour period (131). A thermo-activated gel which incorporated a mucoadhesive was also developed from various poloxamer grades and carbopol, and demonstrated long retention times and good bioadhesion (95). This technology appears ideal for the topical treatment of ophthalmic crystals, and may reduce the dosage frequency required by anchoring the dosage form to the site of action.

The mechanisms of bioadhesion and mucoadhesion are debated, but appear to involve initial surface interaction with the epithelium, where polymers gather to reduce the surface tension, followed by stabilisation through or via hydrogen, covalent or ionic bonding, electrostatic or hydrophobic interactions (121). These bonding mechanisms correspond to six theories of exact interaction, of which the wetting theory is the most likely explanation in this case. This applies to liquids, and their ability to spread over a surface and subsequently adhere to it. Surface tension is involved, and the energy required to separate the two phases is referred to as the work of adhesion,  $W_A$ .

$$W_A = \gamma_A + \gamma_B - \gamma_{AB}$$

Where  $\gamma_A$  is the surface energy of the liquid,  $\gamma_B$  is the surface energy of the solid, and  $\gamma_{AB}$  is the interfacial energy between the liquid and solid (120).

In mucoadhesion, the more flexible the polymer chains are, the more the polymer will be able to penetrate the mucin coat, thereby increasing the adhesive strength (121). There is a link between mucoadhesive strength and polymer chain length. Complete hydration of the polymer is another factor, although care has to be taken to avoid over-hydration, as the polymer network will be weakened and the gel structure lost (120,132).

It is difficult to distinguish between bioadhesion and mucoadhesion, especially in this case as the eye will always be coated in a mucin layer. There are references to both with respect to corneal binding; however, for the purposes of clarity in this project, and because there is likely to be a combination of effects involved, the two terms will be synonymous after this point.

Mucoadhesive polymers have been used to promote bioavailability, by improving drug retention times as well as reducing the rate of drainage (133). In addition, the non-Newtonian pseudoplastic or 'shear thinning' rheology inherent in PAA hydrogels facilitates the process of blinking by dramatic reductions in apparent viscosity as a function of the high external

shear stresses applied by the leading-edge and inside surface of the eye-lid (112). These high shear stresses are associated with equivalent shear rates of  $0 \text{ s}^{-1}$  at rest to  $10,000 - 40,000 \text{ s}^{-1}$  when blinking (134). Pseudoplastic fluids therefore offer significantly less resistance to blinking than Newtonian liquids of equivalent consistency ('viscosity'). High apparent viscosities under zero external stresses result in longer contact times on the surface of the eye. By allowing intimate contact with mucus and epithelium for prolonged periods, an improved efficacy and subsequent reduced dosing frequency may be possible (123). There appears to be no reasonable objection to this novel pharmaceutical form, and yet there are very few of them made commercially. The benefits are potentially enormous, and could revolutionise the way ophthalmic conditions are treated, certainly for chronic conditions such as glaucoma and cystinosis where the difference in dosing frequency would be extremely beneficial to the patient (135). Many trials demonstrate the value of these dosage forms (112,114,118). Three gums were analysed for suitability to formulate an eye gel; HPMC, xanthan gum and carbomer. Gellan gum was also investigated, but eliminated after pre-formulation studies.

#### **4.1.5 Gellan gum**

Gellan gum is frequently used in the pharmaceutical industry as a thickener and emulsifier (74). The gel is also bioadhesive and has been shown to provide a sustained release, and was initially investigated for use in this project. However, gellan gum gels in the presence of mono and divalent cations, and was unsuitable for use with cysteamine hydrochloride as an active component (136).

#### **4.1.6 Carbomer 934**

Carbomer 934 is commonly used for its excellent gelling characteristics and optimum rheological properties (Figure 25). Its viscosity is pH dependent,

and to a lesser extent the presence of electrolytes (137). It is a well-documented mucoadhesive gel (95,129,130,138).

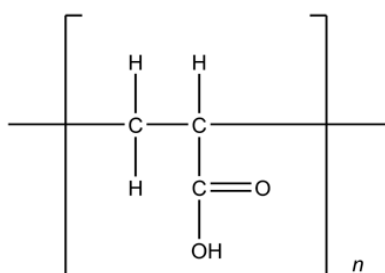


Figure 25. Structural repeating unit of carbomer 934, where  $n \approx 2000$  (139).

Carbomer 934 is a negatively-charged, high molecular weight synthetic polymer. It is composed of poly(acrylic acid) (PAA) cross linked with allyl sucrose. The primary functional group is carboxylic acid, making the gels hydrophilic and able to form hydrogen bonds. When dry or un-neutralised in solution, the carbomer chains are coiled and unexpanded. Sodium hydroxide is added to a carbomer solution to raise the pH, and the carbomer becomes ionised above its dissociation constant ( $pK_a$ ) of 4.75. This ionisation is increased the more the pH is raised beyond the  $pK_a$  value. The polymer's carboxylate groups then repel each other, producing a rigid gel structure (140). A pH of 7 produces a gel with optimum viscosity and clarity (137). Carbomer can tolerate alcohol, however the gels become more viscous and opaque (141).

#### 4.1.7 Xanthan gum

Xanthan gum is widely used in both food and pharmaceutical industries. It is a negatively-charged polysaccharide produced by the bacteria *Xanthomonas campestris* (Figure 26). Higher than ambient temperatures produce a decrease in viscosity and it is known to be bioadhesive (142). After installation into the eye, xanthan gum is an ordered double-stranded helix, due to the lachrymal salts (143).

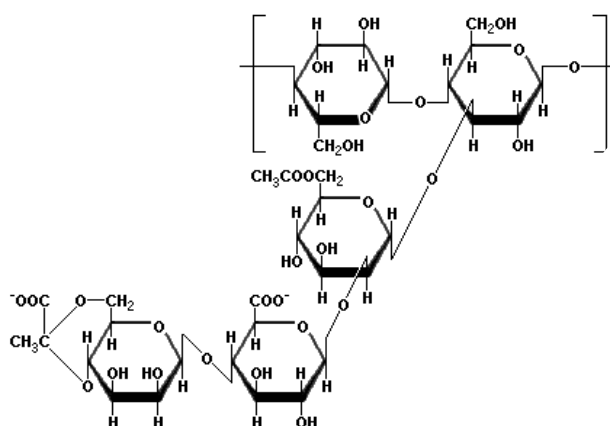


Figure 26. Structural repeating unit of xanthan gum,  $n \approx 500$  (144).

#### 4.1.8 Hydroxypropyl methylcellulose (HPMC)

Hydroxypropyl methylcellulose (HPMC) is frequently used in oral and topical applications within the pharmaceutical industry (Figure 27). Viscosity is reduced at higher temperatures, although no significant viscosity change is seen between 30°C and 40°C (51,145). Water soluble drugs are released from an HPMC matrix by a combination of diffusion through and dissolution of the matrix (125). HPMC is neutral.

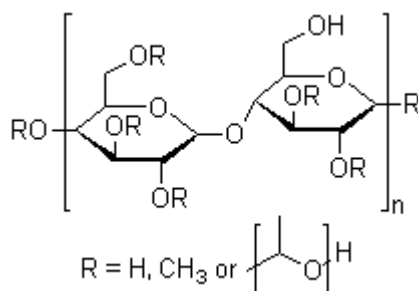


Figure 27. Structural repeating unit of HPMC,  $n \approx 500$  (146).

#### 4.1.9 Thiolated polymers

In an attempt to improve the mucoadhesion of the xanthan, HPMC and carbomer polymers, work has been undertaken in which thiol-containing compounds have been included in the formulations, including cysteine and cysteamine (120). Bernkop-Schnurch et al hypothesized that in situ the

'thiomer' gels would form disulphide links not only between the polymer itself, but also between the polymer and the mucin layer, leading to a strengthened adhesive joint (147-150).

Thiomers achieve this increase in strength through disulphide bond formation as they possess thiol-bearing side chains. These side chains form disulphide bonds with cysteine-rich sub domains of the mucus, which is present on every mucus membrane in the body (147,149,150). These polymers can also inhibit enzymes, gel in situ and enhance permeation, and examples include chitosan, deacylated gellan gum or poly(acrylates). Bernkop-Schnurch's research published in 2005 describes how various different sulfhydryl ligands can be attached to the polymers, such as cysteine or cysteamine (Figure 28).

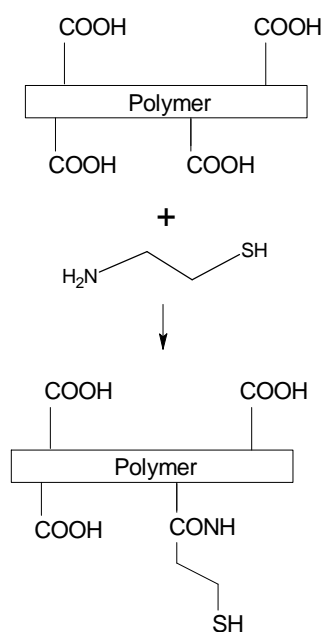


Figure 28. Synthesis scheme for the generation of polymer–cysteamine conjugates.

Thiomers have been reported as unstable in aqueous solution, although there are ways to overcome this (148). When formulated into ophthalmic inserts, the thiomers were well-accepted by volunteers and achieved a drug concentration on the ocular surface for more than 8 hours (150). It is unclear if these polymers could be used in this context; by binding to

cysteine within the mucus, the absorption of the active through the rest of the cell layers may be inhibited (147).

#### **4.1.10 In Vitro testing**

There is no definitive test for bioadhesion. However, the bioadhesion of the three gels used is well documented (130,140,151,152). Bioadhesion was measured by two methods: A Texture Analyser (Stable Micro Systems, Surrey, UK) was used to measure the force required to remove the gel from an area of bovine cornea (153). Agar was used as a comparison to the tissue, being itself a known tissue substitute (154).

As a comparison, rheological studies were performed, analysing the effect of the gels when combined with porcine mucin. It has been proposed that rheological synergism between the polymer and the mucin, observed through changes in storage and loss moduli, can be used as a parameter to measure bioadhesion (155,156). However, Wong et al questioned the validity of this method due to the lack of biological tissue (157). Freeze-dried crude mucin from porcine stomach (type II) was combined with the gels. Ceulmans et al have reported a dispersion of gastric mucin in a salt solution is a suitable equivalent to ocular mucin (143).

## **4.2 Materials and Methods**

### **4.2.1 Materials**

Carbomer 934 was purchased from Universal Biologicals, UK. Cysteamine, cysteamine hydrochloride, potassium chloride, sodium chloride, sodium carbonate, calcium carbonate, magnesium chloride and freeze-dried crude mucin from porcine stomach (type II) were purchased from Sigma, UK. Tubing membrane 12-14,000 kDa was purchased from Visking, UK. Agar No.1 LP0011 was obtained from Oxoid Ltd (Hampshire, UK). All other chemicals were of pharmaceutical grade.

#### 4.2.2 Gel manufacture

All gels were made by addition of the respective polymer to Simulated Lachrymal Fluid (SLF) at pH 7.4 with some modifications.

SLF was used to mimic tear fluid during tests. It was also used in the production of the ophthalmic gels to provide additional buffering capacity. The following salts were weighed out and stirred in a 1 L volumetric flask: potassium chloride 0.179% w/v, sodium chloride 0.631% w/v, sodium carbonate 0.218% w/v, calcium carbonate 0.004% w/v and magnesium chloride 0.005% w/v.

Once dissolved, the pH of the carbomer 934, xanthan gum and HPMC solutions was adjusted to 7.4, which is that of biological tissues, by addition of 2 M hydrochloric acid or 2 M sodium hydroxide. Distilled water was added to 85% final volume. The gel was then stored for 24h at 4°C. Sorensen's Modified Phosphate Buffer (SMPB) was added, along with either cysteamine hydrochloride or phe conjugate. Phe conjugate also required ethanol as a cosolvent. The pH was maintained at 7.4. SLF addition achieved the final weight. Final gels were allowed to rest at 4°C for 24h until further testing commenced (94,129,158). Table 11 summarises all gels tested.

In addition, the HPMC gels were prepared in deionised water, heated to 90°C and stirred vigorously (51). The xanthan gum was prepared in 0.01% w/w benzalkonium chloride solution in deionised water. This was heated to 40°C for 10 minutes and sonicated for 1 hour (143,159). Xanthan gum supports bacterial growth easily without a preservative (160). Multidose ophthalmic preparations must include a preservative to ensure sterility, as the bottle could receive contamination from contact with eyelids, lashes or tears (161). The quaternary ammonium preservative benzalkonium chloride is known to be safe and efficacious in ophthalmic preparations (162,163), and is the most frequently used (161). It is weakly allergenic, and has reported drug penetration enhancing effects, through disruption of the hydrophobic barrier of the corneal epithelium (161).

Table 11. Summary of all gels tested.

Concentration of gel	No active	Phe conjugate 0.5% w/w*	Cysteamine HCl 0.5% w/w	Cysteamine 5% w/w
1.0% w/w carbomer 934	✓			
1.0% w/w carbomer 934		✓		
1.0% w/w carbomer 934			✓	
1.0% w/w carbomer 934				✓
1.0% w/w xanthan	✓			
1.0% w/w xanthan		✓		
1.0% w/w xanthan			✓	
1.0% w/v HPMC	✓			
1.0% w/v HPMC		✓		
1.0% w/v HPMC			✓	

\* Phe conjugate requires ethanol as a cosolvent to dissolve.

#### 4.2.3 pH studies

The effect of active addition on pH was measured using a handheld MP120 pH meter from Mettler Toledo (Columbus, Ohio, USA). Measurements were recorded at 21°C. Gels for this study were neutralised at pH7.4, and the pH allowed to alter upon addition of the active, with no further addition of NaOH.

#### 4.2.4 Optical Transmission

The eye gels should be optically clear to allow minimal interference with vision. The optical transmission of each gel was measured using a Cecil CE 3021 Spectrometer (Cambridge, England). Transmission is the ratio of the amount of light unabsorbed by the gel to the total amount of light the gel is exposed to, expressed as a percentage. A transmission of 480 nm was used, as this is the middle of human light wavelength perception (164). The gels were measured with a 1cm path length, although in situ they

would be less than a millimetre thick. The gels were referenced to deionised water at room temperature, which was taken as 100%. A figure greater than 90% is classed as transparent, between 10 and 90% as translucent, and less than 10% as opaque. As a comparison, some commercial ophthalmic preparations were also measured.

#### **4.2.5 Rheology studies**

The rheological properties of the gels were studied using an Advanced Rheometer AR1000 from TA Instruments (Delaware, USA). A 60 mm, 2° angle cone geometry was used, with a truncation value of 65 µm. All measurements were made at 34°C, the temperature at the cornea surface (165,166). Continuous shear measurements were made initially, using a linear mode and a continuous ramp of 0-600 s<sup>-1</sup>, and 600-0 s<sup>-1</sup> over 20 minutes, to establish flow types such as Newtonian or plastic.

Oscillatory measurements were performed on the gels to characterise the linear visco-elastic behaviour and relate the rheological parameters to molecular structure. A linear mode was used with a frequency of 1-10 Hz, and 20 sample points. The controlled variable was percentage strain. The sample volume was approximately 1.5 ml. All tests were performed in triplicate.

#### **4.2.6 Dissolution studies**

##### **4.2.6.1 Phe conjugate (6) studies**

Prior to the dissolution studies commencing, tests confirmed that SLF as a dissolution medium did not alter the lambda max of either the phe conjugate or cysteamine hydrochloride. A 100 ml round-bottomed flask with sidearm was held in a water bath, heated to 34°C (166). To the sidearm, a condenser was attached. 50 ml SLF was added to the flask, and stirred magnetically using an IKA RET basic hotplate stirrer (Staufen, Germany). The dialysis membrane (12-14,000 kDa) contained 7 ml of gel

and, tied in a rod shape (length 2.23 cm; radius 1 cm, average of 3 measurements) to exclude air bubbles, was added at time zero. The medium was sampled every 2 minutes for the first ten minutes, every 5 minutes for an hour, and every 15 minutes after the first hour.

To allow quantification of the dissolution results, the  $A_1$  of the phe conjugate was determined. Thus, 100% release would be quantifiable. Samples were analysed at 256 nm, the  $\lambda$  max for phe conjugate, using an UV spectrometer from Unicam (Winsford, Cheshire, UK). All experiments were carried out under sink conditions and triplicates were obtained for each experiment. The area of each membrane was calculated using:

$$A = 2\pi r^2 + 2\pi rh$$

Where  $r$  = radius and  $h$  = height of the membrane cylinder. This was used in conjunction with the Higuchi equation to determine the rate-order of the drug release.

$$Q = \frac{AM_t}{A_F \cdot S}$$

$$Q = k_H t^{1/2}$$

Where  $Q$  is the cumulative amount of drug release in  $\text{mg}/\text{cm}^2$ ,  $A$  is the absorbance,  $M_t$  is the total mass of drug in mg,  $A_F$  is the final absorbance,  $S$  is the surface area in  $\text{cm}^2$ ,  $k_H$  is the Higuchi dissolution constant and  $t^{1/2}$  is the square root of time in minutes. A value of  $k_H$  below 0.45 is indicative of Fickian diffusion (167).

#### **4.2.6.2 Cysteamine hydrochloride studies**

Ellman's reagent was used for analysis of the cysteamine hydrochloride dissolution tests (168). The setup was similar to that for the phe conjugate dissolution tests, with some modifications (section 4.2.6). The 50 ml deionised water also contained 10% Tris buffer, to allow the Ellman's

reagent to solubilise. The dialysis membrane contained 0.5 ml of 0.5% w/v cysteamine hydrochloride in a 1% gel. Samples were scanned on a UV spectrophotometer from Unicam (Cheshire, UK) at 440 nm, the  $\lambda_{\text{max}}$  for Ellman's reagent. The Higuchi method was used to analyse the results. All experiments were carried out under sink conditions and triplicates were obtained for each experiment.

#### **4.2.7 Bioadhesion studies**

Bioadhesion was quantified by two methods: A Texture Analyser (Stable Micro Systems, Surrey, UK) was used to measure the force required to remove the gel from an area of bovine cornea (153). Agar was used as a tissue substitute (154). Fresh bovine eyes were collected immediately after slaughter, and washed with deionised water. The whole cornea was then excised and washed in SLF at room temperature. Prior to testing, the corneas were placed on a tissue to remove excess fluid. Cyanoacrylate glue was then used to attach a cornea to a 2 cm<sup>2</sup> stainless steel plate. Care was taken not to allow the glue to come into contact with the upper surface of the tissue. Immediately after this, the steel plates were attached (in pairs) to the Texture Analyser, one positioned directly above the other. Each gel sample was placed between the cornea samples and held together for 60 seconds; the force required to separate the plates was then measured (contact force of 0.05 N, contact time 60 s, probe speed 0.5 mm/s). The force was plotted against distance; the area under the curve (AUC) being equal to the work of adhesion ( $W_{\text{ad}}$ ) (123,153). As a comparison, 3 cm diameter nutrient agar plates were poured, allowed to cool and used in place of the corneal tissue. All other parameters were identical to the tissue studies. Each individual test was undertaken nine times. The statistical significance was determined using a Mann-Whitney test. All outliers and extreme values were removed. The bioadhesion attachment area was 4 cm<sup>2</sup>.

As a comparison, rheological studies were performed, analysing the effect of the gels when combined with porcine mucin. Mucoadhesion analysis using this method is well documented (94,140,155,169,170). A range of mucin concentrations and test conditions were used. Mucin dispersions of 12% and 20% w/w were made in both simulated lachrymal fluid and deionised water, and stirred magnetically for 3 hours. The samples were then homogenised for 10 minutes and sonicated for 45 minutes. They were then made to pH 7.4 by drop wise addition of 2 M sodium hydroxide, and left in the refrigerator overnight before use. Oscillatory tests using the rheometer were performed at 15°C (to minimise sample dehydration and degradation (171)), and 34°C (the temperature at the cornea surface (165,166)), using ratios of 50:50 (129), 40:7 (representative of in vivo volumes upon installation (172)), 4:1 and 1:4. The geometry and parameters used were identical to those outlined in section 4.2.5.

#### **4.2.8 Stability tests**

To determine the long-term stability of each formulation, the gels were monitored over a 4-month period at 4°C. The rheology of each gel was measured at time zero, and periodically over the subsequent 4 months. The gels were also monitored visually for any signs of colour change, turbidity or bacterial growth (173).

### **4.3 Results and discussion**

#### **4.3.1 pH studies**

The change in pH of the gel after addition of the actives was noted (table 12).

Table 12. pH effect on all gels after active addition (n = 3).

Concentration of gel <sup>#</sup>	Active	pH after addition of the active ( $\pm$ SD)
1.0% w/w carbomer 934	Phe conjugate*	7.00 ( $\pm$ 0.09)
1.0 % w/w carbomer 934	Cysteamine HCl	7.20 ( $\pm$ 0.04)
1.0 %w/w carbomer 934	Cysteamine	7.40
1.0% w/w xanthan gum	Phe conjugate*	5.31 ( $\pm$ 0.09)
1.0% w/w xanthan gum	Cysteamine HCl	5.90 ( $\pm$ 0.08)
1.0% w/v HPMC	Phe conjugate*	7.01 ( $\pm$ 0.04)
1.0% w/v HPMC	Cysteamine HCl	7.40

\* Phe conjugate required ethanol as a cosolvent to dissolve. <sup>#</sup> Initial pH 7.4

When formulated at a pH of between 4 and 6, PAA solutions act as in situ forming gels (pH-dependent). When inserted into the eye, these carbomer colloidal dispersions show a sol to gel transition as the pH is raised to that of the eye, pH 7.4. In this study, all three of the hydrogels xanthan, HPMC and carbomer were initially neutralised using sodium hydroxide and the actives were added subsequently in SMPB (pH=7.4). These carbomer gels are considered 'preformed' as opposed to in situ (112,114,116). It has been reported that the ocular surface can tolerate a pH range of 6.6-7.8, beyond this range patients can experience stinging or discomfort (127,174-176). The inclusion of phe conjugate, cysteamine hydrochloride or cysteamine to neutralised hydrogels was to cause changes to the pH dependent on the initial concentration of polymer. All samples qualify as preformed gels according to the definition used for an in situ gel, with the exception of the xanthan gels (116). The xanthan gels will become more viscous when inserted into the eye due to the presence of lachrymal salts, and therefore are in situ gelling.

#### 4.3.2 Optical Transmission

The optical transmission of the three gels was tested, along with the two commercial gels Timoptol<sup>®</sup> and Viscotears<sup>®</sup> (table 13).

Table 13. Optical transmission of the three gels and two commercial gels (n = 3).

	Optical Transmission of gels (%) ( $\pm$ SD)		
	Carbomer 934	Xanthan gum	HPMC
No active	9.3 ( $\pm$ 0.16)	3.4 ( $\pm$ 0.35)	98.3 ( $\pm$ 0.06)
Phe conjugate	0.6 ( $\pm$ 0.2)	2.2 ( $\pm$ 0.06)	94.2 ( $\pm$ 0.06)
Cysteamine HCl	5.7 ( $\pm$ 0.18)	4.5 ( $\pm$ 0.36)	97.9 ( $\pm$ 0.12)
Timoptol <sup>®</sup> LA	95.6 ( $\pm$ 0.15)		
Viscotears <sup>®</sup> Liquid gel	92.7 ( $\pm$ 0.13)		

HPMC displayed the most ideal transmission of the three gels, consistently above 90% with both the phe conjugate and cysteamine hydrochloride as actives. Both carbomer 934 and xanthan gum showed less than 10%, which is classed as opaque. In the case of the phe conjugate, this is due to the presence of alcohol as a cosolvent (137). There may also be precipitation due to the salt content of the gels causing opacity. The commercial preparations displayed excellent transmission of light. Timoptol<sup>®</sup> LA and Viscotears<sup>®</sup> liquid gel contain gellan gum and carbomer, respectively, and are two of a small group of gel-based ophthalmic drops on the market.

In situ, these gels would be less than a fraction of a millimetre thick, and thus transmission would be increased greatly. The tear film has a thickness of 7-8  $\mu$ m (135). Only through in vivo work will the true transparency of the gels be demonstrated.

### 4.3.3 Rheology studies

#### 4.3.3.1 Carbomer 934 gels

All of the carbomer samples displayed pseudoplastic flow behaviour as previously reported for PAA hydrogels of this concentration (130)(figure 29). This is thought to occur through Brownian motion, whereby the polymer chains regroup into positions with lower kinetic energy (177). An initially high increase in shear stress as a function of shear rate ('apparent viscosity') followed by a more gradual or constant increase can also be interpreted as an 'apparent yield stress'. Polymers that form weak gel networks often display an apparent yield stress at low shear rates and the elastic component of the viscoelastic behaviour can be quantified using oscillatory measurements. To measure this component, a small stress,  $\sigma$  (mPa) applied at a frequency,  $\omega$  ( $\text{rad.s}^{-1}$ ) will create a reactionary strain,  $\gamma$  (mPa) with a smaller amplitude and associated phase lag,  $\delta$  (degrees) due to the non-ideal nature of the gels' viscoelastic properties (74).

A 1% w/w concentration was considered necessary to produce the consistency required for a functional eye gel as the initial 0.1% w/w gels produced were too fluid with viscosities akin to that of water. It has been hypothesised that a viscosity of 12-15 mPa.s is optimal for ophthalmic delivery (124,138), demonstrated through in vivo work with rabbits. A viscosity of around 20 mPa is known to be acceptable to patients (143), and preparations for ophthalmic instillation such as eye gels should ideally be less than 30 mPas to maximise patient comfort (135). The power law was used to quantify the flow type, as there was no apparent yield stress:

$$\sigma = \eta' \gamma^n$$

Where  $\sigma$  = shear stress (pa),  $\eta'$  = viscosity coefficient (Pa.s),  $\gamma$  = shear rate ( $\text{s}^{-1}$ ) and  $n$  = the rate index of pseudoplasticity.

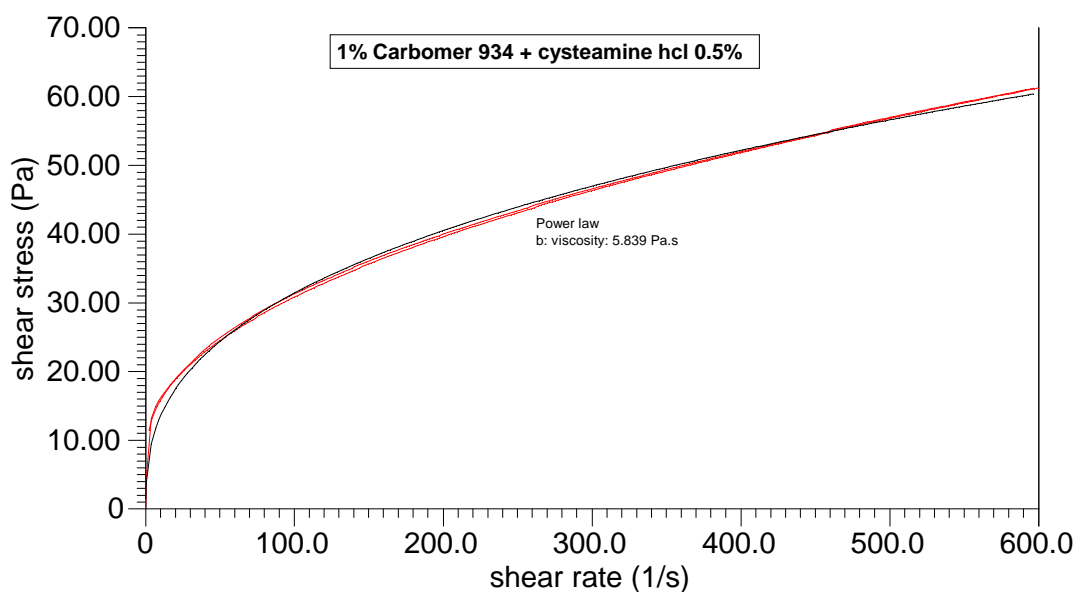


Figure 29. Rheology of 1% w/w carbomer 934 with 0.5% cysteamine hydrochloride.

Continuous flow measurements with a 1% w/w carbomer 934 gel and carbomer 934 gels containing cysteamine compounds are represented in Figure 30. This indicates an increase in consistency with addition of phe conjugate and cysteamine hydrochloride, and a slight decrease with inclusion of cysteamine (table 14). As all of the samples are at equal pH due to the use of SMPB, these differences may be due to strengthened network interactions for the conjugate and the hydrochloride, and decreased interactions for the cysteamine. This change in viscosity may also have been as a result of the salt in the actives causing the side chains to align against the backbone of the polymer structures, reducing flexibility (178). The use of ethanol as a cosolvent decreased the viscosity and the clarity of the gel.

Table 14. Viscosity coefficient values for carbomer 934 gels containing different cysteamine compounds (n = 3).

Gel active	Viscosity coefficient, $\eta'$ (Pa.s) ( $\pm$ SD)
No active	0.095 ( $\pm$ 0.03)
Cysteamine HCl	0.1 ( $\pm$ 0.02)
Cysteamine	0.9 ( $\pm$ 0.01)
Phe conjugate	0.095 ( $\pm$ 0.02)

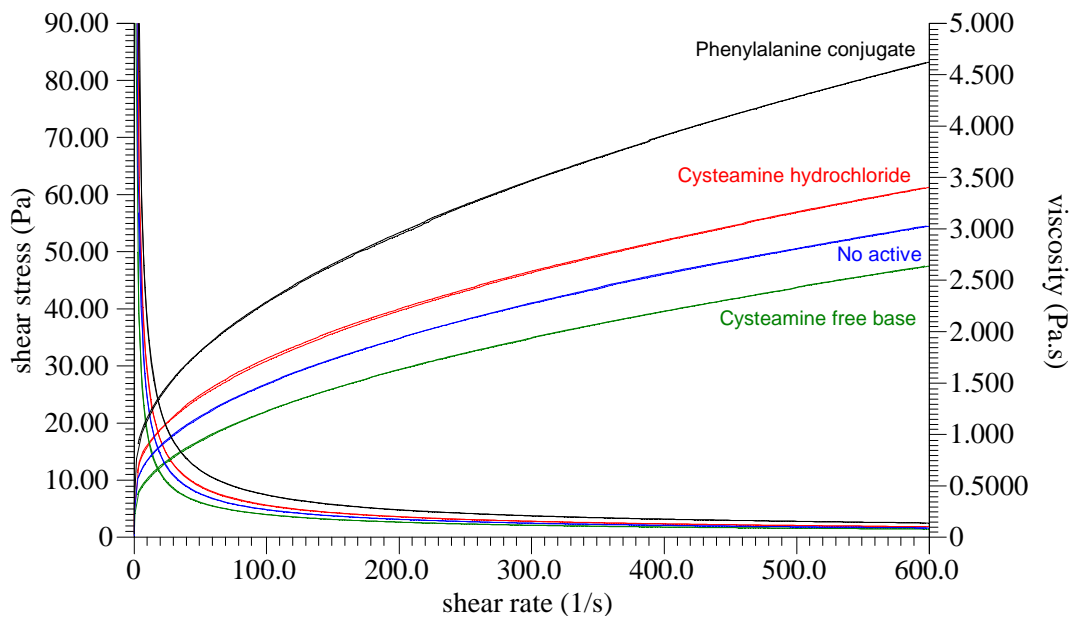


Figure 30. Continuous flow curves for carbomer 934 gels containing different cysteamine compounds at 34°C.

The oscillatory shear results provide information on the gel structure. When a stress is applied at a constant frequency, some of the energy is dissipated in viscous flow and the remainder is stored, which is recovered when the stress is removed. Viscosity and gel behaviour (viscoelasticity) can be examined by determining the effect that an oscillatory force has on the movement of the material. If the strain is within the linear viscoelastic region, and therefore the yield stress is not reached, then the sample is not destroyed. The storage modulus,  $G'$ , is a measure of 'dynamic rigidity', the amount of energy stored and recovered per cycle of deformation. The loss modulus,  $G''$ , is a measure of energy dissipated per cycle. A  $G'$  value greater than the  $G''$  value is indicative of secondary bond formation (124). Tan delta (loss tangent) gives information on the elasticity of a system, and can be calculated from the ratio:

$$\text{Tan } \delta = G''/G'$$

A  $\text{Tan } \delta$  less than 1 indicates a solid, elastic, gel-like network, whereas a  $\text{Tan } \delta$  greater than 1 indicates that the structure is more like that of a liquid (124). A  $\text{Tan } \delta$  value less than 1 is advantageous for mucoadhesive systems.

All of the carbomer 934 gels were found to exhibit a  $G'$  greater than  $G''$ , and a  $\tan \delta$  less than 1. This is indicative of secondary bond formation (74,143). Results from the oscillatory measurements described in figure 31 and table 15 indicate very little effect of cysteamine hydrochloride, phe conjugate and cysteamine on the loss tangent, suggesting the same degree of elasticity for all carbomer 934 gels studied. A degree of elastic behaviour at low shear stress reflects the weak gel properties of these formulations. This propensity to form a gel under conditions of zero to low shear is desirable for increased residence on the ocular surface. The oscillatory results presented clearly indicate that the addition of cysteamine actives (cysteamine, cysteamine hydrochloride and phe conjugate) to carbomer 934 gels does not appear to destroy these weak gel properties. The results for the gel where ethanol was used as a cosolvent were comparable to those with no active.

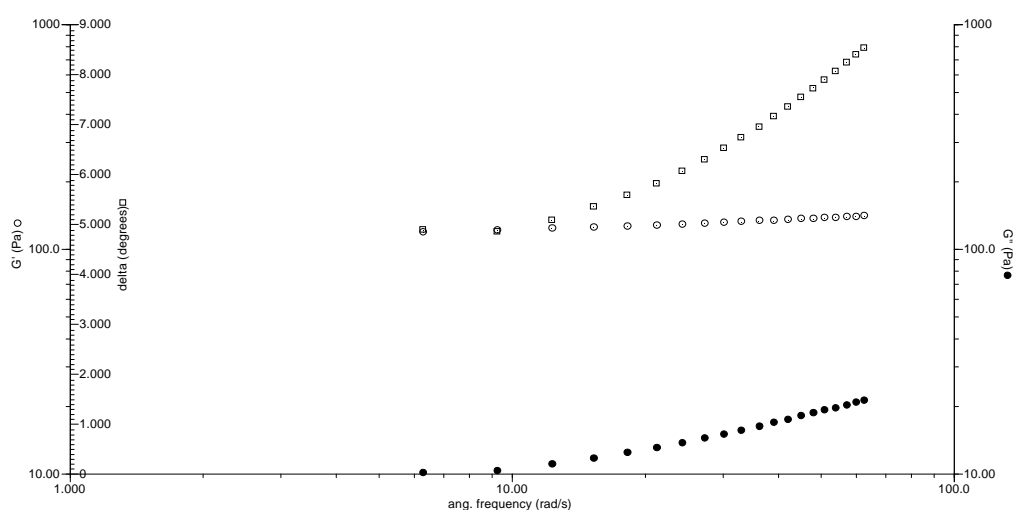


Figure 31. 1% w/w carbomer 934 with 0.5% cysteamine hydrochloride oscillation results.

Table 15. Oscillatory data for carbomer 934 gels ( $n = 3$ )( $\pm$  SD).

Gel	$G'$ (Pa)	$G''$ (Pa)	Tan $\delta$
Carbomer 934 no active	70 ( $\pm$ 1.8)	6 ( $\pm$ 0.5)	0.09 ( $\pm$ 0.02)
Carbomer 934 cysteamine HCL	119 ( $\pm$ 2.1)	10 ( $\pm$ 0.4)	0.09 ( $\pm$ 0.01)
Carbomer 934 phe conjugate	65 ( $\pm$ 1.1)	6 ( $\pm$ 0.6)	0.10 ( $\pm$ 0.02)
Carbomer 934 cysteamine	43 ( $\pm$ 0.7)	4 ( $\pm$ 0.8)	0.09 ( $\pm$ 0.02)

#### 4.3.3.2 Xanthan gum gels

Xanthan gum also displayed shear-thinning behaviour, with a slight yield stress. It was also mildly thixotropic as previously reported (179) (Figure 32). These characteristics will be useful in preventing dosage loss during initial installation into the eye.

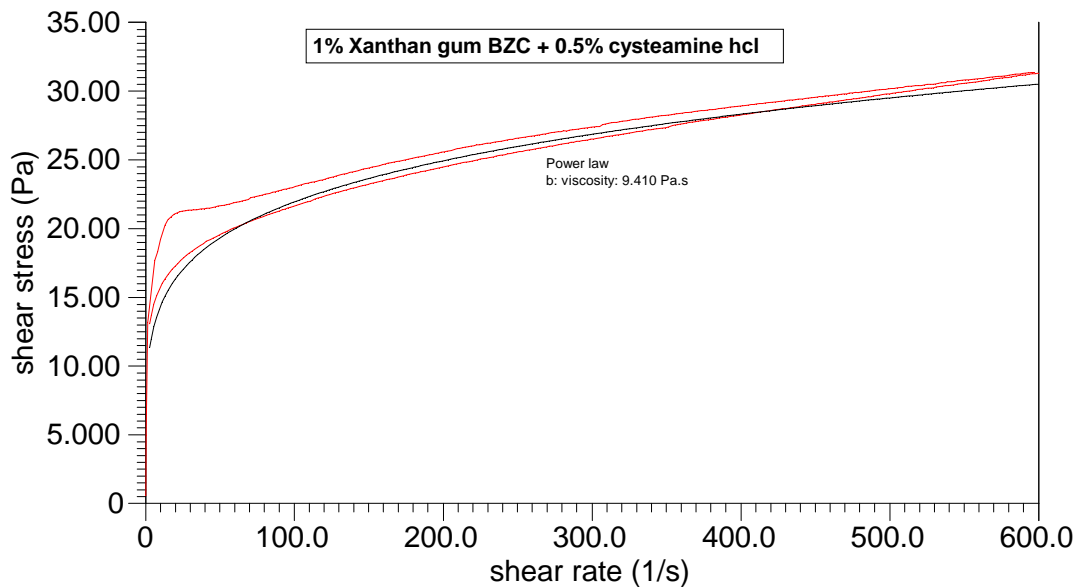


Figure 32. 1% w/w xanthan gum with 0.5% cysteamine hydrochloride.

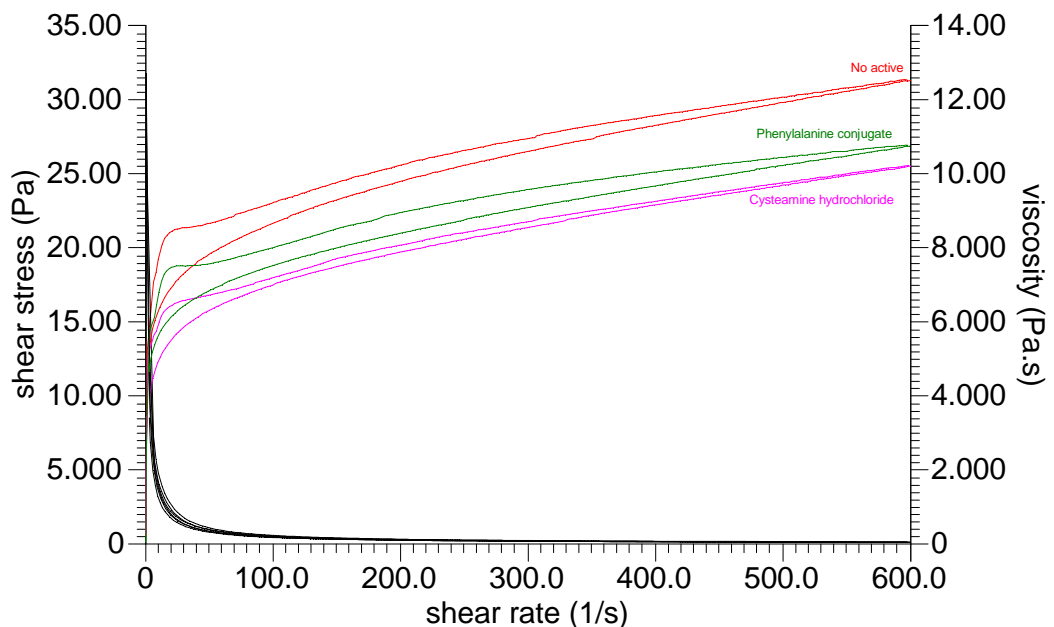


Figure 33. Effect of active addition on xanthan gels.

Table 16. Viscosity coefficient values for xanthan gels containing different cysteamine compounds (n = 3).

Gel active	Viscosity coefficient, $\eta'$ (Pa.s) ( $\pm$ SD)
No active	0.05 ( $\pm$ 0.01)
Cysteamine HCl	0.05 ( $\pm$ 0.01)
Phe conjugate	0.05 ( $\pm$ 0.02)

The addition of actives phe conjugate and cysteamine hydrochloride to the gel base does not alter the consistency of the gels (figure 33 and table 16). This may be due to strong interactions within the xanthan double helix structure (143).

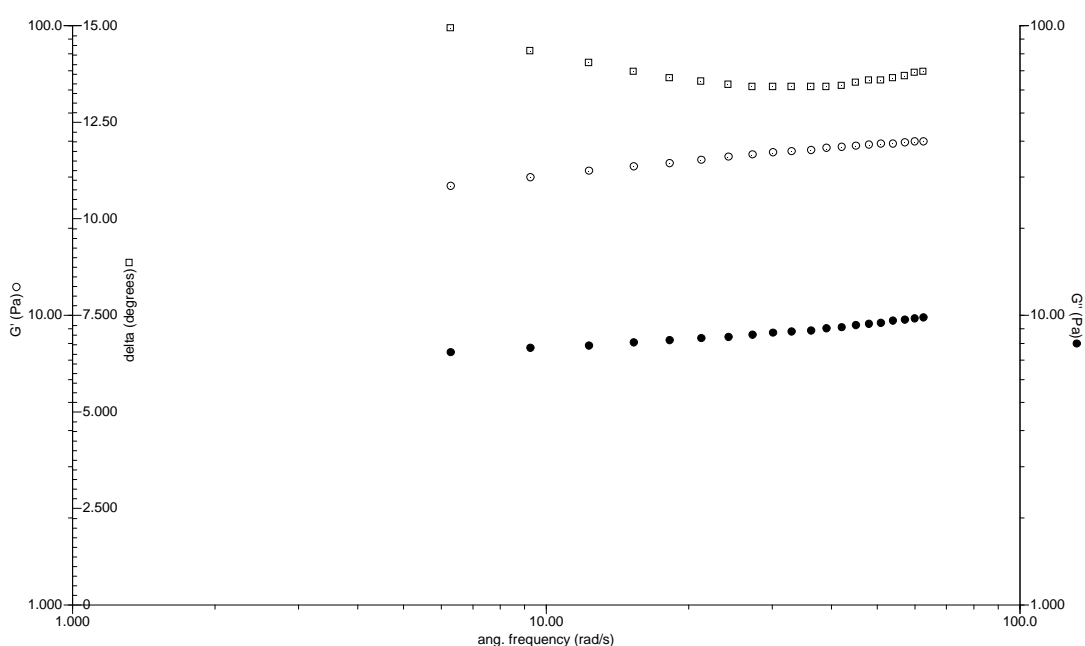


Figure 34. Oscillatory shear data for xanthan gels.

Table 17. Oscillatory data for xanthan gels (n = 3) ( $\pm$  SD).

Gel	G' (Pa)	G'' (Pa)	Tan $\delta$
Carbomer 934 no active	27 ( $\pm$ 0.2)	7.9 ( $\pm$ 0.1)	0.29 ( $\pm$ 0.01)
Carbomer 934 cysteamine HCL	28 ( $\pm$ 0.2)	7.5 ( $\pm$ 0.4)	0.27 ( $\pm$ 0.03)
Carbomer 934 phe conjugate	27 ( $\pm$ 0.3)	7.2 ( $\pm$ 0.2)	0.27 ( $\pm$ 0.01)

All of the xanthan gum gels were found to exhibit a  $G'$  greater than  $G''$ , and a  $\tan \delta$  less than 1 (figure 34 and table 17). This indicates that very little change in structure was produced by the addition of actives, and that the gel network remained intact.

#### 4.3.3.3 HPMC gels

HPMC at 1% w/v was found to behave as a Newtonian fluid, and had the appearance of water as previously reported at low concentrations (180) (Figure 35). There was no yield stress or thixotropy. After installation into the eye, this gel will most likely be lost through the nasal-lachrymal ducts, as it is weakly bioadhesive.

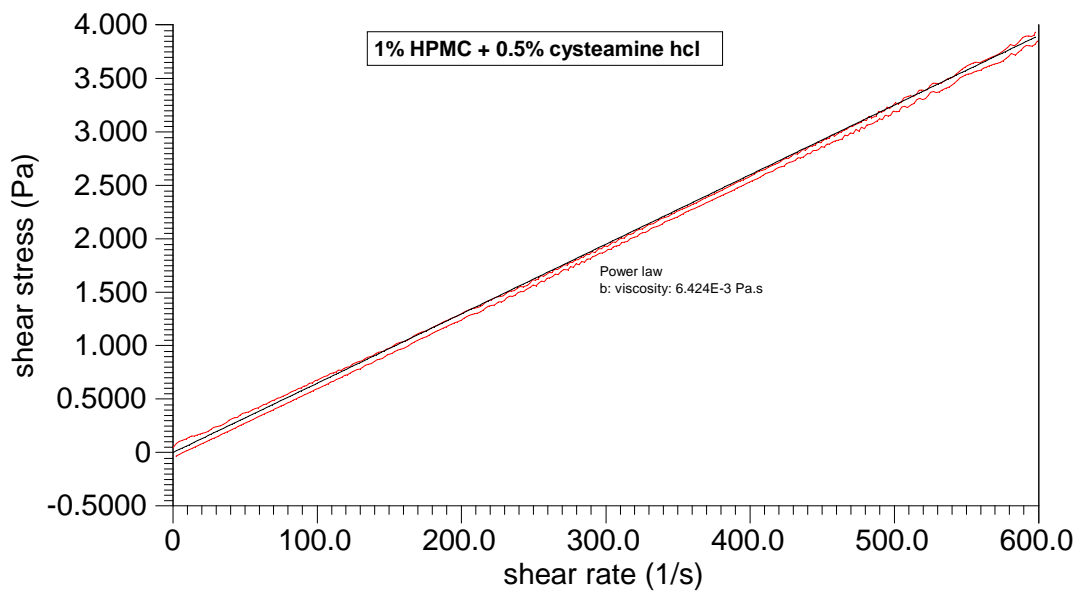
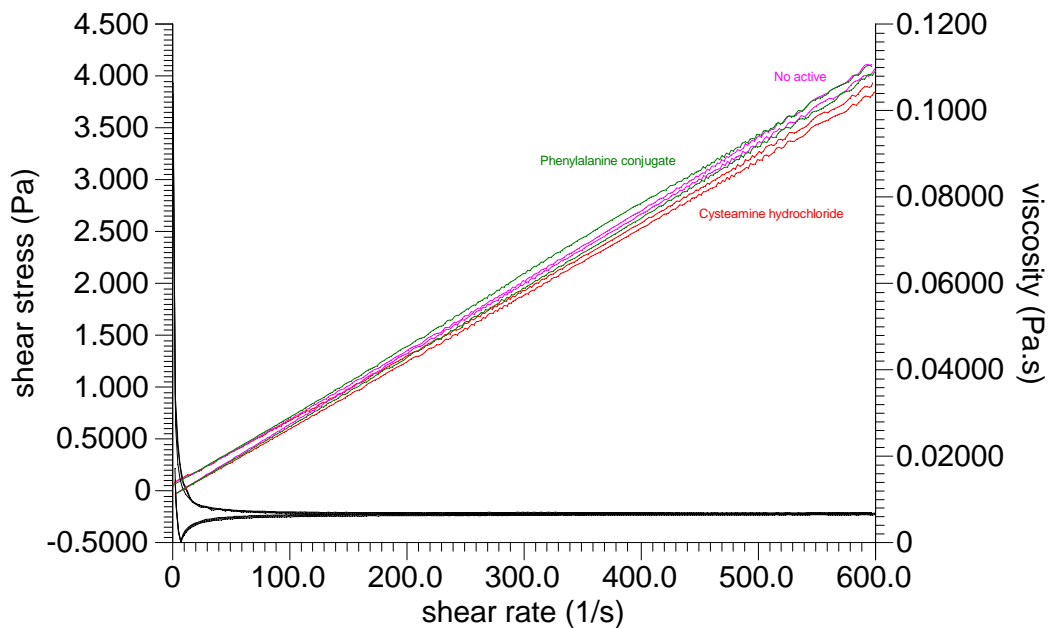


Figure 35. 1% w/v HPMC displayed a Newtonian rheology.



c  
Figure 36. Effect of active addition on the viscosity of HPMC gels.

The viscosity is almost unchanged upon addition of the actives, with cysteamine hydrochloride producing a marginal reduction in viscosity (figure 36 and table 18). HPMC is unaffected by pH, temperature or ionic changes.

Table 18. Viscosity coefficient values for HPMC gels containing different cysteamine compounds (n = 3).

Gel active	Viscosity coefficient, $\eta'$ (mPa.s)( $\pm$ SD)
No active	6.5 ( $\pm$ 0.01)
Cysteamine HCl	6.7 ( $\pm$ 0.01)
Phe conjugate	6.6 ( $\pm$ 0.02)

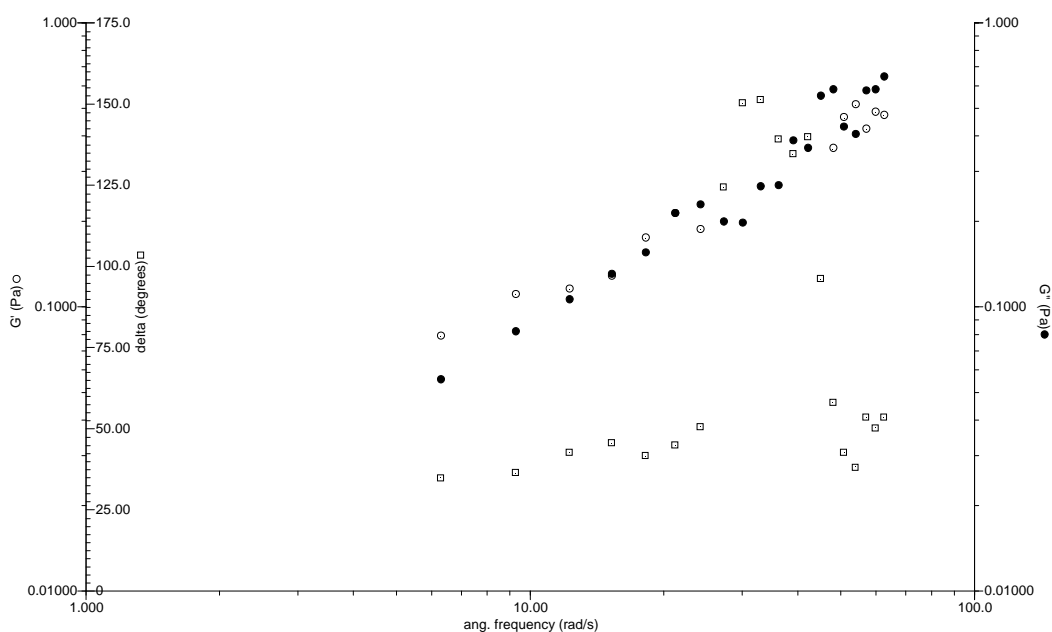


Figure 37. 1% w/v HPMC with 0.5% cysteamine hydrochloride oscillation results.

The cross-over observed between  $G'$  and  $G''$  in figure 37 is indicative of the destruction of secondary bonds within the HPMC gel (124). The gel would lose viscosity in the eye when sheared by the action of the eye lids, allowing it to flow out of the eye unless the gel network was quickly reformed. The HPMC gels were found to display neither  $G'$  greater than  $G''$ , nor a  $\tan \delta$  less than 1, suggesting no secondary bond formation or gel-like networks. The exception to this was when cysteamine hydrochloride was added, as demonstrated in figure 37 and table 19.

Table 19. Oscillatory data for HPMC gels (n = 3) ( $\pm$  SD).

Gel	G'(Pa)	G''(Pa)	Tan $\delta$
HPMC no active	0.05 ( $\pm$ 0.01)	0.07 ( $\pm$ 0.01)	1.48 ( $\pm$ 0.2)
HPMC cysteamine HCL	0.08 ( $\pm$ 0.01)	0.06 ( $\pm$ 0.01)	0.7 ( $\pm$ 0.1)
HPMC phe conjugate	0.005 ( $\pm$ 0.002)	0.05 ( $\pm$ 0.01)	8.9 ( $\pm$ 0.3)

#### 4.3.4 Dissolution studies

##### 4.3.4.1 Phe conjugate as active

Figures 38 to 40 show the percentage release of the phe conjugate from each gel. The release from the gel was analysed by the Higuchi method (Table 21). The average area of each membrane rod is shown in table 20.

Table 20. Average membrane rod areas for each gel (n = 3).

Gel	Average membrane rod area (cm <sup>2</sup> )( $\pm$ SD)
Carbomer 934, phe conjugate	20.32 ( $\pm$ 0.15)
Xanthan gum, phe conjugate	19.97 ( $\pm$ 0.15)
HPMC, phe conjugate	23.45 ( $\pm$ 0.15)
Carbomer 934, cysteamine HCl	6.28 ( $\pm$ 0.12)

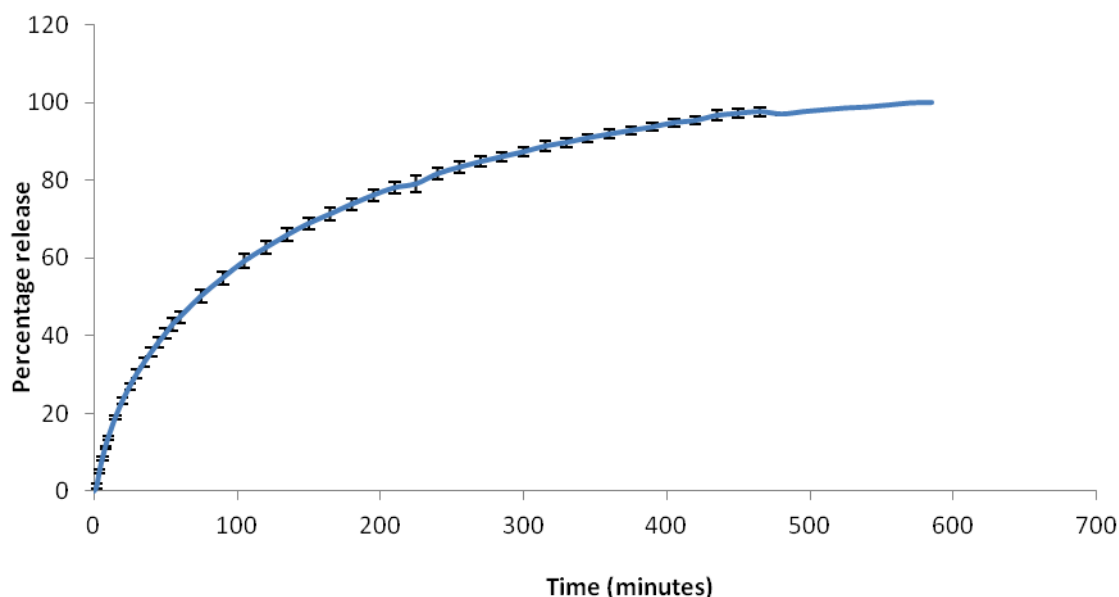


Figure 38. Percentage release of phe conjugate from carbomer 934.

On average 95% of the phe conjugate was released from the carbomer 934 gels after 420 minutes.

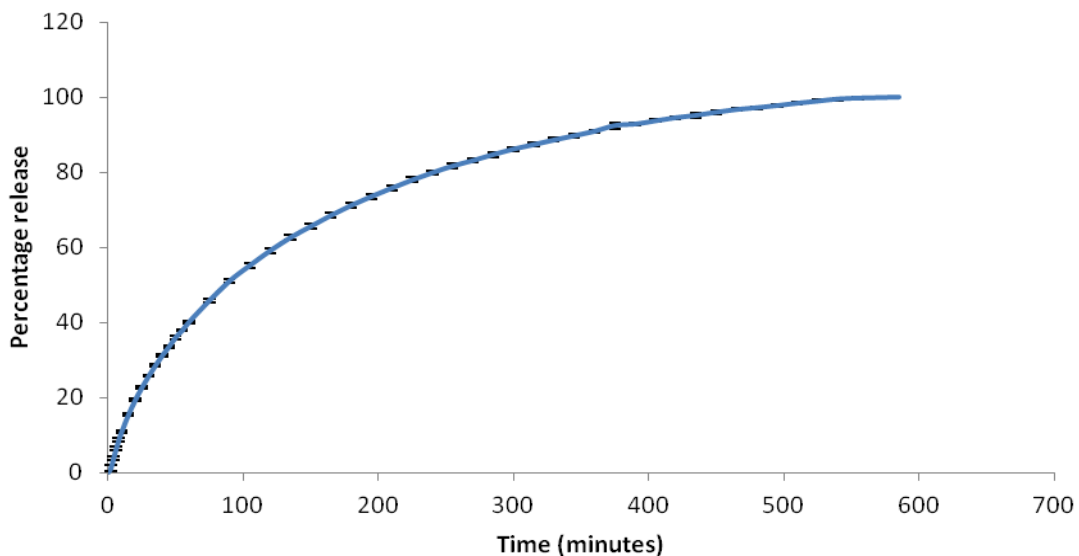


Figure 39. Percentage release of phe conjugate from xanthan gum.

The xanthan gum gels released 95% of phe conjugate after 435 minutes on average. The triplicate results were identical.

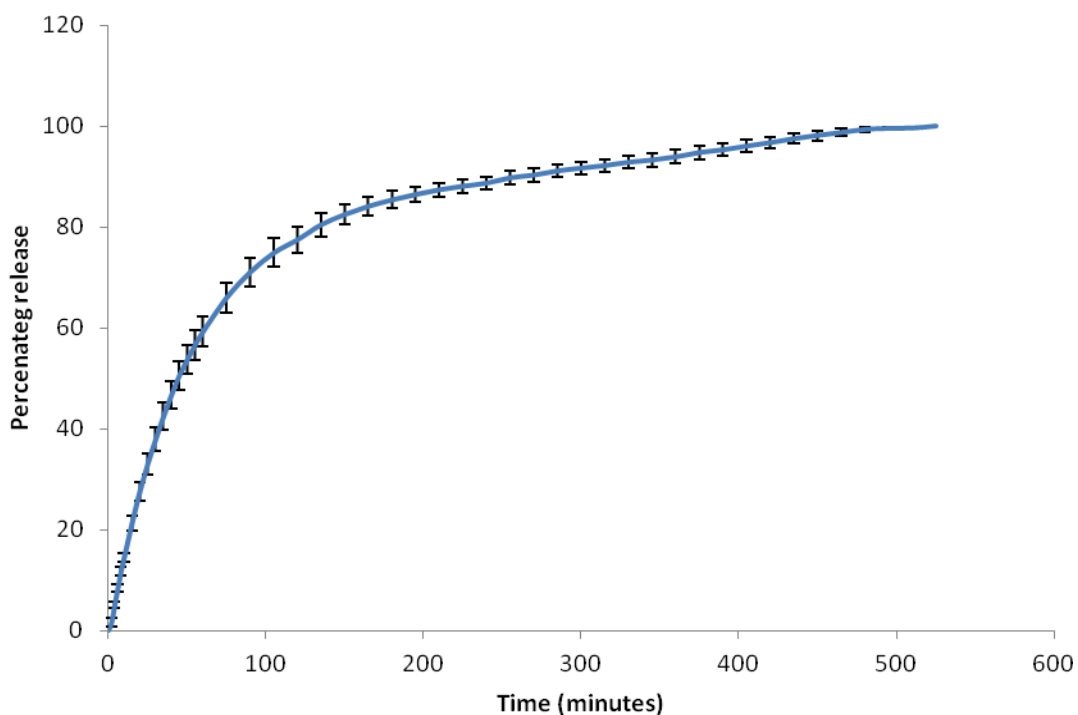


Figure 40. Percentage release of phe conjugate from HPMC.

HPMC released 95% of phe conjugate after 390 minutes on average.

Table 21. Results of the Higuchi model analysis on each of the three gels.

Gel sample time (minutes)	Higuchi model, $k_H$					
	2	35	75	240	420	540
Carbomer 934, phe conjugate	0.05	0.08	0.08	0.07	0.06	0.04
Xanthan gum, phe conjugate	0.06	0.08	0.09	0.08	0.07	0.07
HPMC, phe conjugate	0.07	0.11	0.12	0.09	0.07	0.07*
Carbomer 934, cysteamine HCl	0.25	0.24	-	-	-	-

\*495 minutes

The in vitro release from each gel could be categorised as first-order Fickian diffusion. This is indicative of reversible interactions between the polymer matrix and the active and uninterrupted drug release from the gels.

The dissolution tests for the three gels demonstrated that the gels released the phe conjugate over a prolonged period of time. This is in support of previous studies which demonstrated sustained drug release over an 8-hour period from gels for ophthalmic delivery (181). This slow release of drug may be as a result of ionic interactions between the negatively charged polymers carbomer and xanthan and the positively charged phe conjugate (124). Where the constant administration of eye-drops is the routine method of drug delivery, as is the case with cystinosis, the development of a controlled release formulation is desirable. These results indicate that this may be achieved using ophthalmic gels as a vehicle for ophthalmic delivery.

#### 4.3.4.2 Cysteamine hydrochloride as active

Figure 41 shows the release of cysteamine hydrochloride from carbomer 934 gels.

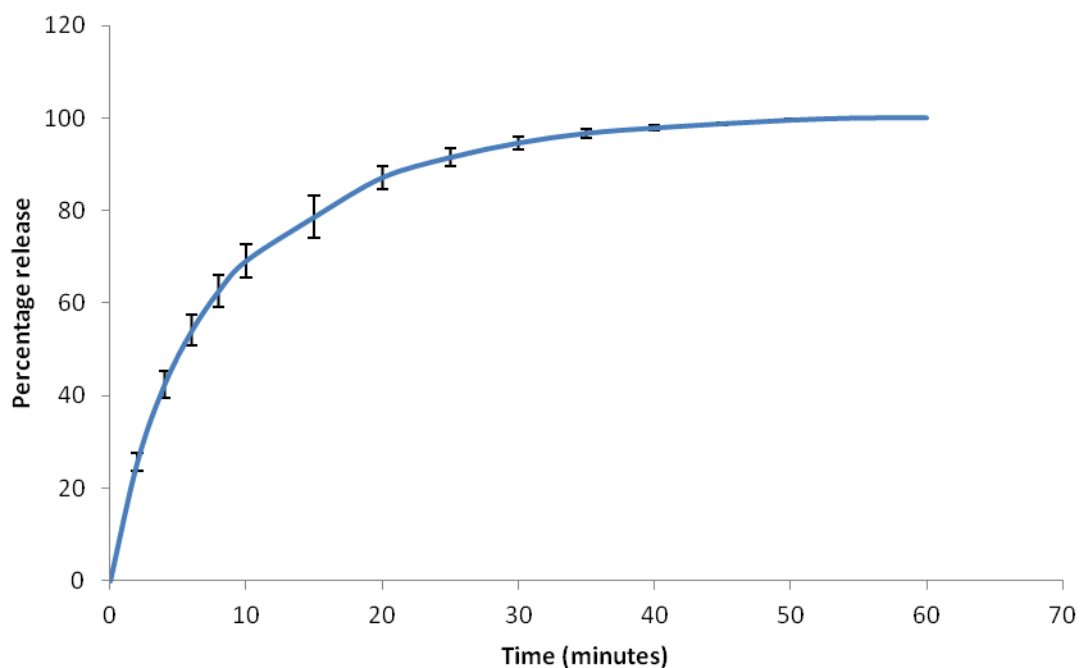


Figure 41. Percentage release of cysteamine hydrochloride from carbomer 934 gels.

On average, 95% of the cysteamine hydrochloride was released after 30 minutes. This is a faster release than was recorded with the phe conjugate, although in combination with the bioadhesive properties, this gel should be a marked improvement over traditional eye drops. The work conducted by Bozdog et al in 2008 (51), showed an incompatibility between cysteamine hydrochloride and carbopol. However, they did achieve in vitro release over 8 hours using HPMC.

It is hypothesised that the faster release rate observed with cysteamine hydrochloride is due to the smaller, more hydrophilic nature of the drug when compared to the phe conjugate.

Using both the phe conjugate and cysteamine hydrochloride as actives, equilibrium solubility has been displayed, where drug particles reach equilibrium between the gel and the aqueous media. In vivo, the drug would be absorbed by the cornea or surrounding tissues, and allow more drug to be released by the gel.

#### 4.3.5 Bioadhesion studies

PAA has been shown to have excellent bioadhesive properties in comparison to other gels as reported by Slovin and Robinson (121) and its ability to increase ocular residence time, relative to traditional eye drops, has also been reported (182). It should be noted however that the negative charge on the corneal epithelium (183,184) would be expected to provide a natural barrier to adhesion of a highly anionic polymer such as PAA. In practice, the significant yield stress of PAA gels, particularly at a concentration of 1.0% w/v, would appear to counteract this effect causing the gel to remain on the surface of the corneal epithelium despite microadhesion being weak or non-existent.

The force required to remove the gels from the tissue corresponds to secondary, chemical interactions, while the AUC values relate to physical entanglements between the polymer gel and the tissue (153,169). The Mann-Whitney analysis reveals significant bioadhesion between the corneal tissue and the carbomer gels containing both phe conjugate and cysteamine hydrochloride, although this is not the case for AUC (Table 22). The agar tests confirm these results to some extent, with cysteamine hydrochloride gels showing significant bioadhesion for AUC data. Physical entanglements will probably occur in vivo, due to the presence of mucus.

Table 22. Results of bioadhesion assay for carbomer 934.

Carbomer 934	Force (N)	AUC
Tissue vs plain gel	0.067 <sup>b</sup>	0.205 <sup>b</sup>
Tissue vs gel with cysteamine HCL	0.107 <sup>b</sup>	0.177 <sup>a</sup>
Tissue vs gel with phe conjugate	0.107 <sup>b</sup>	0.196 <sup>b</sup>
Agar vs plain gel	0.134	0.29 <sup>b</sup>
Agar vs gel with cysteamine HCL	0.177 <sup>a</sup>	0.35 <sup>b</sup>
Agar vs gel with phe conjugate	0.159 <sup>a</sup>	0.27 <sup>b</sup>

p<0.05 a, p<0.01 b.

The Mann-Whitney analysis of the xanthan gum gels shows significant bioadhesion for the tissue tests only, while the agar tests are devoid of bioadhesion (Table 23).

Table 23. Results of bioadhesion assay for xanthan gum gels.

Xanthan gum	Force (N)	AUC
Tissue vs plain gel	0.051 <sup>b</sup>	0.091 <sup>b</sup>
Tissue vs gel with cysteamine HCL	0.108 <sup>b</sup>	0.150 <sup>b</sup>
Tissue vs gel with phe conjugate	0.76 <sup>b</sup>	0.145 <sup>b</sup>
Agar vs plain gel	0.276 <sup>b</sup>	0.39 <sup>b</sup>
Agar vs gel with cysteamine HCL	0.242 <sup>b</sup>	0.314 <sup>b</sup>
Agar vs gel with phe conjugate	0.223 <sup>b</sup>	0.28 <sup>b</sup>

p<0.05 a, p<0.01 b.

Analysis of the HPMC gels show bioadhesion between the agar plates and all gel types. However, the tissue tests show significant bioadhesion only with cysteamine hydrochloride (force) and the phe conjugate (AUC) (Table 24).

Table 24. Results of bioadhesion assay for HPMC gels.

HPMC	Force (N)	AUC
Tissue vs plain gel	0.076	0.051 <sup>b</sup>
Tissue vs gel with cysteamine HCL	0.081 <sup>a</sup>	0.048 <sup>b</sup>
Tissue vs gel with phe conjugate	0.065 <sup>a</sup>	0.061 <sup>b</sup>
Agar vs plain gel	0.095 <sup>b</sup>	0.091 <sup>b</sup>
Agar vs gel with cysteamine HCL	0.110	0.098 <sup>b</sup>
Agar vs gel with phe conjugate	0.161	0.113 <sup>b</sup>

p<0.05 a, p<0.01 b.

It has been reported that pH, ionic strength, molecular weight and chain flexibility all affect the bioadhesive properties of PAA gels (155,185) however, it appears that the mechanisms of polymer attachment to mucosal surfaces are still not fully understood (186). There is speculation that bioadhesion is the net effect of many physicochemical factors that include attractive forces such as hydrophobic interactions, hydrogen bonding and van der Waals attraction; physical entanglement of polymer chains via diffusional processes and electrostatic interaction of an attractive or repulsive nature all contribute to the bioadhesive process. It appears that the inherent rheological properties of ophthalmic gels may also have a decisive role to play with respect to improved residence on the eye. The precise reasons for the apparent bioadhesiveness of gels requires more study (121,132).

Carbomer 934 and xanthan gum gels both display excellent bioadhesion, providing the possibility of sustained release through improved residence time. HPMC displayed the weakest bioadhesion, possibly due to its low

viscosity and non-ionic nature. This finding is in agreement with other studies (138). Carbomer 934 has been shown to be less mucoadhesive than another carbomer grade, 974, which is manufactured without the use of benzene (123). While the 934 grade is cross linked with allyl sucrose and polymerised in benzene, the 974 grade is cross linked with allyl penta erythritol and polymerised in ethyl acetate.

The presence of thiol groups in cysteamine hydrochloride is likely to aid the bioadhesion of the gels to the corneal epithelium, by forming disulphide bonds with the thiols of the lachrymal mucus (133). In addition, tear fluid contains positive ions (cations) while lachrymal mucus contains negative ions (anions), allowing various ionic interactions to occur, regardless of the electric charge on the polymer used (138). These interactions will increase the corneal residence time, further improving cysteamine bioavailability. Physical entanglements are also likely to occur between the mucin glycoproteins and polymer chains in vivo, thereby strengthening the bioadhesion effect.

#### **4.3.5.1 Oscillation rheology**

The absence of rheological synergy, observed as values for  $\Delta G'$  and  $\Delta G''$  below 100% under all test conditions (table 25), may be as a result of ions in commercially-prepared mucins (155,156). The ions released through the extraction process can interfere with and disrupt the gel structure. Mucus rheology is also affected by the mucins composition and glycosilation, degree of hydration and ionic composition (123).

Table 25. Synergy tests using oscillatory rheology (selected data only, n = 3, ± SD).

Gel/mucus	G'(Pa)	G''(Pa)	ΔG'(Pa)	ΔG''(Pa)
Carbomer 934 1% w/w no active	118.7	10.15	119.31	12.94
Mucus	0.61	2.79	(±1.2)	(± 0.4)
Carbomer gel no active, mucin 50:50	0.88	1.27	0.74%	9.8%
Carbomer gel phe conjugate, mucin 50:50	0.90	1.27	0.75%	9.8%
Carbomer gel no active, mucin 1:4	0.24	1.43	0.2%	11.1%
Carbomer gel no active, mucin 4:1	12.51	3.78	10.49%	29.2%

Close contact between the gel and mucus layer (particularly if the mucus layer becomes dehydrated) can promote interdiffusion and entanglements between polymer and mucin chains which can strengthen the mucoadhesive bond (123). Carboxylic groups along the polymer chain can further strengthen the mucoadhesive joint by hydrogen bonding with the mucin layer.

#### 4.3.6 Stability tests

The average storage temperature for all samples over the four-month stability test period was 4.5°C.

##### 4.3.6.1 Carbomer 934

Figures 42 to 45 show the plots from the rheological tests of the carbomer gels over time.

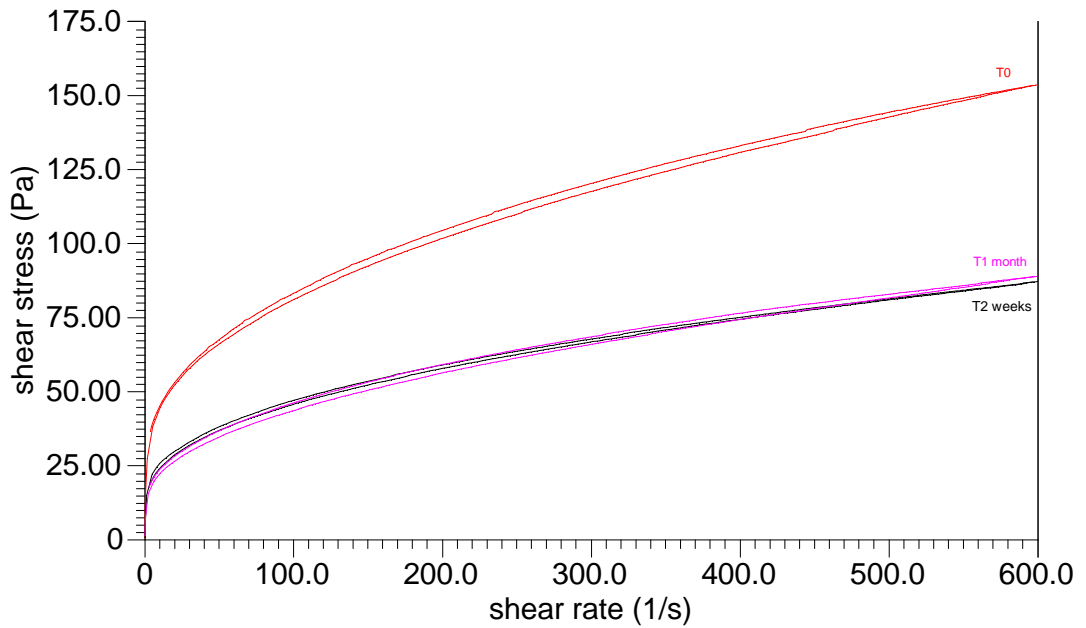


Figure 42. Carbomer 934 gel stability containing no active.

The reduction in viscosity observed between time zero and two weeks is possibly due to bacterial contamination causing polymer degradation.

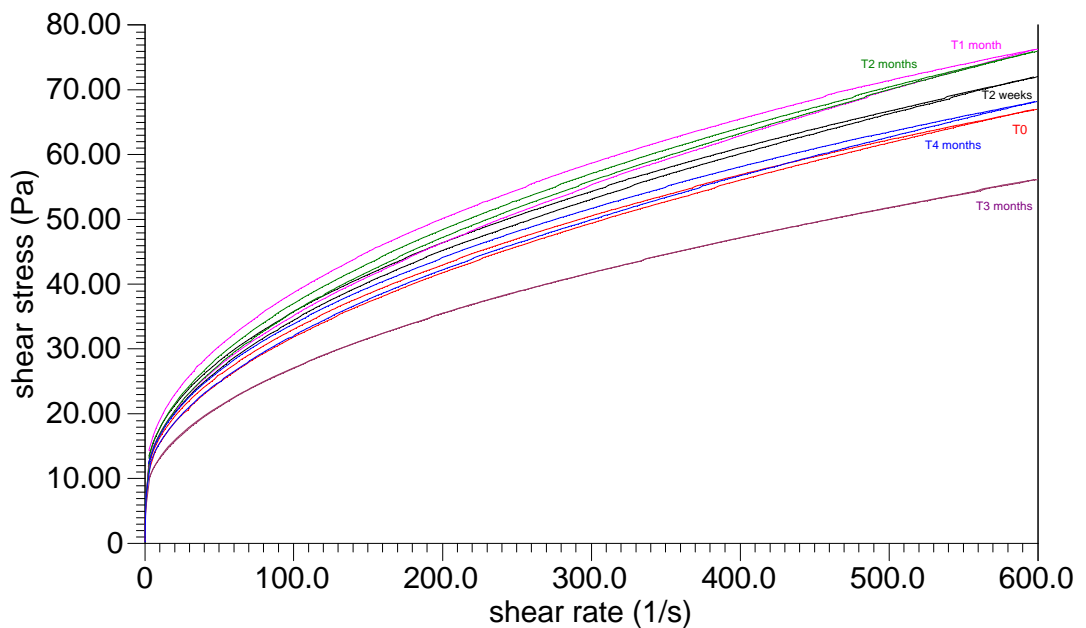


Figure 43. Carbomer gel stability over time containing phe conjugate.

The phe conjugate imparts a greater stability to the gel, observed as a reduction in viscosity variation over time when compared to carbomer gel alone (figure 42). This may be as a result of the presence of salts in the phe conjugate strengthening the polymer structure.

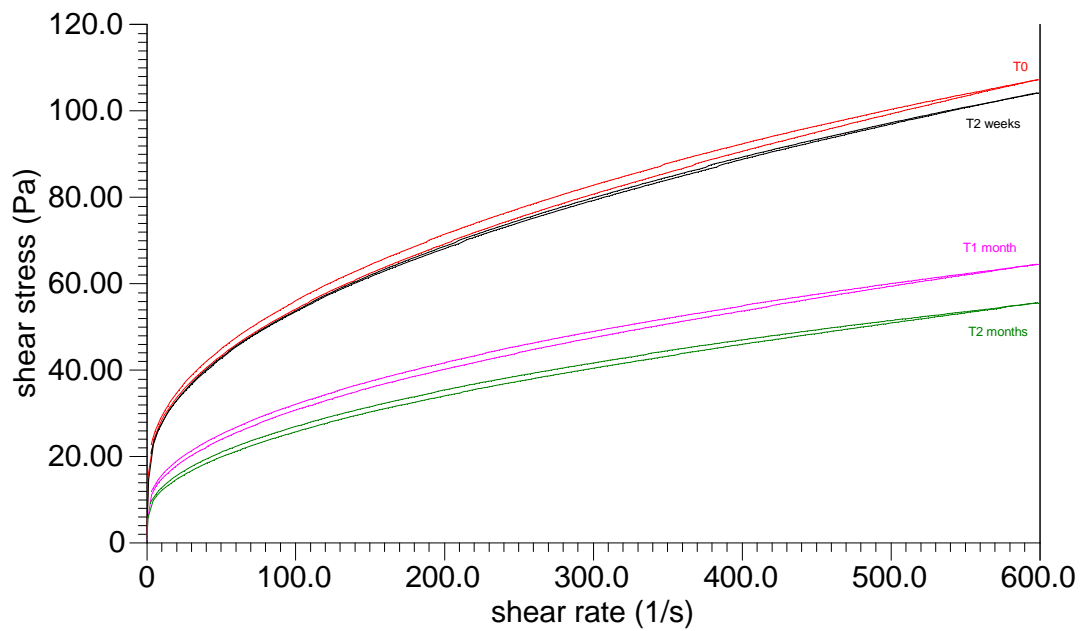


Figure 44. Carbomer gel stability over time containing cysteamine hydrochloride.

There has been a decrease in viscosity over time, particularly between 2 weeks and 1 month.

The carbomer 934 gels containing the phe conjugate as the active are the most stable, with almost no change observed in the rheology over four months. The gels containing cysteamine hydrochloride appeared stable at 2 weeks, but by 4 weeks the rheology had altered dramatically. This may be due to the presence of salts in the actives affecting the stability of the gel structure.

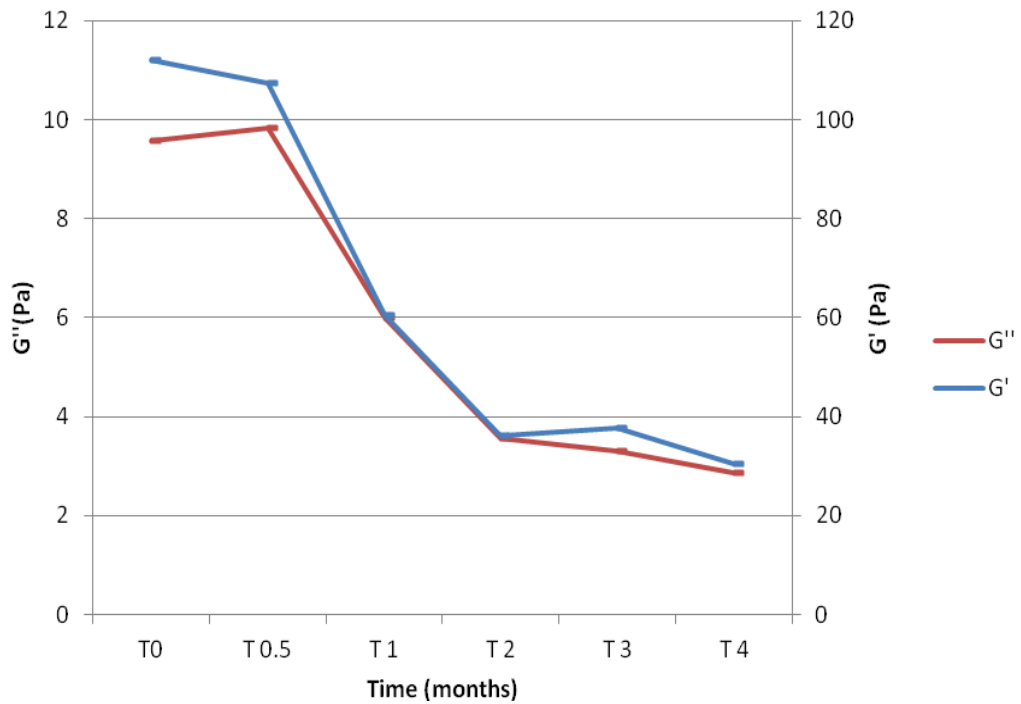


Figure 45. Carbomer 934 oscillation data over time.

The oscillation results support the continuous shear measurements. All of the carbomer gels still displayed a  $G'$  greater than  $G''$ , and a  $\tan \delta$  less than 1 after 12 months, demonstrating that the gel structure was intact.

#### 4.3.6.2 Xanthan gum

Figures 46-48 demonstrate the rheology of the xanthan gum gels over time.

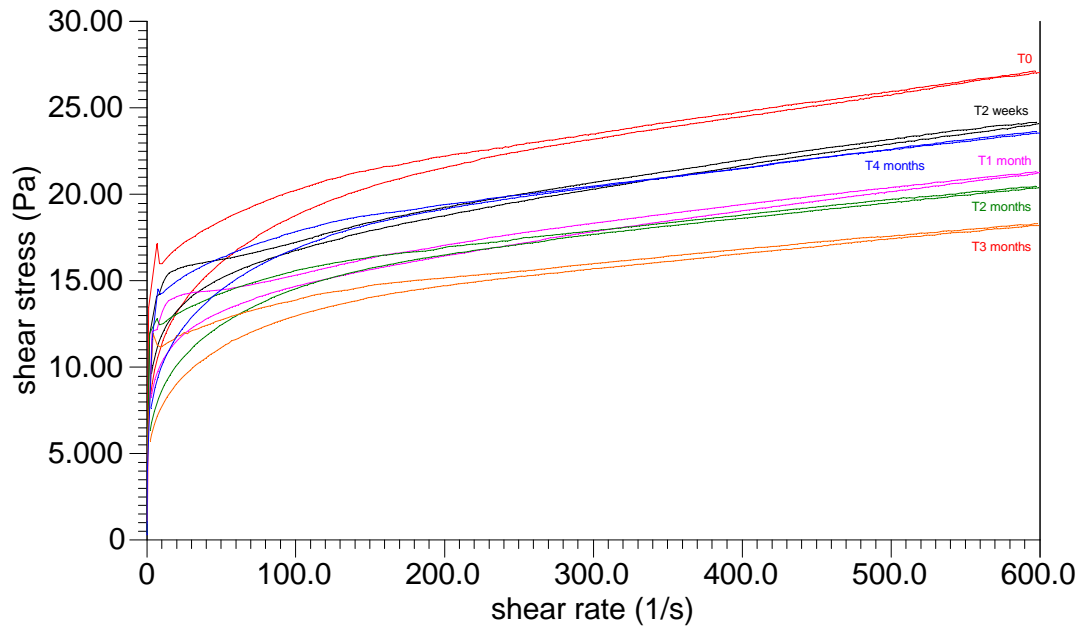


Figure 46. Effect of time on the viscosity of xanthan gels containing no active.

This reduction in viscosity over time may be as a result of degradation of the polymer over time due to hydrolysis.

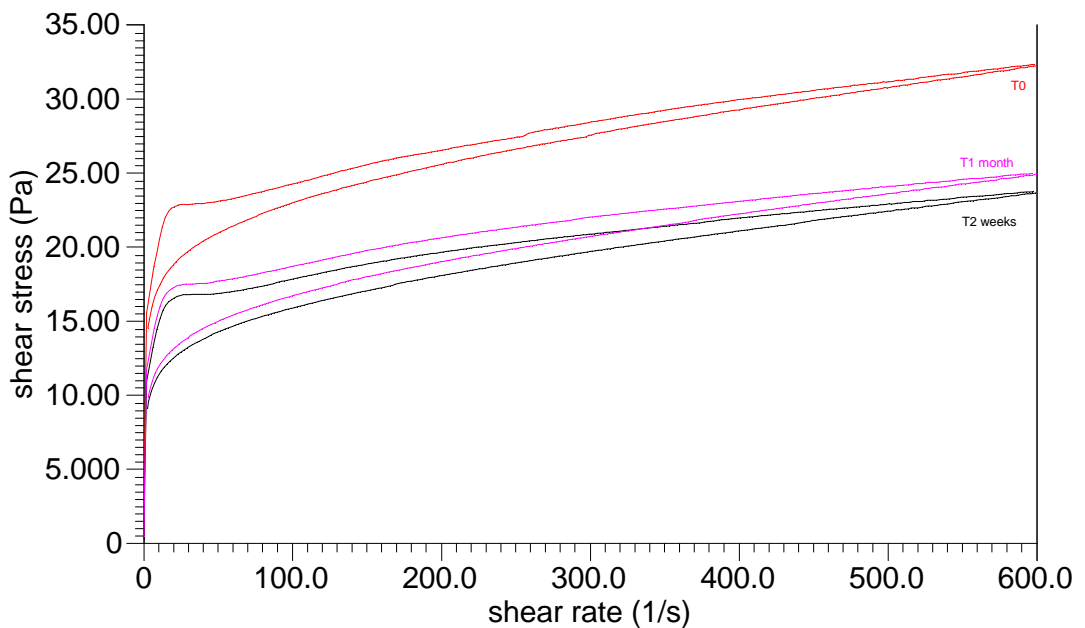


Figure 47. The rheology of xanthan gum containing cysteamine hydrochloride over time.

The reduction in viscosity observed between time zero and two weeks may be as a result of polymer degradation.

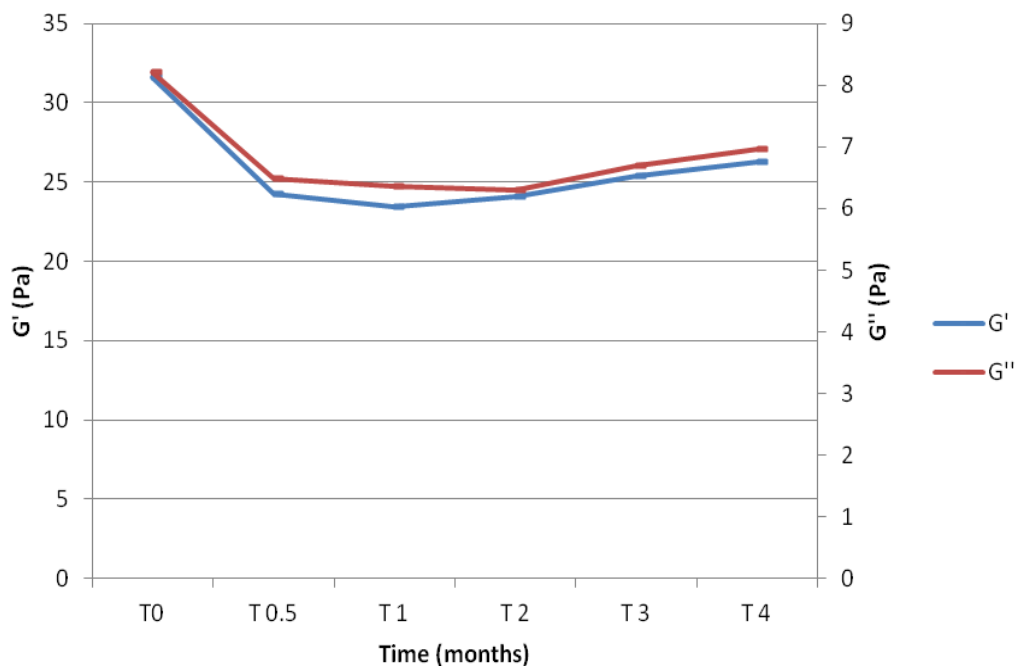


Figure 48. Oscillatory results for xanthan gum over time.

The lack of a gel network, illustrated by  $G'' > G'$ , suggests that the xanthan gels are instable over time. The presence of benzalkonium chloride may have destroyed any secondary bonds which were present.

#### 4.3.6.3 HPMC

Figures 49-51 display the rheology of HPMC gels over time.

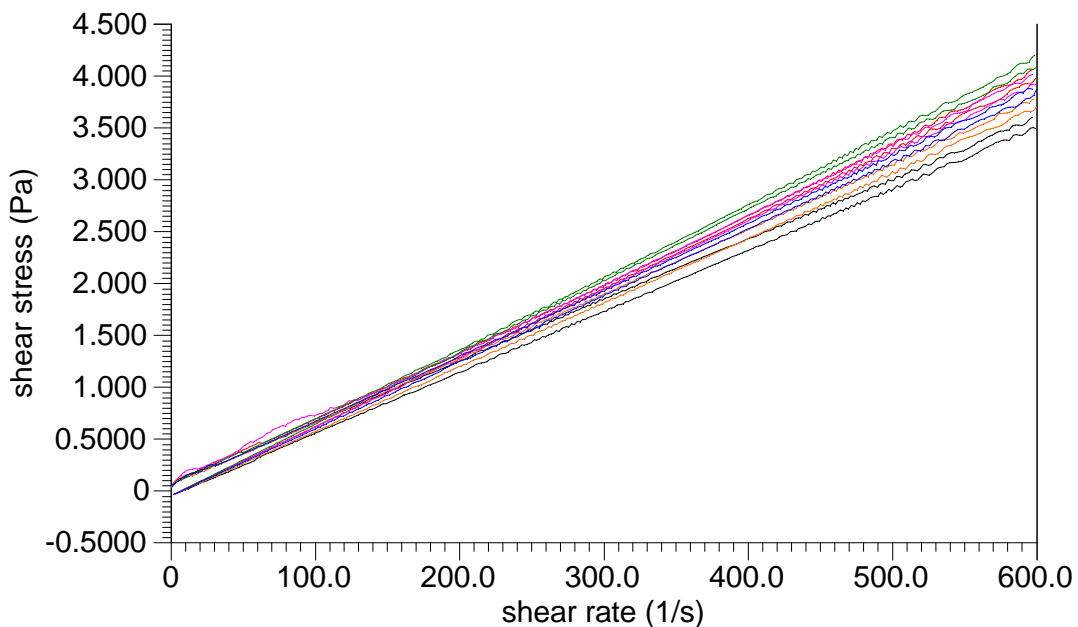


Figure 49. Rheology of HPMC containing no active over time.

There is virtually no change in the rheology of the gels over time, suggesting that HPMC gels are very stable over four months.

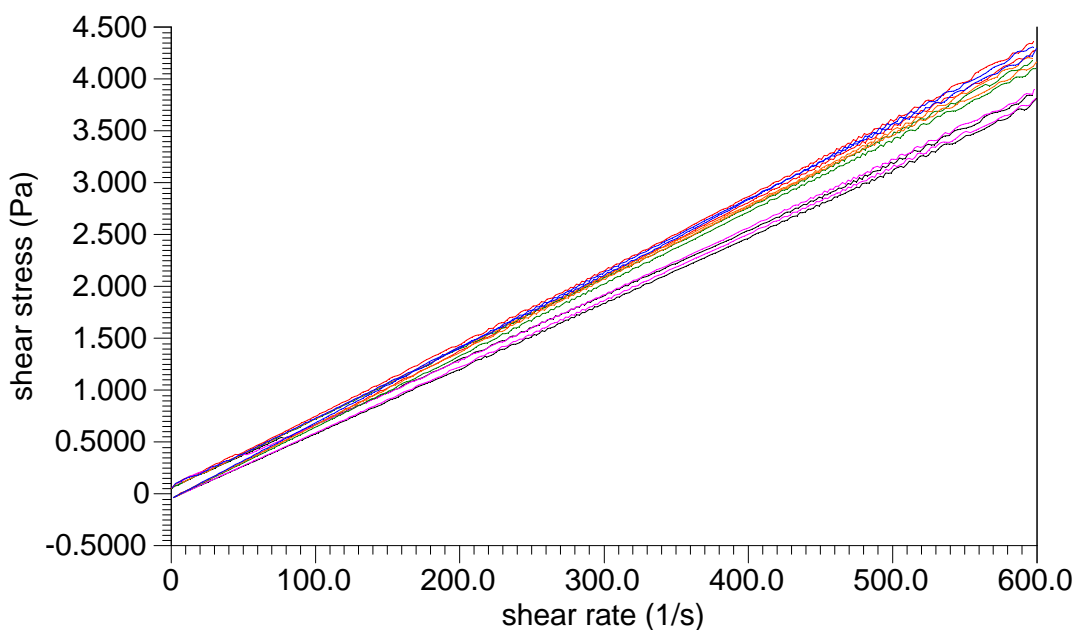


Figure 50. The rheology of HPMC over time, containing cysteamine hydrochloride.

The HPMC gels containing cysteamine hydrochloride appear to be as stable over time as the gel alone without any active component (figure 49).

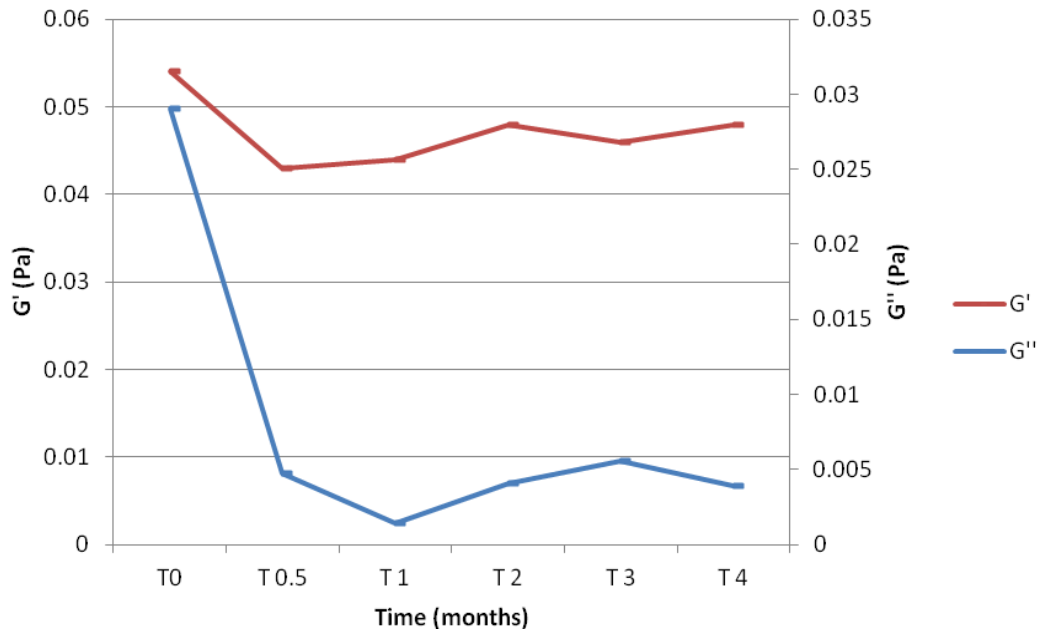


Figure 51. Oscillatory data of HPMC gels over time.

There has been a large reduction of  $G''$  over time, although evidence of a gel network can still be seen as  $G' > G''$ .

#### 4.4 Conclusion

The gels were formulated to be weakly adherent to the eye tissue and tests confirmed this for both the carbomer and xanthan gum gels. Carbomer 934 showed statistically significant bioadhesion, against tissue and agar. Xanthan gum was found to display the most comprehensive and statistically significant bioadhesion of all three gels, against tissue only. HPMC displayed the weakest bioadhesion of all three gels, against tissue and agar. This may be due to a low viscosity. Stability tests show carbomer gels to be stable without a preservative over 2 weeks, and the gel structure is intact after 4 months of storage at 4°C. Overall, the carbomer and xanthan gum gels appear promising for improved performance upon the current eye drops.

The results demonstrate that the formulation of cysteamine hydrochloride as a gel for ophthalmic delivery is achievable. The three ophthalmic gels were found to possess similar characteristics and exhibit properties desirable for eye gels. The xanthan and carbomer gels tested formed weak gel networks at zero to low shear stresses, desirable properties for increased residence time on the ocular surface. A net bioadhesion and first order release of the active from the sample matrix was also apparent. On average the experimental compound was released over an eight-hour period. The current ophthalmic treatment requires hourly administration whilst the patient is awake, allowing a treatment-free period overnight. It is thought that these gels could provide overnight drug treatment, through prolonged contact and decreased drainage, thereby permitting a decrease in daytime administration. Furthermore, the addition of cysteamine did not destroy the gel properties.

These results offer the possibility of a gel formulation of cysteamine, which would considerably enhance the quality of life for patients with the ocular complications of cystinosis. They may also be suitable as a base gel for other ophthalmic drugs.



## **Chapter 5 – Pulmonary delivery**

## Chapter 5 – Pulmonary delivery

### 5.1 Introduction

#### 5.1.1 History of respiratory delivery

The lungs have been targeted to treat respiratory disease since the first century, when Pedanus Discorides, the Greek physician and pharmacologist, prescribed inhaled fumigation (187). Thomas Clover first described inhalers for general anaesthesia in Britain in 1877 (187). However, it wasn't until the 1940s that nebulisers were first used to treat respiratory diseases. In 1956, MDIs were invented to treat respiratory diseases such as asthma, while dry powder inhalers have been used since the early 1960s (74). Some of the most commonly prescribed inhalers are Ventolin<sup>®</sup> (GSK), QVAR<sup>®</sup> (Teva), Serevent<sup>®</sup> (GSK) and Bricanyl<sup>®</sup> (AZ), which are all used to treat asthma.

More recently, the lungs have become a target for systemic treatments. In 2006 the inhaled insulin product Exubera<sup>®</sup> (Pfizer) was launched for the treatment of diabetes (188). However, the manufacturers withdrew the product after 14 months due to poor sales levels (189). It was found to be equivalent in efficacy to the existing short-acting insulin, meaning at least one daily injection of insulin was still needed. It was also double the cost of the existing therapy, leading the National Institute of Clinical Excellence (NICE) to advise local health boards to prescribe it only for patients with serious needle phobia, or injection site problems (190). After withdrawal from the market, a report was published which found an increased risk of lung cancer in ex-smokers using Exubera<sup>®</sup> (189). As such, there is currently only one inhaled drug licensed for systemic treatment. Relenza<sup>®</sup> (GSK) was the first inhaled drug to be marketed for systemic treatment (191). It is used to prevent and treat influenza. Studies have shown that Relenza<sup>®</sup> has around a 2% bioavailability, and should be used with caution in asthmatics and people with respiratory ailments, a patient group particularly susceptible to the flu (192,193). There are issues over the drug's cost, and this further limits its use (194).

### **5.1.2 Pulmonary delivery in cystinosis**

Despite cystinosis affecting nearly every tissue in the body, lung disease has not been reported. Evidence suggests that late-stage lung dysfunction is caused by intercostal muscle impairment, the muscles which power inhalation, and not lung disease itself (5,195). This complication primarily affects individuals who have not received oral cysteamine therapy from infancy. Pulmonary function tests show a 50% reduction in lung volume for size and age. A cystinosis patient's chest cavity may also be conical due to early rickets, lowering inspirational volume (5). The impact of disease states on the absorptive capacity of the lung is undetermined (196).

There is only one study to date that has examined inhaled cysteamine (197). Mice were exposed to nebulised cysteamine prior to receiving chemotherapy, in an attempt to reduce radiation-induced lung damage, i.e. not for the treatment of cystinosis. They were also given intraperitoneal doses. Cysteamine is effective for this indication when administered orally. The aerosol proved to be ineffective however, while the intraperitoneal doses were effective. It was concluded that the concentration of cysteamine reaching the peripheral lung was inadequate when delivered by nebuliser. Aerosol particle size was too large to reach the alveoli, as medical nebulisers are designed to target the airways and not the alveoli. The author states that cysteamine is active in the lung, and that future studies should aim to increase the dose and decrease the particle size (197).

### **5.1.3 Lung anatomy**

The structure of the lungs is shown in Figure 52. The trachea or windpipe divides into two branches, called bronchi, where the lungs begin. These bronchi continue to divide into bronchioles, which lead to alveolar sacs. These are clusters of alveoli, tightly wrapped in blood vessels. There are millions of alveoli in each lung. The total alveoli surface area for both lungs is 100 square meters (198,199), with 70 square meters in contact with

capillaries (196). The capillaries stretch for 2000 km (200). All of these factors endow the inhaled route with a potentially high bioavailability (189).

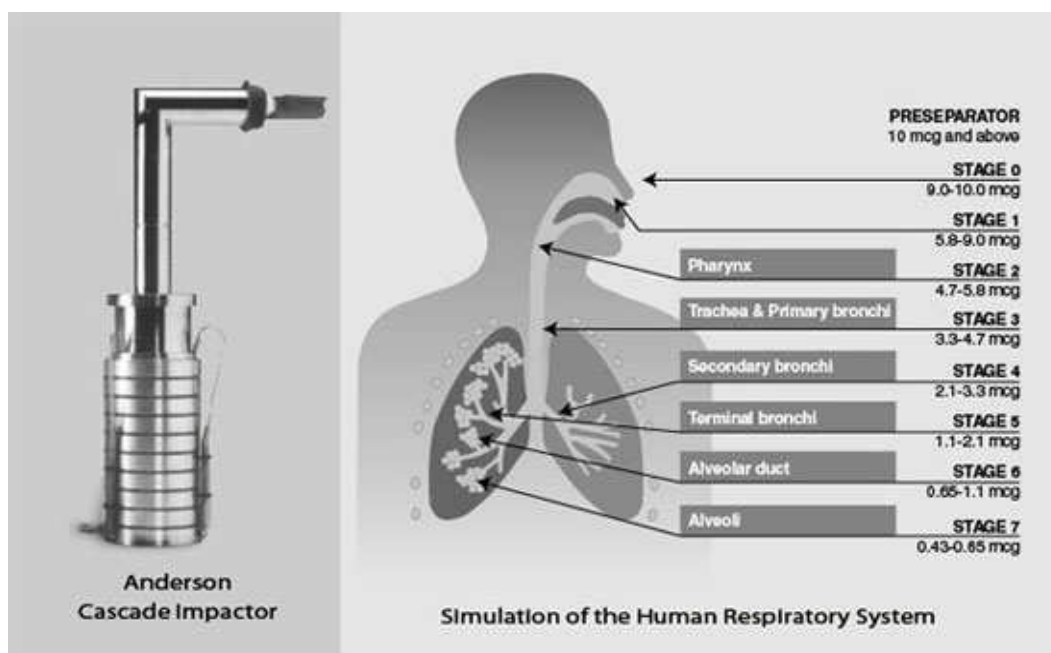


Figure 52. Diagram of particle sizes for lung delivery, with the corresponding Andersen Cascade Impactor (ACI) stages (201).

Small molecules can be absorbed within seconds of inhalation via this route (202), either by absorption through epithelial cells or by alveolar macrophages. Hydrophilic molecules in particular are favoured in lung epithelial transport (203), and this should maximise the absorption of cysteamine. Particles of aerodynamic diameter 3  $\mu\text{m}$  are an optimum target for ensuring drug absorption via alveolar macrophages (204). There is reduced uptake by alveolar macrophages of particles below 0.26  $\mu\text{m}$  (205).

The epithelium of the airways is lined with tiny hairs called cilia, which carry any insoluble particles up to the throat for swallowing (74). The mucociliary pathway carries mucus out of the lungs at an estimated 4 mm/min (206). Larger particles will be swept away by cilia (188), which particularly affects the upper airways. Phagocytic activity is more prevalent in the lower airways (188). Larger particles tend to impact on the back of the throat, or get swept out of the lungs by cilia, while smaller particles are carried out of the lungs upon expiration. Another factor leading to large drug absorption

is the thickness of the epithelium, which can be as much as 60  $\mu\text{m}$  in the trachea, but as little as 0.2  $\mu\text{m}$  in the alveoli (189,199,202).

The mucus layer in the trachea is thicker than in the lower airways (188). In addition, an elevated blood flow of 5 L/min ensures rapid drug circulation. The lungs do not have a low degrading pH or enzymes like the GI tract, and once absorbed, the drug directly enters the system circulation and avoids the first pass effect (189,207). This allows a smaller dose to be given, further reducing the likelihood of side effects.

Lung-Lining fluid (LLF) has several roles, the main one being host defence. It is also vital for lung structure and function, by providing lubrication to the pulmonary epithelium, and maintaining fluid surface tension (208). It is important in gaseous exchange. The volume of the LLF has been calculated to be 15-70 ml in healthy adults (208,209). LLF is further categorised into airway surface liquid (ASL), which covers the conducting airways, and alveolar subphase fluid (ASVF), which is only found lining the alveolar sacs. ASL is composed mainly of water, with a mucus component of mucin glycoproteins and proteoglycans, which endow a gel-like structure. The glycoproteins are present both on the surface of the epithelium and secreted, the rate of secretion being largely controlled by inflammatory mediators and neurotransmitters. This is the most likely explanation for mucus hypersecretion present during airway inflammation (208). ASL operates in conjunction with the cilia, as particles of diameter 5  $\mu\text{m}$  or greater are trapped in the ASL, which are then cleared from the lungs via the mucociliary escalator to the throat for swallowing.

ASL contains lysozymes, lactoferrin, immunoglobins and phagocytes amongst other antimicrobial factors, which all aid in limiting foreign particulate invasion (208). These antibacterial molecules also add to the rheological character, endowing it with increased viscosity and elasticity (206). It is pH 6.6 during periods of health and non-inflammation, but becomes more acidic when the person has disease or lung inflammation (208).

ASVF is composed of mainly water with a surfactant. It is 0.1-0.2  $\mu\text{m}$  thick, and is sterile due to the large number of macrophages. It traps particles of diameter 5  $\mu\text{m}$  or less, which are then taken up by macrophages, and either carried up to the throat by cilia, or absorbed and released into the blood stream (208). The surfactant is composed mainly of phospholipids, and also contains cholesterol and proteins (210).

The humid atmosphere of the lungs has a large impact on the aspirated particles. Inside the airways it is approximately 99% relative humidity (RH), compared to the ambient room humidity of around 50% (74). As it enters the lungs, the particle collects condensation on its surface. The particle will continue to collect water until equilibrium exists between the vapour pressures. This way, the inhaled particle will gradually increase in size, altering the predicted flow into the lungs. This phenomenon can be avoided by coating the particle with a lipophilic coating (207).

#### **5.1.4 Inhaled bioavailability**

The bioavailability of inhaled drugs is reportedly as low as 8% (200,202,211). The dose which impacts on the throat and upper airways is subsequently swallowed, and is then available to the systemic circulation once absorbed from the gut (212). The total percentage which actually reaches the lungs is typically between 20 and 40% (211,212). The lungs do not possess degrading enzymes, and also avoid the first pass effect. This allows a smaller dose to be delivered, and circumvents the issues of low drug delivery.

#### **5.1.5 Inhaler types**

There are three main inhaler types currently available: Metered-Dose Inhalers (MDIs), Dry Powder Inhalers (DPIs) and nebulisers.

### MDIs

The drug is dissolved or suspended in a liquid propellant, along with excipients, and sealed in a pressurised canister. Upon actuation, the patient must inhale simultaneously to avoid the dose being lost (74).

### DPIs

The patient inhales the drug in a propellant-free cloud of fine particles. DPIs are mainly breath-actuated devices, although some modern devices incorporate a powered system to aid particle break-up. DPIs avoid problems with the coordination of actuation and inhalation required for MDIs, and larger doses can be delivered than with an MDI. DPIs also allow a greater stability for the drug (207).

### Nebulisers

The drug is dispersed in an aqueous solution, and fine droplets as a mist are produced for inhalation. This delivery device is useful if the drug is unsuitable for MDI or DPI formulation, or if the dose is large. The patient can also breathe normally, and the drug will be delivered efficiently (74).

A DPI was chosen for the delivery device of the drug, due to practical and economical factors (213). Formulated powder is filled into hard gelatine capsules, which are subsequently loaded individually into a Handihaler<sup>®</sup> device (Figure 53).



Figure 53. The Handihaler<sup>®</sup> device used in this project (214).

Once the capsule has been pierced and air flow is initiated, the capsule spins within a chamber inside the device, allowing the powder to escape through a hole at each end. The de-agglomeration of powders is a complex process involving centrifugal force, fluid mechanics, adhesion, turbulence, shear forces, impaction, the impact of the capsule with the device, and of the powder with a grid or mesh. These factors all contribute to the fluidisation and de-agglomeration of the powder, particularly the mechanical impaction of the powder with the impact angle on the throat (215). The free-flowing powder then leaves the device through the mouthpiece, and into the patient's lungs.

DPIs are termed 'passive' devices, in that the patient's inspiration alone operates the device. DPIs require the patient to inhale deeply and with some force, as particle de-aggregation is dependent on this (216). Inside a DPI, inhalation flow and the resistance within the inhaler gives rise to turbulent flow, which leads to flow-dependant dose emission. It is extremely important that the patient receives counselling on the use of their inhaler, as poorly de-aggregated particles will impact on the throat and oropharynx, with a result of the loss of the dose. The strength and duration of the patient's breath are therefore critical parameters in the in vitro testing process. When testing DPIs, both the European and US Pharmacopoeias state that the flow rate used should produce a pressure drop across the inhaler of 4 kPa, while the duration of flow should give a volume of 4 Litres. This is broadly representative of a normal, healthy adult male of 70 kilos in weight, inhaling 'as deeply and as hard as possible' (217). The initial acceleration rate is important to detach the drug molecules from the carrier particles. Cystinosis patients are generally underweight, and children will not be able to achieve these values. Most patients inhale for a period of 2 seconds on average, which is half the recommended period in the USP. However, as most DPIs deliver their dose within 100-300 ms of initiation of use, this should not be a problem (218). Measuring the pressure down-stream of the device, and comparing this with atmospheric pressure can be used to calculate the pressure drop across the device. There is a consensus that a flow of 30 L/min should be achieved

when using a DPI (217). The European and US pharmacopoeias state that the flow rate should be within +/-5% of the target flow.

The following relationship can be used to calculate the pressure drop across an inhaler:

$$R = Q/\sqrt{\Delta P}$$

Where R is the resistance, Q is the flow rate in L/min, and  $\Delta P$  is the pressure drop (cm H<sub>2</sub>O) (217). The Handihaler<sup>®</sup> device has been reported as having one of the highest resistance values of commonly prescribed inhalers, which is probably due to the basic nature of the device (217). In most DPIs, the patient 'activates' the dose by twisting the device, or in some cases just by opening it. This produces a free bolus of drug powder which can be inhaled with minimal effort. However in the case of the Handihaler<sup>®</sup>, the powder remains in a pierced capsule, and it is the patient's inhalation alone which liberates it. Nevertheless, a flow of 40.4 L/min has been shown to produce a 4 kPa pressure drop across the device, and it has been demonstrated that most patients in a study achieved this, despite suffering from chronic obstructive pulmonary disease (COPD) (217). This should give reassurance to critics who may suggest that small, weak cystinotic children cannot inhale at the flow necessary for successful respiratory delivery.

### **5.1.6 Fate of inhaled microparticles**

The deposition of powder in the respiratory tract is influenced by particle size, size distribution, breathing pattern and the delivery device (188), particle size being the most influential factor in lung targeting efficacy. To target the lungs efficiently, particles must have an aerodynamic diameter of 1-5  $\mu\text{m}$  (196,207,211,213). Aerodynamic particle size takes into account the particle's size, shape and density, and therefore it is widely accepted as the key parameter in determining lung deposition (219). Particles below 2  $\mu\text{m}$  are perfect for targeting the alveoli (74).

Once inhaled, aerosols deposit in the airways in three main ways; gravitational sedimentation, inertial impaction and Brownian diffusion (74).

#### Gravitational sedimentation

This is the main mechanism of distribution for particles with an aerodynamic size range of 0.5-5  $\mu\text{m}$ . It is mainly influenced by increasing particle size and residence time, but decreases as respiration increases. This is the main factor influencing particles in the small conducting spaces with low air flow (215).

#### Inertial impaction

This mainly affects particles with sizes of 5  $\mu\text{m}$  and greater. It is an important mechanism, particularly affecting the upper respiratory tract and large conducting airways. The changing physical contours of the throat and larynx and large flow velocities are responsible for this phenomenon. The likelihood of impaction increases with increased air flow, rate of breathing and particle size (216).

#### Brownian diffusion

This only affects particles with diameters less than 0.5  $\mu\text{m}$ . These micro particles impact with surrounding air molecules, and tend to migrate to the vessel walls, especially in areas with low airflow such as alveoli (220).

### **5.1.7 Microsphere production**

There are several techniques available to produce micro particles suitable for inhalation. Milling, emulsion solvent evaporation (ESE) and spray drying are the most commonly employed methods (207). Milling has the advantage of producing solvent-free particles, but allows poor control of particle size. ESE is much slower than spray drying, in the magnitude of days compared to minutes, but is excellent for use with thermo labile compounds. Spray drying is a popular choice due to its numerous advantages over alternative methods, and was the method chosen for this

project. None of these methods can precisely control the geometric particle size distribution (219).

#### **5.1.7.1 Milling**

Milling is the traditional method of choice for producing micronised particles. There are many different types of mills, including ball, colloid, hammer and jet mills. A jet mill is most commonly used for micronisation of particles for inhalation (204). Large particles are broken down into smaller particles through inter-particle collision and attrition. Most of the particles produced will be within the size range of 1-20  $\mu\text{m}$ , although there is little control over size, shape or surface properties (204). The particles produced by this method also tend to be chemically degraded and highly charged due to the high energy input of the process, which can then lead to static electricity build up and agglomeration, which can produce instability of the drug.

#### **5.1.7.2 Emulsion solvent evaporation**

Microspheres are produced through the evaporation of a constantly-stirring emulsion mix of drug and excipients. Heat is supplied to accelerate the process. The significant exposure of the drug to the environment and high temperatures precluded this method from the study.

#### **5.1.7.3 Spray drying**

Spray drying has been used to produce powders for inhalation since the 1980s, to produce uniform particles of microscopic diameter (213,219). Solvent containing active ingredients and excipients are forced through a small jet nozzle into a stream of hot air, which vaporises, leaving behind individual solid particles (74) (Figure 54).

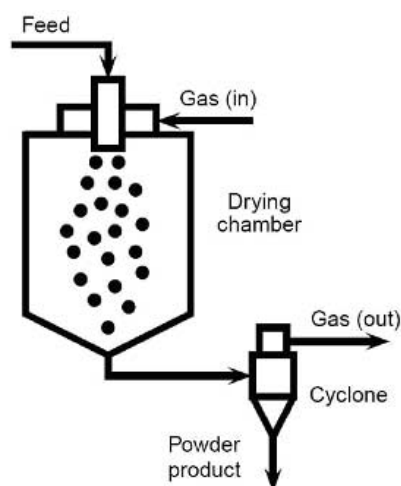


Figure 54. Diagram of a typical bench top spray dryer (221).

These particles are typically amorphous hollow spheres, sometimes with a small hole (219). This is due to the drying process, whereby the outer surface dries to a crust before the centre, and the liquid centre then vaporises and escapes through a hole blown in the crust. There are several advantages of spray drying, including:

1. Rapid, one step process
2. Uniform particles with excellent flow properties
3. Evaporation is extremely quick, thermo-labile drugs can be used without being destroyed
4. A high yield is achievable
5. Can be used for a wide range of substances, in solution or suspension (74).
6. Particles are usually organic solvent-free.

The mini (bench top) spray dryer used in this project is useful for initial stage testing, when only a minimal weight of drug is available. However, there are some disadvantages of using this system. The drying chamber is too small, typically less than 10 litres, which makes the drying-gas residence time less than one second. This limits the drying capacity of the apparatus, and allows only the smallest droplets to become completely dry, leaving a larger volume of residual solvent than is desirable. In an attempt

to offset this effect, a lower flow rate than preferred has been used in the process (222).

There is an intricate relationship between process variables such as inlet temperature and flow rate, and feed variables such as concentration and solvent choice, and these all affect particulate kinetics and morphology (223). Particle size can be influenced within the spray drying technique by altering the concentration of drug in the feed solution: the lower the concentration, the smaller the particle size (224). Increasing the temperature can also reduce the particle size. The molecular weight of the polymer is also important for successful microsphere formation. A concentration of between 0.5-2.5% w/v is typically used. Too low a concentration can result in incomplete microspheres, where too high a concentration can produce agglomeration (223).

Due to the minute size of the particles produced, static electricity can be a problem, leading to agglomeration. There can therefore be a poor recovery rate from the inside walls of the dryer, which may also give poor aerolisation (220,225). It has also been reported that particles less than 2  $\mu\text{m}$  have low collection efficiencies (204). There is also a high risk of the pneumatic nozzle clogging. An alternative ultrasonic nozzle may lower the likelihood of this occurring, as well as producing particles with a more uniform size distribution (204).

#### **5.1.8 Static electricity and agglomeration**

Agglomeration is a problem commonly seen in DPIs (226). The low size range necessary for optimum lung delivery produces a large surface-area-to-volume ratio, which favours interparticulate forces over gravity and aerodynamicity. This gives rise to static electricity problems, where minute particles aggregate together producing a powder with agglomeration and poor flow properties (227). DPIs require good flow properties to allow the patient to breathe in the powder and direct it accurately at the deep lung,

with minimal losses to the GI tract. Agglomeration due to friction causes inconsistent drug delivery.

The most common method used to solve the aggregation problem is to combine the drug molecules in a homogenous blend with an inactive carrier, such as lactose (224,227). The lactose grade used in this project was  $\alpha$ -lactose monohydrate, which possesses relatively flat particle surfaces (227). The lactose molecules are much larger than the drug molecules attached to them (typically 20-100  $\mu\text{m}$ ), and therefore the lactose impacts in the oropharynx, while the drug particles are carried deep into the lungs (228). There is a fine balance between adhering the drug to the lactose with enough force to carry the drug to the lungs, but not so strongly that it won't disperse upon inhalation (227). The specific force of interaction must be surpassed to dislodge drug particles (199). There are four main forces adhering drug particles to carriers:

1. Mechanical adhesion through irregularities on the surface
2. Capillary action from water
3. Static electrical charges
4. Van der Waals forces

These forces prevent adequate aerosol production. Keeping moisture content at a minimum reduces the capillary forces. Capillary forces are reciprocally related to surface charge, and develop from the condensation of water onto particle surfaces. If a large enough volume of water is condensed, an attractive force is induced. The moisture which condenses can also produce irreversible aggregation and solid bridge formation, giving larger particles and poorer lung penetration (199). Therefore, immediate protection from environmental moisture upon manufacture is extremely important.

Low deposition efficacy in DPIs is most commonly caused by poor drug separation from the carrier particle (199), which is governed by drug-drug and drug-carrier interactions. Interactions which are too weak lead to re-separation, and interactions which are too strong lead to upper airway

deposition (229). The balance must be perfect to ensure the drug remains attached to the carrier during manufacture and transit, but releases upon inspiration. Separation occurs through three main mechanisms:

1. Shear flow and turbulence
2. Particle-device impaction
3. Particle-particle impaction

For carrier particles with a large surface area and significant asperities, as is the case in this project, impaction is the predominating mechanism (227). This occurs when the particle impacts with the device, and is dependent on momentum. Momentum is related to particle size, therefore the larger particles will generate larger impaction forces (227). If the surface roughness of the carrier particle is too great, drug molecules may be shielded from detachment forces (227), and have areas of higher energy to attach to. Some strongly adhered particles may not break apart, even after leaving the device (219).

The optimum impact angle for de-agglomeration is 45 degrees (226). Higher velocity air flow also improves de-agglomeration, but increases throat impaction and drug loss. There is a delicate balance between improved deep-lung penetration and loss to impaction (226). Fine particle fraction is maximised using a combination of two 45-degree angles, with minimal loss to impaction. Studies analysing air flow patterns within the 90-degree throat of the ACI show particles initially drop to the bottom of the throat, accelerate along the throat and are lifted by the airflow. The centre of the pipe has the maximum velocity, and this reduces gradually to the slowest, virtually still part nearest the wall of the throat (226). Surfactants can also be used to de-aggregate particles, but can prematurely release drug through lowered microsphere/medium interfacial tension (223).

### 5.1.9 Poly(D,L-lactide) (PLA)

Biodegradable polymers are becoming a popular method of ensuring controlled drug release, through encapsulating drug particles. The higher molecular weight PLAs are also established as surgical implants and devices (230,231). Low molecular weight RESOMER<sup>®</sup> R 202s, Poly(D,L-lactide) (PLA) was chosen for encapsulating cysteamine bitartrate, due to its biodegradable, biocompatible and non-toxic nature (188,205,231-234) (Figure 55). Cysteamine bitartrate was used for the respiratory powder work as it was less deliquescent than the hydrochloride salt (see section 5.2.2). PLA was granted approval by the FDA in 1984 for use in drug formulations (223). Poly(lactic-co-glycolic acid) (PLGA) was also investigated for suitability in lung delivery but was found to be extremely slowly degraded in the lung (205). As this formulation is for the treatment of a chronic condition, it was eliminated from the study over concerns of polymer build-up.

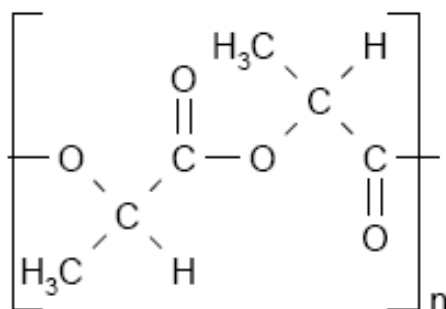


Figure 55. Monomeric repeating unit of Poly(D,L-lactic acid), where  $n \approx 7700$  (235)

Biodegradable polymer encapsulation also enhances the stability of the drug (188). It has been used previously for sustained release to the lungs (188,210,234,236,237). Recently, it has been used to provide encapsulation and controlled release for anti-cancer agents (238). Polymers have also demonstrated an ability to promote the mucus penetration of coated particles in the lungs (239). Poly(D,L-lactide) is the racemic polymer of two stereoisomeric forms, D-PLA and L-PLA (230). PLA is optically inactive. Upon degradation, the Krebs cycle component lactic acid is liberated, and thus the polymer is atoxic (240). It is also

amorphous. Poly(D,L-lactide) produces superior particle morphology than D-PLA and L-PLA, which are liable to exhibit craters, pores and collapsed particles, possibly due to crystallinity (223). Poly(D,L-lactide) displays superior film-forming characteristics, and is solubilised under moderate conditions, which may lead to improved encapsulation (223). To date there are no sustained release preparations available for targeted lung delivery. If achieved, duration of action could be improved, along with a reduction of administration frequency and side effects, which brings improved compliance and economic viability (210).

Due to the numerous and complex factors affecting dissolution, it can be difficult to predict how a drug will be released from a microsphere. There are two main mechanisms involved in drug release from a polymer: diffusion of the drug, and degradation of the polymer (231). Biodegradation of poly(D,L-lactide) occurs through hydrolysis (223), by a mechanism known as 'homogenous degradation'. Hydrolysis cleaves ester bonds at random, and any short chain fractions below 15 kD in size are solubilised, and the mass is gradually broken down (223). There is a gradual formation of small pores, through which both drug and aqueous media can penetrate (240).

The rate at which this occurs is largely influenced by environmental pH; the polymer has been shown to degrade most rapidly and efficiently at pH 9.6, and slowest and more incompletely at pH 5 (240). PLA degradation is maximised by hydrophilicity, low crystallinity and low average molecular weight. The most influential factor is composition of polymer, which affects hydrophilicity (241). The rate of drug release from microspheres is influenced by carrier/drug ratio, degree of stabilisation, polymerisation, and particle size (188).

There has been concern over polymer accumulation within the lungs (204). Cysteamine bitartrate has a half life of around 1.88 hours, and the leukocyte cystine content returns to baseline levels after 6 hours, requiring very accurate, frequent dosing (33). The lung can generally clear particles easily, therefore a biodegradable polymer should be quickly broken down

and absorbed. A pulmonary preparation of cysteamine may provide relief from the punishing oral dosage regime.

#### **5.1.10 In vitro testing**

The most commonly used in vitro model for testing the delivery of drugs to the lungs is the impactor. The impactor used in this project was the Andersen Cascade Impactor (ACI, Copely Scientific Ltd, Nottingham, UK). Through a series of eight stages with progressively smaller holes, the aerodynamic size distribution of the powder is analysed. This defines where aspirated particles are expected to deposit in the lung. The ACI satisfies the assessment specifications for inhaled products of both the United States Pharmacopoeia (USP), and the European Pharmacopoeia (Ph.Eur.). It is also a widely used technique in quality control analyses. Figure 56 shows a comparison of the ACI stages with the lungs. The stream of aerosols travel down through each stage of the ACI, which represent the narrowing airways within the lungs as larger particles impact on a stage plate, and particles that are small enough are carried on to the next stage. The particles are separated according to their mass median aerodynamic diameter (MMAD), allowing subsequent analysis on size fractions (74). It is the particle's inertia that determines at what stage it will impact, and as this is a function of velocity and aerodynamic particle size, the shape and density of the particle is not required to be known. The more inertia a particle has, the more likely it is to impact upon a collection plate, while smaller particles with less inertia will be carried past the plate by the air stream.

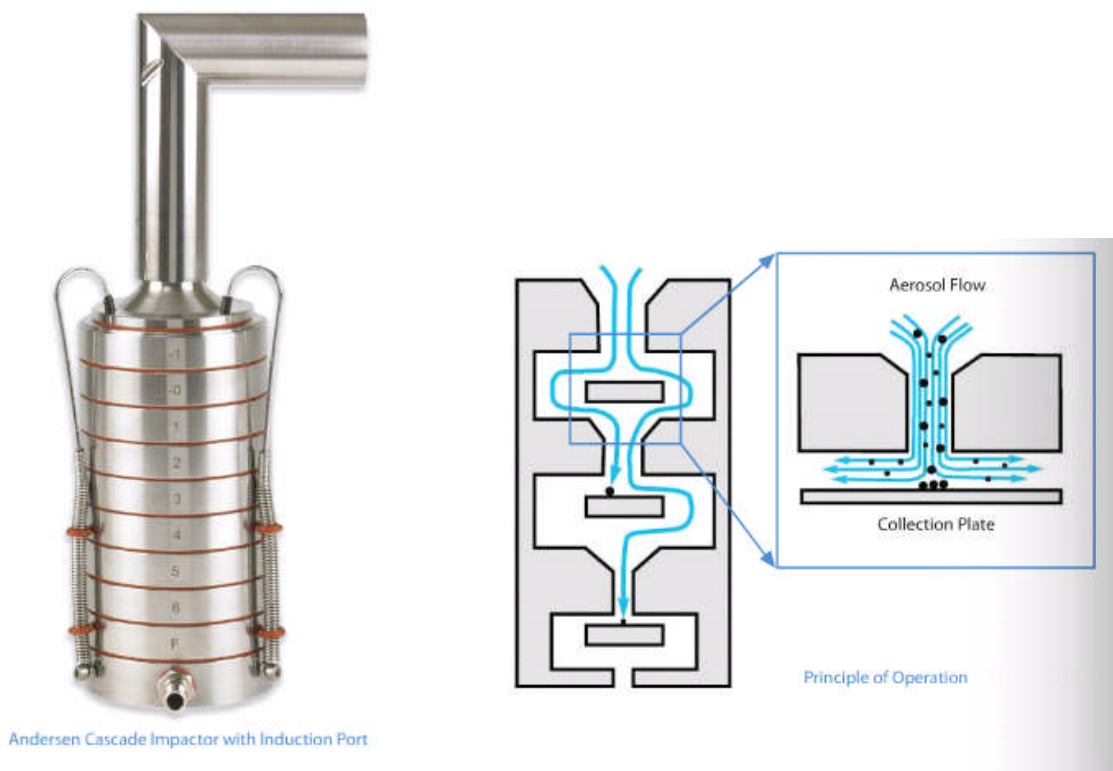


Figure 56. Detail of the internal structure of the ACI (Copely Scientific Ltd, Nottingham, UK).

Particle bounce can be a problem; instead of impacting upon a plate, particles bounce off and continue down the impactor and settle on an incorrect stage, giving false results (242). In order to lessen this effect, each plate can be coated with silicon oil, as per the Industry Standard (GlaxoSmithKline, Ware, UK). The ACI also has the benefit of retaining 100% of the delivered dose for analysis. The operation of the ACI (Copely) is outlined in the documents received during training on the device at Glaxo SmithKline’s laboratories in Ware, Hertfordshire (242,243). Measured cut-off diameters in the ACI stack used for testing are shown in table 26.

Table 26. Cut-off diameters in the ACI

ACI stage	Cut-off diameter at 60 L/min ( $\mu\text{m}$ ) <sup>a</sup>	Cut-off diameter at 28.3 L/min ( $\mu\text{m}$ ) <sup>b</sup>
Stage 0	5.9	9.0
Stage 1	4.1	5.8-9.0
Stage 2	3.2	4.7-5.8
Stage 3	2.1	3.3-4.7
Stage 4	1.4	2.1-3.3
Stage 5	0.62	1.1-2.1
Stage 6	0.35	0.7-1.1
Stage 7	0.15	0.4-0.7

<sup>a</sup>(244,245), <sup>b</sup>Copely, usp 601

Cut-off diameters are altered when a 28.3 L/min flow is used, although a converter kit consisting of additional stages is available, as well as a formula to calculate the new cut-offs. The cut-offs stated here are taken from the European Pharmacopoeia (244,245).

The advantages of the ACI method include its well-established and widely accepted method by regulatory authorities, a choice of construction materials, conversion kits available for 60 and 90 L/min flow rates allowing retention of the 28.3 L/min cut-off diameters, small footprint and attachments available for nasal sprays and nebulisers. However, the ACI method of in vitro testing has been criticized over its labour-intensive nature and convoluted analysis, and consequently, large variability in results (246). Despite this, the technique is the most commonly used, particularly during the development stage.

The ACI does not allow analysis of formulation biodegradability on, or permeability or absorption across epithelium. Systems are being developed which incorporate pulmonary epithelial cells into impactors in an attempt to rectify this (203).

It is hypothesised that a dry powder inhaler for systemic treatment may eliminate many of the problems seen with the current oral dose. The

malodorous nature of the drug may be disguised, allowing easier administration. It has the possibility of being a simple, portable and economically viable drug delivery system. It is also a more environmentally friendly method compared to MDIs. It is hoped that systemic treatment for cystinosis may become as straightforward as that for asthma and other respiratory diseases

## **5.2 Materials and methods**

### **5.2.1 Materials**

L-Tartaric acid, cysteamine, ethanol, methanol, DCM, ethyl acetate, hexane, acetonitrile, acetone, silicon oil and glass microfibre filters were purchased from Sigma. Tris buffer was purchased from Fisher. Poly(D,L-lactide), (Resomer R202s) and a Handihaler® device were obtained from Boehringer Ingelheim Pharma GmbH & Co. (Ingelheim am Rhein, Germany). The spray-dried/USP lactose grade (granulated  $\alpha$ -lactose monohydrate) was obtained from Domo (Goch, Germany). Lactose BP was purchased from Lactochem (Tamil Nadu, India). The 100  $\mu$ m lactose was obtained from DMV International bv (Veghel, Netherlands). Empty gelatine capsules (size 3) were purchased from Davcaps (Hertfordshire, UK). DTNB was purchased from Molekula (Gillingham, UK).

### **5.2.2 Cysteamine bitartrate synthesis**

During preformulation studies, cysteamine hydrochloride was found to be unsuitable for use in the spray drier. It is extremely hygroscopic and deliquesces, and therefore extremely difficult to achieve a dry powder with. It is also insoluble in most solvents, making a DCM: methanol mix the only suitable vehicle. There is a reluctance to use DCM as a vehicle for spray-drying, due to its toxic nature, which the patient may be exposed to if residual solvent remains (247). It was decided to use cysteamine bitartrate as an alternative, given that the bitartrate salt is used in the current medication.

To a stirring solution of L-tartaric acid (1.5 g, 0.01 moles) in degassed anhydrous ethanol (200 cm<sup>3</sup>) at room temperature, cysteamine (0.77 g, 0.01 moles) was added. The precipitate mixture was then stirred continuously for 5 minutes at room temperature, and filtered under vacuum. The resultant white powder was then placed in a vacuum oven overnight at 50°C. It was characterised by <sup>1</sup>HNMR, and compared with the commercial preparation of cysteamine bitartrate, Cystagon™ (Appendix III).

### 5.2.3 Microsphere preparation

Suspensions containing components in varying ratios were prepared and spray-dried as per table 27. Spray dried microspheres can be hygroscopic. To avoid uptake of environmental moisture, particles were sealed in a vial immediately after harvesting from the collection vessel, and stored in a desiccator at 4°C. Microspheres were stored at different temperatures and conditions prior to testing, including a desiccator cabinet (Bel-Art Secador, New Jersey, USA) at 25°C, a desiccator at 4°C and 21°C. The in vitro deposition of these particles was then compared with that of non-desiccated microspheres. Microspheres alone and a 50:50 blend with lactose were tested, and also cysteamine bitartrate which had been micronised for 5 minutes in a ball mill at medium amplitude (AS200 Basic, Retsch GmbH, Germany). The batch with the most discreet, spherical and non-aggregated microspheres was selected for further analysis (batch 9). Table 28 describes the final production parameters chosen.

Table 27. The 10 batches of microspheres were manufactured according to the conditions shown.

Microsphere batch number	Components	Spray dryer conditions	Appearance
1	DCM:Methanol, 9:1, PLA 3% w/v, cysteamine HCl 2% w/v	55C, 700 L/h, 40% pump, 100% aspirator	Off white, adheres to jar walls
2	DCM:Methanol, 9:1, PLA 3% w/v, cysteamine HCl 2% w/v	39C, 700 L/h, 40% pump, 100% aspirator	Off white, some adherence to jar walls
3	Ethyl acetate, PLA 3% w/v, cysteamine bitartrate 2% w/v	39C, 700 L/h, 40% pump, 100% aspirator	White, some adherence to jar walls
4	Ethyl acetate, PLA 2.5% w/v, cysteamine bitartrate 1% w/v	39C, 700 L/h, 40% pump, 100% aspirator	no defined particles
5	Ethyl acetate, PLA 2.5% w/v, cysteamine bitartrate 2% w/v	39C, 700 L/h, 40% pump, 100% aspirator	white powder, some adherence to jar walls
6	Ethyl acetate, PLA 2% w/v, cysteamine bitartrate 2% w/v	39C, 700 L/h, 40% pump, 100% aspirator	white powder, some adherence to jar walls
7	Ethyl acetate, PLA 1.5% w/v, cysteamine bitartrate 2% w/v	39C, 700 L/h, 30% pump, 100% aspirator	white powder, minimum adherence to jar walls
8	Ethyl acetate, PLA 2.5% w/v, cysteamine bitartrate 2% w/v	35C, 700 L/h, 30% pump, 100% aspirator	white powder, lots of static, difficult to harvest
9	Ethyl acetate, PLA 2% w/v, cysteamine bitartrate 2% w/v	35C, 700 L/h, 30% pump, 100% aspirator	white powder, lots of static, very difficult to harvest
10	Ethyl acetate, PLA 1.5% w/v, cysteamine bitartrate 2% w/v	35C, 700 L/h, 30% pump, 100% aspirator	white powder, lots of static, difficult to harvest

Table 28. Final spray drying conditions used for optimum microsphere preparation.

Optimal spray drying conditions	
Inlet temperature	35°C
Outlet temperature	27°C
Air flow	700 L/h*
Pump	30%*
Aspirator	100%*
Total solids	4% w/v

\*(248,249)

The dose used in DPIs is dependent on four factors:

1. Formulation properties, such as powder flow, particle size, shape and surface properties and drug carrier interaction
2. Aerosol generation and delivery from the inhaler device
3. Inhalation technique
4. Inspiratory flow rate

Only a few milligrams of drug needs to be delivered into the lungs, therefore a carrier also provides additional bulk to improve handling and metering of the drug (199). Generally, excipients contribute 60-99% by weight of the total dose in respiratory powders (199).

#### 5.2.4 Microscope analysis

Drug particles were viewed through a Leica DM 2500M microscope connected to a Leica DFC 420 camera (Leica Microsystems GmbH, Germany) for pre-electron microscope analysis. The microscope was fitted with 5x, 10x, 20x, 50x and 100x lenses.

### 5.2.5 Scanning Electron Microscopy (SEM)

The shape and particle architecture of the microspheres was observed by a Leo S430 SEM (Leo, UK), with a secondary electron detector. The microspheres were fixed to the specimen stub using carbon tape and dusted to remove excess. The stubs were sputter coated in a Polaron SC7640 (Quorum, West Sussex, UK), in a vacuum for 250 s at 100 mTorr. The photographs were taken at an accelerating potential of 20 kV, beam diameter of 10 pA and a scan rate of 40 seconds.

### 5.2.6 Particle size analysis

The particle size and size distribution of the microspheres was analysed by laser diffraction using a Mastersizer MSS from Malvern (Worcestershire, UK). Analysis of particle size was performed on batch 9 only, as these were found to be the most discreet microspheres within the desired size range (1-5  $\mu\text{m}$ ). The microspheres were placed in the dry powder feeder, and drawn into the Mastersizer by the airflow. Due to the aggregation seen under the microscope, it was performed 6 times. One sample was mixed for 30 seconds on a whirlmixer, and then scanned. The other sample was treated identically, and then sieved through a 45  $\mu\text{m}$  stainless steel mesh (Retsch GmbH, Germany).

It was noted that agglomeration was more apparent after sieving, and, in an attempt to eliminate this, a suspension of microspheres were prepared in triplicate in hexane, acetone and chloroform and sonicated for 1 minute. The sample was then analysed with a liquid sampling system 6 times (220).

The results are expressed in terms of volume distribution,  $d[v,0.1]$ ,  $d[v,0.5]$  and  $d[v,0.9]$  representing the 10<sup>th</sup>, 50<sup>th</sup> and 90<sup>th</sup> percentiles, respectively.  $D[4,3]$  is the mean particle size.  $D[3,2]$  is the equivalent surface area mean diameter. The mass median aerodynamic diameter (MMAD), defined as the mean geometric aerodynamic diameter, was also calculated from particle size analysis.

The distribution of particle diameters is represented by the span, where:

$$\text{span} = (d[v,0.9] - d[v,0.1]) / d[v,0.5]$$

### **5.2.7 Moisture content of microspheres**

The hygroscopicity of the microspheres was a potential problem as stated in the introduction. Moisture content analysis was performed on three identical batches of Batch 9 microspheres, using a TGA Q500 from TA Instruments (Delaware, USA). Once tared, the titanium pans were loaded with a uniform covering of sample, and the furnace raised. Using a ramp mode, the samples were heated at 20°C/min to 250°C, and the percentage weight loss analysed. The change in moisture content was noted over time.

### **5.2.8 Drug content of microspheres**

To analyse the percentage drug loading of the microspheres, 300 mg of the blend 9 microspheres were weighed accurately, and dissolved in 5 ml 1M Tris buffer, pH 8, and deionised water was added to 50 ml. The flask was then whirl mixed and sonicated. An equimolar weight of Ellman's reagent was added to the flask in the absence of light, and the UV absorbance measured at 440 nm. The absorbance reading was then entered into the equation of the straight line obtained by the linear regression of a calibration curve. This was performed in triplicate.

### **5.2.9 Blend with lactose**

The poor flowability displayed by the microspheres, caused by static forces between the minute particles makes the use of an inert 'carrier' particle necessary. Three different lactose grades were tested: 100 micrometer, spray dried USP and BP. The carrier generally makes up 60-99% of the total weight of a dry powder (199,228). As a starting mixture, drug loaded

microspheres were blended with carrier lactose particles in the ratio 50:50. Lactose supplied for inhalation is typically below 200 µm (227). The lactose was sieved through a 90 µm stainless steel mesh, and collected on a 63 µm mesh (Retch GmbH, Germany) (250,251). The drug-lactose blend was then mixed on a Denley Spiramix 10 (Thermo Scientific, USA) for 30 minutes, and subsequently placed on a whirl mixer for 30 seconds (Fisherbrand, Leicestershire, UK).

#### **5.2.10 In vitro powder aerolisation: Pre-clean**

Microsphere aerolisation was analysed using a calibrated Andersen Cascade Impactor (ACI; Copely Scientific Ltd, Nottingham, UK), attached to a vacuum pump with a variable free flow rate from 0-133 L/min (Copely, Nottingham, UK). Before initial use, the whole ACI stack must be dismantled, sonicated with warm, soapy water for 10 minutes, before being rinsed in deionised water and acetone and left to air dry. Each 'o' ring and rubber mouthpiece must also be removed, soaked for a minimum of 12 hours in acetonitrile, and a further 12 hours minimum in methanol, before being rinsed in acetone and left to air dry. Prior to the first run, each stage and plate must be washed in hexane and rinsed in acetone, and left to air dry. To eliminate static electricity, no gloves were worn whilst using the ACI, and the stack was grounded before use.

#### **5.2.11 Andersen Cascade Impactor: Testing**

##### **5.2.11.1 ACI Set up**

Before each test, the ACI had to be set up as outlined in the Standard Operating Procedure (GlaxoSmithKline, Ware, UK). Briefly, to minimise any 'bounce' between the particles and the plates, the stainless steel collecting plates were soaked in a 1% w/v silicon oil solution in hexane for 10 seconds, before being removed, placed horizontally and the hexane allowed to evaporate, leaving a thin film of silicon oil on the surface. The plates

were then handled with tweezers to ensure the film remained intact, and the stack reassembled. This included a methanol pre-soaked glass fibre filter in stage F, and 10 ml of deionised water in the preseparator. When testing a DPI, a preseparator must be inserted between the throat and stage 0 of the ACI. This collects the larger inert carrier particles typically used in DPI formulations, and also removes any particles greater than 10  $\mu\text{m}$ .

The alignment marks were checked for accuracy of the stack assembly. The stack was attached to the pump, and the flow rate checked using a flow meter DFM2 from Copely (Nottingham, UK), and adjusted if necessary. A flow of 60 L/min  $\pm$  1.5 L/min is required for DPIs, however flows of 55 L/min and 28.3 L/min were used in this project, as values above this were beyond the capacity of the vacuum pump.

#### **5.2.11.2 Respiratory powder testing**

Powder aliquots (approximately 100 mg) were loaded into size 3 hard gelatine capsules, and were placed individually into a Handihaler® dry powder device. To test a drug-containing powder, the capsule was pierced and held firmly against the mouthpiece, ensuring a good seal was made. The pump was activated for 3 seconds for 55 L/min and 5 seconds for 28.3 L/min using a foot pedal, and the powder drawn through the ACI (table 29). An airflow of 60 L/min for 3 seconds through the impactor is representative of the patient inhaling one dose from a DPI, and an airflow of 28.3 L/min is used for MDIs, although this may be more representative of the patient group in this study (246,252). Temperature and relative humidity are important for hygroscopic materials, and were measured before and after testing using a Rotronic Hygropalm 21 (Bassersdorf, Switzerland).

Table 29. Summary of the powders tested.

ACI batch, each run at flow rates of 28.3 and 55 L/min
Batch 9 alone, 21°C
Batch 9 alone (desiccator, 25°C)
Batch 9 alone (desiccator, 4°C)
Batch 9 with lactose 50:50, 4°C
Batch 9 with lactose 50:50, 21°C
Milled cysteamine bitartrate alone, 4°C

#### 5.2.11.3 ACI Wash down

The Handihaler<sup>®</sup> was carefully separated from the mouthpiece of the ACI, and cleaned with water. The amount of drug deposited in each area of the ACI stack was then determined, by careful sequential rinsing with deionised water of the mouthpiece, throat, pre-separator, stages and collection plates and backup filter into volumetric flasks. Table 30 shows the sizes of flasks used for the corresponding stages, and the component grouping. Care was taken at this stage to ensure that no powder was lost.

#### 5.2.11.4 Respiratory powder analysis

To each flask 10% v/v 1M Tris buffer at pH 8 was added, and made up to the mark with deionised water. The flasks were shaken and sonicated for 10 minutes prior to analysis. Table 30 shows the stages with the corresponding flask sizes used.

Table 30. Sequential ACI stages, with corresponding flask size.

ACI stage	Corresponding flask name abbreviation	Flask size (ml)
Mouthpiece, throat	T	250
Lid, pre separator, stage 0, plate 0	P	500
Stage 1, plate 1	1	100
Stage 2, plate 2	2	50
Stage 3, plate 3	3	50
Stage 4, plate 4	4	50
Stage 5, plate 5	5	50
Stage 6, plate 6, stage 7, plate 7, o ring, filter	6-F	100

Ellman's reagent was added, and the flasks inverted. Absorbance was measured at 440 nm in the absence of natural light, and with minimal artificial light. The resultant readings were inserted into the equation of the straight line to determine concentration. Stages 1-8 of the impactor contain the most important size fraction, i.e. below 5  $\mu\text{m}$ .

The fine particle dose (FPD) is defined as the respirable fraction of the delivered dose, which is the weight of powder less than 5  $\mu\text{m}$ , and was calculated from the sum of the powder collected on stages 1-7. The fine particle fraction (FPF) was calculated from the ratio of FPD to total powder weight. The emitted dose (ED) is the percentage of the total powder mass in the capsule which exits and deposits in the ACI. The respirable dose (RD) is the mass of drug recovered from the lower ACI stages (cut off 6.4  $\mu\text{m}$ ). The respirable fraction (RF) is the ratio of RD to total loaded dose (188).

### 5.2.12 ACI pressure and flow testing

To analyse the pressure drop across the inhaler device produced when a flow is initiated, a digital Manometer (P200 pressure meter, Digitron, England) was attached downstream on the ACI (without mouthpiece), in place of the flow meter. Readings were taken in triplicate at 55.8 L/min for 3 seconds, and 28.3 L/min for 5 seconds, and the results compared to atmospheric pressure using a calibrated barometer, using the equation:

$$R = Q/\sqrt{\Delta P}$$

Where R is the resistance, Q is the flow rate in L/min, and  $\Delta P$  is the pressure drop (cm H<sub>2</sub>O) (217).

### 5.2.13 Dissolution testing

A 100ml round-bottomed flask with sidearm was held in a water bath, and was heated to 37°C (body temperature). To the sidearm, a water condenser was attached. A 10% v/v solution of 1 M Tris buffer in deionised water was added to the flask (50ml), along with an equimolar weight of DTNB. The solution was stirred magnetically using an IKA RET basic hotplate stirrer (Staufen, Germany). At time zero, 50mg of the (50:50 blend) microspheres were added. The medium was sampled every 2 minutes. Samples were scanned on a UV from Unicam (Cheshire, UK) at 440 nm, the  $\lambda_{max}$  for TNB. This was performed in triplicate.

### 5.2.14 Stability testing

Upon manufacture ( $T_0$ ), the microspheres were analysed by TGA and IR spectroscopy, and stored under three different conditions in order to analyse their stability; a refrigerator (4°C) containing a desiccator, a store at room temperature and an Environmental Test Chamber (Copely, Nottingham, England) set at 30°C and 75% Relative Humidity (74). These conditions were chosen to cover cold storage, typical home storage and accelerated testing. The temperature in each of the storage conditions was monitored daily. TGA and IR spectroscopy tests were then performed, and compared with the results from the microspheres at  $T_0$  (74). The microspheres were also checked for any visual changes.

### **5.3 Results and discussion**

#### **5.3.1 Cysteamine bitartrate synthesis and analysis**

Cysteamine bitartrate was synthesised and characterised using  $^1\text{H}$ NMR and melting point analysis, the results compared with the commercial preparation Cystagon<sup>™</sup>.

The melting point of Cystagon<sup>™</sup> was measured at 95°C, 1°C higher than the melting point of the synthesised cysteamine bitartrate which was measured at 94°C. It was concluded from these results that cysteamine bitartrate had been synthesised.

#### **5.3.2 Microscope analysis**

Preliminary analysis was performed using a microscope fitted with a 100x objective lens, using mineral oil (figures 57-58). Although not as detailed as the SEM, it enabled qualitative assessment of the powders.

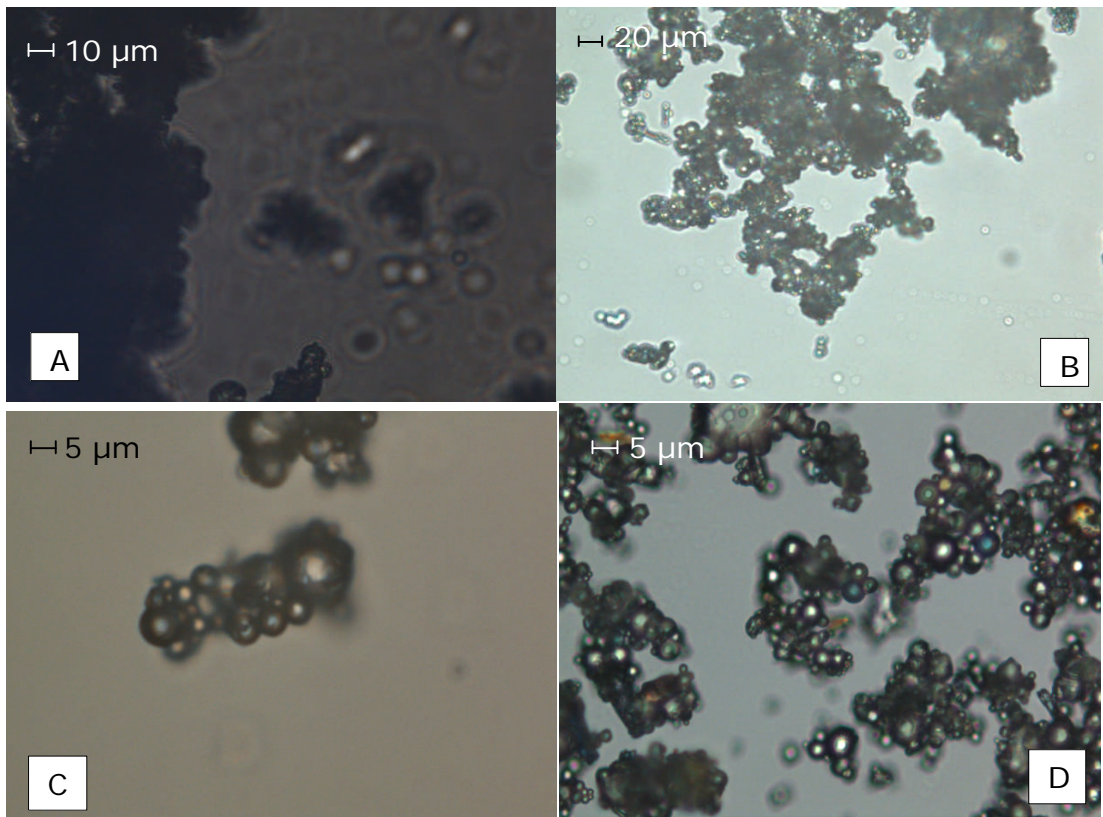


Figure 57. Optical micrographs of the progressing blends, illustrating the particles becoming more discreet; A. Batch 2, B. Batch 3, C. Batch 8, and D. Batch 8 showing particles of 3-5  $\mu\text{m}$ .

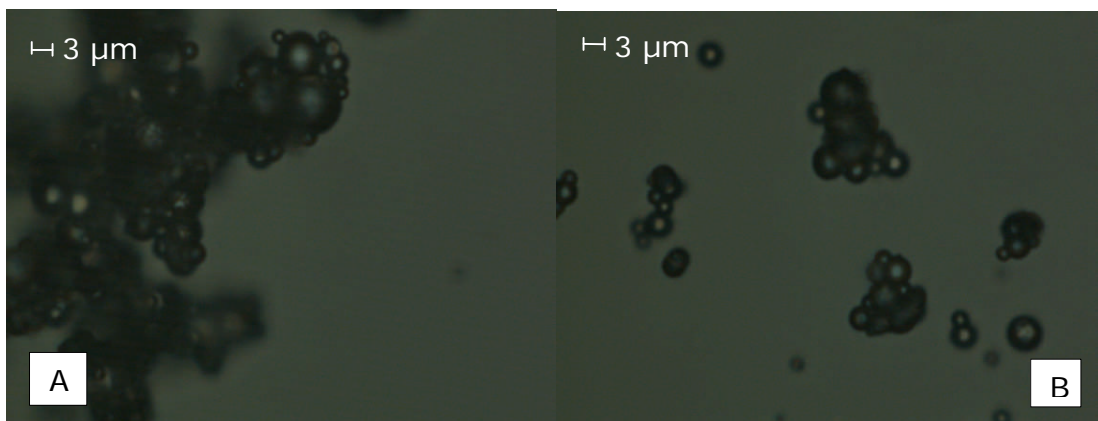


Figure 58. Optical micrographs illustrating the spherical final particles, A. Batch 9 particles of 2-3  $\mu\text{m}$ , and B. Batch 9 particles of 2-4  $\mu\text{m}$ .

The particles became more discreet and spherical as testing progressed due to a reduction in polymer concentration. Batches 8-10 were the most suitable for further testing, as they existed as discreet, spherical particles within the desired size range of 1-10  $\mu\text{m}$ , and were fully formed spheres when viewed by microscope. Initial batches of microspheres (batches 1 - 4)

were found to be highly agglomerated when viewed under the microscope. This was due to an excessively high polymer concentration, making the microspheres sticky and adhere together (253), and was confirmed by SEM analysis. Particle size is controlled by drug and polymer concentration (254,255). Too high a concentration of either drug or polymer produces a solution with increased viscosity, which is less readily separated into small droplets, and hence larger particles are produced. Too low a concentration gives particles which aren't fully encapsulated (255). Drug encapsulation is also influenced by polymer precipitation rate.

Another reason for this 'clumping' may have been an excessively high inlet temperature in the spray dryer. The Glass Transition temperature (T<sub>g</sub>) of a non-crystalline (amorphous) material is a critical point of physical change. If a polymer is used below its T<sub>g</sub>, the polymer is described as 'glassy' (brittle), and is not susceptible to molecular change. When used above the T<sub>g</sub>, polymers are soft and flexible ('rubbery'), allowing molecular change to take place (256,257). The T<sub>g</sub> for PLA is reportedly 45-55°C (data sheet), and 38-42 °C from Boehringer, therefore a wide temperature range was tested.

### **5.3.3 Scanning Electron Microscope (SEM) analysis**

The ten batches of polymer and drug were sequentially analysed by SEM (table 27). Spray dryer conditions were altered according to the results, until microspheres were formed. Initially, too high an inlet temperature and too high a polymer concentration lead to irregular morphology (figure 59). By slowly lowering the temperature and polymer concentration, discreet uniform spheres were formed (figure 60), within the required particle size range of 1.5 – 5 µm. Batch 9 was found to be ideal (figure 61), displaying discreet and uniform particles within the desired size range of 1-5 µm. The magnification used is displayed in the figure headings.

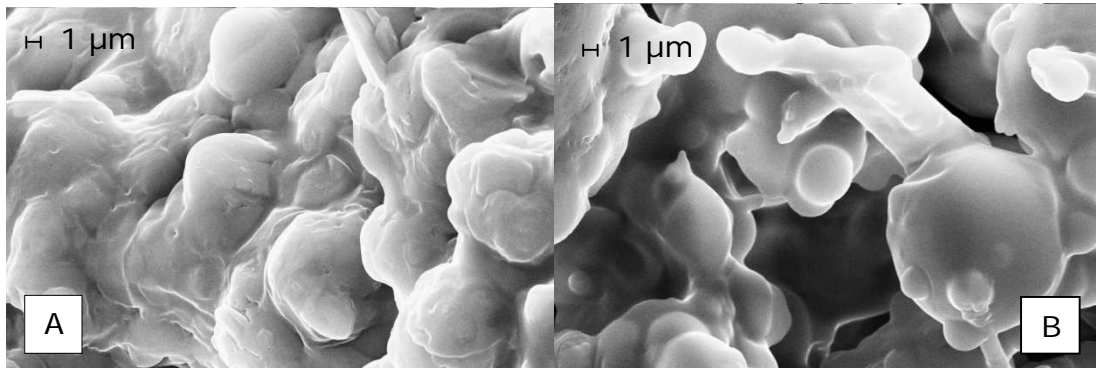


Figure 59. SEM images showing, A. Batch 2 showing signs of spheres (x10K), and B. Batch 3 becoming more spherical and displaying hard bridges between particles (x10K).

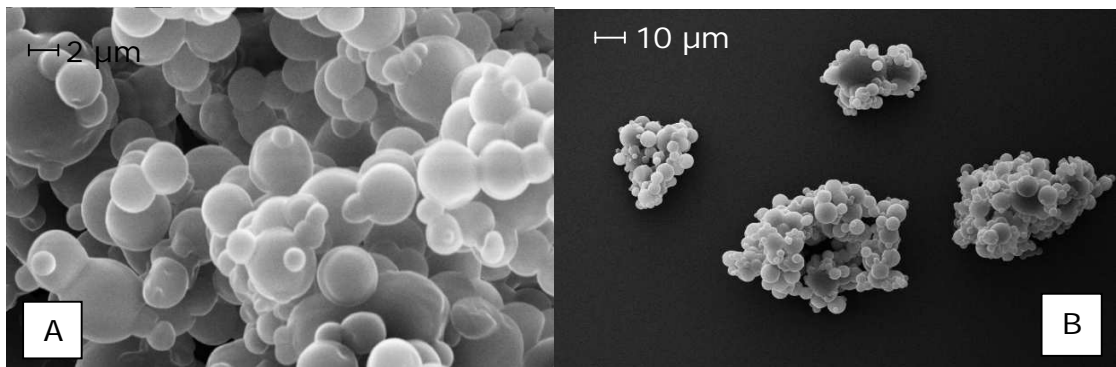


Figure 60. SEM images showing, A. Batch 8 showing fully formed microspheres, with many still connected (x10K), and B. Batch 9 with complete microspheres within the desired size range (1-6 μm) (x2K).

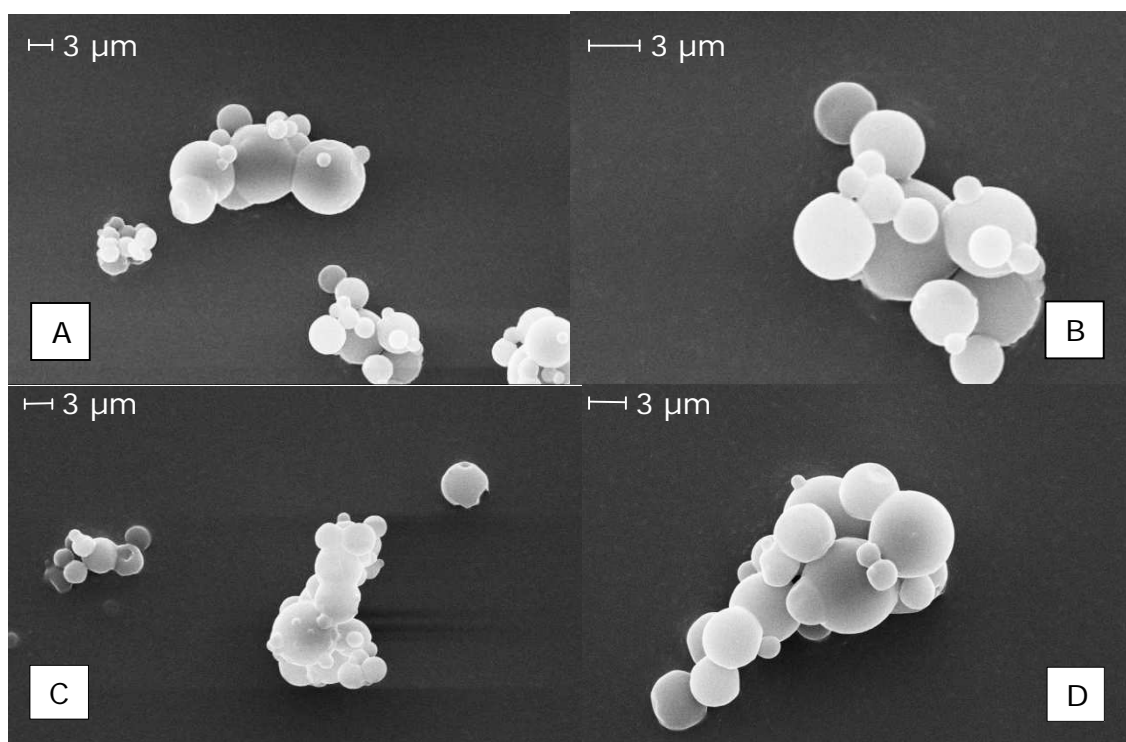


Figure 61. SEM images of Batch 9, the batch chosen for further analysis (magnification: A, x5.37K, B, x11.71K, C, x6.28K, D, x8.06K).

The Batch 9 microspheres exist as discrete particles, with smooth morphology. Batch 10 appeared to have insufficient polymer, as particles were not fully coated spheres (results not shown). Batch 9 microspheres were chosen as the particles with the most ideal size and shape, and with the optimum spray dryer conditions (table 28). SEM analysis gives only a 'snapshot' of particle size, therefore the powders were also tested using laser light scattering.

#### 5.3.4 Particle size analysis

Batch 9 microspheres were prepared in five ways and analysed. The results are shown in table 31.

Table 31. Summary of the particle size results for Batch 9 microspheres (n = 3).

Statistics	D[v, 0.1]	D[v,0.5] (MMAD)	D[v, 0.9]	D[4,3]	D[3,2]	Span
Batch 9 dry powder mean ( $\mu\text{m}$ )	3.71	25.37	304.49	95.42	8.54	11.86
Batch 9 dry powder mean sieved ( $\mu\text{m}$ )	13.38	200.83	504.76	222.30	39.04	2.45
Batch 9 hexane solution mean ( $\mu\text{m}$ )	5.89	57.09	127.20	87.81	18.42	2.12
Batch 9 acetone solution mean ( $\mu\text{m}$ )	10.25	25.82	54.85	29.65	18.88	1.73
Batch 9 chloroform solution mean ( $\mu\text{m}$ )	10.04	25.64	50.95	28.40	19.24	1.60

D(v, 0.1) is the size of particle for which 10% of the sample is below this size. D(v, 0.5) is the size of particle at which 50% of the sample is smaller and 50% is larger than this size. This value is known as the Mass Median Aerodynamic Diameter (MMAD). D(v, 0.9) gives a size of particle for which 90% of the sample is below this size. D[4.3] is the equivalent volume mean diameter or the De Broncker mean diameter. D[3,2] is the equivalent surface area mean diameter or the Sauter mean diameter. Sauter mean diameter is defined as the diameter of a sphere that has the same volume/surface area as the particle of interest. The lower the span, the more homogenous the powder's particle size distribution (220).

Aerodynamic diameter ( $d_{ae}$ ) particle size (MMAD) is critical for determining the performance of a particle. It is affected by size, shape and density (204). This is important to understand how a particle behaves in a moving air stream, like the respiratory tract, information which diameter alone does not explain. Therefore for a given density, small particles have lower aerodynamic diameters compared to larger ones. Porous particles would have an even lower  $d_{ae}$  (204).

Scanning electron images show the microspheres to be less than 5  $\mu\text{m}$  in diameter. However, the particle size results do not support this, which is probably due to friction agglomeration causing particles to adhere together, and failing to break up during the analysis. For this reason, microspheres were subjected to different methods of preparation before analysis,

including sieving. However, this produced more agglomeration in the powders. Solubility of the powders in the dispersing agents could cause agglomeration. Particles should be insoluble in any dispersing agent, and were found to be insoluble in all three of the solvents used. Wet analysis confirms that agglomeration is a major problem with these microspheres. There are reports of correlation between light scattering particle size measurements and impaction analysis (219). Comparisons between the results are made in section 5.3.7.

### 5.3.5 Moisture content of microspheres

The moisture content of the microspheres was analysed by TGA immediately after harvesting ( $T_0$ ), and at subsequent time intervals for two weeks. The results are shown in table 32. TGA analyses the mass of the sample during heating to determine weight change due the loss of volatile components.

Table 32. Moisture content of Batch 9 microspheres over time (n = 3).

Batch 9	Moisture content (%) ( $\pm$ SD)
$T_0$	0.83 ( $\pm$ 0.04)
$T_{1 \text{ day}}$	0.33 ( $\pm$ 0.03)
$T_{2 \text{ days}}$	1.23 ( $\pm$ 0.03)
$T_{1 \text{ week}}$	0.54 ( $\pm$ 0.04)
$T_{2 \text{ weeks}}$	0.70 ( $\pm$ 0.03)

Hygroscopic microspheres are removed from the air stream quicker than non-hygroscopic particles, as described in the introduction. By coating cysteamine bitartrate with PLA, the hygroscopic nature of the drug should largely be avoided. The water content of PLA is reported as being less than or equal to 0.5% (data sheet), however this is dependent on temperature and relative humidity. There is no significant absorption of moisture by the microspheres when monitored over a two-week period.

### **5.3.6 Drug content of microspheres**

The calibration curve was obtained from UV analysis of a set of standard solutions containing Ellman's reagent, producing a curve of absorbance versus cysteamine bitartrate concentration as follows:  $y = 1.2808x + 0.05$ , where  $y$  = absorbance and  $x$  = cysteamine bitartrate concentration, with an excellent correlation coefficient of  $r^2 = 0.9995$ . Using this method, calculation of cysteamine bitartrate concentration was made for drug content, dissolution and ACI analyses. The drug content of the microspheres was calculated to be 50% ( $n = 6$ ,  $SD \pm 0.2$ ).

### **5.3.7 Blend with lactose**

The microspheres possessed very poor flow properties, and were subject to large static forces due to their minute size range (1-5  $\mu\text{m}$ ). This was demonstrated when sieved microspheres were found to be larger than prior to sieving (table 31). Due to this property, it was unlikely that they would leave the inhaler and travel through the airways without a carrier particle. Batch 9 microspheres were combined with three different lactose grades at 1.5%, and viewed using SEM (figures 62 – 64).

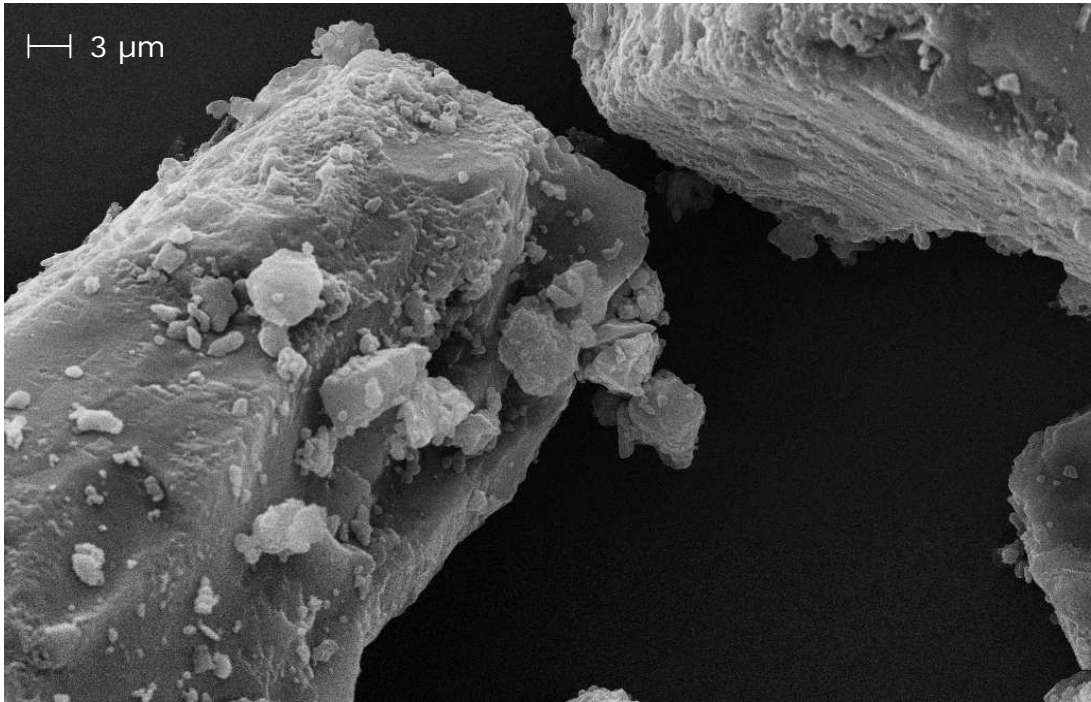


Figure 62. SEM of 100  $\mu\text{m}$  lactose, showing large planar particles with minor asperities (x4.68K).

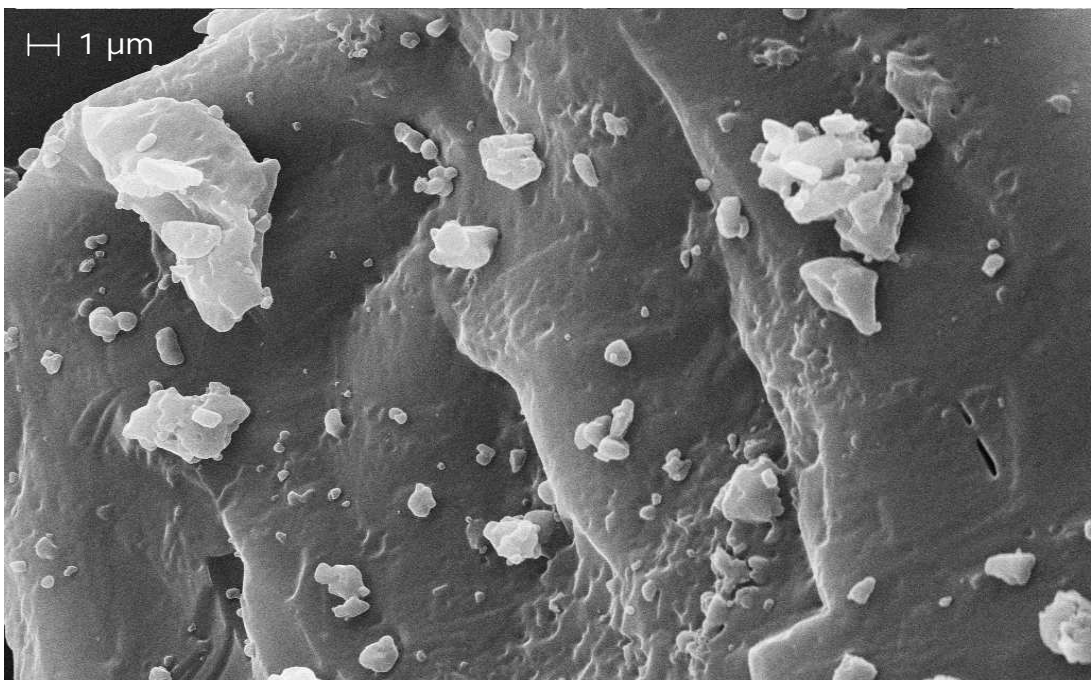


Figure 63. The BP lactose grade possesses many areas for drug particle attachment (x10K).

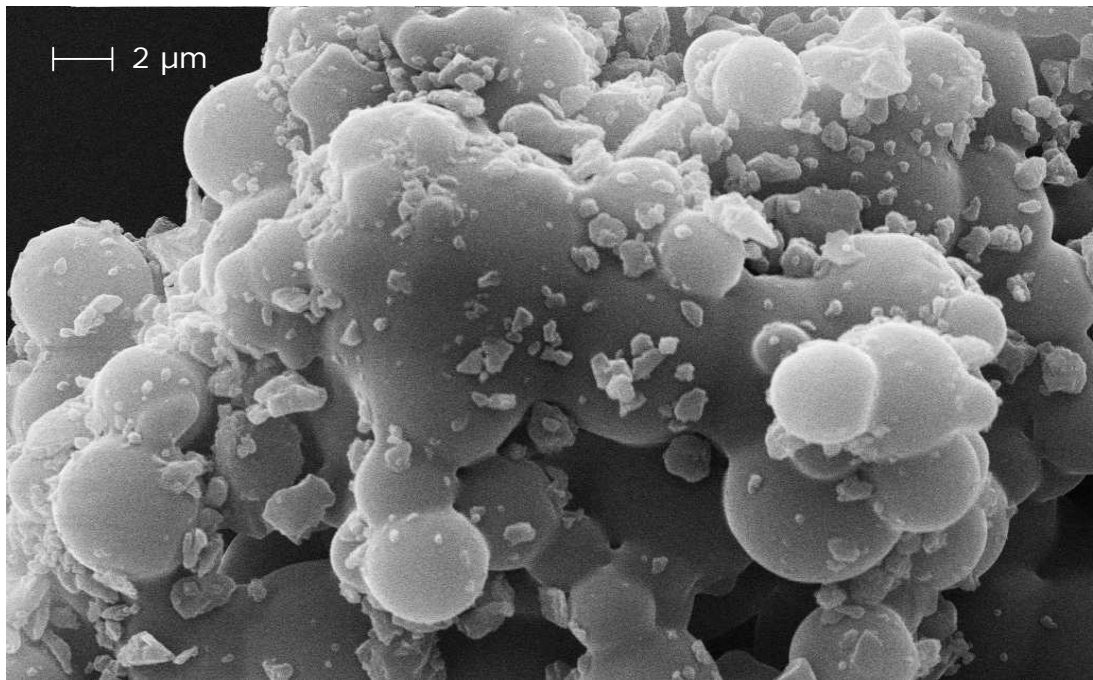


Figure 64. The spray dried/USP lactose has extensive regions for particle attachment (x10K).

Both the spray dried/USP and BP grades are processed to produce particles with major asperities, whereas the 100 μm grade is planar with few asperities. Lactose which has been spray dried can be prohibitive to drug particle release, producing active areas of high surface energy (roughness) which the microspheres cannot detach from (227). Therefore, of the three lactose grades tested, sieved 100 μm grade was selected for further analysis. The standard lactose blend ratio of 67.5:1 used in some asthma inhaler powders was difficult to view with the SEM, as the lactose was larger than the microspheres by a magnitude of approximately fifteen. When blended in a ratio of 50:50, the microspheres can be seen attached to the surface of the lactose (figure 65).

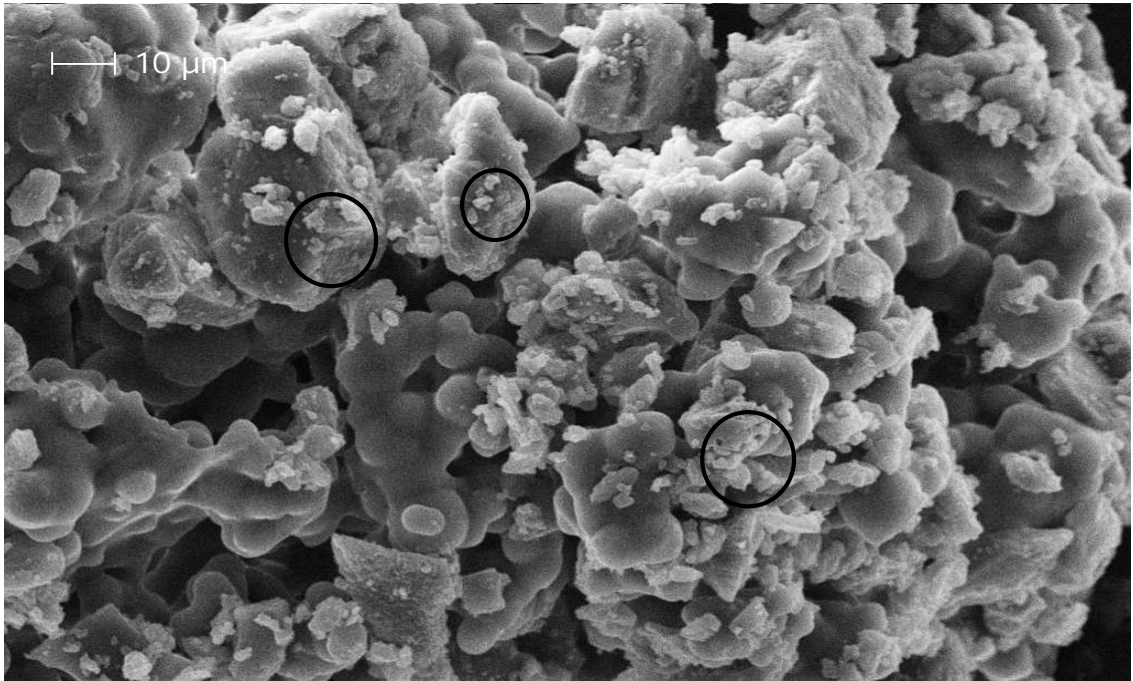


Figure 65. SEM of a 50:50 mix of 100 µm lactose with Batch 9 microspheres, with the microspheres clearly attached to the carrier lactose particles (x2.1K).

Due to the unknown level of metabolism and pharmacokinetics of the microspheres in the lungs, it was decided to maintain the blend at a 50:50 level for the subsequent tests. The powder characteristics should be improved at this level, while allowing a larger dose of drug to be loaded into the capsules if required.

The quantity of lactose present in powders for inhalation is low enough that even in patients with lactose intolerance there should be no problems (199). Any lactose which impacts in the upper airways is hydrolysed by enzymes and swallowed, and that which reaches the deep lung is absorbed and metabolised.

Recently, studies have been conducted to find alternatives to coarse carrier particles to improve powder flowability. Incorporating dispersability enhancers before spray drying has been shown to enhance aerolisation properties (220).

### 5.3.8 Andersen Cascade Impactor: Analysis

The temperature and relative humidity were monitored before and after ACI testing, and the average values are shown in table 33. The powder batches were analysed by ACI, and the results are summarised in table 34.

Table 33. The average room temperature and relative humidity at ACI testing, and standard deviation between readings.

Average temperature (°C)	20.9 (± 0.02)
Average RH (%)	35.2 (± 0.36)

Table 34. Summary of the powder batch characteristics (mean, n = 3)

Powder batch	FPD <sup>a</sup> (µg)	FPF <sup>b</sup> (%)
Batch 9, 10%RH 25°C, 55 L/min	25 (± 0.5)	0.0032
Batch 9, 21°C, 55 L/min	33 (± 0.4)	0.042
Batch 9, 4°C, 55 L/min	19 (± 0.5)	0.045
Batch 9, lactose 50:50, 4°C minimal handling, 55 L/min	72.3 (± 0.3)	0.073
Batch 9, lactose 50:50, 4°C minimal handling, 28 L/min	62 (± 0.4)	0.051
Batch 9, lactose 50:50, 21°C, 55 L/min	75 (± 0.2)	0.07
Milled cysteamine bitartrate, 4°C, 28 L/min	38 (± 0.3)	0.046
Milled cysteamine bitartrate, 4°C, 55 L/min	47 (± 0.5)	0.043

<sup>a</sup> Fine particle dose < 5 µm.

<sup>b</sup> Fine particle fraction, as percentage of total loaded dose (220).

Of the batches tested, the powders which contained lactose produced a higher FPD, suggesting that the carrier particle has aided the drug further into the deep lung tissue. Initially, a flow of 55 L/min was used during the ACI testing. However, poor particle deposition was seen in the critical stages, i.e. 2-5. A comparative flow of 28.3 L/min was then used, in an attempt to minimise losses to the throat and preseparator through inertial impaction. The powders which were tested using a flow of 55 L/min produced higher FPD values. This could be due to the high resistance of the inhaler device, requiring more effort to remove the powder. An attempt to reduce the static agglomeration through minimised contact had minimal effect. Table 35 shows the percentage deposition on the corresponding plate of the most successful powder batch (Batch 9, lactose 50:50, 21°C, 55 L/min). Figure 66 compares the effect of storage upon the same powder.

Table 35. ACI cut-off diameters and the corresponding powder deposition.

ACI stage	Cut-off diameter ( $\mu\text{m}$ ) <sup>a</sup>	% deposition ( $\pm$ SD)
Stage 1	4.1	2.27 ( $\pm$ 0.3)
Stage 2	3.2	1.42 ( $\pm$ 0.4)
Stage 3	2.1	1.43 ( $\pm$ 0.4)
Stage 4	1.4	1.26 ( $\pm$ 0.3)
Stage 5	0.62	1.60 ( $\pm$ 0.3)
Stage 6 + 7	0.35 – 0.15	3.26 ( $\pm$ 0.2)

<sup>a</sup> (244,245)

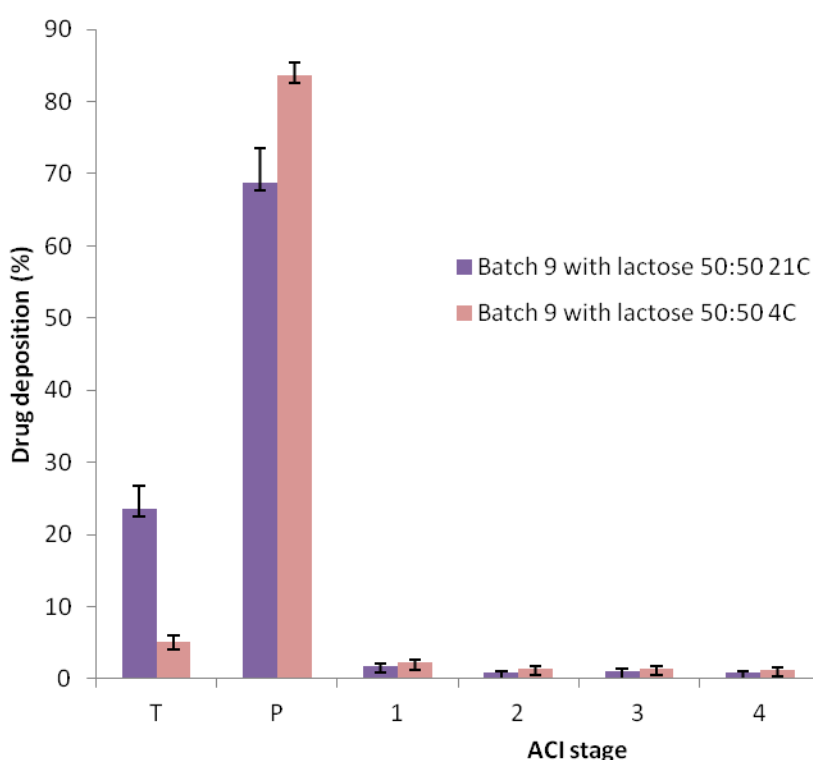


Figure 66. Comparison of storage effects on the most successful powder blend, T = throat, P = preseparator.

The low in vitro deposition seen is probably due to particulate agglomeration, which inhibits powder flow from the capsule into the ACI. This is the most likely cause of large upper airways impaction seen. It is common to see more than half of a drug powder deposit in the preseparator and stage 0 (246), particularly if a carrier particle is employed. However, the excessively large losses seen here may be due to the carrier particles failing to release the drug particles. The process of sieving may

also have increased lactose surface roughness and produced high surface energy sites, improving the bond between drug and carrier particle (246).

Targeting of the alveolar region is crucial for efficient systemic delivery (220). Studies have shown that for the granulated lactose, a larger particle size produces a larger respirable fraction (227). This is corroborated by a correspondingly low MMAD. A particle size of around 200  $\mu\text{m}$  is ideal; any larger and the drag forces become prohibitive (227). The powder developed during this project is therefore unsuitable for deep lung targeting without substantial further work. The powders may be improved with a simple change in the carrier particle, or may require a more fundamental alteration.

#### **5.3.9 ACI pressure and flow testing**

The average atmospheric pressure was recorded at 753 mmHg. Resistance for the device at 55.8 L/min was calculated to be 15.89 kPa, and 25.89 kPa at 28.3 L/min. In both cases the required minimum pressure drop of 4 kPa across the device was achieved, satisfying both the European and US Pharmacopoeias. The predictably high resistance of the Handihaler<sup>®</sup> device is important, and produces a good balance between usability and efficiency (258).

The US and European Pharmacopoeias also recommend that the duration of flow should give a volume of 4 Litres. Inhalers are usually tested based on the inspiratory capacity of 3.5 L for men and 2.7 L for women (USP 601). This is the maximum volume that can be inspired following a normal, unforced expiration. However, shorter, lighter people will naturally have a lower lung capacity, and, as most of the cystinosis patients are children or are short in stature and underweight, these figures are unlikely to be achieved. Therefore, flow volumes were used which were more representative of the patient group. A flow of 55.8 L/min for 3 seconds produced a volume of 2.79 L, while 28.3 L/min for 5 seconds produced a volume of 2.36 L.

### 5.3.10 Dissolution testing

The drug was released almost instantly from the microspheres, and after 8 minutes 100% of the drug had been released (Figure 67). This measurement was performed four times, and the average release plotted.

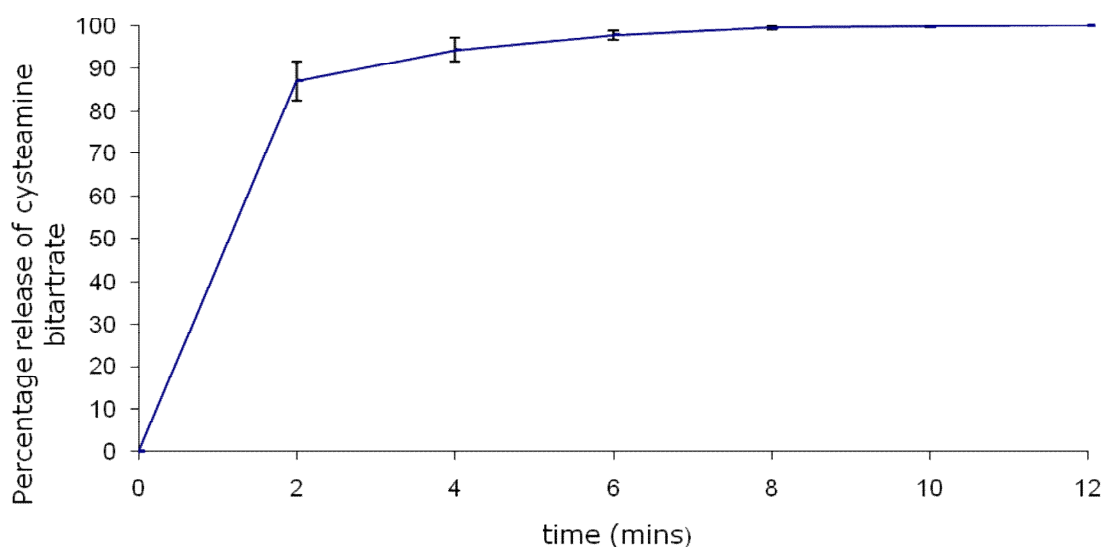


Figure 67. Cysteamine bitartrate release from the microspheres over time (n = 4).

The small size of the particles has a large surface area, and therefore quicker release. The volume used in this experiment was 50 ml, which is within lung lining fluid limits, while the weight of microspheres was double the dose used in the capsules, eliminating concerns of dose accumulation issues.

### 5.3.11 Stability tests

TGA analysis was performed at intervals over a two-month period, and IR analysis for two weeks. At T1week, it was observed that the batch of microspheres subjected to 30°C and 75% RH had degraded significantly and irreversibly. The particles had largely dissolved in the high humidity, and had recrystallised as large agglomerated crystals which had fused to the

base of the container. The particles stored at 4°C and room temperature were still present as a white, fluffy powder (Figure 68).

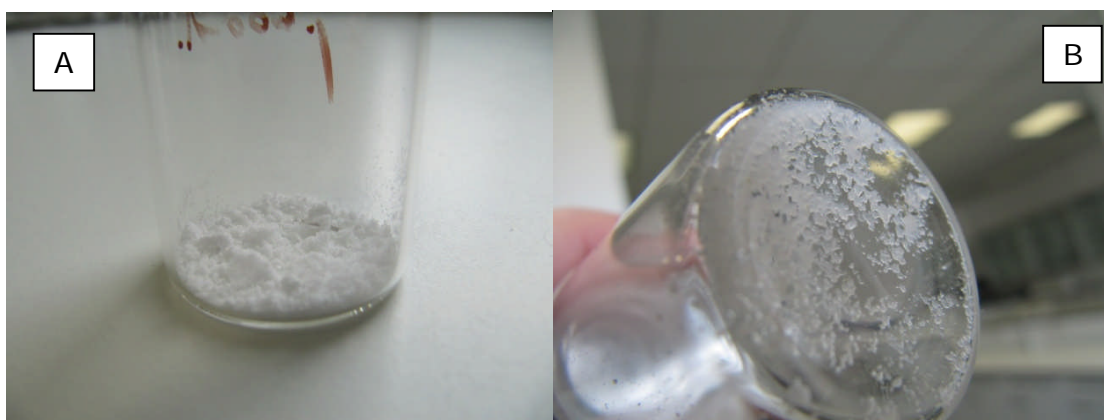


Figure 68. Images of, A. Batch 9 microspheres stored at 4°C for 1 week, and B. Batch 9 microspheres stored at 30°C, 75% RH for 1 week.

IR analysis showed a 96.78% match of the microsphere batch stored at 30°C and 75% RH after one week (table 36). After two weeks this had decreased to a 79.19% match with microspheres at time zero,  $T_0$ . Figure 68 shows evidence of microsphere degradation after only one week of storage at 30°C. The microspheres stored at 4°C displayed greater stability over time, as demonstrated by an 11.6% change in percentage match over seven days, compared to a 19.8% change (21°C storage) and a 17.6% change (30°C storage)

Table 36. IR analysis of Batch 9 microspheres stored in varying storage conditions, compared with  $T_0$ .

Drug powder	Percentage overall match to microspheres at $T_0$
T1 week 4°C	98.12%
T1 week 21°C	97.77%
T1 week 30°C	96.78%
T2 weeks 4°C	86.53%
T2 weeks 21°C	77.94%
T2 weeks 30°C	79.19%

TGA analysis showed minor changes in the microspheres over time, with a consistent 0.5% weight loss at lower temperatures with the loss of water,

and the beginning of decomposition at around 150°C. Figure 69 is a representative plot.

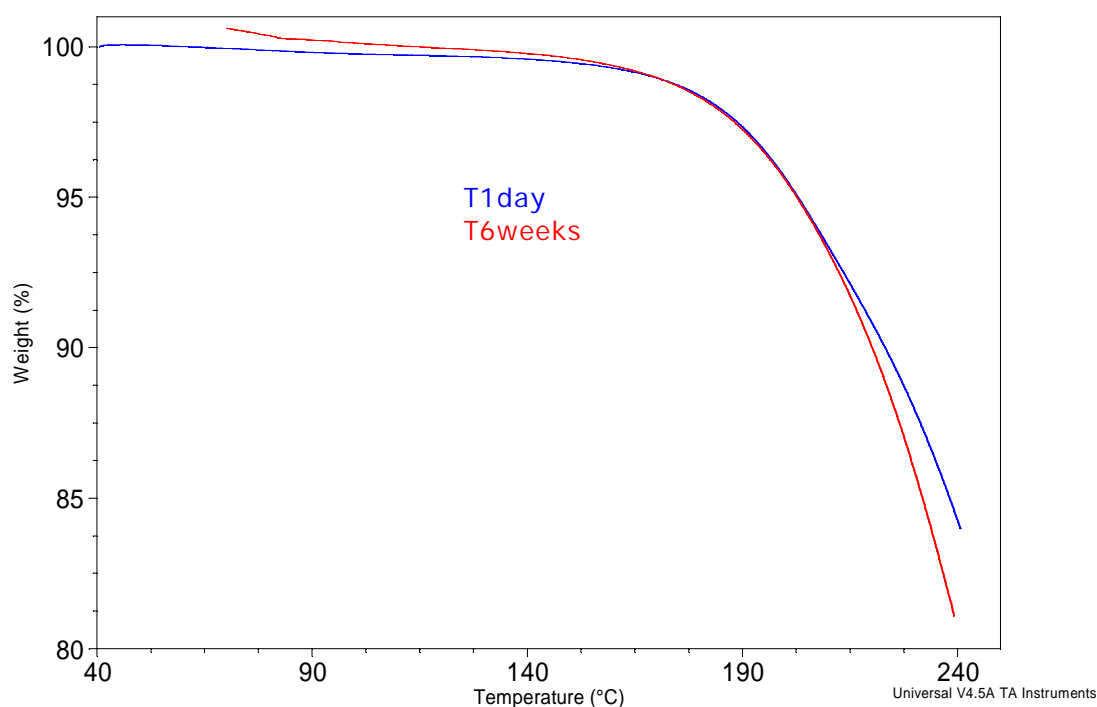


Figure 69. TGA plot comparing Batch 9 microspheres from T1 day and T6 weeks, stored at 30°C and at 75% RH.

The amorphous nature of the particles produced by spray drying can become more crystalline when exposed to high temperatures and/or humidity (219). This change can have a dramatic effect on particle deposition, and can lead to strong irreversible bridge formation, through dissolution in condensed water vapour as capillary forces are strong (246). Moisture can also act as a plasticiser leading to softening, and as a lubricant aiding the detachment of drug from carrier particles (246). Relative humidity should not exceed 55% in any stage of manufacture or storage to prevent the formation of capillary forces (246).

The microsphere degradation observed when a storage temperature of 30°C and 75% RH was used (figure 68 and table 36) cannot be explained by an uptake in moisture as previously hypothesised, as TGA analysis shows insignificant moisture uptake over time (table 32). Poly(D,L-lactide) is a thermoplastic polymer. This allows molecular movement within the polymer

when it is subjected to a temperature around or above its T<sub>g</sub>. At 4°C, the polymer is below its glass transition temperature, and is in a glassy state (240). When the T<sub>g</sub> is reached (45 - 55°C), the polymer 'softens' at a molecular level. The rubbery state is at a higher level of free energy than the glassy state, so the polymer has the potential to be more reactive in this state. Storage of the microspheres at this elevated temperature and relative humidity should be avoided to prevent degradation of the polymer and subsequent loss of activity.

#### **5.4 Conclusion**

Cysteamine bitartrate was spray-coated with the polymer PLA to produce microspheres suitable for delivery to the lungs. The ideal ratios and solvents required were determined in extensive preformulation tests. Each batch was analysed by microscope, and the polymer concentration altered until discreet, spherical particles were produced. Cysteamine hydrochloride was unsuitable for spray drying due to its hygroscopic and deliquescent nature, as shown by almost instant uptake of environmental moisture. Cysteamine bitartrate was synthesised and used as the active component. Polymer coated microspheres in the size range required for targeted lung delivery (1-5 µm) were produced and analysed. Drug release from the microspheres was complete after 8 minutes. Moisture content analysis revealed minimal moisture absorption over two weeks. Microspheres were blended in a ratio of 50:50 with a carrier lactose particle. In vitro analysis revealed a large preseparator loss of microspheres. This could have been caused by the static agglomeration of particles or the poor separation of drug particles from the carrier lactose particles. Microspheres stored in the refrigerator displayed the greatest stability over time.

The PLA-coated cysteamine bitartrate microspheres were developed during this project as a potential alternative to the current oral capsule treatment of cystinosis. Analysis of the respiratory powders demonstrated unsuitability for deep lung targeting without substantial further work. There was evidence of insufficient powder penetration to the deep lung. This is a

fundamental requirement for targeted delivery to the lungs, as the lower airways are mainly involved in drug absorption. The likely cause for this poor lung penetration is static agglomeration, caused by minute particle size. The powders may be improved with a simple change in the carrier particle, or may require a more fundamental alteration (chapter 6). These results demonstrated that more development work was required to produce a useful pulmonary formulation of cysteamine bitartrate. Further work on the respiratory powders was beyond the scope of this project.



## **Chapter 6 – General discussion and future work**

## **Chapter 6 – General discussion and future work**

The purpose of this project was to investigate alternative formulations to the current oral capsule and eye drop preparations for the treatment of cystinosis. Rectal, ophthalmic and pulmonary deliveries were investigated.

### **6.1 Rectal delivery**

The side effects and dosage regime of the current oral capsule form of cysteamine are serious barriers to compliance. Much of the drug is lost to first-pass metabolism and protein binding, which necessitates a high dose. The oral treatment for cystinosis causes frequent emesis, and possesses an offensive taste and smell. It requires strict six-hourly dosing, which disturbs sleep. As a consequence, compliance can be poor. This limits the benefits of cysteamine therapy significantly. Early initiation of disciplined therapy has been demonstrated to improve long-term morbidity and mortality of cystinotic patients (41,259). Studies have also demonstrated that diligent therapy, if started early in life, could maintain glomerular function at the same level or even prevent the need for renal transplantation completely (22). It is challenging to administer the currently available capsules to infants (4). A suppository formulation may allow easier systemic administration of cysteamine to infants and young children. This would ensure the delivery of the crucial early therapy, with long-term implications. The avoidance of the GI tract and first-pass effect will allow a lower dose to be administered, reducing the side effects and also removing the disagreeable taste and gastric effects currently experienced with the capsules. This will reduce the fluid and salt losses through frequent emesis, and in addition may allow relief from the overnight dose and provide a more stable daily routine for the patients. Compliance for other treatments is likely to be improved as a result, easing the burden of care for the patient's families and carers.

Various suppository bases were investigated for suitability of delivery of cysteamine hydrochloride. PEG bases were found to possess the most ideal characteristics, i.e. compatibility with cysteamine hydrochloride, prolonged release over time and stability upon handling. Upon subsequent testing and analysis, the suppositories demonstrated complete cysteamine hydrochloride release after 40-60 minutes. There was also evidence of stability over 12 months. In particular, PEG Blend C possessed the most ideal characteristics of the three suppository bases investigated, demonstrating long-term stability and ease of manufacturing, handling and storage when compared to PEG Blends A and B.

Cysteamine hydrochloride was successfully formulated as a suppository. Further testing of these forms will determine their viability. Future work should include in vivo testing of the suppositories to investigate their suitability for the treatment of cystinosis. Only through in vivo studies can the true efficacy of the forms be determined. There are concerns over the long-term use of PEG, as the osmotic nature of dissolution can irritate the rectal mucosa over time. This problem can be avoided by moistening the suppository prior to insertion, however the hygroscopicity of cysteamine may lead to drug loss from the suppository. Future studies would determine the significance of any drug loss due to this practice.

Stability of the forms over time may be improved by a more controlled cooling rate within the moulds, allowing larger PEG crystals to develop. This may be achieved by pouring the suppositories into moulds within a temperature-controlled unit, slowly reducing the temperature over time. The suppositories could be further developed into in situ gelling forms, with the incorporation of a gel such as HPMC. This may improve patient comfort upon administration.

The formulation and characterisation of cysteamine suppositories has demonstrated that the rectal route of delivery could greatly relieve many of the side effects currently experienced, thereby improving patient's compliance with treatment, quality of life and subsequent morbidity. Cystamine has demonstrated efficacy in a number of other disease states,

and therefore there is the potential for a much larger patient population to benefit (see section 6.4).

## **6.2 Ophthalmic delivery**

The corneal crystals present in cystinosis are treated by the regular insertion of an eye drop. The oral cysteamine capsules have no effect on this symptom, as the cornea has no blood supply (21). The current eye drops sting upon insertion, causing discomfort. They also require hourly administration to be most effective, as they have a very short residence time of 1-2 minutes. Compliance with this current medication is poor (106), leading to severe ophthalmic conditions. Blindness is a potential endpoint. Ophthalmic gels were investigated as an alternative to the current eye drop formulation.

Cysteamine hydrochloride was formulated as a bioadhesive eye gel using three different gel bases (carbomer, xanthan gum and HPMC). Carbomer gel exhibited ideal properties for a formulation to replace and improve upon the current eye drop, i.e. pseudoplastic rheology, drug release over 40 minutes and long-term stability. The carbomer gel also displayed bioadhesion, and this, in combination with increased viscosity, should improve bioavailability through prolonged contact time with the cornea. Formulated at pH 7.4 for maximum comfort, the carbomer gels will allow blinking to occur without interference (112). However, the optical transmission of the gel was very poor, and would cause blurred vision unless improved. The high salt content of the gels may be causing precipitation, which is observed as opacity. Currently, the eye gels would be useful as an overnight treatment. This may reduce the dosage required during the day, and allow once or twice-daily dosing. Future work may improve this factor, and permit daytime administration.

The transmission of light through the gel should be investigated using a smaller path length such as 1 mm instead of 10 mm, to allow the

investigation of a more realistic in vivo situation. Subsequent analysis should include in vivo testing of the developed ophthalmic forms, allowing safety analysis to be performed. Rabbits are frequently used as test models for ophthalmic formulations, due to structural similarities of the rabbit eye with human eyes, as well as an increased sensitivity to irritants allowing a conservative result to be obtained (107,113). In combination with this in vivo work, gamma scintigraphy could be utilised as a method of monitoring the residence of the instilled eye gel, from installation in the eye to ultimate metabolism in the liver (138). It allows observation without interference, and may be a useful tool in the further analysis of the ophthalmic gels.

Future work with the carbomer gels should also involve the incorporation of a preservative such as benzalkonium chloride. This was previously only included in the xanthan gels due to the propensity of xanthan gum to support bacterial growth. The gels should be formulated with cysteamine bitartrate, and the rheology, bioadhesion and stability analysed. Incorporating cysteamine bitartrate as the active in comparison to the hydrochloride form may also bring an improvement to stability over time, as the bitartrate form is less hygroscopic (260).

Bioadhesive, pseudoplastic, pH neutral, prolonged release hydrogels were developed for the treatment of the corneal crystals. Full characterisation demonstrated the suitability of the carbomer gel as a replacement for the current eye drop. The gel may be useful as an overnight treatment of the ophthalmic crystals, eliminating the therapeutic break during sleep. This may also allow for less frequent dosing during the day, thereby increasing compliance and reducing serious ophthalmic complications such as corneal rupture. The optical clarity may be improved to permit daytime dosing.

The gel base may also be suitable as a carrier for other ophthalmic treatments which require chronic application. Drug bioavailability for eye drops is typically very low, necessitating frequent dosing. Subsequent compliance for chronic ailments such as for glaucoma can be poor. By maximising the drug contact time and aiding patient comfort, these gels may boost compliance by greatly improving the bioavailability, reducing the

dosage frequency to once or twice a day. This 'universal gel base' could revolutionise ophthalmic treatment, greatly improving a drug's efficacy and reducing subsequent health costs. Currently there are very few ophthalmic gels on the market, however the benefits could potentially be enormous.

### **6.3 Pulmonary delivery**

The delivery of cysteamine to the lungs as a systemic treatment for cystinosis may allow the avoidance of the first-pass effect, reducing the dosage required and subsequent side effects. The drug's foul taste and smell can also be removed through polymer coating. Cysteamine bitartrate was spray-coated with a biodegradable polymer (PLA), producing microsphere-sized particles suitable for respiratory delivery. The polymer coating was designed to improve the handling and stability and eliminate the odour of the cysteamine bitartrate. The particles were analysed for size and morphology by Scanning Electron Microscope and particle size analyser. The microspheres were found to be spherical and uniform, and within the size ranges required for optimum deep lung targeting (2-5  $\mu\text{m}$ ). The microspheres were found to release 100% of the cysteamine bitartrate after 8 minutes.

However, much of the drug was lost to the 'throat' section of the Andersen Cascade Impactor in vitro testing apparatus. Deep lung penetration is critical for successful delivery of drugs to the lungs for systemic treatments. There are many possible causes for this drug loss, including static agglomeration, too large particles and poor flowability. The bench-top spray dryer used in this project also may have contributed to this poor deep lung penetration, as the drying chamber is too small and may permit residual solvent. Although these factors were not fully investigated during the course of these studies due to time constraints, they present opportunities for further research in the area.

Significant additional work is required to produce a viable respiratory dosage form. Deep lung penetration is critical for the dosage form to be successful. Further studies of the respiratory powder should include testing with a carrier particle in the size range of 200 micrometers, as this has recently been demonstrated as an ideal carrier particle size for maximising deep lung drug delivery (227). This simple adjustment to the formulation may dramatically improve powder penetration to the lungs. A novel method of improving powder flowability is to coat the microspheres with magnesium stearate, which can dramatically improve aerolisation by lowering cohesion (225). This may be another simple method to improve the deep lung penetration of the microspheres.

Jet milling the cysteamine bitartrate would produce a powder with a smaller and more uniform particle size distribution, and may significantly improve deep lung penetration. Jet milling is the most widely-used method for the production of microspheres for inhalation (219). However, it is an expensive method of particle size reduction and also requires large batch sizes of around 1 kg, which makes it an unsuitable technique for small-scale research.

Cysteamine absorption in the lung has been demonstrated (197), and therefore an inhaler could be a useful route of delivery. Patients of all ages would benefit from the advantages of a dry powder inhaler, except babies and very young children. This patient group would be more suitable for the suppository formulation. A DPI would mask the taste of the cysteamine and allow a lower dose to be administered, further reducing the side effects. Compliance with the treatment should improve, as administration becomes easier and less stressful, perhaps in combination with the suppositories.

#### **6.4 Cysteamine bitartrate's indications in other disease states**

Cysteamine bitartrate has demonstrated efficacy in a range of other conditions such as Huntington's disease, Parkinson's disease, Alzheimer's disease, malaria, and radiation sickness (2,46,260-263), and is being investigated as a potential treatment of schizophrenia (264-266).

Huntington's disease is much more prevalent than previously thought, and there are currently 12.4 sufferers per 100,000 population (267). By 2050 it is estimated that 16 million people in the US alone will be suffering from Alzheimer's disease (268). This imparts greater versatility upon the formulations developed during this project, and potentially allows a much wider patient population to benefit from the improvements made to the oral cysteamine bitartrate formulation. Currently there are around 2000 diagnosed cystinosis patients in the world. If cysteamine becomes a routine treatment for these more common diseases, the improvement of efficacy, side effects and quality of life that the suppository or inhaler forms could bring over the current oral capsule may be experienced by millions of patients.

## **6.5 General conclusion**

The aim of this project was to develop alternative formulations of cysteamine with the potential to reduce or eliminate some of the side effects which are evident using the current oral capsule and ophthalmic eye drop, thereby improving the quality of life for those affected. Cysteamine hydrochloride was successfully formulated as a suppository in a PEG base, however further work is required to determine the in vivo efficacy and long term safety of this formulation. It may be a useful dosage form in paediatric treatment of cystinosis or when the oral route is compromised. A bioadhesive ophthalmic gel was developed to replace the current eye drop, and may allow a reduction in administration from 15-times per day to once or twice daily dosing although currently the optical clarity is extremely poor. A reduction in salt content may improve this to allow daytime administration. A dry powder inhaler was also developed, however further work is required to improve deep lung penetration. It is hypothesised that further development of these new formulations may lead to increased compliance through puberty and into adulthood, and subsequently reduce morbidity and mortality in the latter stages of the disease.

## References

- (1) Almond PS, Matas AJ, Nakhleh RE, Morel P, Troppmann C, Najarian et al. Renal Transplantation for Infantile Cystinosis: Long-Term Follow-Up. *Journal of Pediatric Surgery*. 1993; 28(2):232-238.
- (2) Gahl WA, Kleta R. Nephropathic Cystinosis in Adults: Natural History and Effects of Oral Cysteamine Therapy. *Annals of Internal Medicine*. 2007; 147(4):242.
- (3) Syres K, Harrison F, Tadlock M, Jester JV, Simpson J, Roy S, et al. Successful treatment of the murine model of cystinosis using bone marrow cell transplantation. *Blood*. 2009; 114(12):2542-2552.
- (4) Cystinosis Research Network. About Cystinosis. [homepage on the Internet]. Illinois, USA: Cystinosis Research Network; 2007 cited 2007 20/5/07]. Available from: [www.cystinosis.org/aboutcystinosis.html](http://www.cystinosis.org/aboutcystinosis.html).
- (5) Gahl WA. Cystinosis. *Pediatric Nephrology*. 2009; 6:1019-1038.
- (6) Gahl WA, Thoene JG, Schneider JA. Cystinosis. *New England Journal of Medicine*. 2002; 347(2):111-121.
- (7) Gahl WA, Kleta R. Cystinosis: Antibodies and Healthy Bodies. *Journal of the American Society of Nephrology*. 2002; 13:2189-2191.
- (8) Williamson DAJ. Cystinosis. *British Medical Journal*. 1952; 27(134):356-363.
- (9) Fanconi G, Uehlinger E, Knauer C. The Coeliakiesyndrom with congenital cystic Pankreasfibromatose and bronchiektasien. *Viennese Medical Weekly*. 1936; 86:753-756.
- (10) Tiddens HAWM. The Renal De Toni Syndrome with Dwarfism. [PhD thesis on the Internet]. 1957: University of Utrecht; 1957 [cited 9/10/07] Available from: <http://www.urolog.nl/urolog/theses/theses.php?doc=tiddens&profmenu=yess>.
- (11) Burki E. *Annales Paediatrici, Basel*. 1941; 156:324.
- (12) Gahl WA, Kuehl EM. Corneal Crystals in Nephropathic Cystinosis: Natural History and Treatment with Cysteamine Eyedrops. *Molecular Genetics and Metabolism*. 2000; 71:100.
- (13) Crawhall J.C, Lietman PS, Schneider J.A, Seegmiller JE. Cystinosis: Plasma cystine and cysteine concentrations and the effect of D-penicillamine and dietary treatment. *The American Journal of Medicine*. 1968; 44(3):330-339.

- (14) Schneider JA, Schlesselman JJ, Mendoza JA, Orloff S, Thoene JG, Kroll WA, et al. Ineffectiveness of ascorbic acid therapy in nephropathic cystinosis. *New England Journal of Medicine*. 1979; 300:756-759.
- (15) Schneider JA, Thoene JG, Oshima RG, Crawhall JC, Olson DL. Cystinosis. Intracellular Cystine Depletion by Amino Thiols In Vitro and In Vivo. *Journal of Clinical Investigation*. 1976; 58:180-189.
- (16) Gahl WA, Kaiser-Kupfer MI, Fujikawa L, Kuwabara T, Jain S. Removal of Corneal Crystals by Topical Cysteamine in Nephropathic Cystinosis. *New England Journal of Medicine*. 1987; 316(13):775-779.
- (17) Gahl WA, Tietze F, Bashan N, Schulman JD, Steinherz R. Defective Cystine Exodus from Isolated Lysosome-Rich Fractions of Cystinotic Leucocytes. *Journal of Biological Chemistry*. 1982; 257(16):9570-9575.
- (18) Schneider JA, Jonas AJ, Smith ML. ATP-Dependent Lysosomal Cystine Efflux is Defective in Cystinosis. *Journal of Biological Chemistry*. 1982; 257(22):13185-13188.
- (19) Gahl WA, Tietze F, Butler JD, Schulman JD. Cysteamine Depletes Cystinotic Leucocyte Granular Fractions of Cystine by the Mechanism of Disulphide Interchange. *Biochemistry Journal*. 1985; 228:545-550.
- (20) Thoene JG, Pisoni RL, Christensen HN. Detection and Characterisation of Carrier-Mediated Cationic Amino Acid Transport in Lysosomes of Normal and Cystinotic Human Fibroblasts. *Journal of Biological Chemistry*. 1985; 260(8):4791-4798.
- (21) Dufier JL. Ocular Changes in Long-Term Evolution of Infantile Cystinosis. *Ophthalmic Paediatric Genetics*. 1987; 8(2):131-137.
- (22) Gahl WA, Reed GF, Thoene JG, Schneider JA, Rizzo WB, Schulman JD et al. Cysteamine Therapy for Children with Nephropathic Cystinosis. *New England Journal of Medicine*. 1987; 316(16):971-977.
- (23) Smolin LA, Clark KF, Gahl WA, Thoene JG, Schneider JA. A Comparison of the Effectiveness of Cysteamine and Phosphocysteamine in Elevating Plasma Cysteamine Concentration and Decreasing Leukocyte Free Cystine in Nephropathic Cystinosis. *Pediatric Research*. 1988; 23(6):616-620.
- (24) Broyer, Tete MJ, Gubler MC. Late Symptoms in Infantile Cystinosis. *Pediatric Nephrology*. 1987; 1(3):519-524.
- (25) Gahl WA, Sonies BC, Ekman EF, Andersson HC, Adamson M, Markello TC et al. Swallowing Dysfunction in Nephropathic Cystinosis. *New England Journal of Medicine*. 1990; 323(9):565-570.
- (26) Gahl WA, Schneider JA, Adamson M, Reznik VM, Adelman RD, Clark KF et al. Treatment of Cystinosis with Cysteamine from Early Infancy. *Journal of Pediatrics*. 1991; 119(3):491-493.

- (27) Gahl WA, Markello TC, Bernardini IM. Improved Renal Function in Children with Cystinosis Treated with Cysteamine. *New England Journal of Medicine*. 1993; 328(16):1157-1162.
- (28) Gahl WA. Coronary Artery and Other Vascular Calcifications in Patients with Cystinosis after Kidney Transplantation. *Clinical Journal of the American Society of Nephrology*. 2006; 1:555-562.
- (29) Skovby F, Kleita R, Anikster Y, Christensen R, Gahl WA. Cystinosis in Denmark: Mutation analysis and treatment with cystamine, the disulphide of cysteamine. *American Journal of Human Genetics*. 2002; 71(4).
- (30) Antignac C, Hippert C, Dubois G, Morin C, Disson O, Ibanes S, et al. Gene Transfer May Be Preventative But Not Curative for a Lysosomal Transport Disorder. *Molecular Therapy*. 2008; 16(8):1372-1381.
- (31) van't Hoff W, Town M, Jean G, Attard M, Whitmore SA, Broyer M et al. A Novel gene Encoding an Integral membrane Protein is Mutated in Nephropathic Cystinosis. *Nature Genetics*. 1998; 18:319-324.
- (32) US National Library of medicines. CTNS. [homepage on the Internet]. USA: US Department of Health; 2008 [updated February 2008; cited 2011 May 2011]. Available from: <http://ghr.nlm.nih.gov/gene/CTNS>.
- (33) Kleita R, Gahl WA. Pharmacological treatment of nephropathic cystinosis with cysteamine. *Expert Opinion on Pharmacotherapy*. 2004; 5(11):2255-2262.
- (34) Thoene JG. A Review of the Role of Enhanced Apoptosis in the Pathophysiology of Cystinosis. *Molecular Genetics and Metabolism*. 2007; :1-5.
- (35) Chevalier R, Forbes M. Generation and evolution of atubular glomeruli in the progression of renal disorders. *American Society of Nephrology*. 2008; 19:197-206.
- (36) Dohil R, Fidler M, Gangoiti JA, Kaskel F, Schneider JA, Barshop BA. Twice-daily cysteamine bitartrate therapy for children with cystinosis. *The Journal of Pediatrics*. 2010; 156(1):71-75.
- (37) Gahl WA, Iwata F, Kuehl EM, Reed GF, Kaiser-Kupfer MI, McCain LM. A Randomised Clinical Trial of Topical Cysteamine Disulfide (Cystamine) Versus Free Thiol (Cysteamine) in the Treatment of Corneal Cystine Crystals in Cystinosis. *Molecular Genetics and Metabolism*. 1998; 64:237-242.
- (38) Anderson RJ, Cairns D, Cardwell WA, Case M, Groundwater PW, Hall AG et al. Design, Synthesis and Initial In Vitro Evaluation of Novel Prodrugs for the Treatment of Cystinosis. *Letters in Drug Design and Discovery*. 2006; 3:336-345.

- (39) Sansanwal P, Yen B, Gahl WA, Ma Y, Ying L, Wong LC, et al. Mitochondrial autophagy promotes cellular injury in nephropathic cystinosis. *Journal of the American Society of Nephrology*. 2010; 21:272-283.
- (40) Schneider JA, Belldina EB, Huang MY, Brundage RC, Tracy TS. Steady-State Pharmacokinetics and Pharmacodynamics of Cysteamine Bitartrate in Pediatric Nephropathic Cystinosis Patients. *British Journal of Clinical Pharmacology*. 2003; 56:520-525.
- (41) Gahl WA, Markello TC, Yang ML, Rose SR, Kimonis VE, Troendle J. Effects of Early Cysteamine Therapy on Thyroid Function and Growth in Nephropathic Cystinosis. *Journal of Clinical Endocrinology and metabolism*. 1995; 80(11):3257-3261.
- (42) Lim J, Pellois JP, Simanek EE. A retro-inverso TAT-like peptide designed to deliver cysteamine to cells. *Bioorganic & Medicinal Chemistry Letters*. 2010; accepted manuscript.
- (43) Schneider JA. Treatment of Cystinosis: Simple in Principle, Difficult in Practice. *Journal of Pediatrics*. 2004; 145(4):436-438.
- (44) Elenberg E. Feeding Problems in Cystinosis. *Pediatric Nephrology*. 1998; 12:365-370.
- (45) Gahl WA, Tsilou E, Zhou m, Chan C-C, Sieving PC. Ophthalmic Manifestations and Histopathology of Infantile Nephropathic Cystinosis: Report of a Case and Review of the Literature. *Survey of Ophthalmology*. 2007; 52(1):97-105.
- (46) Van Raamsdonk JM, Pearson J, Bailey CDC, Rogers DA, Johnson DVW, Hayden MR, et al. Cystamine treatment is neuroprotective in the TAC128 mouse model of Huntington disease. *Journal of Neurochemistry*. 2005; 95:210-220.
- (47) Schneider JA, Fidler MC, Barshop BA, Deutsch R, Martin M, Dohil R et al. Pharmacokinetics of Cysteamine Bitartrate Following Gastrointestinal Infusion. *British Journal of Clinical Pharmacology*. 2006; 63(1):36-40.
- (48) Sun L, Xu S, Zhou M, Wang C, Wu Y, Chan P. Effects of cysteamine on MPTP-induced dopaminergic neurodegeneration in mice. *Brain research*. 2010; 1335:74-82.
- (49) Gentile V, Cooper AJ. Transglutaminases - possible drug targets in human diseases. *Current Drug Targets - CNS and Neurological Disorders*. 2004; 3(2):99-104.
- (50) Tarawneh R, Galvin J. Potential future neuroprotective therapies for neurodegenerative disorders and stroke. *Clinics in Geriatric Medicine*. 2010; 26(1):125-147.

- (51) Bozdag S, Gumus K, Gumus O, Unlu N. Formulation and in vitro evaluation of Cysteamine hydrochloride viscous solutions for the treatment of corneal cystinosis. *European Journal of Pharmaceutics and Biopharmaceutics*. 2008; 70(1):260-290.
- (52) Cairns D, Anderson RJ, Terry J, Coulthard M. Cystinosis and its Treatment. *Pharmaceutical Journal*. 2002; 269:615-616.
- (53) Choy YB, Park JH, Prausnitz MR. Mucoadhesive microparticles engineered for ophthalmic drug delivery. *Journal of Physics and Chemistry of Solids*. 2008; 69:1533-1536.
- (54) Wenner WJ, Murphy JL. The Effects of Cysteamine on the upper Gastrointestinal Tract of Children with Cystinosis. *Pediatric Nephrology*. 1997; 11(5):600-603.
- (55) Schneider JA, Dohil R, Newbury RO, Sellers ZM, Deutsch R. The Evaluation and Treatment of Gastrointestinal Disease in Children with Cystinosis Receiving Cysteamine. *Journal of Pediatrics*. 2003; 143(2):224-230.
- (56) Bendel-Stenzel MR, Steinke J, Dohil R, Kim Y. Intravenous delivery of cysteamine for the treatment of cystinosis: association with hepatotoxicity. *Pediatric Nephrology*. 2008; 23:311-315.
- (57) Walker WA. The stomach and duodenum. In: Walker WA, editor. *Pediatric gastrointestinal disease: pathophysiology, diagnosis, management*, Volume 1. Fourth ed. USA: PMPH-USA; 2004. p. 516.
- (58) Schneider JA, Soohoo N, Kaplan RM. A Cost-Effectiveness Analysis of the Orphan Drug Cysteamine in the Treatment of Infantile Cystinosis. *Medical Decision Making*. 1997; 17:193-198.
- (59) electronic Medicines Compendium (eMC). Cystagon 150mg hard capsules. [homepage on the Internet]. online: Datapharm Communications Ltd.; 2008 [updated 16/4/08; cited 2010 29/9/10]. Available from: <http://www.medicines.org.uk/emc/medicine/20798/SPC/cystagon%20150%20mg%20hard%20capsules/>.
- (60) Amos J. Protective organ wash engineered. [homepage on the Internet]. London: BBC; 2010 [updated 15/9/10; cited 2010 15/9/10]. Available from: <http://www.bbc.co.uk/news/science-environment-11322197>.
- (61) Schneider JA, Dohil R. Enterically Coated Cysteamine, Cystamine and Derivatives Thereof. [homepage on the Internet]. 9/8/07: WIPO; 2007 [updated 26/1/07; cited 2007 13/12/07]. Available from: <http://www.wipo.int/pctdb/en/wo.jsp?wo=2007089670>.

- (62) Schneider JA, Fidler MC, Barshop BA, Deutsch R, Martin M, Dohil R et al. understanding Intestinal Cysteamine Bitartrate Absorption. *Journal of Pediatrics*. 2006; 148(6):764-769.
- (63) Dohil R, Gangoiti JA, Cabrera BL, Fidler M, Schneider JA, Barshop BA. Long-Term Treatment of Cystinosis in Children with Twice-Daily Cysteamine. *The Journal of Pediatrics*. 2010; 156(5):823-827.
- (64) Terryn S, Devuyst O, Antignac C. Cell therapy for cystinosis. *Nephrology Dialysis Transplantation*. 2010; :1-4.
- (65) Cairns D, McCaughan B, Kay G, Knott RM. A Potential New Prodrug for the Treatment of Cystinosis: Design, synthesis and In-Vitro Evaluation. *Bioorganic & Medicinal Chemistry Letters*. 2008; 18(5):1716-1719.
- (66) Omran Z, Kay G, Hector EE, Knott RM, Cairns D. Folate pro-drug of cystamine as an enhanced treatment for nephropathic cystinosis. *Bioorganic & medicinal chemistry letters*. 2011; 21(8):2502-2504.
- (67) Omran Z, Kay G, Salvo AD, Knott RM, Cairns D. PEGylated derivatives of cystamine as enhanced treatments for nephropathic cystinosis. *Bioorganic & medicinal chemistry letters*. 2011; 21(1):45-47.
- (68) Omran Z, Moloney KA, Benylles A, Kay G, Knott RM, Cairns D. Synthesis and in vitro evaluation of novel pro-drugs for the treatment of nephropathic cystinosis. *Bioorganic & medicinal chemistry*. 2011; 19(11):3492-3496.
- (69) World Health Organisation. Adherence to Long-Term Therapies: Evidence for Action. Geneva: WHO; 2003.
- (70) Molinspiration. Log P calculator. [homepage on the Internet]. molinspiration; 2008 cited 2008 12/8]. Available from: [www.molinspiration.com/cgi-bin/properties](http://www.molinspiration.com/cgi-bin/properties).
- (71) Pirika. Log P calculator. [homepage on the Internet]. Pirika; 2008 cited 2008 11/8]. Available from: [www.pirika.com/chem/TCPEE/LOGKOW/ourlogkow.htm](http://www.pirika.com/chem/TCPEE/LOGKOW/ourlogkow.htm).
- (72) Europa, European Commission Joint Research Centre. Partition Coefficient. [homepage on the Internet]. Europa; 2009 [updated 2009; cited March 2009 Available from: <http://ecb.jrc.ec.europa.eu/DOCUMENTS/Testing-Methods/ANNEXV/A08web1992.pdf>.
- (73) Eksterowicz JE, Miller JL, Kollman PA. Calculation of Chloroform/Water Partition Coefficients for the N-methylated Nucleic Acid Bases. *Journal of Physical Chemistry B*. 1997; 101(50):10971-10975.
- (74) Aulton M. E. *Pharmaceutics. The Science of Dosage Form Design*. 2nd ed. London: Churchill Livingstone; 2002.

- (75) Black SD. Ellman's Reagent/DTNB (Protocol). [homepage on the Internet]. Texas: University of Texas Health Centre; 1994 [updated 26/10/94; cited 2008 24/3/08]. Available from: <http://www.bio.net/bionet/mm/methods/1994-October/020180.html>.
- (76) Lewin A, Crow A, Oubrie A, Le Brun NE. Molecular basis for precificity of the extracytoplasmic thioredoxin ResA. *The Journal of Biological Chemistry*. 2006; 281(46):35467-35477.
- (77) Huffman RW, McBride P, Brown DM. On the cleavage of Ellman's reagent (5,5'-dithiobis(2-nitrobenzoic acid)) by dithionite in the presence of dioctadecyldimethylammonium chloride [Dodac] surfactant vesicles laced with cholesterol. *Journal of Organic Chemistry*. 1994; 59:1633-1637.
- (78) Walmsley TA, Abernethy MH, Fitzgerald HP. Effect of Daylight on the Reaction of Thiols with Ellman's Reagent, 5,5'-(2-Nitrobenzoic acid). *Clinical Chemistry*. 1987; 33(10):1928-1931.
- (79) Allen LV. *Suppositories*. first edition ed. 2008: Pharmaceutical Press; 2008.
- (80) Coben LJ. *Modern Suppository Manufacturing*. *Drug Development and Industrial Pharmacy*. 1977; 3(6):523-546.
- (81) Aungst BJ, Lam G, Shefter E. Oral and rectal nalbuphine bioavailability: First-pass metabolism in rats and dogs. *Biopharmaceutics and Drug Disposition*. 1984; 6(4):413-421.
- (82) De Boer AG, De Leede LG, Breimer DD. Drug absorption by sublingual and rectal routes. *British Journal of Anaesthesia*. 1984; 56(1):69-82.
- (83) Hermann TW. Recent Research on Bioavailability of Drugs from Suppositories. *International Journal of Pharmaceutics*. 1995; 123:1-11.
- (84) Choi HG, Jung JH, Ryu JM, Yoon SJ, Oh YK, Kim KK. Development of In Situ-Gelling and Mucoadhesive Acetoaminophen Liquid Suppository. *International Journal of Pharmaceutics*. 1998; 165(1):33-44.
- (85) Chicco D, Grabnar I, Vojnovic D, Maurich V, Realdon N, Ragazzi E et al. Correlation of In Vitro and In Vivo Paracetamol Availability from Layered Excipient Suppositories. *International Journal of Pharmaceutics*. 1999; 189(2):147-160.
- (86) Kim CK, Choi HG, Lee MK, Kim MH. Effect of Additives on the Physiochemical Properties of Liquid Suppository Bases. *International Journal of Pharmaceutics*. 1999; 190:13-19.
- (87) Kim CK, Lee SW, Choi HG, Lee MK, Gao ZG, Kim IS et al. Trials of In Situ-Gelling and Mucoadhesive Acetaminophen Liquid Suppository in Human Subjects. *International Journal of Pharmaceutics*. 1998; 174:201-207.

- (88) Kim CK, Oh YK, Choi HG. In Situ Gelling and Mucoadhesive Liquid Suppository Containing Acetaminophen: Enhanced Bioavailability. *International Journal of Pharmaceutics*. 1998; 165(1):23-32.
- (89) Ryu JM, Chung SJ, Lee MH, Kim CK, Shim CK. Increased Bioavailability of Propranolol in Rats by Retaining Thermally Gelling Liquid Suppositories in the Rectum. *Journal of Controlled Release*. 1999; 59:163-172.
- (90) van't Hoff W, Baker T, Dalton RN, Duke LC, Smith SP, Chantler C et al. Effects of Oral Phosphocysteamine and Rectal Cyseamine in Cystinosis. *Archives of Disease in Childhood*. 1991; 66:1434-1437.
- (91) De Muynck C, Cuvelier C, Van Steenkiste D, Bonnarens L, Remon JP. Rectal Mucosa Damage in Rabbits After Subchronical Application of Suppository Bases. *Pharmaceutical Research*. 1991; 8(7):945-950.
- (92) Pasquali RS, Taurozzi MP, Bregni C. Some considerations about the hydrophilic-lipophilic balance system. *International Journal of Pharmaceutics*. 2008; 356(1-2):44-51.
- (93) Ratsimbazafy V, Bourret E, Duclos R, Brossard C. Rheological behavior of drug suspensions in Gelucire® mixtures and proxiphylline release from matrix hard gelatin capsules. *European Journal of Pharmaceutics and Biopharmaceutics*. 1999; 48(3):247-252.
- (94) Mayol L, Quaglia F, Borzacchiello A, Ambrosio L, La Rotonda MI. A novel poloxamers/hyaluronic acid in situ forming hydrogel for drug delivery: Rheological, mucoadhesive and in vitro release properties. *European Journal of Pharmaceutics and Biopharmaceutics*. 2008; 70:199-206.
- (95) Chen C, Qi H, Chen W HC, Li L, Wu C. Development of a Poloxamer Analogs/Carbopol-Based In Situ Gelling and Mucoadhesive Ophthalmic Delivery System for Puerarin. *International Journal of Pharmaceutics*. 2007; 337:178-187.
- (96) Choi H, Jung J, Ryu J, Yoon S, Oh Y, Kim C. Development of in situ-gelling and mucoadhesive acetaminophen liquid suppository. *International journal of pharmaceutics*. 1998; 165(1):33-44.
- (97) Yong CS, Choi JS, Quan Q, Rhee J, Kim C, Lim S, et al. Effect of sodium chloride on the gelation temperature, gel strength and bioadhesive force of poloxamer gels containing diclofenac sodium. *International journal of pharmaceutics*. 2001; 226(1-2):195-205.
- (98) Azarmi S, Roa W, Lobenberg R. Current Perspectives in Dissolution Testing of Conventional and Novel Dosage Forms. *International Journal of Pharmaceutics*. 2007; 328(1):12-21.
- (99) O'Brien FEM. The Control of Humidity by Saturated Salt Solutions. *Journal of Scientific Instruments*. 1948; 25:73-76.

- (100) Millot MC, Martin F, Bousquet D, Sebille B, Levy Y. A reactive macromolecular matrix for protein immobilization on a gold surface. Application in surface plasmon resonance. *Sensors and Actuators*. 1995; 29:268-273.
- (101) Coates J. Interpretation of Infrared Spectra, A Practical Approach. In: Meyers RA, editor. *Encyclopedia of Analytical Chemistry*. Chichester: John Wiley and Sons Ltd; 2000. p. 10815-10837.
- (102) Kim CH, Parkin S, Bharara M, Atwood D. Linear coordination of Hg(II) by cysteamine. *Polyhedron*. 2002; 21(2):225-228.
- (103) Ahmad S, Shaheen MA, Stoeckli-Evans H. A monoclinic polymorph of cysteamine hydrochloride. *Acta Crystallographica Section E; Structure Reports Online*. 2010; 66(1):134.
- (104) Li Y, Kaito A. Highly oriented structure formed in a lamella-forming diblock copolymer with high molar mass. *European Polymer Journal*. 2006; 42:1986-1993.
- (105) Dufier JL. Evolution of Ocular Manifestations in Nephropathic Cystinosis: A Long-Term Study of a Population Treated with Cysteamine. *Journal of Pediatric Ophthalmology Strabismus*. 2003; 40(3):142-146.
- (106) Gahl WA, Tsilou E, Thompson D, Lindblad AS, Thoene JG, Schneider JA et al. A Multicentre Randomised Double Masked Clinical Trial of a New Formulation of Topical Cysteamine for the Treatment of Corneal Cystine Crystals in Cystinosis. *British Journal of Ophthalmology*. 2003; 87:28-31.
- (107) Gahl WA, Jain S, Kuwabara T, Kaiser-Kupfer MI. Range of Toxicity of Topical Cysteamine in Rabbit Eyes. *Journal of Ocular Pharmacology*. 1988; 4(2):127-131.
- (108) Gahl WA, Kaiser-Kupfer MI, Gazzo MA, Kuehl EM, Caruso RC, Datiles MB. A Randomised Placebo-Controlled Trial of Cysteamine Eye Drops in Nephropathic Cystinosis. *Archives of Ophthalmology*. 1990; 108(5):689-693.
- (109) Noble JL, Jones NP, Postlethwaite RJ. Clearance of Corneal Crystals in Nephropathic Cystinosis by Topical Cysteamine 0.5%. *British Journal of Ophthalmology*. 1991; 75:311-312.
- (110) Washington University School of Medicine. Cornea Structure and Function. [homepage on the Internet]. St. Louis: Washington University School of Medicine; 2010 cited 2010 1/26]. Available from: <http://wuphysicians.wustl.edu/dept.aspx?pageID=17&ID=6>.
- (111) Jansook P, Stefánsson E, Thorsteinsdóttir M, Sigurdsson BB, Kristjánssdóttir SS, Bas JF, et al. Cyclodextrin solubilization of carbonic anhydrase inhibitor drugs: Formulation of dorzolamide eye drop

- microparticle suspension. *European Journal of Pharmaceutics and Biopharmaceutics*. 2010; 76(2):208-214.
- (112) Nanjawade BK, Manvi FV, Manjappa AS. In Situ-Forming Hydrogels for Sustained Ophthalmic Drug Delivery. *Journal of Controlled Release*. 2007; 122:119-134.
- (113) Ahmed I, Patton TF. Disposition of timolol and inulin in the rabbit eye following corneal versus non-corneal absorption. *International journal of pharmaceutics*. 1987; 38(1-3):9-21.
- (114) Le Boursais C, Acar L, Zia H, Sado PA, Needham T, Leverage R. Ophthalmic Drug Delivery Systems - Recent Advances. *Progress in Retinal and Eye Research*. 1998; 17(1):33-58.
- (115) Shell JW. Ophthalmic drug delivery systems. *Survey of Ophthalmology*. 1984; 29(2):117-128.
- (116) Mali MN, Hajare AA. In situ gel-forming systems for sustained ocular drug delivery. *European Industrial Pharmacy*. 2010; (5):17-20.
- (117) Saettone MF, Salminen L. Ocular Inserts for Topical Delivery. *Advanced Drug Delivery Reviews*. 1995; 16:95-106.
- (118) Kaur IP, Kanwar M. Ocular Preparations: The Formulation Approach. *Drug Development and Industrial Pharmacy*. 2002; 28(5):473-493.
- (119) Cone RA. Barrier properties of mucus. Accepted manuscript ed. Baltimore: 2008.
- (120) Smart JD. The basics and underlying mechanisms of mucoadhesion. *Advanced Drug Delivery Reviews*. 2005; 57:1556-1568.
- (121) Robinson JR, Mlynek GM. Bioadhesive and phase-change polymers for ocular drug delivery. *Advanced Drug Delivery Reviews*. 1995; 16:45-50.
- (122) Lai SK, Wang YY, Wirtz D, Hanes J. Micro- and macrorheology of mucus. Accepted manuscript ed. Baltimore: 2008.
- (123) Varum FJO, Veiga F, Sousa JS, Basit AW. An investigation into the role of mucus thickness on mucoadhesion in the gastrointestinal tract of pig. *European Journal of Pharmaceutical Sciences*. 2010; .
- (124) Rupenthal ID, Green CR, Alany RG. Comparison of ion-activated in situ gelling systems for ocular drug delivery. Part 1: Physicochemical characterisation and in vitro release. *International journal of pharmaceutics*. 2011; 411(1-2):69-77.
- (125) Harris P. *Food Gels*. First ed. London: Elsevier; 1990.

(126) Amin PD, Srividya B, Cardoza RM. Sustained Ophthalmic Delivery of Ofloxacin from a pH Triggered In Situ Gelling System. *Journal of Controlled Release*. 2001; 73:205-211.

(127) Andrews GP, Laverty TP, Jones DS. Mucoadhesive polymeric platforms for controlled drug delivery. Corrected proof ed. belfast: Elsevier; 2008.

(128) Barbu E, Verestiuc L, Nevell TG, Tsibouklis J. Polymeric Materials for Ophthalmic Drug Delivery: Trends and Perspectives. *Journal of Materials Chemistry*. 2006; 16:3439-3443.

(129) Ceulemans J, Ludwig A. Optimisation of carbomer viscous eye drops: an in vitro experimental design approach using rheological techniques. *European Journal of Pharmaceutics and Biopharmaceutics*. 2002; 54:41-50.

(130) Edsman K, Carlfors J, Harju K. Rheological evaluation and ocular contact time of some carbomer gels for ophthalmic use. *International Journal of Pharmaceutics*. 1996; 137:233-241.

(131) Pan W, Liu Z, Li J, Nie S, Liu H, Ding P. Study of an Alginate/HPMC-Based In Situ Gelling Ophthalmic Delivery System for Gatifloxacin. *International Journal of Pharmaceutics*. 2006; 315:12-17.

(132) Smart JD. Some formulation factors influencing the rate of drug release from bioadhesive matrices. *Drug Development and Industrial Pharmacy*. 1992; 18(2):223-232.

(133) Zambito Y, Colo GD. Thiolated quaternary ammonium–chitosan conjugates for enhanced precorneal retention, transcorneal permeation and intraocular absorption of dexamethasone. *European Journal of Pharmaceutics and Biopharmaceutics*. 2010; 75(2):194-199.

(134) Bothner H, Waaler T, Wik O. Rheological characterisation of tear substitutes. *Drug Development and Industrial Pharmacy*. 1990; 16:615-616.

(135) Oechsner M, Keipert S. Polyacrylic acid/polyvinylpyrrolidone bipolymeric systems. I. Rheological and mucoadhesive properties of formulations potentially useful for the treatment of dry-eye-syndrome. *European Journal of Pharmaceutics and Biopharmaceutics*. 1999; 47:113-118.

(136) Edsman K, Paulsson M, Hagerstrom H. Rheological Studies of the Gelation of Deacetylated Gellan Gum (Gelrite) in Physiological Conditions. *European Journal of Pharmaceutical Sciences*. 1999; 9:99-105.

(137) Osborne DW, Amann AH. Topical Drug Delivery Formulations. Illustrated ed. London, UK: Informa Health Care; 1990.

(138) Rupenthal ID, Green CR, Alany RG. Comparison of ion-activated in situ gelling systems for ocular drug delivery. Part 2: Precorneal retention and in vivo pharmacodynamic study. *International journal of pharmaceutics*. 2011; 411(1-2):78-85.

(139) Medicinescomplete. Carbomer 934 Structural repeating unit. [homepage on the Internet]. Medicinescomplete; 2009 cited 2009 September 20th]. Available from:  
<http://www.medicinescomplete.com/mc/excipients/current/images/ExcCarbomerC001.png>.

(140) Tamburic S, Craig DQM. A comparison of different in vitro methods for measuring mucoadhesive performance. *European Journal of Pharmaceutics and Biopharmaceutics*. 1997; 44:159-167.

(141) Kulkarni A. Study of polymers and permeation enhancers effects on meloxicam gel formulations. [Master of Pharmacy thesis on the Internet]. Bangalore: Rajiv Gandhi University of Health Sciences; 2006 [cited 5/6/11] Available from:  
<http://119.82.96.198:8080/jspui/bitstream/123456789/2691/1/Kulkarni%20Anant%20Rao.pdf>.

(142) Needleman IG, Martin GP, Smales FC. Characterisation of bioadhesives for periodontal and oral mucosal drug delivery. *Journal of clinical periodontology*. 1998; 25(1):74-82.

(143) Ceulemans J, Vinckier I, Ludwig A. The use of Xanthan gum in an ophthalmic liquid dosage form: Rheological characterization of the interaction with mucin. *Journal of Pharmaceutical Sciences*. 2002; 91(4):1117-1127.

(144) Medicinescomplete. Structural unit of Xanthan gum. [homepage on the Internet]. Medicinescomplete; 2009 cited 2009 September 20th]. Available from:  
<http://www.medicinescomplete.com/mc/excipients/current/images/ExcXanthanGumC001.png>.

(145) Chiellini E. *Biomedical polymers and polymer therapeutics*. : Springer; 2001.

(146) INCHEM. Structural unit of HPMC. [homepage on the Internet]. INCHEM; 2009 cited 2009 September 20th]. Available from:  
<http://www.inchem.org/documents/jecfa/jecmono/40abcj15.gif>.

(147) Bernkop-Schnurch A, Walker GF, Leitner VM. Thiolated Polymers: Evidence for the Formation of Disulphide Bonds with Mucus Glycoproteins. *European Journal of Pharmaceutics and Biopharmaceutics*. 2003; 56(2):207-214.

- (148) Bernkop-Schnurch A, Kast CE, Richter MF. Improvement in the mucoadhesive properties of alginate by the covalent attachment of cysteine. *Journal of Controlled Release*. 2001; 71:277-285.
- (149) Bernkop-Schnurch A, Clausen AE, Hnatyszyn M. Thiolated Polymers: Synthesis and In Vitro Evaluation of Polymer-Cysteamine Conjugates. *International Journal of Pharmaceutics*. 2001; 226:185-194.
- (150) Bernkop-Schnurch A. Thiomers: A New Generation of Mucoadhesive Polymers. *Advanced Drug Delivery Reviews*. 2005; 57(11):1569-1582.
- (151) Singh S, Gajva B, Rawat M, Muthu MS. Enhanced transdermal delivery of ketoprofen from bioadhesive gels. *Pakistan Journal of Pharmaceutical Science*. 2009; 22(2):193-198.
- (152) Bilensoy E, Rouf ME, Vural I, Sen M, Hincal AA. Mucoadhesive, thermosensitive, prolonged-release vaginal gel for clotrimazole:  $\beta$ -cyclodextrin complex. *Pharmaceutical SciTech*. 2006; 7(2):54-60.
- (153) Thirawong N, Nunthanid J, Puttipatkhachorn S, Sriamornsak P. Mucoadhesive properties of various pectins on gastrointestinal mucosa: An in vitro evaluation using texture analyser. *European Journal of Pharmaceutics and Biopharmaceutics*. 2007; 67:132-140.
- (154) Madsen EL, Hobson MA, Shi H, Varghese T, Frank GR. Tissue-mimicking agar/gelatin materials for use in heterogeneous elastography phantoms. *Physics in Medicine and Biology*. 2005; 50:5597-5618.
- (155) Rossi S, Bonferoni MC, Lippoli G, Bertoni M, Ferrari F, Caramella C, et al. Influence of mucin type on polymer-mucin rheological interactions. *Biomaterials*. 1995; 16:1073-1079.
- (156) Rossi S, Bonferoni MC, Lippoli G, Bertoni M, Ferrari F, Caramella C, et al. A rheological approach. In: Mathiowitz E, Chickering DE, Lehr CM, editors. *Bioadhesive drug delivery systems: fundamentals, novel approaches and development*. First edition ed. New York: Taylor and Francis (CRC Press); 1999. 3 p. 55-57.
- (157) Wong CF, Yuen KH, Peh KK. An in-vitro method for buccal adhesion studies: importance of instrument variables. *International Journal of Pharmaceutics*. 1999; 180:47-57.
- (158) Riley RG, Smart JD, Tsibouklis J, Dettmar PW, Hampson F, Davis JA et al. An investigation of mucus/polymer rheological synergism using synthesised and characterised poly(acrylic acid)s. *International Journal of Pharmaceutics*. 2001; 217:87-100.
- (159) Stewart WC, Sharpe ED, Stewart JA, Hott EC. The safety and efficacy of timolol 0.5% in xanthan gum versus timolol gel forming solution 0.5%. *Current Eye Research*. 2002; 24(5):387-391.

- (160) Babbar SB, Jain R. Xanthan gum: An economical partial substitute for agar in microbial culture media. *Current Microbiology*. 2006; 52(4):287-292.
- (161) Baudouin C, Labbe A, Hong L, Pauly A, Brignole-Baudouin F. Preservatives in eye drops: The good, the bad and the ugly. *Progress in Retinal and Eye Research*. 2010; :1-23.
- (162) Lewis RA, Katz GJ, Weiss MJ, Landry TA, Dickerson JE, James JE, et al. Travoprost 0.004% with and without Benzalkonium chloride: A comparison of safety and efficacy. *Journal of Glaucoma*. 2007; 16(1):98-103.
- (163) Marple B, Roland P, Benninger M. Safety review of benzalkonium chloride used as a preservative in intranasal solutions: An overview of conflicting data and opinions. *Otolaryngology-Head and Neck Surgery*. 2004; 130(1):131-141.
- (164) Anumolu SS, Singh Y, Gao D, Stein S, Sinko PJ. Design and evaluation of novel fast forming pilocarpine-loaded ocular hydrogels for sustained pharmacological response. *Journal of Controlled Release*. 2009; 137(2):152-159.
- (165) Sliney DH. Physical factors in cataractogenesis: ambient ultraviolet radiation and temperature. *Investigative Ophthalmology & Visual Science*. 1986; 27:781-790.
- (166) Ooi EH, Ng EYK, Purslow C, Acharya R. Variations in the corneal surface temperature with contact lens wear. *Proceedings of the Institution of Mechanical Engineers, Part H: Journal of Engineering in Medicine*. 2007; 221(4):337-349.
- (167) Peppas NA, Sahlin JJ. A simple equation for the description of solute release. III. Coupling of diffusion and relaxation. *International Journal of Pharmaceutics*. 1989; 57:169-172.
- (168) Riddles PW, Blakeley RL, Zerner B. Ellman's Reagent: 5,5'-Dithiobis(2-nitrobenzoic Acid)- a Reexamination. *Analytical Biochemistry*. 1979; 94:75-81.
- (169) Thirawong N, Kennedy RA, Sriamornsak P. Viscometric study of pectin-mucin interaction and its mucoadhesive bond strength. *Carbohydrate Polymers*. 2008; 71:170-179.
- (170) Hornof M. In Vitro and In Vivo Evaluation of Novel Polymeric Excipients in the Ophthalmic Field. University of Vienna; 2003 [cited 11/09/2007] .
- (171) Madsen F, Eberth K, Smart JD. A rheological examination of the mucadhesive/mucus interaction: the effect of mucoadhesive type and concentration. *Journal of Controlled Release*. 1998; 50:167-178.

- (172) Qi H, Chen W, Huang C, Li L, Chen C, Li W, et al. Development of a poloxamer analogs/carbopol-based in situ gelling and mucoadhesive ophthalmic delivery system for puerarin. *International Journal of Pharmaceutics*. 2007; 337:178-187.
- (173) Uhart M, Pirot F, Boillon A, Senaux E, Tall L, Diouf E, et al. Assessment of sodium hyaluronate gel as vehicle for intra camelar delivery of cefuroxime in endophthalmitis prophylaxis. *International Journal of Pharmaceutics*. 2010; in press.
- (174) Tang I, Wong DM, Yee DJ, Harris MG. The pH of multi-purpose soft contact lens solutions. *Optometry and Vision Science*. 1996; 73(12):746-749.
- (175) Dalton K, Subbaraman LN, Rogers R, Jones L. Physical properties of soft contact lense solutions. *Optometry and Vision Science*. 2008; 85:122-128.
- (176) Carney LG, Fullard LG. Ocular irritation and environmental pH. *Australian Journal of Optometry*. 1979; 62:335-336.
- (177) Lee CH, Moturi V, Lee Y. Thixotropic property in pharmaceutical formulations. Uncorrected proof ed. Elsevier; 2009.
- (178) Oh MH, So JH, Yang SM. Rheological evidence for the silica-mediated gelation of Xanthan gum. *Journal of Colloid and Interface Science*. 1999; 216(320):328.
- (179) Garcia-Ochowa F, Santos VE, Gomez E. Xanthan gum: Production recovery and properties. *Biotechnology Advances*. 2000; 18(7):549-579.
- (180) Chen HH. Rheological properties of HPMC enhanced Surimi analysed by small- and large-strain tests: 1. The effect of concentration and temperature on HPMC flow properties. *Food Hydrocolloids*. 2007; 21(7):1201-1208.
- (181) Wu H, Liu Z, Peng J, Li L, Li N, Li J, et al. Design and evaluation of baicalin-containing in situ pH-triggered gelling system for sustained ophthalmic drug delivery. *International journal of pharmaceutics*. 2011; 410(1-2):31-40.
- (182) Thassu D, Deleers M, Pathak Y. Nanoparticulate drug delivery systems. Illustrated Edition ed. New York, USA: CRC Press; 2007.
- (183) Fitzgerald P, Hadgraft J, Kreuter J, Wilson CG. A  $\gamma$ -scintigraphic evaluation of microparticulate ophthalmic delivery systems: liposomes and nanoparticles. *International journal of pharmaceutics*. 1987; 40(1-2):81-84.
- (184) de la Fuente M, Raviña M, Paolicelli P, Sanchez A, Seijo B, Alonso MJ. Chitosan-based nanostructures: A delivery platform for ocular therapeutics. *Advanced Drug Delivery Reviews*. 2010; 62(1):100-117.

- (185) Park H, Robinson JR. Mechanisms of mucoadhesion of Poly(acrylic acid) hydrogels. *Pharmaceutical Research*. 1987; 4(6):457-464.
- (186) Salamat-Miller N, Chittchang M, Johnston TP. The use of mucoadhesive polymers in buccal drug delivery. *Advanced Drug Delivery Reviews*. 2005; 57(11):1666-1691.
- (187) Dessanges JF. A History of Nebulization. *Journal of Aerosol Medicine*. 2001; 14(1):65-71.
- (188) Zeng XM, Martin GP, Marriott C. The controlled delivery of drugs to the lung. *International Journal of Pharmaceutics*. 1995; 124:149-164.
- (189) Depreter F, Amighi K. Formulation and in vitro evaluation of highly dispersive insulin dry powder formulations for lung administration. *European Journal of Pharmaceutics and Biopharmaceutics*. 2010; 76(3):454-463.
- (190) Fleming N. Diabetes fears as inhaled insulin discontinued. [homepage on the Internet]. London: Telegraph; 2008 [updated 1/14; cited 2010 1/19]. Available from: <http://www.telegraph.co.uk/news/uknews/1575532/Diabetes-fears-as-inhaled-insulin-discontinued.html>.
- (191) Home care provider. Relenza (zanamivir for inhalation) receives FDA approval. Home care provider. 1999; 4(5):174-175.
- (192) Mondal D. Zanamivir. In: S.J. Enna, David B. Bylund, editors. *xPharm: The Comprehensive Pharmacology Reference*. New York: Elsevier; 2007. p. 1-4.
- (193) NICE. Clinical effectiveness and cost effectiveness of zanamivir (Relenza): translating the evidence into clinical practice, a National Institute for Clinical Excellence view. *Philosophical Transactions of the Royal Society of London. Series B: Biological Sciences*. 2001; 356(1416):1899-1903.
- (194) Ewan S. Is flu stronger, or are we weaker? *Drug discovery today*. 2004; 9(5):200-200.
- (195) Anikster Y, Lacbawan F, Brantly M, Gochuico B, Avila NA, Travis W, et al. Pulmonary Dysfunction in Adults With Nephropathic Cystinosis. *Chest*. 2001; 119:394-401.
- (196) Von Wichert P, Seifart C. The Lung, an Organ for Absorption? *Respiration*. 2005; 72:552-558.
- (197) Lockhart SP. Inhaled thiol and phosphorothiol radioprotectors fail to protect the mouse lung. *Radiotherapy and Oncology*. 1990; 19:187-191.
- (198) Brain JD. Respiratory system. [homepage on the Internet]. USA: Merck; 2006 cited 2010 1/19]. Available from: <http://www.merck.com/mmhe/sec04/ch038/ch038b.html>.

- (199) Pilcer G, Amighi K. Formulation strategy and use of excipients in pulmonary drug delivery. *International journal of pharmaceutics*. 2010; 392(1-2):1-192.
- (200) Attwood D, Florence AT. *Physical Pharmacy*. First ed. London, UK: Pharmaceutical Press; 2008.
- (201) Medic. Simulation of the human respiratory system. [homepage on the Internet]. Revolizer; 2006 cited 2009 11/26]. Available from: [http://images.google.co.uk/imgres?imgurl=http://revolizer.com/in\\_img/fine\\_particle.jpg&imgrefurl=http://revolizer.com/udd.htm&usq=\\_\\_qxsYmkZgmB-cTYV3paErRB7stbl=&h=341&w=550&sz=28&hl=en&start=79&um=1&itbs=1&tbnid=Pb425JI0pC48QM:&tbnh=82&tbnw=133&prev=/images%3Fq%3Dlung%2Bdrug%2Bparticle%26ndsp%3D20%26hl%3Den%26safe%3Dactive%26sa%3DN%26start%3D60%26um%3D1](http://images.google.co.uk/imgres?imgurl=http://revolizer.com/in_img/fine_particle.jpg&imgrefurl=http://revolizer.com/udd.htm&usq=__qxsYmkZgmB-cTYV3paErRB7stbl=&h=341&w=550&sz=28&hl=en&start=79&um=1&itbs=1&tbnid=Pb425JI0pC48QM:&tbnh=82&tbnw=133&prev=/images%3Fq%3Dlung%2Bdrug%2Bparticle%26ndsp%3D20%26hl%3Den%26safe%3Dactive%26sa%3DN%26start%3D60%26um%3D1).
- (202) Patton JS, Fishburn CS, Weers JG. The Lungs as a Portal of Entry for Systemic Drug Delivery. *Proceedings of the American Thoracic Society*. 2004; 1:338-344.
- (203) Hein S, Bur M, Schaefer UF, Lehr C. A new Pharmaceutical Aerosol Deposition Device on Cell Cultures (PADD OCC) to evaluate pulmonary drug absorption for metered dose dry powder formulations. *European Journal of Pharmaceutics and Biopharmaceutics*. 2011; 77(1):132-138.
- (204) Shoyele SA, Cawthorne S. Particle engineering techniques for inhaled biopharmaceuticals. *Advanced Drug Delivery Reviews*. 2006; 58:1009-1029.
- (205) Dailey LA, Jekel N, Fink L, Gessler T, Schmehl T, Wittmar M, et al. Investigation of the proinflammatory potential of biodegradable nanoparticle drug delivery systems in the lung. *Toxicology and Applied Pharmacology*. 2006; 215:100-108.
- (206) Widdicombe JH, Widdicombe JG. Regulation of human airway surface liquid. *Respiration Physiology*. 1995; 99:3-12.
- (207) Telko MJ, Hickey AJ. Dry Powder Inhaler Formulation. *Respiratory Care*. 2005; 50(9):1209-1227.
- (208) Ng AW, Bidani A, Heming TA. Innate host defence of the lung: Effects of lung-lining fluid pH. *Lung*. 2004; 182:297-317.
- (209) Rennard SI, Basset G, Lecossier D, O'Donnell KM, Pinkston P, Martin PG, et al. Estimation of volume of epithelial lining fluid recovered by lavage using urea as marker of dilution. *Journal of Applied Physiology*. 1986; 60:532-538.

- (210) Cook RO, Pannu RK, Kellaway IW. Novel sustained release microspheres for pulmonary drug delivery. *Journal of Controlled Release*. 2005; 104:79-90.
- (211) Lipworth BJ. Pharmacokinetics of inhaled drugs. *British Journal of Clinical Pharmacology*. 1996; 42:697-705.
- (212) Rohatagi S, Rhodes GR, Chaikin P. Absolute Oral Versus Inhaled Bioavailability: Significance for Inhaled Drugs with Special Reference to Inhaled Glucocorticoids. *Journal of Clinical Pharmacology*. 1999; 39:661-663.
- (213) Chougule MB, Padhi BK, Jinturkar KA, Misra A. Development of Dry Powder Inhalers. *Recent Patents on Drug Delivery and Formulation*. 2007; 1:11-21.
- (214) PharmQD. Spiriva Handihaler. [homepage on the Internet]. PharmQD; 2010 [updated 15/1; cited 2011 9/7]. Available from: <http://www.pharmqd.com/pharmacy-news/fda-updates-earlier-guidance-respiratory-treatment-spiriva-handihaler>.
- (215) Zhou QT, Armstrong B, Larson I, Stewart PJ, Morton DAV. Understanding the influence of powder flowability, fluidization and de-agglomeration characteristics on the aerosolization of pharmaceutical model powders. *European Journal of Pharmaceutical Sciences*. 2010; 40(5):412-421.
- (216) Nadarassan DK, Assi KH, Chrystyn H. Aerodynamic characteristics of a dry powder inhaler at low inhalation flows using a mixing inlet with an Anderson Cascade Impactor. *European Journal of Pharmaceutical Sciences*. 2010; .
- (217) Al-Showair RAM, Tarsin WY, Assi KH, Pearson SB, Chrystyn H. Can all patients with COPD use the correct inhalation flow with all inhalers and does training help? *Respiratory Medicine*. 2007; 101:2395-2401.
- (218) Harris D. Testing inhalers. [homepage on the Internet]. UK: Pharmaceutical Technology Europe; 2007 [updated 30/9; cited 2010 5/6]. Available from: [http://www.camcon.co.uk/downloads/articles/PTE\\_Testing\\_Inhalers.pdf](http://www.camcon.co.uk/downloads/articles/PTE_Testing_Inhalers.pdf).
- (219) Taki M, Marriott C, Zeng X, Martin GP. The production of 'aerodynamically equivalent' drug and excipient inhalable powders using a novel fractionation technique. *European Journal of Pharmaceutics and Biopharmaceutics*. 2011; 77(2):283-296.
- (220) Rabbani NR, Seville PC. The influence of formulation components on the aerolisation properties of spray-dried powders. *Journal of Controlled Release*. 2005; 110:130-140.

- (221) CHEC research centre. Research. [homepage on the Internet]. Denmark: Denmark Technical University; 2007 [updated 26/3/2007; cited 2011 7/7/11]. Available from: <http://www.chec.kt.dtu.dk/Research/Chemical%20Product%20Design/Particle%20technology/Research.aspx>.
- (222) Bögelein J, Lee G. Cyclone selection influences protein damage during drying in a mini spray-dryer. *International journal of pharmaceutics*. 2010; 401(1-2):68-71.
- (223) Bain DF. Development and characterization of biodegradable microspheres containing selected antimycobacterials. [PhD thesis on the Internet]. Aberdeen: RGU; 1998 [cited 2010] .
- (224) Kawakami K, Sumitani C, Yoshihashi Y, Yonemochi E, Terada K. Investigation of the dynamic process during spray-drying to improve aerodynamic performance of inhalation particles. *International journal of pharmaceutics*. 2010; 390(2):250-259.
- (225) Zhou QT, Qu L, Larson I, Stewart PJ, Morton DAV. Improving aerosolization of drug powders by reducing powder intrinsic cohesion via a mechanical dry coating approach. *International journal of pharmaceutics*. 2010; 394(1-2):50-59.
- (226) Adi S, Tong Z, Chan HK, Yang R, Yu A. Impact angles as an alternative way to improve aerolisation of powders for inhalation? *European Journal of Pharmaceutical Sciences*. 2010; in press.
- (227) Donovan MJ, Smyth HDC. Influence of size and surface roughness of large lactose carrier particles in dry powder inhaler formulations. *International journal of pharmaceutics*. 2010; 402(1-2):1-9.
- (228) Watling CP, Elliott JA, Scruton C, Cameron RE. Surface modification of lactose inhalation blends by moisture. *International journal of pharmaceutics*. 2010; 391(1-2):29-37.
- (229) Cline D, Dalby R. Predicting the quality of powders for inhalation from surface energy and area. *Pharmaceutical Research*. 2002; 19(9):1274-1277.
- (230) Engelberg I, Kohn Joachim. Physico-mechanical properties of degradable polymers used in medical applications: a comparative study. *Biomaterials*. 1991; 12(3):292-304.
- (231) Zhou S, Song B, Li X. In vitro degradation and release profiles for poly dl-lactide film containing paracetamol. *Journal of Material Science*. 2007; 18:1623-1626.
- (232) Kim SY, Lee YM, Kang JS. Indomethacin-loaded methoxy poly(ethylene glycol)/poly(D,L-lactide) amphiphilic diblock copolymeric

nanospheres: Pharmacokinetic and toxicity studies in rodents. *Journal of Biomedical Materials Research*. 2005; 74(4):581-590.

(233) Kontio R, Suuronen R, Konttinen YT, Hallikainen C, Kommonen B, Kellomaki M, et al. Orbital floor reconstruction with poly-L/D-lactide implants: clinical, radiological and immunohistochemical study in sheep. *International Journal of Oral and Maxillofacial Surgery*. 2004; 33:361-368.

(234) Burt HM, Zhang X, Toleikis P, Embree L, Hunter WL. Development of copolymers of poly(D,L-lactide) and methoxypolyethylene glycol as micellar carriers of paclitaxel. *Colloids and Surfaces B: Biointerfaces*. 1999; 16:161-171.

(235) Gander B, Johansen P, Nam-Tran H, Merkle HP. Thermodynamic approach to protein microencapsulation into poly(D,L-lactide) by spray drying. *International Journal of Pharmaceutics*. 1996; 129:51-61.

(236) Zhang X, Jiang X, Hu J, Fu C. Rifampicin polylactic acid microspheres for lung targeting. *Journal of Microencapsulation*. 2000; 17(6):785-788.

(237) Selek H, Sahin S, Ercan MT, Sargon M, Hincal AA, Kas HS. Formulation and in vitro/in vivo evaluation of terbutaline sulphate incorporated in PLGA (25/75) and L-PLA microspheres. *Journal of Microencapsulation*. 2003; 20(2):261-271.

(238) Liu Y, Pan J, Feng S. Nanoparticles of lipid monolayer shell and biodegradable polymer core for controlled release of paclitaxel: Effects of surfactants on particles size, characteristics and in vitro performance. *International journal of pharmaceutics*. 2010; 395(1-2):243-250.

(239) Yang M, Lai SK, Wang Y, Zhong W, Happe C, Zhang M, et al. Biodegradable Nanoparticles Composed Entirely of Safe Materials that Rapidly Penetrate Human Mucus. *Angewandte Chemie International Edition*. 2011; 50(11):2597-2600.

(240) Belbella A, Vauthier C, Fessi H, Devissaguet JP, Puisieux F. In vitro degradation of nanospheres from poly(D,L-lactides) of different molecular weights and polydispersities. *International Journal of Pharmaceutics*. 1996; 129:95-102.

(241) Ravelingien M, Mullens S, Luyten J, D'Hondt M, Boonen J, De Spiegeleer B, et al. Vancomycin release from poly(D,L-lactic acid) spray-coated hydroxyapatite fibers. *European Journal of Pharmaceutics and Biopharmaceutics*. 2010; 76(3):366-370.

(242) Hammer A and Luciani F. Compendium of analytical procedures - Anderson Cascade Impactor Test. Hertfordshire: GSK; 2005.

(243) Hammer A. Equipment used for the determination of the particle size distribution by inertial impaction, excluding NGI - maintenance, calibration and use, PD Global. Hertfordshire: GSK; 2007.

- (244) Nichols SC. Andersen Cascade Impactor; calibration and mensuration issues for the standard and modified impactor. *Pharmeuropa*. 2000; 12:598-602.
- (245) Council of Europe. Preparations for inhalation: aerodynamic assessment of fine particles. *European Pharmacopoeia*. Strasbourg, France: European Pharmacopoeia Convention; 2003. p. 209-219.
- (246) Podczeczek F. Optimization of the operation conditions of an Anderson-Cascade impactor and the relationship to centrifugal adhesion measurements to aid the development of dry powder inhalations. *International Journal of Pharmaceutics*. 1997; 149:51-61.
- (247) Bain DF, Munday DL, Smith A. Solvent influence on spray-dried biodegradable microspheres. *Journal of Microencapsulation*. 1999; 16(4):453-474.
- (248) Narahariseti PK, Lew MDN, Fu YC, Lee DJ, Wang CH. Gentamicin-loaded discs and microspheres and their modifications: characterisation and in vitro release. *Journal of Controlled Release*. 2005; 102:345-359.
- (249) Wang FJ, Wang CH. Sustained release of etanidazole from spray dried microspheres prepared by non-halogenated solvents. *Journal of Controlled Release*. 2002; 81(3):263-280.
- (250) Zeng XM, Martin GP, Tee SK, Ghoush AA, Marriott C. Effects of particle size and adding sequence of fine lactose on the deposition of salbutamol sulphate from a dry powder formulation. *International Journal of Pharmaceutics*. 1999; 182:133-144.
- (251) Lucas P, Anderson K, Staniforth JN. Protein Deposition from Dry Powder Inhalers: Fine Particle Multiplets as Performance Modifiers. *Pharmaceutical Research*. 1998; 15(4):562-569.
- (252) Weda M, Zanen P, de Boer AH, Barends DM, Frijlink HW. An investigation into the predictive value of cascade impactore results for side effects of inhaled salbutamol. *International Journal of Pharmaceutics*. 2004; 287:79-87.
- (253) Giunchedi P, Conte U. Spray-drying as a preparation method of microparticle drug delivery systems: an overview. *STP Pharma sciences*. 1995; 5(4):276-290.
- (254) Grandfils C, Flandroy P, Nihant N, Barbette S, Jerome R, Teyssie P, et al. Preparation of poly (D,L) lactide microspheres by emulsion-solvent evaporation, and their clinical applications as a convenient embolic material. *Journal of Biomedical Materials Research*. 2004; 26(4):467-479.
- (255) Conte U, Conte B, Giunchedi P, Maggi L. Spray dried polylactide microsphere preparation: Influence of the technological parameters. *Drug Development and Industrial Pharmacy*. 1994; 20(3):235-258.

- (256) Migahed MD, Fahmy T. Structural relaxation around the glass transition temperature in amorphous polymer blends: temperature and composition dependence. *Polymer*. 1994; 35(8):1688-1693.
- (257) Liu A, Wang X, Wang L, Wang H, Wang H. Prediction of dielectric constants and glass transition temperatures of polymers by quantitative structure property relationships. *European Polymer Journal*. 2007; 43(3):989-995.
- (258) Selvam P, McNair D, Truman R, Smyth HDC. A novel dry powder inhaler: Effect of device design on dispersion performance. *International journal of pharmaceutics*. 2010; 401(1-2):1-6.
- (259) Gahl WA. Early Oral Cysteamine Therapy for Nephropathic Cystinosis. *European Journal of Pediatrics*. 162; 1:S38-S41.
- (260) Min-Oo G, Fortin A, Poulin JF, Gros P. Cysteamine, the molecule used to treat cystinosis, potentiates the anti-malarial efficacy of artemisinin. *Antimicrobial Agents and Chem*. 2010; in press check name of j.
- (261) Ambroz HB, Kornacka EM, Przybytniak GKGK. Influence of cysteamine on the protection and repair of radiation-induced damage to DNA. *Radiation Physics and Chemistry*. 2004; 70(6):677-686.
- (262) Braun JEF, Sarquis F, Lafleur MVM, Retèl J. Effect of the sulfhydryl compound cysteamine on gamma-radiation-induced mutations in double-stranded M13 DNA. *Mutation Research/DNA Repair*. 1996; 364(3):171-182.
- (263) Inoue M, Church CC, Brayman A, Miller MW, Malcuit MS. Confirmation of the protective effect of cysteamine in in vitro ultrasound exposures. *Ultrasonics*. 1989; 27(6):362-369.
- (264) Douglas A, Hamlyn A, James O. Controlled Trial of Cysteamine in Treatment of Acute Paracetamol (Acetomenophen) Poisoning. *The Lancet*. 1976; 307(7951):111-115.
- (265) Prescott LF, Swainson CP, Forrest ARW, Newton RW, Wright N, Matthew H. Successful Treatment of Severe Paracetamol Overdosage With Cysteamine. *The Lancet*. 1974; 303(7858):588-592.
- (266) Pae C, Lee C, Paik I. Therapeutic possibilities of cysteamine in the treatment of schizophrenia. *Medical hypotheses*. 2007; 69(1):199-202.
- (267) Wexler A. Stigma, history, and Huntington's disease. *The Lancet*. 2010; 376(9734):18-19.
- (268) Alzheimer's Association. Facts and Figures Factsheet. [homepage on the Internet]. USA: Alzheimer's Association; 2011 [updated March 2011; cited 2011 May 2011]. Available from: [http://www.alz.org/documents\\_custom/2011\\_Facts\\_Figures\\_Fact\\_Sheet.pdf](http://www.alz.org/documents_custom/2011_Facts_Figures_Fact_Sheet.pdf)

(269) Safety Officer in Physical Chemistry at Oxford University. Safety data for cysteamine. [homepage on the Internet]. Oxford UK: Oxford University; 2006 [updated 11/9/06; cited 2011 8/7/11]. Available from: <http://msds.chem.ox.ac.uk/CY/cysteamine.html>.

## **Appendix I**

### Phe conjugate synthesis

To a stirring solution of cystamine dihydrochloride (1g, 0.00444 moles) in anhydrous dichloromethane (20 cm<sup>3</sup>) at room temperature, 1,8-diazabicycloundec-7-ene (1.33 ml, 0.0089 moles) was added. The reaction mixture was then stirred continuously for 60 minutes at room temperature. To this was added butoxycarbonyl-L-phenylalanine N-hydroxysuccinimide ester (3.22 g, 0.0089 moles). After thin layer chromatographic (TLC) analysis confirmed that there were no starting materials left the solution was then partitioned between dichloromethane (20 cm<sup>3</sup>) and water at room temperature. The dichloromethane extracts were then washed with water (3 x 50 cm<sup>3</sup>), dried with magnesium sulphate, filtered and evaporated to near dryness. The solution was applied to a silica gel chromatography column (4 x 30 cm<sup>3</sup>) prepared with dichloromethane. The column was initially eluted with the same solvent until all front running impurities had eluted (monitored by TLC). The eluent was then changed to dichloromethane : methanol (9:1) and the major product was eluted, this was monitored and confirmed by TLC analysis, UV visualisation at 254 nm.

The protected compound was dissolved in trifluoroacetic acid (5 cm<sup>3</sup>) at room temperature. After 3.5 hours, the resulting solid was washed in ethanol (3 x 20 cm<sup>3</sup>), and the trifluoroacetic acid and ethanol removed by evaporation. Addition of diethyl ether gave an off a white precipitate that was filtered and dried at 50°C. The solid was analysed by mass spectroscopy.

### Mass spectroscopy method

All analyses were undertaken using a 1200 Series Mass Spectrometer from Agilent Technologies (Berkshire, UK). The small sample of crystal was placed into a vial, and chloroform added. The vial was then sealed and shaken. The sample was selected by the auto sampler and 10.00 µl was

injected into the Mass Spectrometer. The liquid phase was composed of 5% of 0.2% formic acid in methanol and 95% of 0.1% formic acid in water.

Found:

Mass spectroscopy: m/z 453.2 (m + 0) (100%), 447.1 (m - 6.1) (90%), 431.4 (m - 21.8) (75%), 469.1 (m + 15.9) (60%), 306.3 (m - 146.9) (10%). M: C<sub>22</sub>H<sub>22</sub>N<sub>4</sub>S<sub>2</sub>O<sub>2</sub>; Exact Mass: 453.2.

NMR: All analyses were undertaken using a Bruker Topspin Ultrashield 400MHz (Massachusetts, USA). The <sup>1</sup>H NMR spectrum (CD<sub>3</sub>OD) (400MHz) had δ: 2.64 (d, CH<sub>2</sub>S, 4H); 3.1 (d, CH<sub>2</sub>, 2H); 3.39 (d, NCH<sub>2</sub>, 4H); 4 (m, α, H); 7.35 (m, C<sub>6</sub>, 6H); 8.4 (m, NH<sub>3</sub>, 6H); 8.9 (m, NH, H).

Melting point: 164°C

Yield: 42%

## Appendix II

Table 37. A summary of the suppository batches made and their characteristics.

Suppository batch	Composition (% w/w)	Hardness without active; observations	Hardness including active (Phe conjugate)	Appearance
1 (C)	PEG 1500 100%	30N, 3.06 kg	27N, 2.75 kg	Opaque
2	Witepsol W35 100%	23N, 2.35 kg	20N, 2.04 kg	Uniform white
3	Gelucire 39/01 100%	28N, 2.86 kg	26N, 2.65 kg	Uniform white
4	PEG 1500 30% PEG 8000 70%	Brittle 23N, 2.35 kg	-	Mottled
5	PEG 8000 20% PEG 600 80%	Very soft 15N, 1.53 kg	-	Uniform white
6	PEG 14000 20% PEG 600 80%	Extremely soft 12N, 1.22 kg	-	Mottled white
7	PEG 600 30% PEG 4000 70%	Brittle 28N, 2.86 kg	-	Mottled
8	PEG 8000 60% PEG 1500 40%	Slightly brittle 46N, 4.69 kg	-	Mottled
9	Witepsol W35 98% Tween 80 2%	Extremely hard 55N, 5.61 kg	-	Uniform white
10 (B)	PEG 14000 40% PEG 600 60%	17N, 1.73 kg	13N, 1.33 kg	Mottled white
11	PEG 8000 30% PEG 600 70%	Firm, melts easily 7N, 0.714 kg	-	Mottled white
12	PEG 14000 30% PEG 600 70%	Firm, melts easily	-	Mottled white
13	PEG 14000 25% PEG 600 75%	Soft, melts easily	-	Mottled white
14	Poloxamer F68 3% F127 97%	Extremely hard 30N, 3.06 kg	-	White, air bubbles
15	PEG 8000 39% PEG 400 59% Tween 80 1%	14N, 1.43 kg	-	Mottled white
16	PEG 6000 50% PEG 1500 30% PEG 400 20%	26N, 2.65 kg	Firm 27N, 2.75 kg	Mottled white
17 (A)	PEG 8000 40% PEG 600 60%	19N, 1.94 kg	10N, 1.02 kg	Uniform white
18	PEG 1000 100%	Firm 319N, 32.54 kg	-	Uniform white
19	PEG 1000 75% PEG 4000 25%	Brittle 43N, 4.39 kg	-	Mottled
20	PEG 1000 96% PEG 4000 4%	72N, 7.34 kg	-	Uniform opaque white
21	PEG 1000 75% PEG 3000 25%	Brittle 46N, 4.69 kg	-	Mottled
22	PEG 1000 95 % PEG 3000 5%	Brittle 46N, 4.69 kg	-	Mottled opaque

## Appendix III

### Cysteamine bitartrate synthesis

Found:

NMR: The  $^1\text{H}$ NMR spectrum (MeOD) (400MHz) had  $\delta$ : 2.79 ( $\text{CH}_2\text{S}$ , 2H, t); 3.14 ( $\text{CH}_2\text{N}$ , 2H, t); 4.42 ( $\text{CH}_{\text{bitar}}$ , 2H, S)

Melting point: 94°C

Yield: 67%

### Cystagon™ analysis

Found:

NMR: The  $^1\text{H}$ NMR spectrum (MeOD) (400MHz) had  $\delta$ : 2.79 ( $\text{CH}_2\text{S}$ , 2H, t); 3.14 ( $\text{CH}_2\text{N}$ , 2H, t); 4.42 ( $\text{CH}_{\text{bitar}}$ , 2H, S)

Melting point: 95°C (269)

## **Supporting studies**

1. Completion of modules 1 and 2 of the Post Graduate Certificate course: Research Methods.
2. Attendance at RPSGB conference, London 2008: Ophthalmic drug delivery symposium.
3. Attendance at APS conference at GSK, Stevenage: Industrial insights.
4. Participation in the RGU biannual research symposium.
5. Visit to GSK, Ware, for ACI training, October 2009.

## **Communications associated with this thesis**

### **Publications:**

Buchan B, Kay G, Heneghan A, Matthews KH, Cairns D. Gel formulations for treatment of the ophthalmic complications in cystinosis. *International Journal of Pharmaceutics*. 2010; 392, 1-2, p. 192-197.

### **Conference proceedings:**

Fifth International Cystinosis Conference - Dublin 2008 - Formulation and Evaluation of Novel Dosage Forms of Cysteamine for the Potential Treatment of Cystinosis. Poster.

British Pharmaceutical Conference - Manchester 2008 - Formulation and Evaluation of Novel Dosage Forms of Cysteamine for the Potential Treatment of Cystinosis. Poster and supplement in the *Journal of Pharmacy and Pharmacology*:

Buchan B, Kay G, Matthews KH, Cairns D. Formulation and evaluation of novel dosage forms of cysteamine for the potential treatment of cystinosis. *Journal of Pharmacy and Pharmacology, Supplement*. 2008; 139, p. 55.

British Pharmaceutical Conference - Manchester 2009 - Formulation and Evaluation of Cysteamine for Ophthalmic Delivery. Poster and supplement in the *Journal of Pharmacy and Pharmacology*:

Buchan B, Kay G, Matthews KH, Cairns D. Formulation and Evaluation of Cysteamine for Ophthalmic Delivery. *Journal of Pharmacy and Pharmacology, Supplement*. 2009; 61, 98, p. 73.

Thirty-seventh Annual Meeting and Exposition of the Controlled Release Society – Portland, Oregon, USA 2010 - The preparation and evaluation of gel formulations for treatment of the ophthalmic complications in cystinosis. Poster. Abstract published online, available at: <https://www.controlledreleasesociety.org/customer/source/meetings/PresentationFiles/4871-1.pdf>

First UKPharmSci conference - Nottingham 2010 - Dry powder inhaler for the potential systemic treatment of cystinosis. Poster and podium presentation.

Sixth International Cystinosis Conference – Italy 2010 - Formulation and Evaluation of Cysteamine for Ophthalmic Delivery. Poster.

**Invited talks:**

Celtic Pharmacy Conference - Edinburgh 2010 - Chemical Camouflage - Design of Novel Prodrugs for the Treatment of Nephropathic Cystinosis. Podium and poster presentation.

**Funding:**

April 2010, £800 travel bursary received from the UK Resource Centre for Women in Science, Engineering and Technology, for attendance at the Controlled Release Society's annual meeting and exposition in Portland, Oregon.

September 2010, £500 travel grant received from the Cystinosis Foundation UK, for travel to the CRS conference in Portland, Oregon.

April 2011, £100,000 grant secured from Sparks to support further testing of the ophthalmic gels.